ZooKeys 851: 1–15 (2019)
doi: 10.3897/zookeys.851.33351
http://zookeys.pensoft.net

RESEARCH ARTICLE

A peer-reviewed open-access journal
ZooKeys
Launched to accelerate biodiversity research

A new record of the spider family Caponiidae from China (Arachnida, Araneae)

Ke-ke Liu[1,2], Hai-qiang Yin[1], Ji-he Liu[1], Xiang Xu[1,3], Yong-hong Xiao[2], Xian-jin Peng[1,3]

1 *College of Life Science, Hunan Normal University, Changsha 410081, Hunan, China* **2** *College of Life Science, Jinggangshan University, Ji'an 343009, Jiangxi, China* **3** *The National & Local Joint Engineering Laboratory of Animal Peptide Drug Development (Hunan Normal University), National Development and Reform Commission, Changsha, Hunan 410081, China*

Corresponding author: *Hai-qiang Yin* (yinhaiqiang@hunnu.edu.cn); *Xiang Xu* (xux@hunnu.edu.cn)

Academic editor: *Jeremy Miller* | Received 25 January 2019 | Accepted 9 April 2019 | Published 3 June 2019

http://zoobank.org/73187FA9-EAAD-4D53-8472-FCC8ACB0939E

Citation: Liu K-k, Yin H-q, Liu J-h, Xu X, Xiao Y-h, Peng X-j (2019) A new record of the spider family Caponiidae from China (Arachnida, Araneae). ZooKeys 851: 1–15. https://doi.org/10.3897/zookeys.851.33351

Abstract

The family Caponiidae Simon, 1890 is reported for the first time from China. The total number of the known spider families from China increases to 72 with the addition of this family newly recorded in the present paper. Based on male and female specimens collected from Guangxi, China, *Laoponia saetosa* Platnick & Jäger, 2008 is illustrated and a global distribution map is generated.

Keywords

Distribution, Guangxi Zhuang Autonomous Region, *Laoponia*, taxonomy

Introduction

The family Caponiidae is a group of Haplogynae ecribellate spiders with a patchy but nearly global distribution, typically found on the ground, under rocks, and in burrows and leaf litter. At present, the known caponiids are mainly distributed in America and Africa, absent from Australia and New Zealand, with only three species found in Asia (World Spider Catalog 2019). The first Asian spiders of the family Caponiidae were found in Laos in 2007 by Peter Jäger who collected them using the sieving method;

based on these specimens, Platnick and Jäger (2008) established the genus *Laoponia* to contain the first member of the family Caponiidae discovered in Asia: *Laoponia saetosa*, which was also found subsequently in Vietnam (Liu et al. 2010). *Laoponia saetosa* is characterized by having two eyes, a short embolus, an absence of a tegular apophysis on the male palp, normal endites, and a single receptaculum in the female genitalia (Platnick and Jäger 2008; Liu et al. 2010). The second and third Caponiidae species known to occur in Asia are *Iraponia scutata* Kranz-Baltensperger, Platnick & Dupérré, 2009 from Iran and *Laoponia pseudosaetosa* Liu, Li & Pham, 2010 from Vietnam.

Caponiidae consists of 119 species classified into 18 genera worldwide (World Spider Catalog 2019). Recently, more details based on the morphological characters of the genus *Medionops* and *Nops* were revealed by Sánchez-Ruiz (2017) and Brescovit (2018). Many structures of the legs and genitalia were defined as the diagnostic structures which are undoubtedly beneficial to future taxonomic studies (Sánchez-Ruiz and Brescovit 2017, 2018). With the discovery of many unusual characters, such as a male palp with anterior curvature and female genitalia with lateral extensions of the posterior plate, the caponiids are undergoing re-evaluation and re-organization (Dupérré 2014; Sánchez-Ruiz et al. 2015; Sánchez-Ruiz and Brescovit 2017).

During the past four years, several explorations to Guangxi Zhuang Autonomous Region, China, have been made by the authors, and many spider specimens were collected. Among the many specimens from Guangxi, only four specimens were identified as *Laoponia saetosa*. It is the first member of the family Caponiidae to be found in China.

It isn't surprising to find *Laoponia saetosa* in some areas of Guangxi, China which is very near Vietnam. After all this species has been reported in Vietnam. What is interesting is that in southwest Guangxi, three National Nature Reserves located in Chongzuo City (Nonggang National Nature Reserve, Chongzuo White-headed langur National Nature Reserve) and Nanning City (Damingshan National Nature Reserve) have been explored by authors, but it is only in Nonggang National Nature Reserve that *L. saetosa* was collected. There are only two possible reasons for this. One possibility is that *Laoponia* species have very narrow distribution regions in China and they distribute only in the places very near Vietnam. Geographically, Nonggang National Nature Reserve (22°13'56"–22°39'09"N, 106°42'28"–107°04'54"E) is actually closer to Vietnam than both Chongzuo White-headed langur National Nature Reserve (22°10'43"–22°36'55"N, 107°16'53"–107°59'46"E) and Damingshan National Nature Reserve (23°24'–23°30'N, 108°20'–108°24'E). The other possibility is that besides Nonggang, the other regions of Guangxi are also potential distribution regions of *Laoponia* and collectors simply haven't found them yet. However, the reasons why collectors didn't collect them are very complex and are related with at least two factors: time and methods.

The *Laoponia* specimens examined by Liu et al. (2010) were collected during an entire year-long sampling period (1 April 2014 – 31 March 2015) and it is hard to say which season is the peak abundance for this species. The *Laoponia* specimens examined

by Platnick and Jäger (2008) and Jäger and Praxaysombath (2009) were collected in February/March (the dry season in Laos). The specimens in the present study were collected in between October and November (the dry season in southern China). It is possible that from October to March or April of the next year is the mating period of *L. saetosa* and adult specimens are relatively easily found. It seems that this species is inclined to live the dry circumstance and it is also very possible it has a capability for drought resistance.

Caponiids are wandering hunters. According to the previous description of *L. saetosa* and the authors' collecting experience, it is usually by sieving leaf litter or using pitfall traps that this species was successfully collected.

The authors made an exploration in Damingshan National Nature Reserve, Nanning City, Guangxi Zhuang Autonomous Region, China in November (dry season), 2018 and sieving leaf litter was widely used. The authors also made an exploration in Chongzuo White-headed langur National Nature Reserve, Chongzuo City, Guangxi Zhuang Autonomous Region, China in between August and September (rainy season), 2015 and sieving leaf litter was rarely used during exploration because of rainy weather. Though no specimens of *L. saetosa* were collected in both explorations, the authors think, based on the combinations of geographic location, time and methods, it is very possible that Damingshan National Nature Reserve isn't the distribute region of *L. saetosa*, while it is also highly probable that *L. saetosa* can be collected in Chongzuo White-headed langur National Nature Reserve in suitable season by using suitable collecting methods. Certainly, this must to be confirmed by future collecting and further research from Guangxi, China.

Though *L. saetosa* has been described by Platnick and Jäger (2008) and redescribed by Liu et al. (2010), there are also shortcomings in previous taxonomic treatments of this species. The embolus was broken and its distal end was missing in SEM photographs supplied by Platnick and Jäger in the original description. Liu et al. took only a photograph for one side of male palp (only retrolateral view) and omitted at least one standard anatomical view. The present paper supplies more digital color and SEM images based on the intact specimens. The presentation of more detailed features in images makes it more easily to distinguish *Laoponia* from the other genera such as *Iraponia*, *Nops*, *Nopsides* and *Tarsonops* in family Caponiidae.

Here this newly recorded spider is reported from China and illustrated in detail, and a global distribution map of *Laoponia saetosa* is also provided. The total number of spider families known from China increases to 72 with the addition of this record.

Materials and methods

Specimens were examined and photographed using a LEICA M205C stereomicroscope with a LEICA MC170 HD. Both the male palps and female genitalia were detached from the spider's body and observed in 75% ethanol. For the photographs of

the female vulva, the specimens were previously digested with pancreatin and cleaned after 2 h of digestion. Specimens including detached copulatory organs were stored in 75% ethanol after examination. All the specimens are deposited in Hunan Normal University (HNU), Changsha.

All morphological measurements were calculated using a stereomicroscope (LEICA M205C) and are given in millimeters. Leg measurements are given as total length (femur, patella, tibia, metatarsus, tarsus).

That leg I and IV, not leg II and III were supplied with SEM photographs is following the references on caponiids (Sánchez-Ruiz 2017; Brescovit 2018; Sánchez-Ruiz and Brescovit 2017; 2018). Leg I and IV have more important characteristics than Leg II and III.

Terminology of the male and female genitalia follows Sánchez-Ruiz et al. (2015) and Sánchez-Ruiz and Brescovit (2017). The abbreviations used in the present paper are as follows:

AL abdomen length;
Ar arolium;
AP anterior plate;
AW abdomen width;
Bu bulb;
CL carapace length;
CW carapace width;
CWLNNR Chongzuo White-headed langur National Nature Reserve;
DMR distal margin of receptaculum;
DNNR Damingshan National Nature Reserve;
Em embolus;
ESS external sclerotization around spiracles;
Fu furrow;
LEP lateral extensions of posterior plate;
LO lyriform organs;
MC median concavity;
MS membranous sac;
MTS metatarsal stopper furrow;
NNNR Nonggang National Nature Reserve;
PP posterior plate;
Re receptaculum;
SDO sperm duct opening;
SS slit sensillum;
TT tracheal trunk.

Taxonomy

Family Caponiidae Simon, 1890

Genus *Laoponia* Platnick & Jäger, 2008

Laoponia: Platnick and Jäger 2008: 2, figs 1–25.

Type species. *Laoponia saetosa* Platnick & Jäger, 2008: 4, figs 1–25, 31–34, type locality Laos.

Diagnosis. *Laoponia* species is similar to *Nops* species (see Sánchez-Ruiz and Brescovit 2015: 133, fig. 6; 135, fig. 18) and *Tarsonops* species (see Sánchez-Ruiz et al. 2015: 47, fig. 15; Sánchez-Ruiz and Brescovit 2018, 62, fig. 38H) in having a slit sensillum at the base of fan on chelicerae and the lyriform organ distally located at metatarsi, but can be distinguished from other genera by the relatively shorter, slender embolus with a sharp tip in males (wide, membranous in *Nopsides* Chamberlin, 1924; broad, ribbon-shaped in *Iraponia* Kranz-Baltensperger, Platnick & Dupérré, 2009; with small extensions on tip or a sclerotized margin in *Nops* MacLeay, 1839), and the normal legs without some appendages (such as the median translucent ventral longitudinal keel, the translucent extension of the membrane, subsegmented tarsi, and the presence of a gladius between the anterior metatarsi and tarsi in *Nops* MacLeay, 1839) (Platnick and Jäger 2008; Liu et al. 2010; Jiménez et al. 2011; Sánchez-Ruiz and Brescovit 2018). Female internal genitalia with clearly sclerotized distal margin and simple invagination of receptaculum and relatively wide base of uterus externus (narrow in *Iraponia* Kranz-Baltensperger, Platnick and Dupérré 2009). Unfortunately, there are only two *Laoponia* species reported worldwide: one is known with both male and female specimens and the other only with male specimens. More information on the females of this genus is needed.

Laoponia saetosa Platnick & Jäger, 2008

Figs 1–8

Laoponia saetosa Platnick & Jäger, 2008: 4, figs 1–25, 31–34; Jäger and Praxaysombath, 2009: 31, figs 7–14; Liu, Li and Pham, 2010: 22, figs 1–5, 9, 11–12, 14.

Material examined. All specimens examined in this study were collected by Ailan He, Keke Liu, Qu Cai, Jihe Liu, Jinxin Liu, and Zongguang Huang from Nonggang National Nature Reserve, Guangxi, China. 1 ♀, Longzhou County, Nonggang Station, the entrance of core area, 22°27'50.94"N, 106°55'56.58"E, 230 m, leaf litter, 26.X.2017; 1 ♂, Longzhou County, Sanlian Station, 22°32'4.93"N, 106°50'13.07"E, 310 m, leaf litter, 30.X.2017; 1 ♀, Longzhou County, Xiangshui Station, 18th bound-

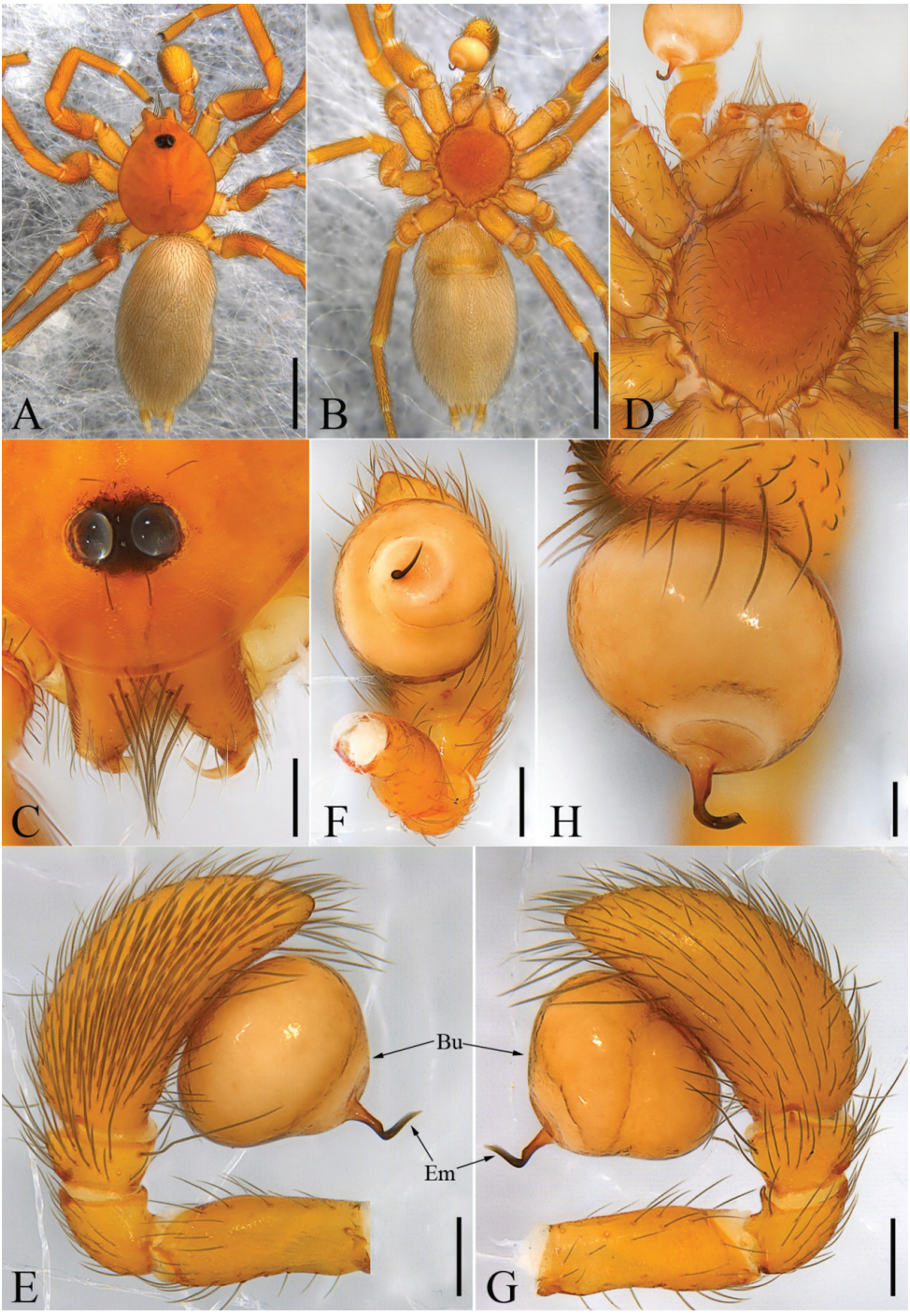

Figure 1. *Laoponia saetosa* Platnick & Jäger, 2008, male **A** habitus, dorsal view **B** habitus, ventral view **C** prosoma, frontal view, slightly lateral **D** prosoma, ventral view **E** palp, prolateral view **F** palp, left, ventral view **G** palp, retrolateral view **H** palp, dorsal view. Scale bars: 1 mm (**A, B**); 0.2 mm (**C, E–G**); 0.5 mm (**D**); 0.1 mm (**H**).

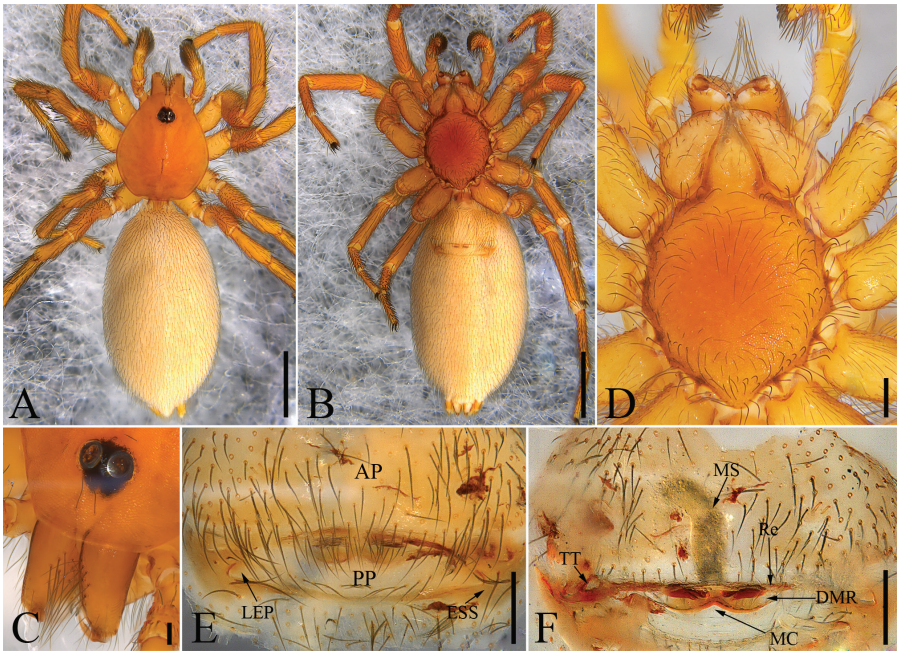

Figure 2. *Laoponia saetosa* Platnick & Jäger, 2008, female **A** habitus, dorsal view **B** habitus, ventral view **C** prosoma, frontal view, slightly lateral **D** prosoma, ventral view **E** epigyne, ventral view **F** vulva, dorsal view. Scale bars: 1 mm (**A, B**); 0.1 mm (**C**); 0.2 mm (**D–F**).

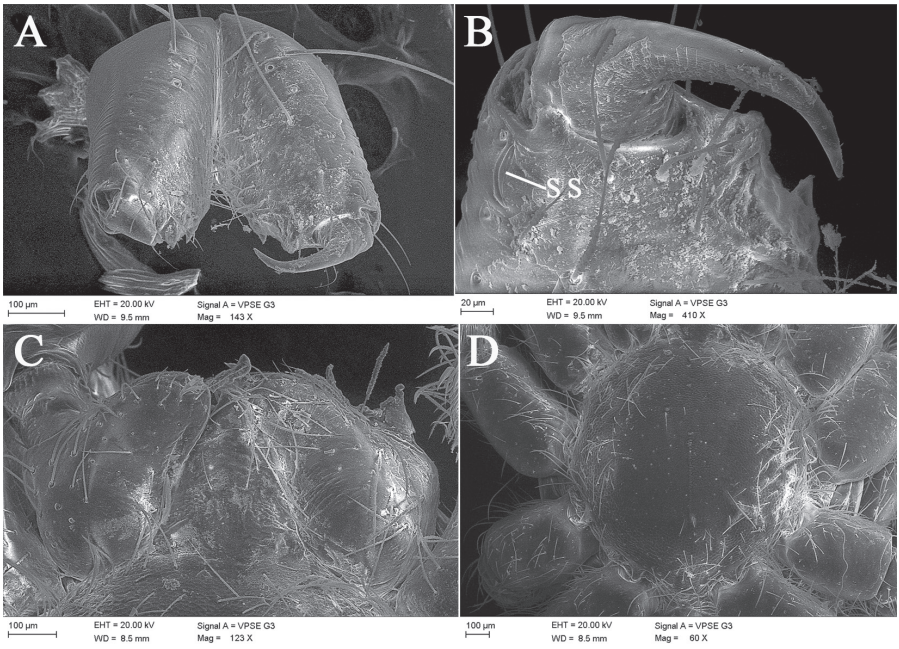

Figure 3. *Laoponia saetosa* Platnick & Jäger, 2008, male mouthpart and sternum **A** chelicerae, frontal view **B** left chelicera, frontal view **C** endites and labium, ventral view **D** sternum, ventral view.

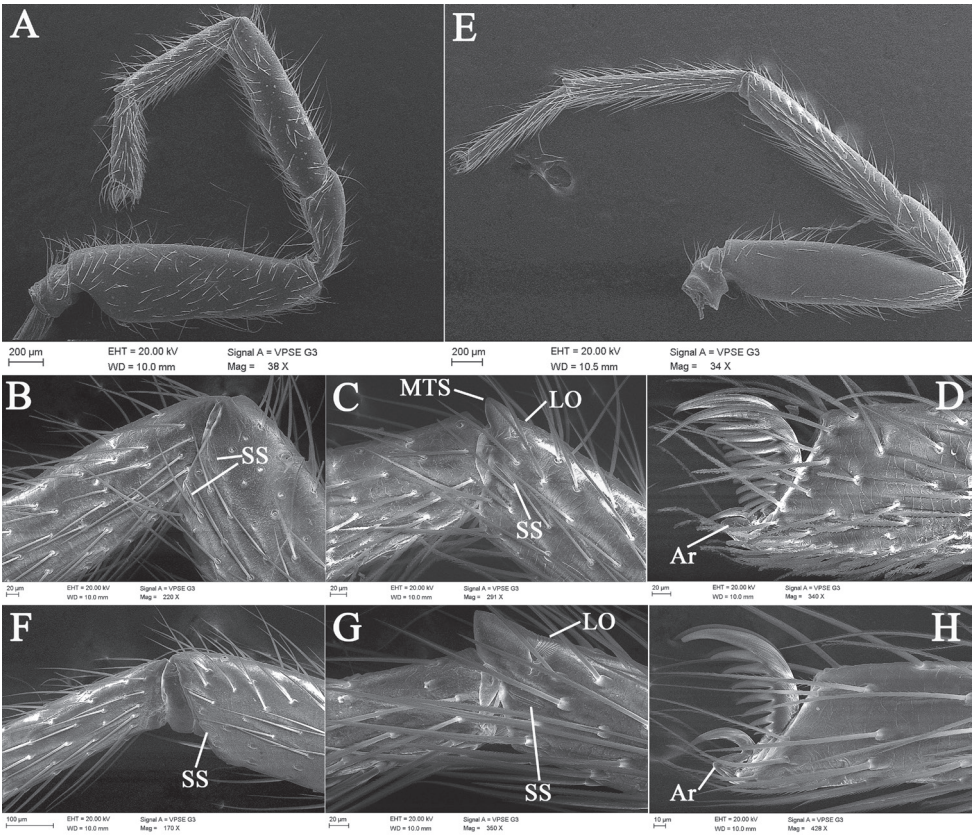

Figure 4. *Laoponia saetosa* Platnick & Jäger, 2008, male legs **A** left leg I, retrolateral view **B** same, join of tibia and metatarsus, retrolateral view **C** same, join of tarsus and metatarsus, retrolateral view **D** same, tarsal claws, retrolateral view **E** left leg IV, retrolateral view **F** same, join of tibia and metatarsus, retrolateral view **G** same, join of tarsus and metatarsus, retrolateral view **H** same, tarsal claws, retrolateral view.

ary tablet, 22°26'8.38"N, 107°1'26.37"E, 260 m, leaf litter, 1.XI.2017; 1 ♂, Ningming County, Longrui Station, Huashan National Village, the road behind the hill, 22°14'29.45"N, 107°3'32.01"E, 260 m, leaf litter, 4.XI.2017.

Diagnosis. The male of this species resembles that of *L. pseudosaetosa* Liu, Li & Pham, 2010 in having short, slender embolus with a sharp tip and entire legs without translucent ventral keel on metatarsi (see Liu et al. 2010: 24, figs 10, 13), but can be distinguished by a stout bulb and the embolus with a distinctively strongly curved median part (Figs 1E–H, 5). The female can be easily distinguished from another Asian species, *Iraponia scutata* Kranz-Baltensperger, Platnick & Dupérré, 2009, by the presence of only two eyes (six eyes in *I. scutata*), abdomen lacking the postepigastric scutum, the shape of median membranous sac (large in *I. scutata*), and relatively wide base of the uterus externus (narrow in *I. scutata*) (Kranz-Baltensperger et al. 2009).

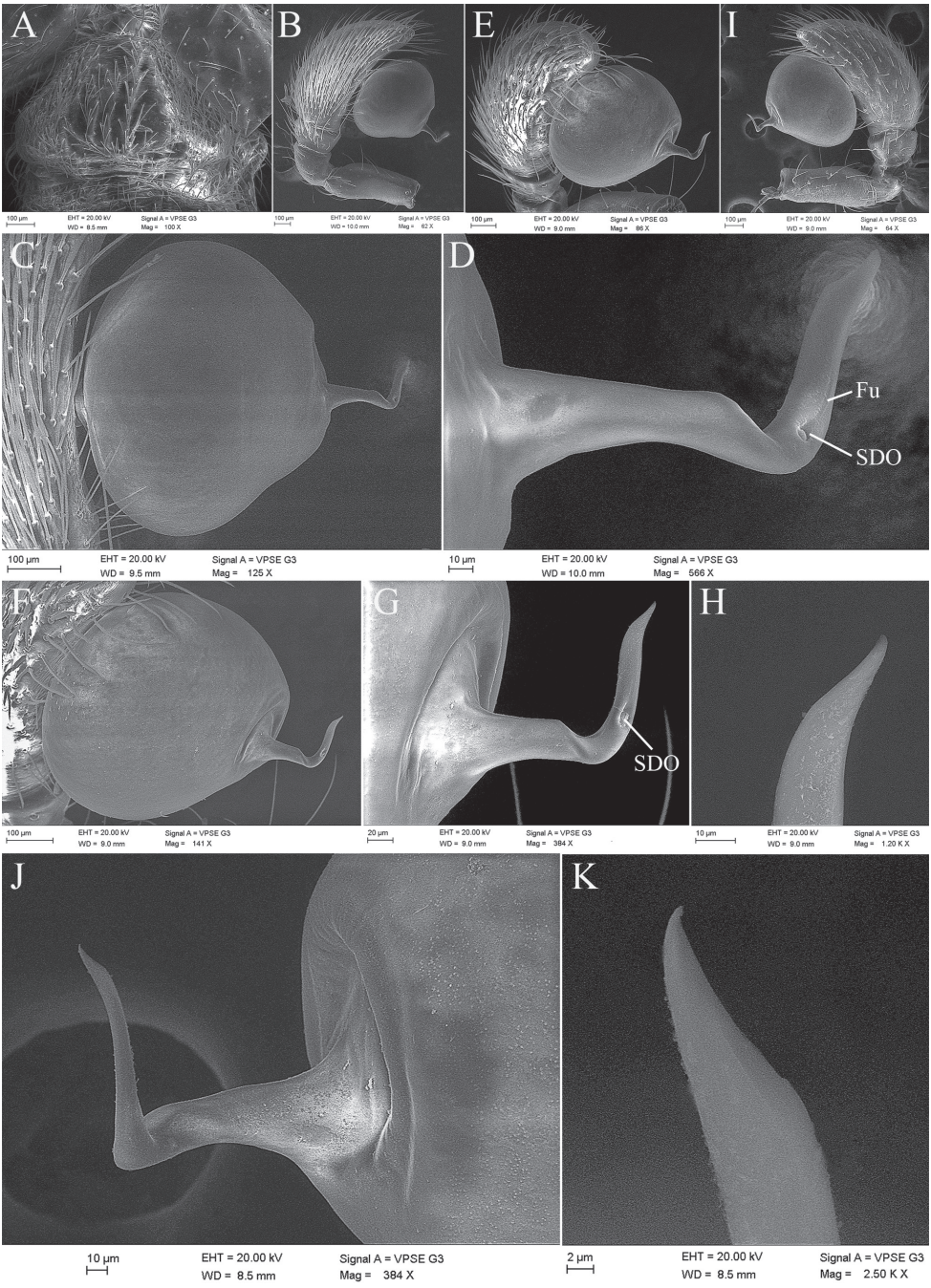

Figure 5. *Laoponia saetosa* Platnick & Jäger, 2008, male genital area and left palp **A** genital area, ventral view **B** palp, prolateral view **C** same, detail of bulb and embolus **D** same, detail of embolus **E** dorsal view, slightly prolateral **F** same, detail of bulb and embolus **G** same, detail of embolus **H** same, the apex of embolus **I** retrolateral view **J** same, detail of bulb and embolus **K** same, the apex of embolus.

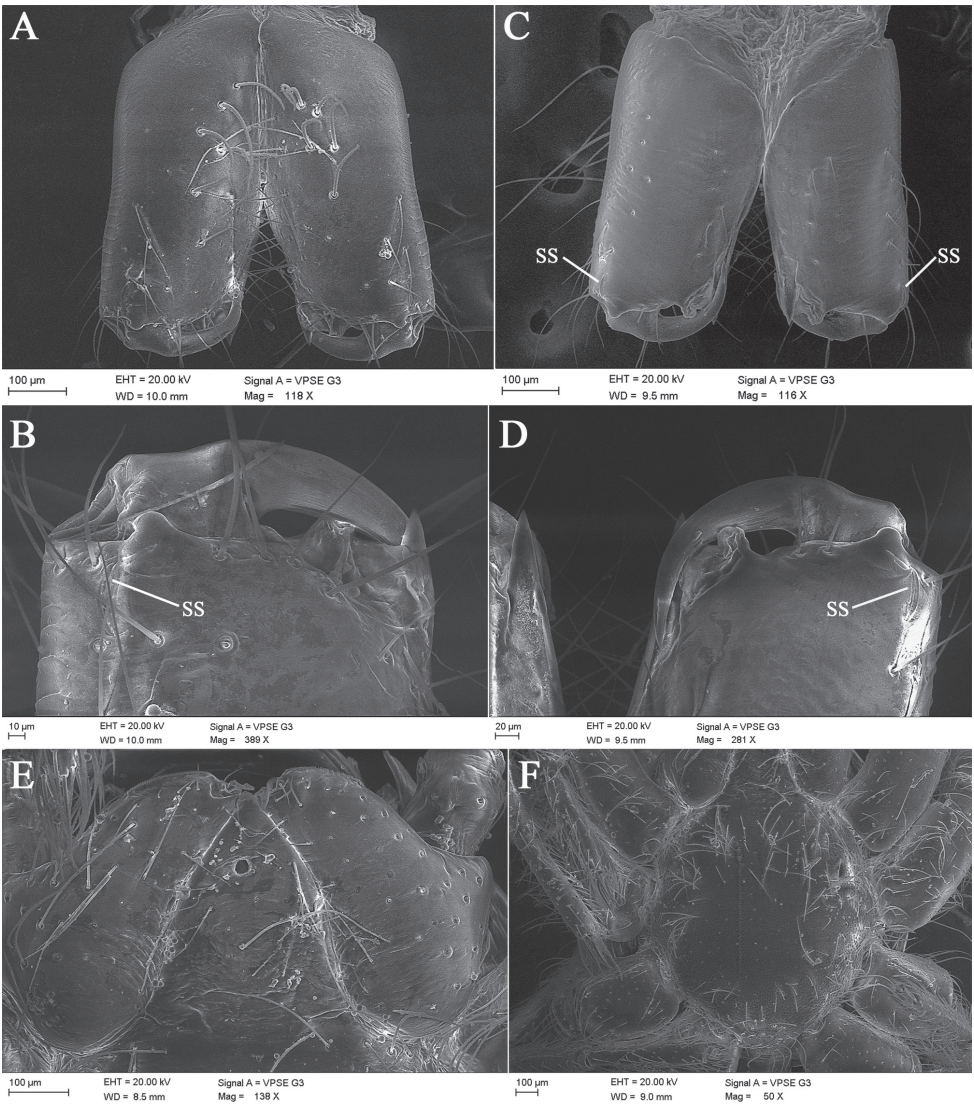

Figure 6. *Laoponia saetosa* Platnick & Jäger, 2008, female mouthpart and sternum **A** chelicerae, frontal view **B** left chelicera, frontal view **C** chelicerae, posterior view **D** left chelicera, frontal view **E** endites and labium, ventral view **F** sternum, ventral view.

Description. Male. Habitus as in Fig. 1A, B. Total length 4.37. Carapace (Fig. 1A) length 1.66, width 1.39, orange, broadly oval in dorsal view (CW/CL ≈ 0.84), pars cephalica slightly domed in lateral view, anteriorly narrowed to 0.3 times its maximum width, with abundant scale-shaped lattices on the surface, indistinct cervical groove and distinct fovea. Eyes (Fig. 1C): circular, with dark pigment around them; diameters

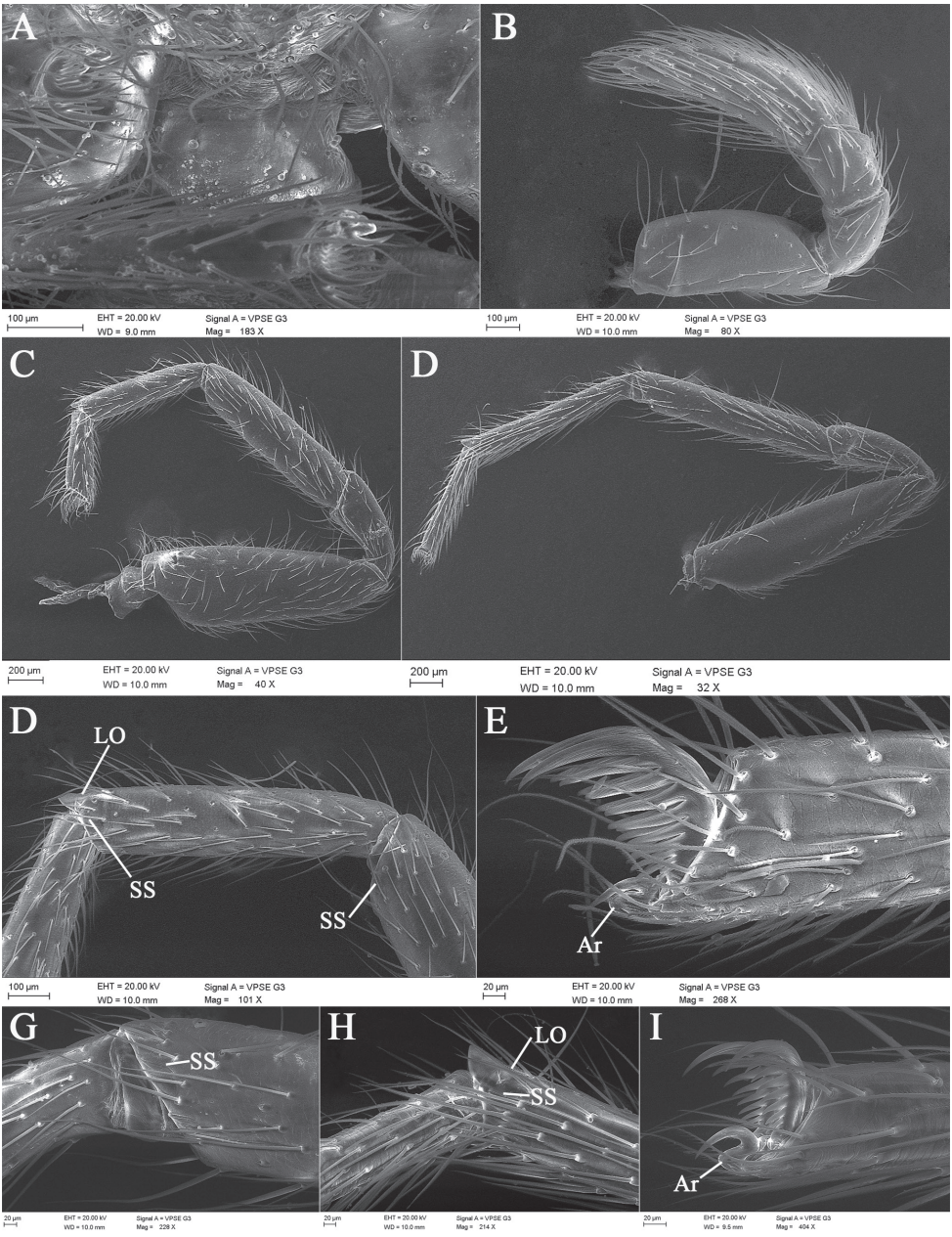

Figure 7. *Laoponia saetosa* Platnick & Jäger, 2008, female **A** pedicel, ventral view **B** left palp, retrolateral view **C** left leg I, retrolateral view **D** same, join of tibia and metatarsus, and patella and tibia, retrolateral view **E** same, tarsal claws, retrolateral view **F** left leg IV, retrolateral view **G** same, join of tibia and metatarsus, retrolateral view **H** same, join of tarsus and metatarsus, retrolateral view **I** same, tarsal claws, retrolateral view.

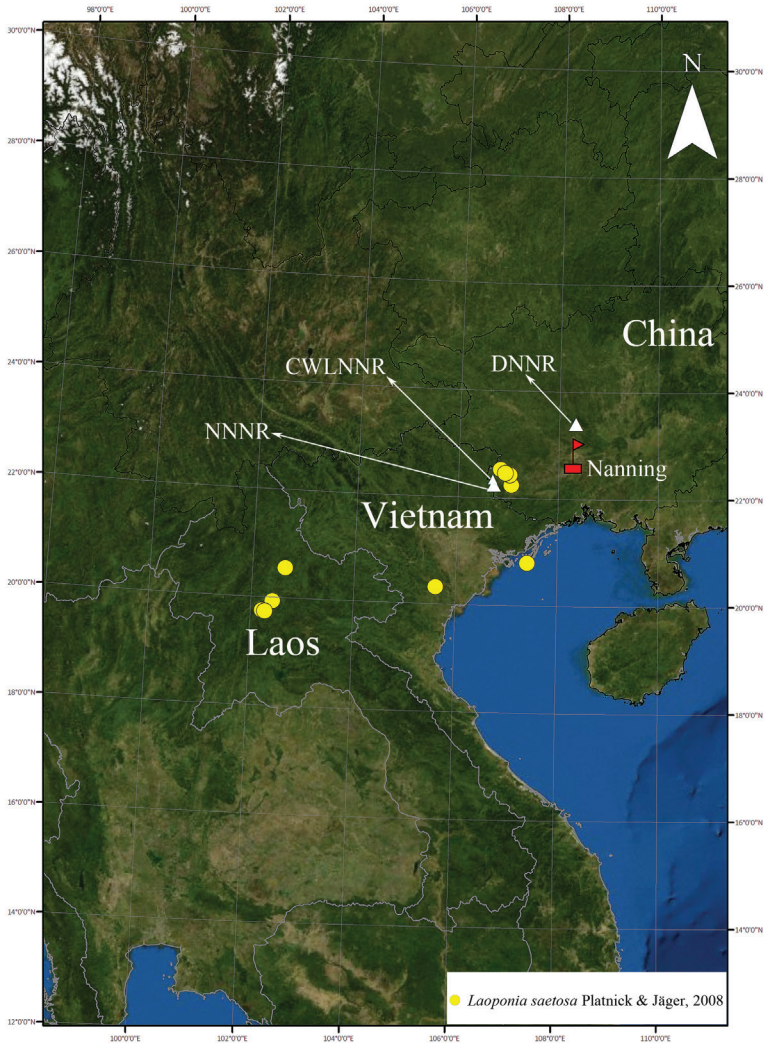

Figure 8. Localities of records of *Laoponia saetosa* Platnick & Jäger, 2008 in the world (see World Spider Catalog 2019 and Material examined for details).

0.14; interdistance 0.05, separated by about one third their diameters; with a group of setae in front of and behind eyes respectively. Mouthparts (Figs 1B, 3A–C): chelicerae straight, light orange, each with an apical group of 6–10 strong and converging setae from basal to median part in frontal view; median lamina long, with dark, heavily sclerotized tip in the furrow; a membranous lobe located at the median part between lamina and fang base; the base of fan with a slit sensillum laterally in frontal view; stridulatory ridges clear, covering more than 1/2 of prolateral surface; endites convergent anteriorly but not touching, light orange, anteriorly with a relatively long membranous projection, serrula present, tiny, middle part wider than distal and proximal margins

and forming an obtuse angle of about 100 degrees, covered with scattered long setae from median to posterior surface; labium almost diamond-shaped, fused to sternum, anterior surface of labium with long, longitudinal, submarginally sclerotized strips and the apical part narrow, a bit round. Sternum (Fig. 1D, 3D) slightly longer than wide, ovoid, with abundant setae and fine reticular lines around the edge, orange, darker at the edge. Pedicel, short, smooth, without setae on the surface. Abdomen (Figs 1A, B, 5A) uniformly white, length 2.62, width 1.48, strongly elongate oval in dorsal view (AW/AL ≈ 0.56), with abundant setae dorsally and two pairs of respiratory spiracles clustered around epigastric groove. Legs (Figs 1A, B, 4) orange, with abundant setae, the base of femur thickened, without sub-segmentation or membranous processes and strong spines on each segment; femora enlarged anteriorly; patella shorter than femora, tibia, metatarsus, and tarsus in legs I, III, IV; the distal part of tibia with few slit sensilla in retrolateral view; metatarsi entire, with obvious metatarsal dorsal stopper and lyriform organ distally in retrolateral view; tarsus with three claws: paired claws with 8–10 teeth, gradually enlarged from base to apex; the unpaired claw small, associated with a relatively small arolium at the base; tibia, metatarsus, and tarsi I–IV with trichobothria in a single row in retrolateral view; leg measurements in mm: I 3.77 (0.92, 0.60, 0.85, 0.79, 0.61); II 3.43 (0.72, 0.65, 0.98, 0.70, 0.38); III 3.30 (0.66, 0.45, 0.89, 0.74, 0.56); IV 4.43 (0.80, 0.69, 1.29, 0.91, 0.74). Leg formula: 4123. Six spinnerets with abundant setae, posterior laterals with two segments.

Genitalia (Figs 1A, B, D–H, 5): epigastric region with faint scutum, furrow broad, slightly bent, slit-shaped with rebordered margins, situated at level of bi-lateral spiracles; palp stout, yellow; patella and tibia short, patella slightly longer than tibia but shorter than femur; cymbium ovoid, with thickened setae at the distal area; bulb light orange, ovoid, 1.2 times as long as its maximum width in frontal view, medially with a constriction in retrolateral view, ventrally with small circular area clearly delimited from remainder of cuticle; embolus sclerotized, hook-shaped, twisted medially, including basal and distal part, apex bent outward in frontal view, forming an angle of approximately 100° with the axis of basal part, with a sperm duct opening associated with a shallow furrow extending towards the apical part.

Female. Habitus as in Fig. 2A, B. As in male except as follows. Total length 4.98, carapace length 1.67, width 1.43, broadly oval in dorsal view (CW/CL ≈ 0.86), anteriorly narrowed to 0.4 times its maximum width. Eyes (Fig. 2C), diameters: 0.14; interdistances: 0.04. Mouthparts (Figs 2B, D, 6A–E): labium with a round hollow anteriorly. Abdomen (Fig. 2A, B), length 3.19, width 1.79, strongly elongate oval in dorsal view (AW/AL ≈ 0.56). Palp (Fig. 7B) and tarsus longer than patella plus tibia, with dense setae. Leg (Figs 2A, B, 7C–I) measurements in mm: I 3.48 (0.67, 0.57, 1.04, 0.61, 0.59); II 3.37 (0.68, 0.61, 0.65, 0.84, 0.59); III 3.27 (0.59, 0.54, 0.74, 0.70, 0.60); IV 4.62 (0.80, 0.76, 1.33, 0.95, 0.78).

Female genitalia (Fig. 2E, F). In ventral view (Fig. 2E), anterior plate distinct, almost reaching proximal part of abdomen; external sclerotization of spiracles yellowish, small, near the lateral extensions of posterior plate; posterior plate oval. In dorsal view (Fig. 2F), tracheal trunk long, anteriorly directed, extending anteriorly as long as cone-

shaped membranous sac, membranous sac located on the receptaculum; with a thin, convex and sclerotized distal margin of receptaculum; postero-medially with distinct median concavity.

Distribution. Laos (Luang Prabang Province), Vietnam (Ninh Binh Province, Hai Phong Province), China (Guangxi Zhuang Autonomous Region).

Remarks. The female genitalia consist of a single receptaculum and a cone-shaped membranous sac in life. The tracheal trunks of the female specimens examined in this study were broken off during preparation. The illustrations of this species were examined by Peter Jäger who first collected and described this species, and who confirmed the identification.

Acknowledgements

We are grateful to Ailan He, Qu Cai, Jinxin Liu and Zongguang Huang for collecting the specimens. Early drafts of this paper benefited greatly from the comments provided by Luyu Wang. We also thank Peter Jäger and Nathalie Yonow for confirming the identification of *Laoponia saetosa* and improving the English of the manuscript, respectively. Special thanks to Jeremy Miller for his tireless encouragement and constructive suggestions and Jie Liu and two anonymous reviewers for their comments. This study was supported by the Natural Science Foundation of China (31772423/31 471963/31372160/31560592), the Hunan Provincial Construct Program of the Key Discipline in Ecology (0713) and by the Opening Fund of The National and Local Joint Engineering Laboratory of Animal Peptide Drug Development (Hunan Normal University), National Development and Reform Commission (2017KF002).

References

Dupérré N (2014) Three new species of Caponiid spiders from Ecuador (Araneae, Caponiidae). Zootaxa 3838 (4): 462–474. https://doi.org/10.11646/zootaxa.3838.4.5

Jäger P, Praxaysombath B (2009) Spiders from Laos: new species and new records (Arachnida: Araneae). Acta Arachnologica 58: 27–51. https://doi.org/10.2476/asjaa.58.27

Jiménez ML, Platnick, NI, Dupérré N (2011) The haplogyne spider genus *Nopsides* (Araneae, Caponiidae), with notes on *Amrishoonops*. American Museum Novitates 3708: 1–18. https://doi.org/10.1206/3708.2

Liu J, Li S, Pham DS (2010) Caponiidae (Arachnida, Araneae), a newly recorded family from Vietnam. Acta Zootaxonomica Sinica 35: 20–26.

Platnick NI, Jäger P (2008) On the first Asian spiders of the family Caponiidae (Araneae, Haplogynae), with notes on the African genus Diploglena. American Museum Novitates 3634: 1–12. https://doi.org/10.1206/624.1

Sánchez-Ruiz A, Brescovit AD (2017) A new genus with seven species of the subfamily Nopinae (Araneae, Caponiidae) from the Neotropical region. Zootaxa 4291(1): 117–143. https://doi.org/10.11646/zootaxa.4291.1.7

Sánchez-Ruiz, A, Brescovit AD (2015) On the taxonomic placement of the Cuban spider *Nops ariguanabo* Alayón and the description of a new Mexican *Tarsonops* (Araneae, Caponiidae). Zootaxa 3914(2): 131–143. https://doi.org/10.11646/zootaxa.3914.2.3

Sánchez-Ruiz A, Brescovit AD, Alayón G (2015) Four new caponiid species (Araneae, Caponiidae) from the West Indies and redescription of *Nops blandus* (Bryant). Zootaxa 3972(1): 43–64. https://doi.org/10.11646/zootaxa.3972.1.3

Sánchez-Ruiz A, Brescovit AD (2018) A revision of the Neotropical spider genus *Nops* MacLeay (Araneae: Caponiidae) with the first phylogenetic hypothesis for the *Nopinae* genera. Zootaxa 4427(1): 1–121. https://doi.org/10.11646/zootaxa.4427.1.1

World Spider Catalog (2019) World Spider Catalog. Natural History Museum Bern. Version 20.0. https://wsc.nmbe.ch/ [accessed 26 March, 2019]

Zhang Z, Wang L (2017) Chinese Spiders Illustrated. Chongqing University Press, Chongqing, 954 pp.

ZooKeys 851: 17–25 (2019)
doi: 10.3897/zookeys.851.31802
http://zookeys.pensoft.net

RESEARCH ARTICLE

A peer-reviewed open-access journal
ZooKeys
Launched to accelerate biodiversity research

A new species of *Pionothele* from Gobabeb, Namibia (Araneae, Mygalomorphae, Nemesiidae)

Jason E. Bond[1], Trip Lamb[2]

1 *Department of Entomology & Nematology, University of California Davis, Davis, California, USA*
2 *Department of Biology, East Carolina University, Greenville, North Carolina, USA*

Corresponding author: *Jason E. Bond* (jbond@ucdavis.edu)

Academic editor: *Chris Hamilton* | Received 20 November 2018 | Accepted 2 February 2019 | Published 3 June 2019

http://zoobank.org/894CD479-72A2-412D-B983-7CE7C2A54E88

Citation: Bond JE, Lamb T (2019) A new species of *Pionothele* from Gobabeb, Namibia (Araneae, Mygalomorphae, Nemesiidae). ZooKeys 851: 17–25. https://doi.org/10.3897/zookeys.851.31802

Abstract

The mygalomorph spider genus *Pionothele* Purcell, 1902 comprises two nominal species known only from South Africa. We describe here a new species, *Pionothele gobabeb* **sp. n.**, from Namibia. This new species is currently only known from a very restricted area in the Namib Desert of western Namibia.

Keywords

Biodiversity, New species, Spider taxonomy, *Pionothele*, Nemesiidae, Mygalomorphae

Introduction

The nemesiid genus *Pionothele* Purcell, 1902 is a poorly known taxon comprising only two species described from southwestern South Africa. In Zonstein's (2016) review of the genus, he redescribed and illustrated *P. straminea* Purcell, 1902 and described a second, new species *P. capensis* Zonstein, 2016. Similarities between female specimens of *Pionothele* and those in the genus *Spiroctenus* Simon 1889a suggest that some species described as the latter may be misidentified as the former (Zonstein 2016); consequently, *Pionothele* may be more widespread and diverse than is currently known. We describe herein a new species, *Pionothele gobabeb* sp. n., from the Namib Desert in

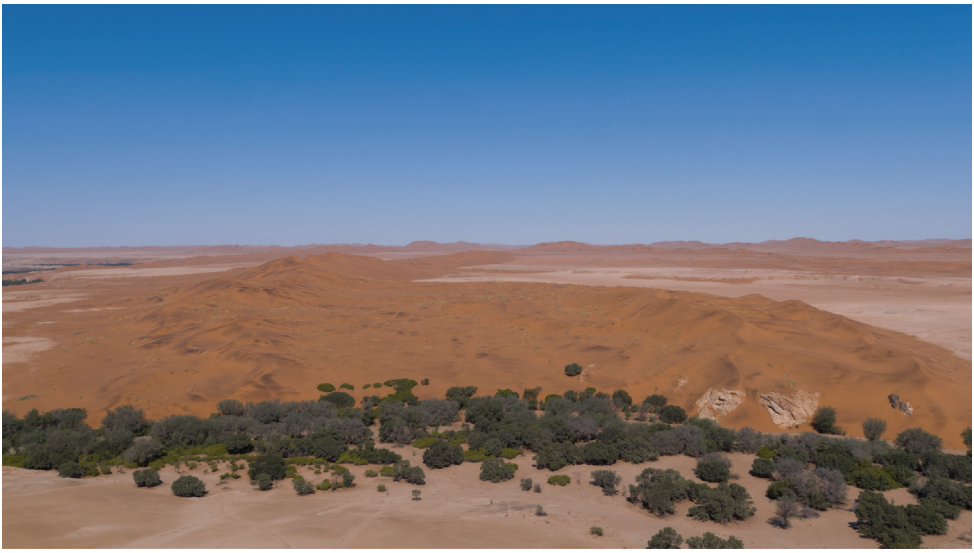

Figure 1. Aerial photograph of type locality. Kuiseb River bed in foreground (tree line); the interdune pitfall trap transect lies beyond the dunes (middle right of image).

central western Namibia; the type locality at the Gobabeb Research & Training Center is about120 km southeast of the Atlantic coastal city of Walvis Bay. The description of this new species extends the distribution of *Pionothele* significantly northward, indicating that the genus may contain considerable undescribed diversity, particularly in the intervening areas.

Habitat and ecology. Fifteen males were collected in pitfall traps after a rain event at Gobabeb; specimens were observed along interdune and gravel plain transects – two of six habitats monitored by long-term pitfall trapping (Henschel et al. 2003). Gobabeb lies adjacent to the Kuiseb River, an ephemeral drainage where the northern terminus of the Namib Sand Sea abuts the gravel plains of the Central Namib. Here dune, riparian, and gravel plain habitats occur in close proximity. Figure 1 illustrates the Gobabeb collecting locality. The single female specimen was collected from a subterranean burrow on a sandy slope. All nominal species of *Pionothele* have been collected from dune ecosystems (or close proximity thereof).

Species concept applied. This new species of *Pionothele* is delineated using a traditional morphological species concept wherein species are defined as those populations with qualitative phenotypic characteristics that differ in a discrete manner from other populations or groups.

Abbreviations, materials and methods

Institutional and quantitative morphological abbreviations used in this paper are defined as follows:

Institutional

BME	Bohart Museum of Entomology, Davis, California.
NMN	National Museum of Namibia, Windhoek, Namibia
CAS	California Academy of Sciences, San Francisco, California.

Quantitative morphological features

The following features are explicitly defined and illustrated in Bond (2012):

ANTd	number of teeth on the anterior margin of cheliceral fang furrow.
Cl, Cw	carapace length and width. Carapace length taken along the mid-line dorsal-most posterior position to the anterofrontal edge of the carapace (chelicerae are not included in length). Carapace width taken at the widest point.
AME, **ALE**, **PME**, **PLE**	anterior median, anterior lateral, posterior median, and posterior lateral eyes, respectively.
LBl, **LBw**	labium length and width taken from the longest and widest points, respectively.
PTl, **PTw**	male palpal tibia length and width.
Bl	palpal bulb length from embolus tip to the bulb base, taken in the ventral plane at its longest point.
PTLs, **TBs**	number of female prolateral patella and tibial spines leg III.
STRl, **STRw**	sternum length and width. Sternum length from the base of the labium to its most posterior point. Width taken across the widest point, usually between legs II and III.
PLS	posterior lateral spinneret
TSrd, **TSp**, **TSr**	number of tibiaI spines on the distal most retrolateral, prolateral, and midline retrolateral positions.
ITC	inferior tarsal claw

Measurement, characterization, and illustration of morphological features

Format, descriptors, and morphological features measured/examined follows closely Bond (2012). Unique voucher numbers were assigned to all specimens (alphanumeric designations beginning with NMB); these data were added to each vial and can be used to cross-reference all images, measurements, and locality data. All measurements are given in millimeters and were made with a Leica MC205 dissecting microscope equipped with the Leica Analysis Suite Software. Lengths of leg articles were taken from the mid-proximal point of the articulation to the mid-distal point of the article (*sensu* Bond 2012, figs 11–16). Leg I and Leg IV article measurements are listed in the species

description in the following order: femur, patella, tibia, metatarsus, tarsus. Carapace and leg coloration are described semi-quantitatively using Munsell® Color Charts (Windsor, NY) and are given using the color name and color notation (hue value/chroma).

Digital images of specimens were made using a BKPlus Digital Imaging System (Dun Inc.™, Richmond, VA) where images were recorded at multiple focal planes and then assembled into a single focused image using Helicon Focus (Helicon Soft, Ltd., Ukraine). The female genital region was removed from the abdominal wall and tissues dissolved using trypsin; spermathecae were examined and photographed in the manner described above. Following Bond (2012), habitus illustrations were constructed from whole body images that were bisected, copied, and reflected in Adobe Photoshop (Adobe Systems, Inc.) to produce a roughly symmetrical image; the actual raw images are available upon request from the first author. Unless otherwise stated, scale bars = 1.0 mm.

Locality data and georeferencing

Latitude and longitude for all collecting localities were recorded in the field using a Garmin Global Positioning System receiver (Garmin International Ltd., Olathe, KS) using WGS84 map datum.

Taxonomy

Family Nemesiidae Simon, 1889b

http://zoobank.org/638FB63E-DB51-4FB5-85AF-C04E81D3DBD7
urn:lsid:nmbe.ch:spiderfam:0007

Genus *Pionothele* Purcell, 1902

http://zoobank.org/4B5E1D34-582C-4259-BAE5-D5FE6AF68BEE
urn:lsid:nmbe.ch:spidergen:00127

Pionothele Purcell, 1902: 380 (type species by monotypy *Pionothele straminea* male holotype from South Africa). – Tucker 1917: 117. – Raven 1985: 93.

Pionothele gobabeb sp. n.

http://zoobank.org/87176CD8-22EB-4428-A293-80D16646EFD2
http://species-id.net/wiki/Pionothele_gobabeb
Figs 1–9

Type material. Male holotype (NMB012_001; deposited in the BME) and additional male paratypes (one each deposited in the NMN, and CAS) from the Erongo Region,

Namibia, in vicinity of Gobabeb Research & Training Center, along D1983 and Kuiseb River, – 23.56984 15.03984, coll. by J. Bond and T. Lamb 27.ix.2013.

Etymology. The specific epithet is a noun taken in apposition and is in reference to the type locality.

Diagnosis. Male and female specimens (Figs 2–4) can be differentiated from the other two described species of *Pionothele* by having posterior median eyes that are reduced in size (Fig. 7), nearly half the diameter of the posterior lateral eyes and much smaller than the anterior median eyes. Like *P. capensis* the male palpal tibia is more slender than in *P. straminea* but like the latter lacks spines (Fig. 8); leg I has more mid-retrolateral spines than *P. capensis*, with a single large mid-distal spine and only two proximal prolateral spines (Figs 5, 6). Males and females both are very light in coloration similar to that of *P. straminea* (Figs 2–4), noted by Raven (1985) as "faded," whereas the abdomen of *P. capensis* is pigmented and mottled. Spermathecal bulbs of *P. gobabeb* are moderately thin and sinuous whereas those illustrated for *P. capensis* are described as "wide and flattened" (Fig. 9); females also appear to have far fewer endite cuspules (25 vs 80).

Description of male holotype. *Specimen preparation and condition.* Specimen preserved in 70% EtOH. Pedipalp, leg I removed, stored in vial with specimen. *General coloration in alcohol.* Carapace yellowish-red 5YR 4/6. Abdomen very pale brown 10YR 7/3. *Cephalothorax.* Carapace 7.58 long, 6.80 wide, very hirsute with fine white setae, pars cephalica slightly elevated. Fringe lacks heavy setae at posterior corners. Foveal groove deep, procurved.Tubercle absent. AER, PER slightly procurved. PME much smaller in diameter than AME, half the size of PLE. Sternum moderately setose, STRl 4.41, STRw 3.40. Posterior sternal sigilla small, round not contiguous; anterior sigilla pair smaller, placed at margin. ANTd comprising 5 large teeth; posterior margin with single row of 6 smaller teeth. Palpal endites, ~21 cuspules restricted to the anteroproximal margin, labium lacking cuspules, LBw 0.92, LBl 0.67. Rastellum absent. *Abdomen.* Moderately setose; apical segment of PLS short, triangular in shape. *Legs.* Leg I: 8.92, 4.62, 5.81, 4.16, 3.14; leg IV: 8.924, 3.31, 7.38, 6.95, 3.93. Light scopulae on all tarsi. Tarsus I with thin band of ~20 trichobothria. ITC legs I–III absent, leg IV small, sharply curved. Paired claws biserially dentate. Leg I spination pattern (Figs 5, 6); TSp 4, TSr 4, TSrd 1. *Pedipalp.* PTw 0.1.18, PTl 3.77, Bl 1.86. Embolus arises sharply from bulb, long thin tapered (Fig. 8).

Variation (n = 5). Cl 6.18–7.59, 6.96±0.27; **Cw** 5.72–6.8, 6.24±0.21; **STRl** 3.56–4.41, 3.99±0.16; **STRw** 2.78–3.4, 3.1±0.12; **LBw** 0.88–1.11, 1.01±0.05; **LBl** 0.54–0.67, 0.62±0.02; **leg I**: 7.66–8.92, 8.45±0.24; 4.07–4.65, 4.39±0.13; 5.11–5.81, 5.39±0.13; 3.61–4.33, 4.03±0.12; 2.9–3.4, 3.14±0.09; **leg IV**: 7.96–8.92, 8.51±0.21; 2.75–3.72, 3.27±0.16; 5.98–7.38, 6.54±0.26; 5.5–6.98, 6.39±0.27; 3.36–3.93, 3.78±0.11; **PTl** 3.45–3.88, 3.72±0.08; **PTw** 0.88–1.18, 1.01±0.06; **Bl** 1.86–2.19, 2.02±0.07; **TSp** 2–4, 3.4±0.4; **TSr** 2–4, 3±0.32; **TSrd** 1–1, 1±0.

Description of non-type female (NMB012_001). *Specimen preparation and condition.* Specimen preserved in same manner as male holotype. *Color.* Carapace yellowish red 5YR 4/6. Abdomen light yellowish-brown 10YR 6/4. *Cephalothorax.* Carapace

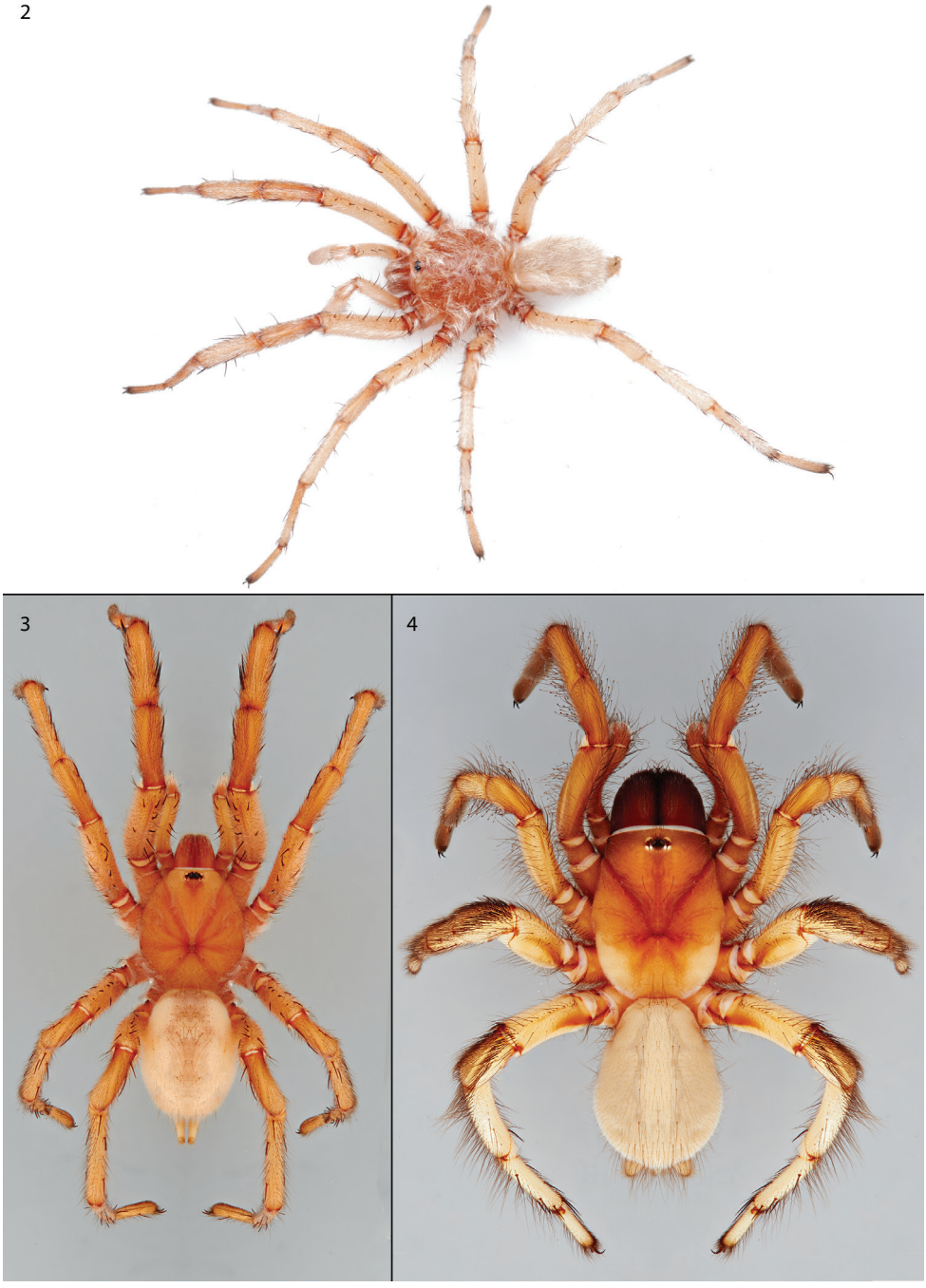

Figures 2–4. Habitus photograph and illustrations of *Pionothele gobabeb* sp. n. **2** Live male specimen **3** habitus digital illustration of male holotype specimen **4** habitus digital illustration of female.

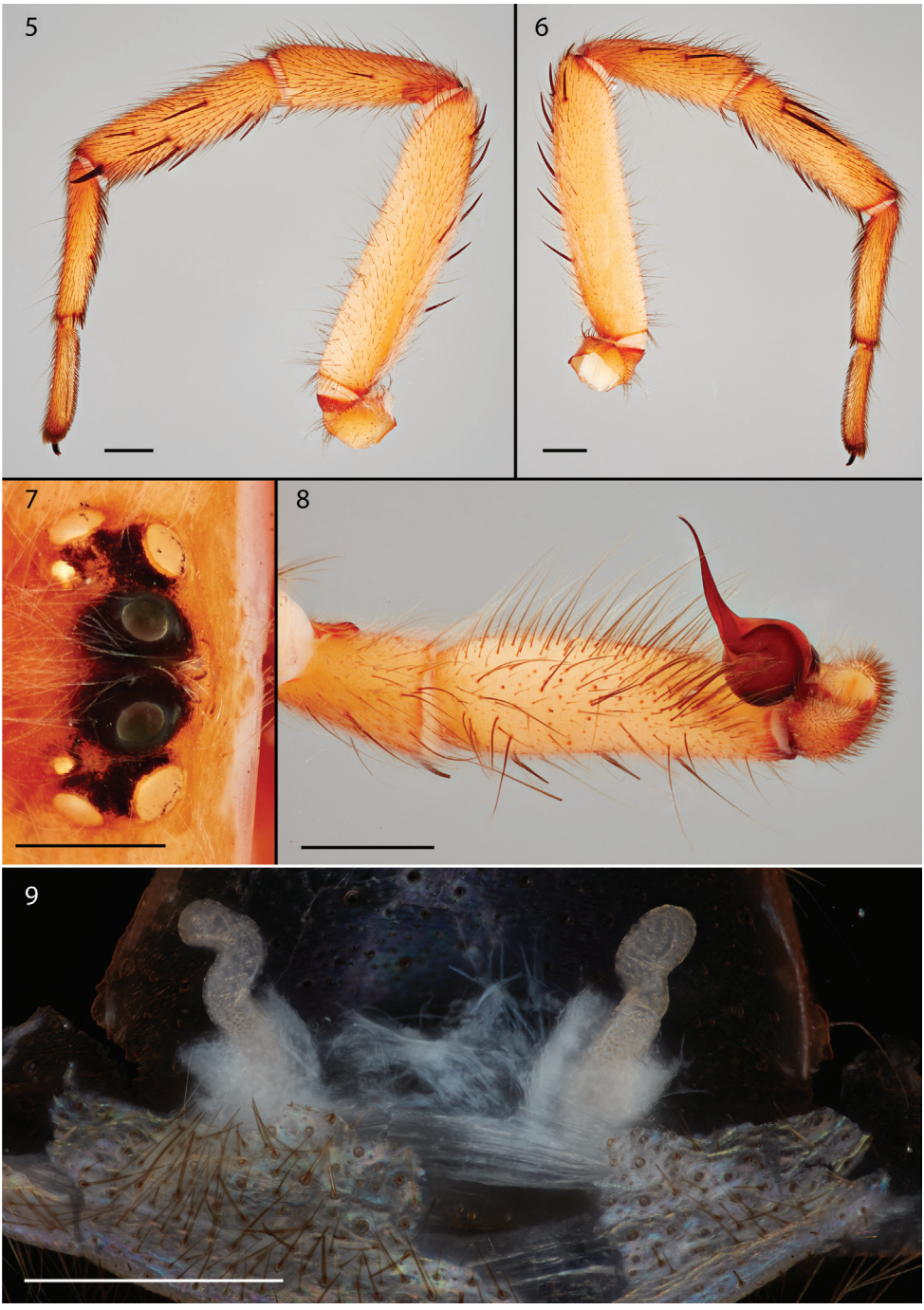

Figures 5–9. Photographic illustrations of male (holotype) and female *Pionothele gobabeb* sp. n. **5** male leg I and mating clasper, retrolateral view **6** male leg I and mating clasper, prolateral view **7** male eye group **8** male pedipalp distal segments and bulb **9** cleared spermathecae. Scale bar: 0.5 mm (**7, 8, 9**).

8.13 long, 6.08 wide, hirsute with fine white setae as in male; lacks fringe. Foveal groove deep and slightly recurved. Tubercle absent. AER very slightly procurved, PER straight to slightly recurved. AME reduced in size, smaller than PME. Sternum moderately setose, STRl 4.49, STRw 3.43. Posterior sigilla small, widely separated; medial anterior sigilla relatively small, positioned laterally. ANTd with 6 teeth with posterior margin comprising 4 teeth. Palpal endites, ~25 cuspules, restricted to the anterior margin endites; labium lacks cuspules, LBw 1.28, LBl 0.97. Rastellum absent. *Legs.* Leg I: 5.69, 3.19, 3.84, 3.09, 2.30; leg IV: 4.29, 3.58, 5.15, 4.46, 2.53. Dense scopulae tarsus/metatarsus of Legs I/II, tarsus/tibia of pedipalp. Tarsus I with ~18 trichobothria arranged in a relatively tight row. PTLs 4, TBs 2. ITC small, sharply precurved; paired claws biserially dentate. Preening combs absent. Female specimen has numerous setae on carapace and legs modified as spatulate (Fig. 4). Spermathecae bulbs thin and sinuous (Fig. 9). Apical segment of PLS short, domed.

Remarks. The female specimen described herein is from a locality some distance from where the male specimens and male holotype/paratypes were collected (formally designated as the type locality). As such we do not describe the female as a paratype so as not to confuse the type locality or the identity of the species if the female specimen is eventually discovered to be a different species – acknowledging that mygalomorph spiders are known to be highly endemic with considerable species crypsis (see Bond & Stockman 2008). Nevertheless, we are reasonably confident that these specimens are conspecifics given similarities in morphology (e.g., size of the PMEs), habitat, and an explicit morphological species concept (applied herein).

Additional material examined. Male specimens (12) collected in pitfall trips in vicinity of the type locality at Gobabeb, deposited in the BME. Single female specimen (NMB012_001) from the Erongo Region, Namibia, in vicinity of Intersection C39 and Huab River, – 20.36035 14.19186898, coll. J. Bond 19.ix.2013, deposited in BME.

Distribution. Known only from the Erongo Region, Namibia.

Acknowledgments

The authors thank Eugene Marais, Rebecca Godwin, Mark Harvey, and one anonymous reviewer for comments on earlier drafts of this manuscript. This work was supported in part by a grant from the National Geographic Society and the Evert & Marion Schlinger Foundation, University of California, Davis.

References

Bond JE (2012) Phylogenetic treatment and taxonomic revision of the trapdoor spider genus *Aptostichus* Simon (Araneae, Mygalomorphae, Euctenizidae). ZooKeys 252: 1–209 https://doi.org/10.3897/zookeys.252.3588.

Bond JE, Stockman AK (2008). An integrative method for delimiting cohesion species: finding the population-species interface in a group of Californian trapdoor spiders with extreme genetic divergence and geographic structuring. Systematic Biology 57: 628–646. https://doi.org/10.1080/10635150802302443

Henschel JR, Mtuleni V, Pallett J, Seely MK (2003) The surface-dwelling arthropod fauna of Gobabeb with a description of the long-term pitfall trapping project. Journal Namibia Scientific Society 51: 65–92.

Purcell WF (1902) New South African trap-door spiders of the family Ctenizidae in the collection of the South African Museum. Transactions of the South African Philosophical Society 11: 348–382. https://doi.org/10.1080/21560382.1900.9525972

Raven RJ (1985) The spider infraorder Mygalomorphae (Araneae): Cladistics and systematics. Bulletin of the American Museum of Natural History 182: 1–180.

Simon E (1889a) Descriptions d'espèces africaines nouvelles de la famille des Avicularíidae. Actes de la Société Linnéenne de Bordeaux 42: 405–415.

Simon E (1889b) Arachnides. In: Voyage de M. E. Simon au Venezuela (décembre 1887-avril 1888). 4e Mémoire. Annales de la Société Entomologique de France 6 9: 169–220.

Tucker RWE (1917) On some South African Avicularíidae (Arachnida). Families Migidae, Ctenizidae, Diplotheleae & Dipluridae. Annals of the South African Museum 17: 79–138.

Zonstein SL (2016) New data on the spider genus Pionothele (Araneae: Nemesiidae) with a description of a new species from South Africa. Israel Journal of Entomology 46: 31–42.

ZooKeys 851: 27–69 (2019)
doi: 10.3897/zookeys.851.31403
http://zookeys.pensoft.net

RESEARCH ARTICLE

A peer-reviewed open-access journal
ZooKeys
Launched to accelerate biodiversity research

Establishment of six new *Rhabdoblatta* species (Blattodea, Blaberidae, Epilamprinae) from China

Rong Yang[1], Zhenzhen Wang[1], Yanshuang Zhou[1], Zongqing Wang[1], Yanli Che[1]

1 *Institute of Entomology, College of Plant Protection, Southwest University, Beibei, Chongqing 400715, China*

Corresponding author: *Yanli Che* (shirleyche2000@126.com)

Academic editor: *E. Cancello* | Received 6 November 2018 | Accepted 2 April 2019 | Published 3 June 2019

http://zoobank.org/69A7925A-7684-404B-A8FC-CC15C4479C19

Citation: Yang R, Wang Z, Zhou Y, Wang Z, Che Y (2019) Establishment of six new *Rhabdoblatta* species (Blattodea, Blaberidae, Epilamprinae) from China. ZooKeys 851: 27–69. https://doi.org/10.3897/zookeys.851.31403

Abstract

This study examined 504 *Rhabdoblatta* specimens sampled from China, of which, 86 *Rhabdoblatta* specimens were used for COI sequencing. A phylogenetic analysis using the ML method and MOTUs estimations by ABGD and GMYC based on COI sequences was performed. Eighteen *Rhabdoblatta* species were identified when these data were combined with morphological data. Six new species were established among these samples, i.e., *Rh. similsinuata* **sp. n.**, *Rh. densimaculata* **sp. n.**, *Rh. gyroflexa* **sp. n.**, *Rh. chaulformis* **sp. n.**, *Rh. maculata* **sp. n.**, and *Rh. ecarinata* **sp. n.** For the first time, females including female genitalia of 14 known *Rhabdoblatta* species are described worldwide. Our study shows that combining molecular species delimitation methods with morphological data helps to delimit species and understand cockroach biodiversity.

Keywords

ABGD, female genitalia, GMYC, new species, species delimitation

Introduction

Kirby established the genus *Rhabdoblatta* in 1903 and designated *Epilampra praecipua* Walker, 1868 as the type species. After the work of many researchers (Shelford 1910; Hanitsch 1915; Bey-Bienko 1950; Princis 1967; Anisyutkin 2000, 2003, 2014), there are now more than 150 species in the largest genus *Rhabdoblatta* in Epilamprinae. Of these, 51 species are from China (Beccaloni 2014). Princis (1958) treated *Polyzosteria terranea* Walker, 1868 as the synonym of *Epilampra praecipua* Walker, 1868, but the type species of *P. terranea* was verified to be a nymph of Epilamprinae when examined by Anisyutkin (2014).

Anisyutkin (2003) divided 22 *Rhabdoblatta* species from Vietnam and Southern China into three groups based on the shape of the apical sclerite of L2D and the sclerite L3 hook: the *Rhabdoblatta klossi* group, the *Rhabdoblatta abdominalis* group and the *Rhabdoblatta elegans* group. Other members of *Rhabdoblatta* exhibit wide variation in the apical sclerite of L2D and sclerite L3 hook (Yang R, pers. obs.), indicating they can't be arranged into any of the above groups. For example, *Rh. monticola*, *Rh. ecarinata* sp. n., *Rh. saussurei,* and *Rh. densimaculata* sp. n. should be placed in the *Rh. klossi* group based on the similar shape of the sclerite L3 hook, which is short, small and without any groove. However, the sclerite L2D of both *Rh. saussurei* and *Rh. densimaculata* sp. n. has the cap-shaped apical membrane and that of the other two species does not. These two could not therefore be assigned into any one of these three species groups. It was inferred from Legendre et al. (2017) and Wang (2018) using molecular data that the genus *Rhabdoblatta* was not a monophyletic group, and consists of members with distant relationships. The genus *Rhabdoblatta* still needs further revision; it is early to make a conclusion on the division of *Rhabdoblatta* species groups.

Since Hebert et al. (2003) came up with the conception of DNA barcodes; this methodology has gained wide acceptance as a supplementary method to identify species. This technique has been proven to be highly informative and to successfully resolve problems of polymorphism, sexual dimorphism and the identification of nymphs in cockroaches (Yue et al. 2014; Che et al. 2017; Bai et al. 2018; Evangelista et al. 2013). Two species delineation methods, Automatic Barcode Gap Discovery (ABGD) (Puillandre et al. 2012) and the General Mixed Yule-coalescent (GMYC) (Pons et al. 2006; Monaghan et al. 2009; Fujisawa and Barraclough 2013), applying the single-locus data to delimit species, have become the most popular approaches in DNA barcoding studies (Yue et al. 2014; Che et al. 2017; Bai et al. 2018; Evangelista et al. 2013).

To date, *Rhabdoblatta* species were described primarily on the basis of morphological characters and DNA barcoding has not been employed to investigate the diversity of *Rhabdoblatta*. In order to infer the diversity of *Rhabdoblatta* and resolve the issues of sexual dimorphism and matching nymphs, we generated new COI sequence data from a wide variety of representatives of this group combined, combined it with published data, and performed phylogenetic analyses, including ABGD and GMYC.

Materials and methods

Morphological study

Terminologies of male genitalia mainly follow Klass (1997) and Anisyutkin (2014). Genitalia abbreviations in the figures are as follows:

R1, R2, R3, R4, R5, L2D and L3	sclerite of the male genitalia;
IX	the ninth abdominal tergite;
X	the tenth abdominal tergite;

teVIII. tergal process of the eighth abdominal tergite;
teIX. tergal process of the ninth abdominal tergite;
V.I. first valves of ovipositor;
V.II. second valves of ovipositor;
V.III. third valves of ovipositor;
gg. gonangulum of the female genitalia;
pl. sclerotized lobes of the second and third pairs of valves in the female genitalia;
a.a. anterior arch of second valvifer of the female genitalia;
bsv. basivalvula of the female genitalia;
vs. vestibular sclerite in the female genitalia;
t.s.p. transverse sclerotized plate in the female genitalia;
bd.s. brood sac of the female genitalia.

Measurements are based on specimens examined. The genital segments of the examined specimens were soaked in 10% NaOH, and then stored in glycerin for observation. All segments observed in glycerin jelly using a Motic K400 stereomicroscope. Photographs of the genitalia and body parts were taken using a Leica M205A stereomicroscope with Leica DFC Camera. Specimens were photographed using a Canon 50D with a Canon EF100mm f/2.8L Macro IS USM lens, and stacked with Helicon Focus software. All photos and images were edited with Adobe Photoshop CS5. The type materials are deposited in the Institute of Entomology, College of Plant Protection, Southwest University, Chongqing, China (SWU).

PCR amplification and sequencing

The hind legs were used for molecular studies, and the other body parts were stored in 95% ethanol as voucher specimens. In total, 86 specimens were used for COI sequencing in this study and all sequences are deposited at the National Center for Biotechnology Information GenBank (Table 1).

The extraction procedure was according to the Hipure Tissue DNA Mini Kit. Total DNA was stored at –20 °C. Primers for the amplifications are COI-F_3 (5'-CAACYAATCATAAAGANATTGGAAC-3') and COI-R_3 (5'-TAAACTTCTGGRTGACCAAARAATCA-3'). Each PCR was performed in Analytik Jena Easy Cycler with 25μL volumes using the aforementioned primers. The amplified samples were tested using agarose gel electrophoresis and sent for sequencing at BGI Technology Solutions Company Limited (BGI-Tech) (Beijing, China). All voucher specimens are deposited in the Institute of Entomology, College of Plant Protection, Southwest University, Chongqing, China.

Sequences processing and phylogenetic analyses

A total of 94 COI sequences was analyzed (86 sequences representing *Rhabdoblatta* species by our own study and six sequences downloaded from GenBank, and two

Table 1. Samples used in species delimitation: sample collection localities, specimen voucher, and GenBank accession numbers.

Species	Location	Accession Number (specimen voucher)
Rh. monticola	Jiulonghu Lake, Guangdong	MK547352 (RhabMont01)
	Dayaoshan, Guangxi	MK547353 (RhabMont02), MK547354 (RhabMont03)
	Dinghushan, Guangdong	MK547355 (RhabMont04)
Rh. ecarinata sp. n.	Yinggeling, Hainan	MK547356 (Rhabcari01)
	Diaoluoshan, Hainan	MK547357 (Rhabcari02), MK547358 (Rhabcari03)
Rh. atra	Dayaoshan, Guangxi	MK547359 (RhabAtra01), MK547361 (RhabAtra03)
	Longtan Park, Guangxi	MK547360 (RhabAtra02)
Rh. rattanakiriensis	Wuzhishan, Hainan	MK547363 (RhabRatt01), MK547362 (RhabRatt02)
	Diaoluoshan, Hainan	MK547364 (RhabRatt03)
	Jianfengling, Hainan	MK547365 (RhabRatt04)
Rh. elegans	Jinzhongshan, Guangxi	MK547366 (RhabEleg01)
	Mengla, Yunnan	MK547367 (RhabEleg02)
	Baoshan, Yunnan	MK547368 (RhabEleg05)
Rh. nigrovittata	Gulin, Sichuan	MK547371 (RhabNigr01), MK547370 (RhabNigr02)
	Nanling, Guangdong	MK547372 (RhabNigr03)
	Simianshan, Chongqing	MK547373 (RhabNigr04), MK547375 (RhabNigr08)
	Dayaoshan, Guangxi	MK547374 (RhabNigr07)
	Shengtangshan , Guangxi	MK547376 (RhabNigr09)
	Tianmushan, Zhejiang	MK547377 (RhabNigr10)
	Mangshan, Hunan	MK547369 (RhabNigr11)
	Emeishan, Sichuan	MK547379 (RhabNigr12)
	Damingshan, Guangxi	MK547378 (RhabNigr13)
Rh. simulans	Medog, Xizang	MK547437 (RhabSimu02), MK547436 (RhabSimu05)
Rh. marginata	Jianfengling, Hainan	MK547381 (RhabMarg01), MK547380 (RhabMarg02)
	Wuzhishan, Hainan	MK547382 (RhabMarg03), MK547390 (RhabMarg11)
	Limushan, Hainan	MK547383 (RhabMarg04), MK547384 (RhabMarg05)
	Wuzhishan Scenic, Guangdong	MK547385 (RhabMarg06), MK547386 (RhabMarg07)
	Maogan, Hainan	MK547387 (RhabMarg08), MK547388 (RhabMarg09)
	Shengtangshan, Guangxi	MK547389 (RhabMarg10)
	Bawangling, Hainan	MK547391 (RhabMarg12)
Rh. sinuata	Butterfly Valley, Yunnan	MK547392 (RhabSinu01), MK547393 (RhabSinu02)
	Daheishan, Sichuan	MK547394 (RhabSinu03), MK547395 (RhabSinu04)
Rh. mascifera	Mengla, Yunnan	MK547407 (RhabMasc01)
	Menglun, Yunnan	MK547408 (RhabMasc02)
Rh. incisa	Ailaoshanshan, Yunnan	MK547399 (RhabInci01), MK547400 (RhabInci03)
	Daweishan, Yunnan	MK547401 (RhabInci04)
Rh. krasnovi	Maandi Village, Yunnan	MK547409 (RhabKras01), MK547411 (RhabKras02), MK547410 (RhabKras03), MK547412 (RhabKras04)
	Daweishan, Yunnan	MK547413 (RhabKras05)
Rh. melancholica	Diaoluoshan, Hainan	MK547425 (RhabMela01), MK547422 (RhabMela12), MK547421 (RhabMela13)
	Dayaoshan, Guangxi	MK547426 (RhabMela02)
	Dabieshan, Hubei	MK547427 (RhabMela03), MK547428 (RhabMela04)
	Huangshan, Anhui	MK547429 (RhabMela05)
	Kuankuoshui, Guizhou	MK547431 (RhabMela06), MK547430 (RhabMela07)
	Simianshan, Chongqing	MK547417 (RhabMela08), MK547418 (RhabMela09)
	Qingchengshan, Sichuan	MK547419 (RhabMela10), MK547420 (RhabMela11)
	Tianmushan, Zhejiang	MK547423 (RhabMela14), MK547424 (RhabMela15)
	Jinxiu, Guagnxi	MK547432 (RhabMela17)
Rh. bicolor	Jiangshan, Zhejiang	MK547414 (RhabBico01), MK547415 (RhabBico02)
	Huangshan, Anhui	MK547416 (RhabBico03)

Species	Location	Accession Number (specimen voucher)
Rh. saussurei	Huanjing, Guangxi	MK547434 (RhabSaus02)
	Mengla, Yunan	MK547433 (RhabSaus01)
Rh. similsinuata sp. n.	Ailaoshan, Yunnan	MK547397 (RhabSimi01), MK547396 (RhabSimi02), MK547398 (RhabSimi03)
Rh. densimaculata sp. n.	Jiguanshan, Sichuan	MK547402 (Rhabdens01)
	Ya'an, Sichuan	MK547403 (Rhabdens02), MK547404 (Rhabdens03)
	Ailaoshan, Yunnan	MK547405 (Rhabdens04)
	Medog, Xizang	MK547406 (RhabDens05)
Rh. maculata sp. n.	Leigongshan, Guizhou	MK547435 (RhabMacu)
Rh. sp. 3		MF804773 (RhabSp)
Rh. atra		KF640066 (RhabAtra)
Rh. bielawskii		KF640067 (RhabBiel)
Rh. sp. 1		KY497676 (RhabBl140)
Rh. sp. 2		KY497678 (RhabBl148)
Rh. sp. 4		KY497684 (RhabBl7)
Mantis religiosa		KR148854
		KM529415

sequences representing the mantis outgroup downloaded from GenBank) (Table 1). Wang (2018) tried to use Blattellidae as outgroup, because Blattellidae is close to Blaberidae; the result is that Blattellidae inserts into the ingroup Blaberidae, and the topology is disorderly. Therefore, we chose the mantis as outgroup. All COI sequences were aligned using MEGA 7.0 and adjusted visually after translation into amino acid sequences. Intraspecific and interspecific genetic divergence values were quantified based on the Kimura 2-parameter (K2P) distance model (Kimura 1980), and variance was estimated by using the bootstrap method with 1000 bootstrap replications in MEGA 7.0 (Kumar et al. 2016). Maximum Likelihood (ML) analysis was implemented in RAxML 7.3.0 (Stamatakis et al. 2008) using GTRGAMMA model with 1000 bootstrap replicates.

We performed two molecular species delimitation methods, the Automatic Barcode Gap Discovery (ABGD: Puillandre et al. 2012) and the General Mixed Yule-coalescent (GMYC: Pons et al. 2006), in order to estimate the number of molecular operational taxonomic units (MOTUs) from the genus *Rhabdoblatta*. Automatic Barcode Gap Discovery (ABGD) was available at the web interface (http://wwwabi.snv.jussieu.fr/ public/abgd/) and was used as a simple, quick and efficient method with the default settings by Jukes-Cantor (JC69) and p distance model with a relative gap width (X = 1.0), it used the 92 COI sequences (excluding outgroups). The GMYC method requires a fully-resolved ultrametric tree for the analysis to define species. Time-resolved gene trees were inferred in BEAST 1.8.1 (Drummond and Rambaut 2007) using the best models from PartitionFinder V1.1.1 (Lanfear et al. 2012). The best-fitting models were as follows: COI_pos1, TrN+G; COI_pos2, TrN+G; COI_pos3, TrN+I. The following settings were used: rate variation was modeled among branches using a strict clock model with the mean clock rate fixed to 1 and the Birth-Death speciation was used as a tree prior. We then selected the GMYC method to the ultrametric gene tree using the SPLITS package (Ezard et al. 2009) in R (R Core

Team 2013). The species delimited were compared to a one species null model using a likelihood ratio test. It used 70 COI sequences (the exact same sequence is left with only one) and excluding outgroups.

Results

Morphological delimitation of *Rhabdoblatta*

On the basis of morphological characters including male genitalia, we were able to identify 20 morphospecies of *Rhabdoblatta* among the 504 samples from China that we examined. Herein six new species, *Rh. similsinuata* sp. n., *Rh. densimaculata* sp. n., *Rh. gyroflexa* sp. n., *Rh. chaulformis* sp. n., *Rh. maculata* sp. n., and *Rh. ecarinata* sp. n. are established only according to morphological characters including male genitalia (Figs 2–7). Species descriptions are provided below.

Phylogenetic analysis based on COI and MOTUs estimation

In this study, we acquired 86 *Rhabdoblatta* COI sequences representing 18 *Rhabdoblatta* morphospecies (other two morphospecies without molecular data), 83 of which, length excluding primers, were 658bp, the remaining were 619bp, 621bp and 634bp respectively. The COI region we sequenced had a relatively high AT content (66.3%) with an average nucleotide composition of A = 30.1%, T = 36.2%, C = 17.6%, and G = 16.1%. Sequence analysis revealed that 266 (40.30%) sites were variable, of which 243 (36.81%) sites were parsimoniously informative. ML analysis revealed that clades from the same morphospecies, including females and nymphs, constituted monophyletic groups (Figure 1).

We used two molecular species delimitation methods (ABGD, GMYC) in our study to delimit *Rhabdoblatta* samples. These two methods have yielded significantly different results using COI data; ABGD produced 46 MOTUs and GMYC 45 MOTUs respectively (Figure 1). ABGD analysis for MOTUs detection was estimated with JC69 and P = 0.001, and the likelihoods of the null and GMYC models from COI analysis were 264.71 and 281.99 respectively. The six sequences (downloaded from GenBank) provided six MOTUs by ABGD and five MOTUs by GMYC: RhabAtra and data of this study (RhabAtra01, RhabAtra02, RhabAtra03) resulted in one MOTU in GMYC, while two MOTUs in ABGD (RhabAtra were recovered as a single MOTU); the remaining five sequences were recovered as single MOTU under both methods. The same MOTUs were detected for remaining data (12 morphospecies) in both ABGD and GMYC analysis: *Rh. similsinuata* sp. n., *Rh. sinuata*, *Rh. atra*, *Rh. mascifera*, *Rh. simulans*, *Rh. bicolor*, *Rh. krasnovi*, *Rh. incisa*, *Rh. densimaculata* sp. n., *Rh. maculata* sp. n., *Rh. monticola*, and *Rh. saussurei*, of which, eight morphospecies were recovered as single MOTU under both methods; however, there were wide discrepancies of MOTU in the remaining six morphospecies (Figure 1), for example, seven MOTUs in ABGD and four MOTUs in GMYC

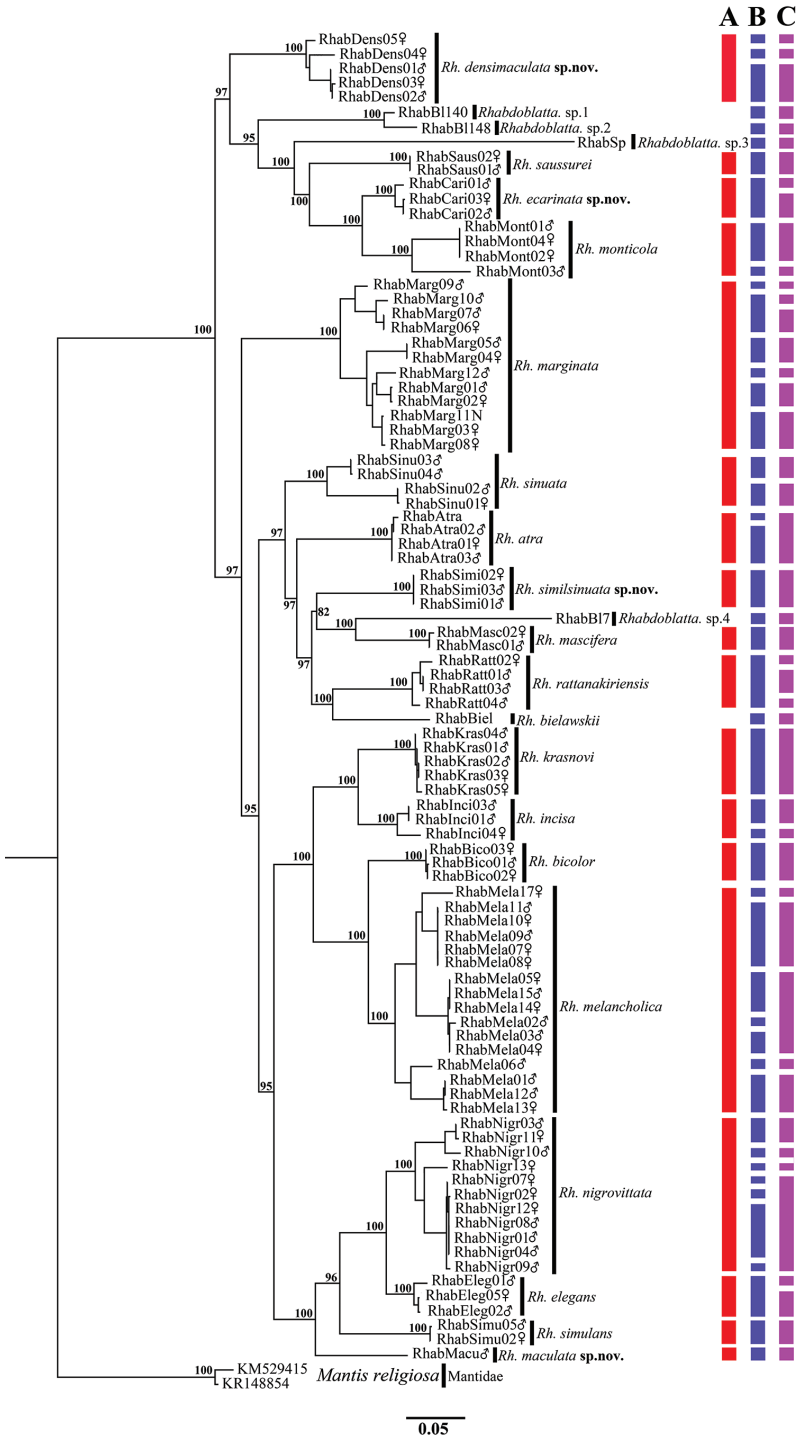

Figure 1. Maximum likelihood (ML) tree derived from COI gene analysis following GTR GAMMA model with 1000 bootstrap replicates. In red, referring to the morphospecies; in blue, referring to MOTUs in ABGD; in purple, referring to MOTUs in GMYC.

Table 2. Pairwise genetic divergence and the variance of the underlying distribution of distances calculated by using K2P model and bootstrap method respectively using cytochrome oxidase subunit I (COI) gene sequences in MEGA. Bold text denotes the variance of the underlying distribution of distances and black denotes pairwise genetic divergence.

Species	1	2	3	4	5	6	7	8	9	10	11	12	13	14	15	16	17	18
Rh. monticola		**0.011**	**0.016**	**0.015**	**0.016**	**0.016**	**0.014**	**0.014**	**0.015**	**0.015**	**0.014**	**0.015**	**0.015**	**0.016**	**0.015**	**0.014**	**0.017**	**0.017**
Rh. ecarinata sp. n.	0.097		**0.015**	**0.015**	**0.016**	**0.017**	**0.014**	**0.013**	**0.016**	**0.016**	**0.014**	**0.015**	**0.016**	**0.017**	**0.015**	**0.014**	**0.016**	**0.018**
Rh. atra	0.178	0.147		**0.013**	**0.015**	**0.015**	**0.014**	**0.013**	**0.014**	**0.013**	**0.015**	**0.014**	**0.014**	**0.015**	**0.014**	**0.015**	**0.015**	**0.017**
Rh. rattanakiriensis	0.172	0.166	0.131		**0.015**	**0.015**	**0.014**	**0.012**	**0.013**	**0.014**	**0.015**	**0.014**	**0.015**	**0.014**	**0.013**	**0.015**	**0.015**	**0.016**
Rh. elegans	0.183	0.180	0.151	0.163		**0.010**	**0.013**	**0.014**	**0.015**	**0.014**	**0.015**	**0.015**	**0.015**	**0.017**	**0.015**	**0.016**	**0.014**	**0.014**
Rh. nigrovittata	0.198	0.191	0.172	0.162	0.082		**0.014**	**0.014**	**0.015**	**0.015**	**0.014**	**0.016**	**0.016**	**0.017**	**0.015**	**0.016**	**0.014**	**0.013**
Rh. marginata	0.173	0.151	0.145	0.162	0.150	0.164		**0.013**	**0.014**	**0.013**	**0.014**	**0.014**	**0.015**	**0.015**	**0.014**	**0.014**	**0.014**	**0.015**
Rh. sinuata	0.176	0.138	0.132	0.127	0.149	0.146	0.146		**0.013**	**0.013**	**0.014**	**0.014**	**0.013**	**0.015**	**0.013**	**0.014**	**0.014**	**0.016**
Rh. similsinuata sp. n.	0.164	0.165	0.138	0.118	0.144	0.153	0.157	0.127		**0.014**	**0.015**	**0.014**	**0.015**	**0.016**	**0.013**	**0.014**	**0.015**	**0.015**
Rh. incisa	0.169	0.162	0.130	0.153	0.143	0.164	0.151	0.130	0.137		**0.014**	**0.015**	**0.010**	**0.015**	**0.012**	**0.015**	**0.016**	**0.014**
Rh. densimaculata sp. n.	0.166	0.134	0.148	0.166	0.161	0.159	0.157	0.145	0.156	0.139		**0.015**	**0.015**	**0.015**	**0.014**	**0.015**	**0.016**	**0.015**
Rh. mascifera	0.187	0.163	0.127	0.143	0.151	0.167	0.164	0.136	0.131	0.152	0.160		**0.015**	**0.016**	**0.015**	**0.015**	**0.015**	**0.018**
Rh. krasnovi	0.172	0.160	0.152	0.160	0.163	0.171	0.171	0.135	0.136	0.085	0.149	0.143		**0.015**	**0.012**	**0.016**	**0.016**	**0.017**
Rh. bicolor	0.169	0.173	0.165	0.157	0.171	0.179	0.159	0.154	0.165	0.142	0.152	0.166	0.147		**0.010**	**0.017**	**0.016**	**0.018**
Rh. melancholica	0.181	0.164	0.165	0.158	0.166	0.173	0.166	0.158	0.144	0.123	0.154	0.164	0.126	0.100		**0.016**	**0.015**	**0.015**
Rh. saussurei	0.140	0.111	0.141	0.169	0.168	0.177	0.152	0.161	0.149	0.160	0.140	0.173	0.164	0.178	0.182		**0.016**	**0.017**
Rh. maculata sp. n.	0.183	0.169	0.162	0.167	0.135	0.143	0.157	0.151	0.161	0.159	0.157	0.158	0.161	0.164	0.165	0.178		**0.015**
Rh. simulans	0.189	0.191	0.170	0.174	0.117	0.118	0.170	0.167	0.145	0.149	0.162	0.179	0.168	0.181	0.166	0.183	0.133	

for *Rh. nigrovittata*, and seven MOTUs in ABGD and five MOTUs in GMYC for *Rh. melancholica*.

We observed the largest mean K2P intramorphospecies genetic distance was 5% (*Rh. marginata*). The interspecific genetic distance of *Rhabdoblatta* ranged from 8.2 to 19.8% (Table 2).

Establishment of six new species

On the basis of morphological characters combined with the molecular data, we were able to identify 20 *Rhabdoblatta* species including six new species among the 504 samples that we examined, i.e., *Rh. similsinuata* sp. n., *Rh. densimaculata* sp. n., *Rh. gyroflexa* sp. n., *Rh. chaulformis* sp. n., *Rh. maculata* sp. n., and *Rh. ecarinata* sp. n.

We attempted to assign 20 *Rhabdoblatta* species into three species groups suggested by Anisyutkin (2003) mainly based on the shape of the apical sclerite of L2D and sclerite L3 hook. Finally we found that ten *Rhabdoblatta* species (*Rh. similsinuata* sp. n., *Rh. densimaculata* sp. n., *Rh. gyroflexa* sp. n., *Rh. marginata*, *Rh. sinuata*, *Rh. incisa*, *Rh. krasnovi*, *Rh. melancholica*, *Rh. bicolor* and *Rh. saussurei*) could not be assigned into any one of the three species groups only using the morphological data listed above. So we didn't adopt the taxonomic system of species groups in this study.

Diagnosis of the genus

Vertex slightly exposed; pronotum subelliptical and the widest part in the middle, anterior and lateral margins rounded, middle of hind margin convex; tegmina and wings of male fully developed extending well beyond the end of the abdomen, the apex of the tegmina arc-shaped; anteroventral margin of front femur type B; the metatarsus of hind leg equal length to sum of left tarsi, inner margin with two rows of small spines; the pretarsus with arolium, claws symmetrical and unspecialized; the shape of subgenital plate, apical sclerite of L2D and sclerite L3 hook variously.

Remarks. Male genitalia of the species *Rh. similsinuata* sp. n. is very similar to *Rh. sinuata* Bey-Bienko, 1958 and other characters match with generic diagnosis. However, the species shows sexual dimorphism, in which the male macropterous and the female brachypterous.

Rhabdoblatta similsinuata sp. n.

http://zoobank.org/0B01CA97-0236-45C3-9C03-A09B459A3CB1
Figure 2A–P

Diagnosis. This species is similar to *Rh. sinuata* Bey-Bienko, 1958 in the male genitalia, only with minor differences as follows: hind margin of subgenital plate with an

inverted V-shaped concavity at middle, and left lobe slightly processed (with an inverted U-shaped concavity in the middle and left lobe not processed). But this species can easily be differentiated from *Rh. sinuata* in the following characteristics: 1) existence of sexual dimorphism： male macropterous, but female brachypterous (tegmina and wings of male and female fully developed extending well beyond the end of the abdomen in the latter); 2) abdominal sterna with obviously longitudinal bands in the middle (bands absent in the latter).

Measurements (mm). Male, pronotum: length × width 4.3–4.7 × 6.1–6.5, tegmen length: 25.2–25.6, overall length: 29.5–30.3; female, pronotum: length × width 5.2–5.5 × 7.6–8.0, tegmen length: 12.6–13.2, overall length: 21.9–22.4.

Description. Male. Body pale yellow (Figure 2A). Eyes blackish brown. Ocelli yellowish white. Antennae dark brown. Vertex, frons and basal of clypeus dark brown, the other part yellow (Figure 2B). Pronotum yellow, with many near round small or a few big black spots on the surface (Figure 2E). Tegmina pale yellow, covered with spots similar to those on pronotum, R and M very close to each other basally (Figure 2G). Wings with costal field, radial field and mediocubital field pale yellow and anal field pale gray, whose veins brown (Figure 2H). Legs yellow. The middle of 3rd–6th abdominal sterna with dark brown longitudinal bands forming an inverted triangle, with dispersedly brown spots on the surface of the segments. Cerci brown, apical segment blackish brown (Figure 2B).

Vertex slightly exposed (Figure 2B). Distance between eyes slightly longer than interocular space (Figure 2B). Pronotum subelliptical, the widest part in the middle, anterior and lateral margins rounded, middle of hind margin convex (Figure 2E). Tegmina and wings fully developed extending well beyond the end of the abdomen, the apex of the tegmina arc-shaped and veins distinct (Figure 2A, B, G, H). Anteroventral margin of front femur type B_1. The inner margin of the metatarsus of hind leg with two rows small spines. Tarsal pulvilli present on the apex of 1st-4th tarsomeres, small and spiked, 1st–3rd with spines around. The pretarsus with arolium, claws symmetrical and unspecialized (Figure 2B, F).

Male genitalia. Supra-anal plate symmetrical, subtrapezoid, the middle of the hind margin concave. Right and left paraprocts unsymmetrical, the right with a big, finger-shaped bulge, the end bent (Figure 2K). Subgenital plate with distal part unsymmetrical, with an inverted V-shaped concave in the middle. The base of the inner plate bifurcated and symmetrical. Styli long and flat, whose length approximately 1/3 of interstyli space (Figure 2L). Left phallomere with sclerite R1T apex nearly rectangle, end of R2 rounded, R3 and R5 interlinked, the base of R3 turned over, and without bifurcation at apex, R4 nearly rectangular and existing independently (Figure 2M). The basal sclerite of L2D slender and rod-shaped, with base slightly intumescent; apical sclerite short and small, the surface on the apical membrane with fine bristles, cap-shaped (Figure 2N). Sclerite L3 long, hook deeply bent and with semicircular carina, margin smooth and with a process; inner margin with tooth-shaped convexity at apex (Figure 2O).

Female. Female brachypterous. Tegmina and wings extending to hind margin of 5th abdominal tergum. Cerci yellow, apical segment blackish brown. Abdominal sterna with longitudinal broad band in the middle, and finger-like spots along the hind margin, and brown spots dispersed on the surface of the segments (Figure 2C, D, I, J).

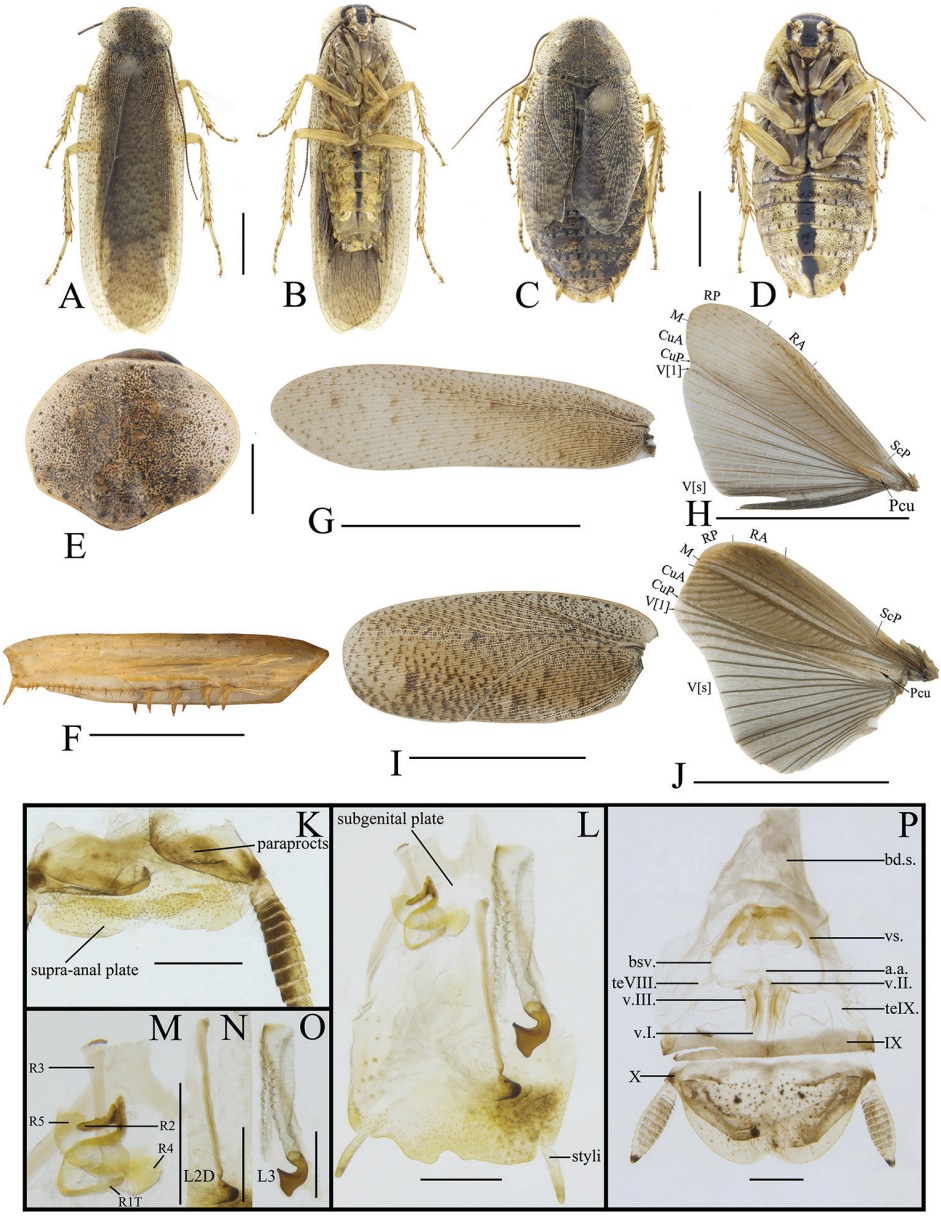

Figure 2. A, B, E–H, K–O *Rhabdoblatta similsinuata* sp. n., male **C, D, I, J, P** female. **A** Holotype, dorsal view **B** holotype, ventral view **C** paratype, dorsal view **D** paratype, ventral view **E** pronotum, dorsal view **F** front femur, ventral view **G** tegmen **H** wings **I** tegmen **J** wings **K** supra-anal plate, dorsal view **L** subgenital plate, ventral view **M** left phallomere, ventral view **N** median phallomere, ventral view **O** right phallomere, ventral view **P** female genitalia. Scale bars: 1.0 cm (**G, H**); 5.0 mm (**A–D, I, J**); 1.0 mm (**E, F, K–P**).

Female genitalia. Weakly sclerotized. Ovipositor back to brood sac. Tergal process of the eighth abdominal tergite obviously vestigial, getting narrower from the base to the end, length approximately half of tergal process of the ninth abdominal tergite.

Tergal process of the ninth abdominal tergite slightly wider, connected to the ninth tergum. First valves of ovipositor with narrow and fine membrane at the apex, inner margin with clearly fine and long bristles. Second valves of ovipositor tube-shaped, completely covered by the first valves of ovipositor. Third valves of ovipositor slightly wider, length shorter than the first valves of ovipositor. Gonangulum and sclerotized lobes of the second and third pairs of valves absent. Anterior arch of second valvifer slender. Basivalvula with semicircular arms, the middle sclerite incompletely separated, semicircular. Vestibular sclerite weakly sclerotized, the middle sclerite slightly membranous. Transverse sclerotized plate absent. Brood sac membranous and without sclerotized section (Figure 2P).

Remarks. The status of *Rhabdoblatta similsinuata* sp. n. is proven to be valid according to our morphological and molecular data (the interspecific genetic distance between this species and *Rh. sinuata*: 0.120).

Etymology. Latin word *similis* means similar, referring to the male genitalia being similar to *Rh. sinuata* Bey-Bienko, 1958.

Type material. *Holotype*: male, Yunnan Prov., Xinping County, Ailao Mountain, Yaonan Village, 11–13-V-2016, Lu Qiu & Zhi-wei Qiu leg. *Paratype*: 11 males and 17 females, same data as holotype; 1 female, Yunnan Prov., Xinping County, Ailao Mountain, Yaonan Village, 23-V-2018, Lu Qiu, Wen-bo Deng & Zhi-wei Dong leg. (all in SWU).

Distribution. China (Yunnan).

Rhabdoblatta densimaculata sp. n.

http://zoobank.org/0DA63989-4C49-46B1-A376-C0D1505942F1
Figure 3A–P

Diagnosis. This species is similar to *Rh. incisa* Bey-Bienko, 1969 in the spots of tegmina. But this species can easily be differentiated from *Rh. incisa* in the following characteristics: 1) body brown, but dark brown in the latter; 2) pronotum yellow, black small spots dispersed on the surface (pronotum dark brown, lateral borders with pale spots in the latter); and 3) sclerite L3 long, hook short and small, and without carina (hook deeply bent and with carina in the latter).

Measurements (mm). Male, pronotum: length × width 6.1–6.5 × 7.3–7.8, tegmen length: 31.8–32.8, overall length: 37.9–39.3; female, pronotum: length × width 7.8 × 9.0–9.3, tegmen length: 31.2–32.3, overall length: 39.0–40.1.

Description. Male. Body dark brown (Figure 3A). Vertex, frons, and eyes black. The 1st–12th segments of antennae dark brown, the others brown. Ocelli and apex of clypeus yellow. Labrum, labial palpi, and maxillary palpi brown (Figure 3B). Pronotum dark brown, lateral borders with pale spots (Figure 3E). Tegmina dark brown, front borders pale brown, with dark brown spots. Wings with costal field and radial field dark brown, mediocubital field brown and anal field gray, with veins obvious and brown (Figure 3G, H). Legs dark brown. Abdominal sterna yellow, 4th–6th segments with dark brown spots. Cerci dark brown (Figure 3B).

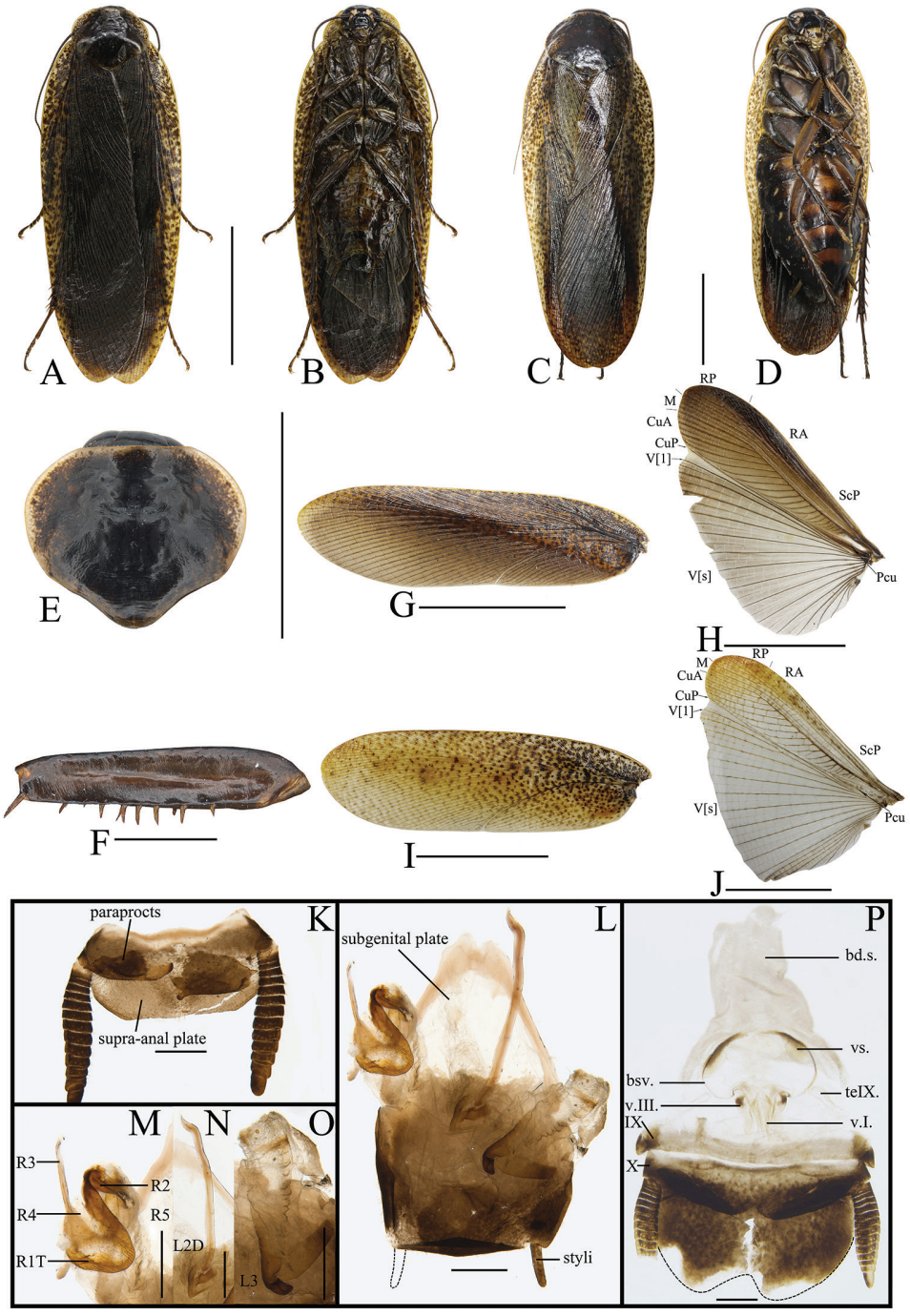

Figure 3. A, B, E–H, K–O *Rhabdoblatta densimaculata* sp. n., male **C, D, I, J, P** female. **A** Holotype, dorsal view **B** holotype, ventral view **C** paratype, dorsal view **D** paratype, ventral view **E** pronotum, dorsal view **F** front femur, ventral view **G** tegmen **H** wings **I** tegmen **J** wings **K** supra-anal plate, dorsal view **L** subgenital plate, ventral view **M** left phallomere, ventral view **N** median phallomere, ventral view **O** right phallomere, ventral view **P** female genitalia. Scale bars: 1.0 cm (**A–D, G–J**); 5.0 mm (**E**); 1.0 mm (**F, K–P**).

Vertex slightly exposed (Figure 3B). Distance between eyes slightly wider than interocular space, the length approximately 2/3 of the space of antennal sockets. The length of third maxillary palpus same as the fifth, both slightly longer than the fourth (Figure 3B). Pronotum subelliptical, the widest part in the middle, anterior and lateral margins rounded, middle of hind margin convex (Figure 3E). Tegmina and wings fully developed extending well beyond the end of the abdomen, the apex of the tegmina arc-shaped and veins distinct (Figure 3A, B, G, H). Anteroventral margin of front femur type B_1 (Figure 3F). The inner margin of the metatarsus of hind leg with two rows small spines. Tarsal pulvilli present on the apex of 1^{st}–4^{th} tarsomeres. The pretarsus with arolium, claws symmetrical and unspecialized (Figure 3B).

Male genitalia. Supra-anal plate subtrapezoid, lateral margins arc-shaped. Right and left paraprocts unsymmetrical, shape similar to other members in the genus (Figure 3K). Subgenital plate with hind margin curved upturn. The base of the inner plate bifurcated. Styli flat, whose length ca. 1/3 of interstyli space (Figure 3L). Left phallomere with bristles, end of sclerite R2 rounded, R3 and R5 interlinked, base of R3 turned over and without bifurcation at apex, and R4 weakly sclerotized and existing independently (Figure 3M). L2D slender, basal part sharp and apex straight; apical sclerite nearly rectangle, the membrane with fine bristles, simple cap-shaped (Figure 3N). Sclerite L3 long, hook short and small, outer-lateral margin arc-shaped, smooth and without carina; inner margin with a tooth-shaped convexity at apex (Figure 3O).

Female. Female similar to male but slightly bigger. Ocelli, apex of clypeus and labrum yellow. Color of the body and spots similar to male (Figure 3C, D, I, J).

Female genitalia. Weakly sclerotized. Ovipositor back to brood sac. Tergal process of the eighth and ninth abdominal tergite obviously vestigial, membranous. First valves of ovipositor with apex membranous, inner margin with fine bristles. Second valves of ovipositor fine, tube-shaped, completely covered by the first valves of ovipositor. Third valves of ovipositor slightly wider and flat, length shorter than the first valves of ovipositor. Gonangulum and sclerotized lobes of the second and third pairs of valves absent. Anterior arch of second valvifer obviously vestigial. Basivalvula weakly sclerotized and with semicircular arms, the mid sclerite separate. Vestibular sclerite wide and weakly sclerotized. Transverse sclerotized plate disappeared. Brood sac membranous and without sclerotized section (Figure 3P).

Etymology. This species name is derived from the Latin words *densus* and *maculatus*, referring to the tegmina having dense spots.

Type material. *Holotype*: male, Sichuan Prov., Ya'an City, Yingjing County, Longcanggou National Forest Park, 19-VI-2016, Jian-yue Qiu leg. *Paratype*: 6 males and 2 females, same data as holotype; 2 males, Sichuan Prov., Chengdu City, Congzhou, Jiguan Mountain, Shaoyaogou, 28-V-2016, Fu-ming Shi leg.; 1 male, Sichuan Prov., Chengdu City, Congzhou, Jiguanshan Township, Anzihe Nature Reserve, 1500m, VI-2015, by light trap, Chao Zhou leg.; 1 male, Sichuan Prov., Chengdu City, Congzhou, Jiguanshan Township, Anzihe Nature Reserve, 1450 m, 2-VI-2016, by light trap, Chao Zhou leg.; 1 female, Yunnan Prov., Dali City, Yunlong County, Mt. Zhiben, 2250 m, 1-VI-1981, Su-bai Liao leg.; 1 female, Yunnan Prov., Xinping County, Ailao

Mountain, Yaonan Village, 11-V-2016, Lu Qiu & Zhi-wei Qiu leg.; 1 male, Yunnan Prov., Tengchong City, Diantan Town, 3–15-VII-2016, light trap, Gui-qiang Huang leg.; 4 females, Yunnan Prov., Gongshan County, Dulongjiang Township, 1400 m, 22–28-VII-2015, Chao Wu leg.; 2 females, Xizang Auto. Regi., Medog County, 80k (Bolonggong), 20–24-VII-2012, Chao Wu leg.; 1 female, Xizang Auto. Regi., Medog County, Beibeng Township, Gelin Village, 12-VII-2016, Hao Xu et Jian-yue Qiu leg. (all in SWU).

Distribution. China (Sichuan, Yunnan, Xizang).

Rhabdoblatta gyroflexa sp. n.

http://zoobank.org/4000A036-211B-4D8E-B02B-FEE2C5C97F21
Figure 4A–K

Diagnosis. This species is similar to *Rh. elegans* Anisyutkin, 2000 in body color, but can be differentiated by the following characters: 1) pronotum reddish yellow with a subtrapezoid dark brown marking at disc (pronotum reddish brown without any marking at disc in the latter); 2) body large (the latter with body medium); and 3) stripes absent in the abdomen (long and black stripes at the hind margin of each segment of the abdominal sterna in the latter); 4) apical part of sclerite R3 of left phallomere turned over (none in the latter).

Measurements (mm). Male, pronotum: length × width 7.5–8.0 × 10.0–10.5, tegmen length: 39.5–42.0, overall length: 44.5–46.0.

Description. Male. Body reddish brown (Figure 4A). Vertex, antennae and eyes dark brown. Ocelli yellowish brown. Frons reddish brown, but space between ocelli dark brown. Clypeus yellowish brown. Mandible and labrum yellowish brown. The first and second of maxillary palpi yellowish brown, the others dark brown (Figure 4B). Pronotum reddish yellow, with a subtrapezoid dark brown marking at disc (Figure 4C). Tegmina with mediocubital field brown, the other field reddish brown. Wings with costal field, radial field, and mediocubital field brown and anal field yellowish brown with veins brown (Figure 4E, F). Coxa, trochanter and femur yellowish brown; the distal part of femur, tibia, tarsomere dark brown. Abdomen brown, abdominal sterna with blackish brown spots along the lateral margins, and with yellow stripes at the lateral and hind margins of the segments. Cerci dark brown (Figure 4B).

Vertex slightly exposed (Figure 4B). Eyes wide, the hind margin extending to the base of the mandible (Figure 4B). Pronotum subelliptical, the widest part in the middle, anterior and lateral margins rounded, middle of hind margin distinctly convex (Figure 4C). Tegmina and wings fully developed extending well beyond the end of the abdomen, the apex of the tegmina and wings with a small convexity and veins clearly (Figure 4A, B, E, F). Anteroventral margin of front femur type B_2 (Figure 4D). The metatarsus of hind leg equal length to sum of left tarsi, inner margin with two rows of small spines. Tarsal pulvilli present on the apex of 1^{st}–4^{th} tarsomeres. The pretarsus with arolium, claws symmetrical and unspecialized (Figure 4B).

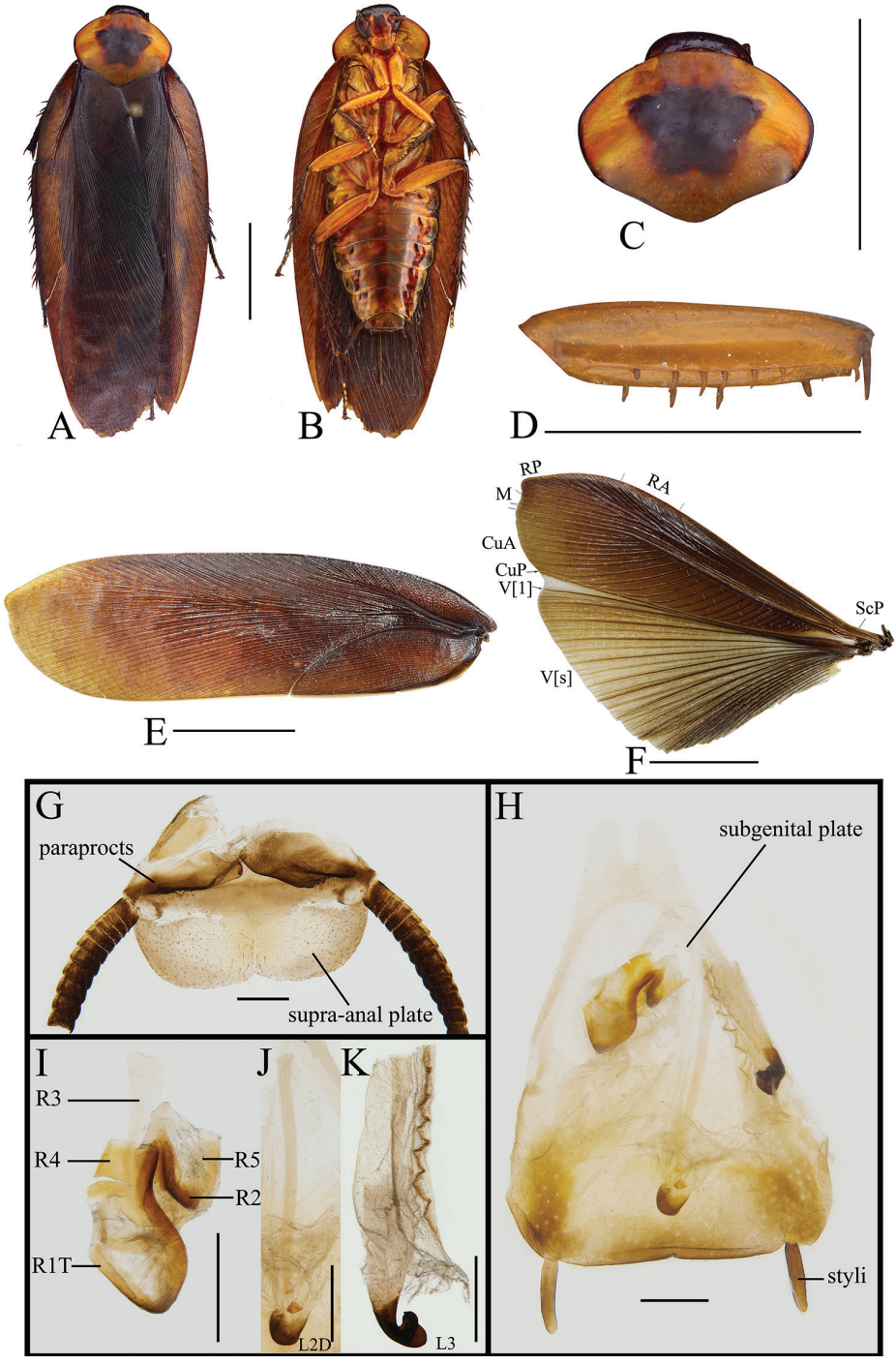

Figure 4. A–H *Rhabdoblatta gyroflexa* sp. n., male. **A** Holotype, dorsal view **B** holotype, ventral view **C** pronotum, dorsal view **D** front femur, ventral view **E** tegmen **F** wings **G** supra-anal plate, dorsal view **H** subgenital plate, ventral view **I** left phallomere, ventral view **J** median phallomere, ventral view **K** right phallomere, ventral view. Scale bars: 1.0 cm (**A–C, E, F**); 5.0 mm (**D**); 1.0 mm (**G–K**).

Male genitalia. Supra-anal plate nearly semicircular, the middle of the hind margin slightly concave. Right and left paraprocts unsymmetrical, shape similar to other members in the genus (Figure 4G). Subgenital plate with hind margin nearly straight. The base of the inner plate bifurcated. Styli long and flat, whose length ca. 1/3 of interstyli space (Figure 4H). Left phallomere with sclerite R1T apex near square, end of R2 rounded, R3 and R5 interlinked, the base of R3 turnover and without bifurcation at apex, R4 nearly rectangle and existing independently (Figure 4I). The basal sclerite of L2D slender and rod-shaped, apical sclerite short and small; the surface of the apical membrane with fine bristles, cap-shaped (Figure 4J). Sclerite L3 hook deeply bent and with semicircular carina with margin smooth; inner margin with groove and a tooth-shaped convexity at apex (Figure 4K).

Female. Female unknown.

Etymology. This species epithet is derived from the Latin words *gyroflexus*, referring to the yellowish brown marking on the pronotum.

Type material. *Holotype*: male, Guangxi Prov., Congzuo City, Pingxiang, 8-V-1963, Ji-kun Yang leg. *Paratype*: 1 male, same data as holotype; 1 male, Guangxi Prov., Congzuo City, Pingxiang, 8-V-1963, Si-kong Liu leg. (all in SWU).

Distribution. China (Guangxi).

Rhabdoblatta chaulformis sp. n.

http://zoobank.org/6CD7D802-2BEF-458B-AE76-0BDE9C983B7B
Figure 5A–K

Diagnosis. Sclerite L2D is strongly sclerotized with a exclamation-shaped process, it is the unique diagnosis of this species.

Measurements (mm). Male, head: length × width 3.5 × 3.0, pronotum: length × width 5.5 × 7.0, tegmen length: 28, overall length: 30.0–31.0.

Description. Male. Body yellowish brown (Figure 5A). Vertex dark brown. Eyes dark brown, border yellow. Ocelli yellow. Scape of antennae yellowish brown, the other dark brown. Frons dark brown. The base of clypeus dark brown, remaining part yellow. Mandible and labrum yellow. Maxillary palpi with the fifth brown, the others yellow (Figure 5B). Pronotum yellow, disc brown, with dark brown spots on the surface, with longitudinal short stripes along hind margin (Figure 5C). Tegmina brown, veins yellow. Wings with costal field, radial field, and mediocubital field yellowish brown and anal field pale brown, veins obvious and brown (Figure 5E, F). Legs brown. Abdominal terga dark brown, sterna yellow and with scattered blackish brown spots. Cerci dark brown (Figure 5B).

Vertex slightly exposed (Figure 5B). Distance between eyes slightly wider than interocular width, the length ca. 2/3 of the space between antennal sockets (Figure 5B). Pronotum subelliptical, the anterior and lateral margins rounded, middle of hind margin distinctly convex (Figure 5C). Tegmina and wings fully developed extending well beyond the end of the abdomen, the apex of the tegmina and wings slightly protruding and veins distinct (Figure 5A, B, E, F). Anteroventral margin of front femur type B_1 (Figure 5D). The metatarsus of hind leg longer than the sum of left tarsi, the inner mar-

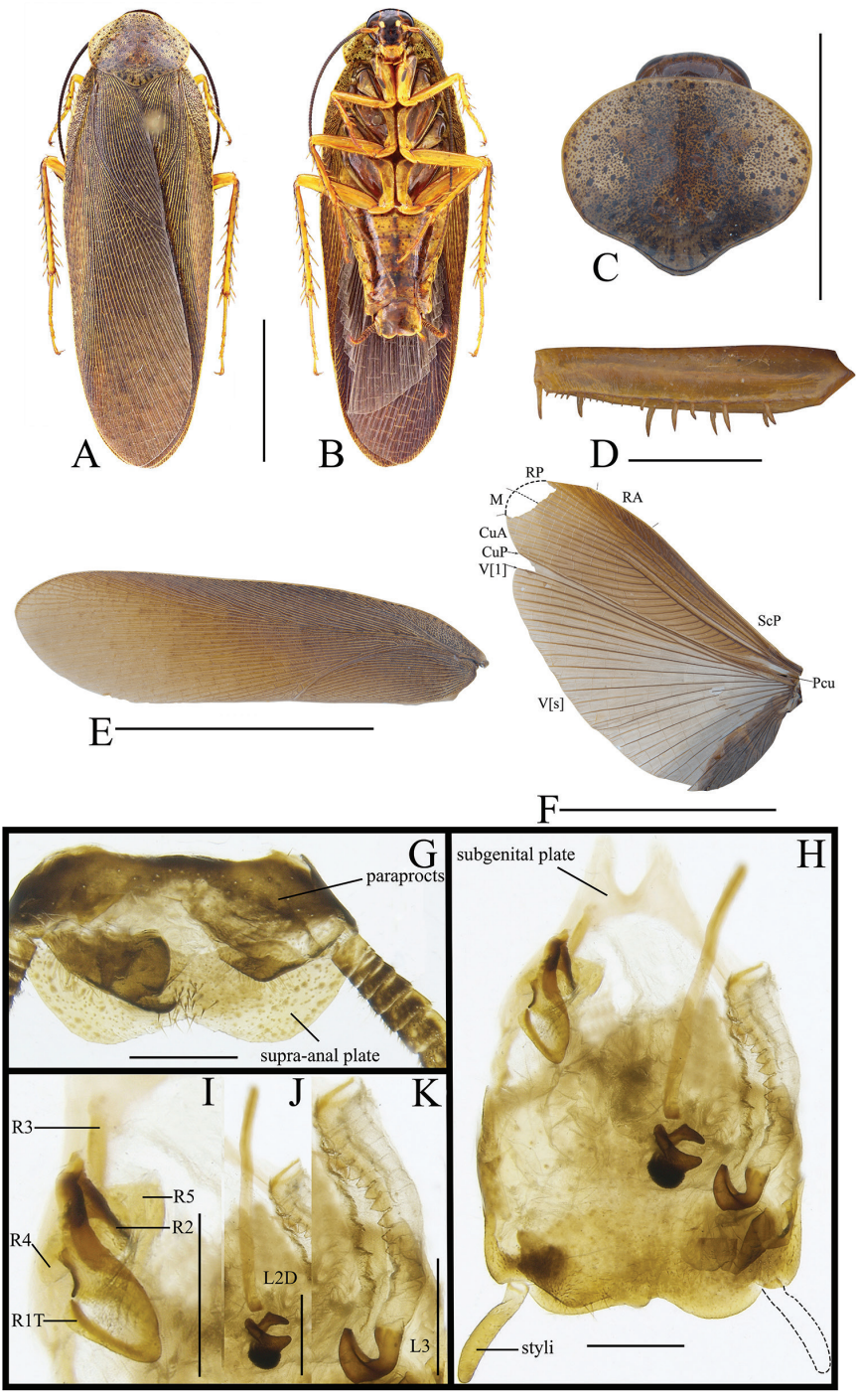

Figure 5. A–H *Rhabdoblatta chaulformis* sp. n., male. **A** Holotype, dorsal view **B** holotype, ventral view **C** pronotum, dorsal view **D** front femur, ventral view **E** tegmen **F** wings **G** supra-anal plate, dorsal view **H** subgenital plate, ventral view **I** left phallomere, ventral view **J** median phallomere, ventral view **K** right phallomere, ventral view. Scale bars: 1.0 cm (**A, B, E, F**); 5.0 mm (**C**); 1.0 mm (**D, G–K**).

gin with two rows of small spines. Tarsal pulvilli present on the apex of 1st–4th tarsomeres, small and spiked. Arolium present, claws symmetrical and unspecialized (Figure 5B).

Male genitalia. Supra-anal plate nearly semicircle, symmetrical, the middle of the hind margin slightly concave. Right and left paraprocts unsymmetrical, shape similar to other members in the genus (Figure 5G). Subgenital plate with hind margin unsymmetrical, slightly M-shaped margin. The base of the inner plate bifurcated. Styli long, whose length ca. 1/2 of interstyli space (Figure 5H). Left phallomere with sclerite R1T with bristles, end of R2 rounded, R3 and R5 interlinked, R4 weakly sclerotized (Figure 5I). The basal sclerite of L2D slender and rod-shaped, almost straight, apical sclerite irregular and with an exclamation-shaped process; the surface on the apical membrane with fine bristles, cap-shaped (Figure 5J). Sclerite L3 slender and hook deeply bent, and with semicircular carina; inner margin with groove and a tooth-shaped convexity at apex (Figure 5K).

Female. Female unknown.

Etymology. This species epithet is derived from the Latin words *chaul* and *formis*, referring to L2D with a exclamation-shaped process.

Type material. *Holotype*: male, Chongqing City, Wanzhou Dist, Wangerbao Nature Reserve, 1700 m, 2-V-2007, Wei-wei Zhang leg. *Paratype*: 1 male, same data as holotype (all in SWU).

Distribution. China (Chongqing).

***Rhabdoblatta maculata* sp. n.**

http://zoobank.org/AAC32271-2194-4D0B-8ECE-AB62FDCA275C

Figure 6A–K

Diagnosis. This species is similar to *Rhabdoblatta omei* Bey-Bienko, 1958, but can be differentiated by the following characters: 1) body wider with darker spots on pronotum and tegmina (body narrower with pale spots on pronotum and tegmina in the latter); 2) the hind margin of subgenital plate slightly concave and nearly symmetrical (the latter with the hind margin obviously concave and asymmetrical); and 3) outer-lateral margin apex of L3 with carina blunt and rounded (sharp and acute in the latter).

Measurements (mm). Male, head: length × width 4.8 × 5.0, pronotum: length × width 7.8 × 10.0, tegmen length: 39.1, overall length: 41.7–43.5.

Description. Male. Body yellow (Figure 6A). Vertex, eyes, and frons black. The apex of clypeus yellow, the remaining black. Ocelli yellow. Scape of antennae brown, the 2nd–15th segments dark brown, other segments pale brown. Mandible and labrum yellow. Maxillary palpi brown (Figure 6B). Pronotum yellow, with an irregular and symmetrical dark brown marking at disc, and with messy and dense brown spots on the border, posterior margin with longitudinal short stripes (Figure 6C). Tegmina yellow, with numerous scattered dark brown or brown spots. Wings pale gray, veins yellowish brown (Figure 6E, F). Legs reddish brown. Abdominal sterna brown. Cerci dark brown (Figure 6B).

Vertex slightly exposed (Figure 6B). Distance between eyes slightly narrower than interocular width, length ca. 1/2 of the space of antennal socket (Figure 6B). Pronotum subelliptical, the anterior and lateral margins rounded, middle of hind margin distinctly

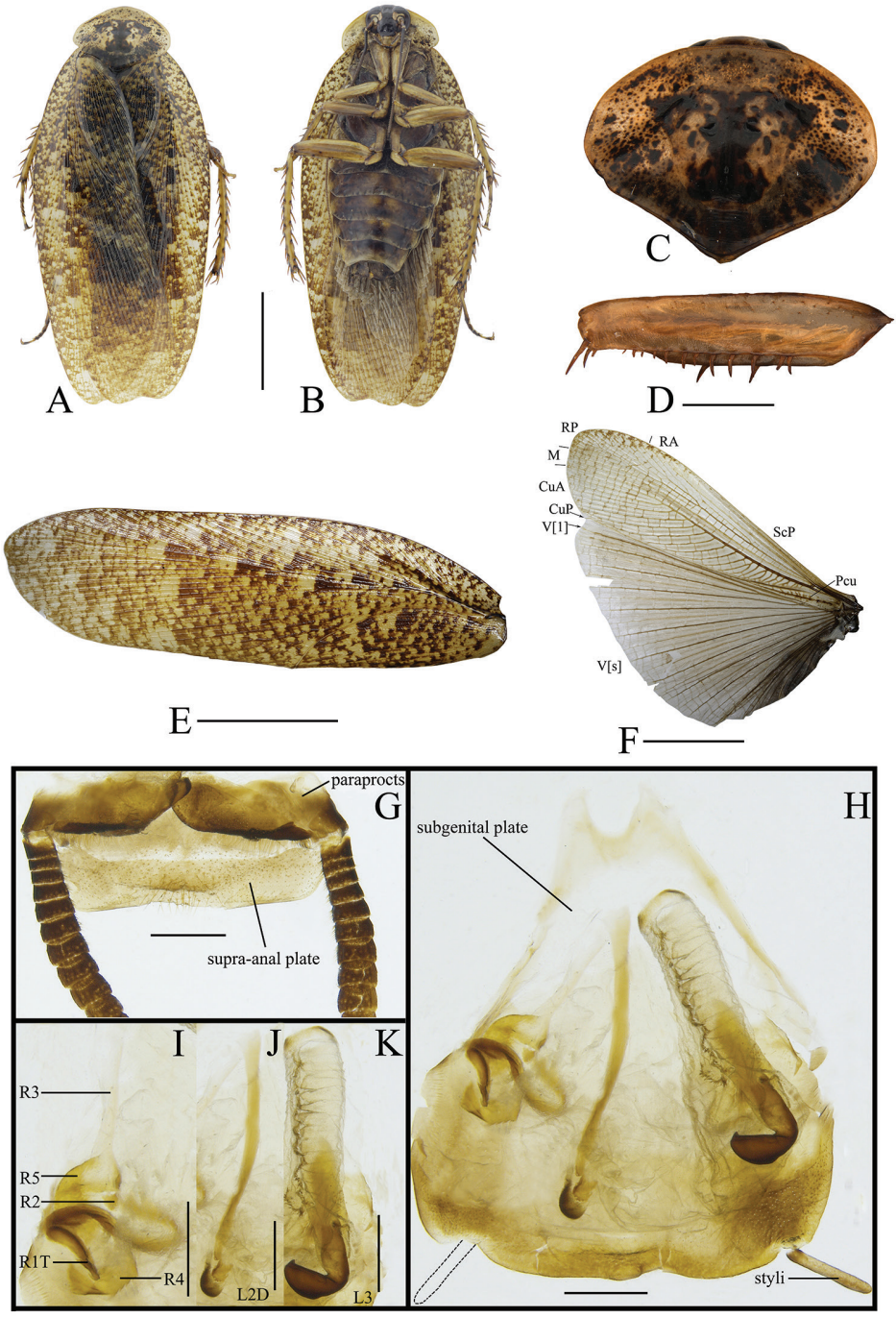

Figure 6. A–H *Rhabdoblatta maculata* sp. n., male. **A** Holotype, dorsal view **B** holotype, ventral view **C** pronotum, dorsal view **D** front femur, ventral view **E** tegmen **F** wings **G** supra-anal plate, dorsal view **H** subgenital plate, ventral view **I** left phallomere, ventral view **J** median phallomere, ventral view **K** right phallomere, ventral view. Scale bars: 1.0 cm (**A, B, E, F**); 5.0 mm (**C**); 1.0 mm (**D, G–K**).

convex (Figure 6C). Tegmina and wings fully developed extending well beyond the end of the abdomen, the apex of the tegmina with a convex and wings blunt and rounded (Figure 6A, B, E, F). Anteroventral margin of front femur type B_2 (Figure 6D). The metatarsus of hind leg equal length to sum of left tarsi, the inner margin with two rows of small spines. Tarsal pulvilli present on the 1st–4th of the tarsomere apex, with 1–2 spines. The pretarsus with arolium, claws symmetrical and unspecialized (Figure 6B).

Male genitalia. Supra-anal plate nearly semicircular, lateral margins rounded, the middle of the hind margin slightly concave. Right and left paraprocts unsymmetrical, shape similar to other members in this genus (Figure 6G). Subgenital plate with hind margin nearly symmetrical, right part with concavity. The base of the inner plate bifurcated. Styli flat, length ca. 1/3 of interstyli space (Figure 6H). The apex of the sclerite R1T peaked, end of R2 rounded, R3 and R5 interlinked; R4 existing independently (Figure 6I). The basal sclerite of L2D slender and rod-shaped; apical sclerite short and small, the surface on the apical membrane with fine bristles, cap-shaped (Figure 6J). Sclerite L3 long, with blunt and rounded carina; inner margin with groove and a tooth-shaped convexity at apex (Figure 6K).

Female. Female unknown.

Etymology. This species epithet is derived from the Latin word *maculatus*, referring to the tegmina having clear spots.

Type material. *Holotype*: male, Guizhou Prov., Leigongshan Mountain, 6-VI-2013, Gui-qiang Huang & Xiang-xiang Zhang leg. *Paratype*: 1 male, same data as holotype; 1 male, Guizhou Prov., Leigongshan Mountain, 29-VI-1988, Min-sheng Wang leg. (all in SWU).

Distribution. China (Guizhou).

***Rhabdoblatta ecarinata* sp. n.**
http://zoobank.org/FD060B05-39AA-4C2A-833A-BAA77DD5DAA1
Figure 7A–T

Rhabdoblatta carinata Liu et al., 2017: 78 (nomen nudum).

Diagnosis. The outer-lateral margin of the sclerite L3 hook without carina, and it is similar to *Rhabdoblatta monticola* (Kirby, 1903), but subcosta of *Rh. monticola* is white (Figure 8A), and this species is yellowish brown.

Measurements (mm). Male, pronotum: length × width 5.0–6.0 × 7.5–8.0, tegmen length: 22.0–24.0, overall length: 26.0–28.0; female, pronotum: length × width 7.8–8.0 × 8.4–9.0, tegmen length: 31.0–32.0, overall length: 37.0–38.0.

Description. Male. Body yellowish brown (Figure 7A). Vertex and apex of frons with scattered brown spots. Eyes black. Ocelli pale yellow. Labrum, labial palpi, and maxillary palpi yellow (Figure 7B). Pronotum yellowish brown, with many near round small or a few big brown spots on the surface and longitudinal short stripes along hind margin (Figure 7I). Tegmina yellowish brown, with several large dark brown spots on

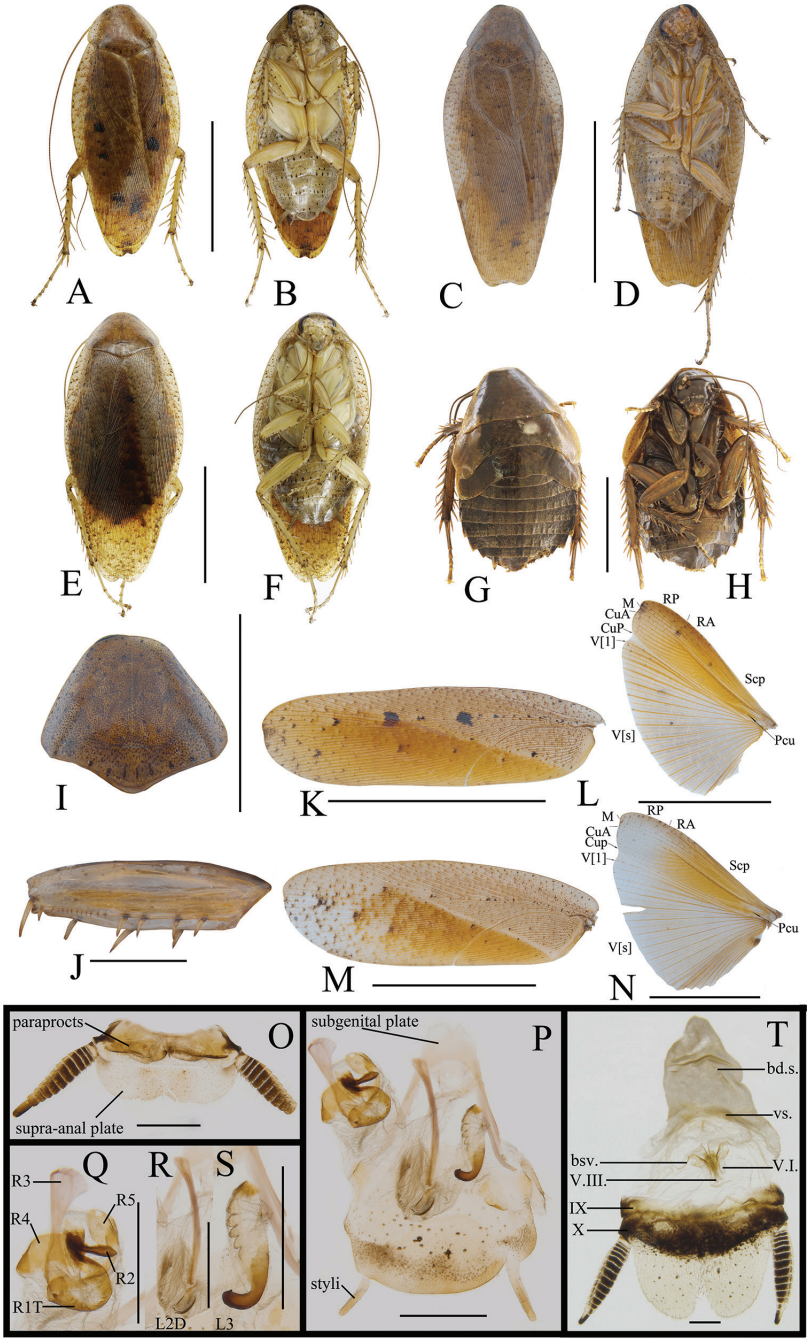

Figure 7. A–D, I–L, O–S *Rhabdoblatta ecarinata* sp. n., male **E, F, M, N, T** female **G, H** nymph. **A** Paratype, dorsal view **B** paratype, ventral view **C** holotype, dorsal view **D** holotype, ventral view **E** paratype, dorsal view **F** paratype, ventral view **G** nymph, dorsal view **H** nymph, ventral view **I** pronotum, dorsal view **J** front femur, ventral view **K** tegmen **L** wings **M** tegmen **N** wings **O** supra-anal plate, dorsal view **P** subgenital plate, ventral view **Q** left phallomere, ventral view **R** median phallomere, ventral view **S** right phallomere, ventral view **T** female genitalia. Scale bars: 1.0 cm (**A–H, K–N**); Scale bars: 5.0 mm (**I**); 1.0 mm (**J, O–T**).

the surface or not. Wings with costal field, radial field, and mediocubital field yellowish brown, and anal field gray, with veins obvious and yellow (Figure 7K, L). Legs yellow. Abdominal sterna yellow, 4^{th}–7^{th} segments with dark brown spots. Cerci dark brown (Figure 7B).

Vertex slightly exposed. Distance between eyes slightly wider than interocular space, the length ca. 2/3 of the space of antennal sockets (Figure 7B). Pronotum subelliptical, the widest part in the middle, anterior and lateral margins rounded, middle of hind margin convex (Figure 7I). Tegmina and wings fully developed extending well beyond the end of the abdomen, the apex of the tegmina arc-shaped and veins distinct (Figure 7A–D, K, L). Anteroventral margin of front femur type B_2 (Figure 7J). The inner margin of the metatarsus of hind leg with two rows small spines. Tarsal pulvilli present on the apex of 1^{st}–4^{th} tarsomeres. The pretarsus with arolium, claws symmetrical and unspecialized (Figure 7B).

Male genitalia. Supra-anal plate symmetrical, nearly rectangular, the middle of the hind margin with concavity (Figure 7O). Subgenital plate with hind margin unsymmetrical, with a cambered convexity in the middle, the left stylus shorter than the right (Figure 7P). Left phallomere with sclerite R3 intamescent at apex, R4 wide and nearly square (Figure 7Q). The basal sclerite of L2D slender and rod-shaped, base slightly intamescent; apical sclerite small, the surface on the apical membrane with fine bristles (Figure 7R). Sclerite L3 with small hook, outer-lateral margin without carina, inner margin with a tooth-shaped convexity at apex (Figure 7S).

Female. Female similar to male but slightly larger (Figure 7E, F, M, N).

Female genitalia. Weakly sclerotized. Ovipositor back to brood sac. Tergal process of the eighth and ninth abdominal tergite obviously vestigial. First valves of ovipositor wide, apex membranous. Second valves of ovipositor fine and tube-shaped, completely covered by the first valves of ovipositor. Third valves of ovipositor slightly wider and flat, length shorter than the first valves of ovipositor. Gonangulum and sclerotized lobes of the second and third pairs of valves not obvious. Anterior arch of second valvifer obviously vestigial. Basivalvula with semicircular arms, the mid sclerite with incomplete separation, linked with membrane. Vestibular sclerite membranous, wider than the basivalvula. Transverse sclerotized plate absent. Brood sac membranous and without sclerotized section (Figure 7T).

Nymph. Body brown. Spine on the tibia robust. The length of antennae nearly equal to the body's length (Figure 7G, H).

Remarks. This species was named as *Rhabdoblatta carinata* by Liu et al. (2017) in the book Cockroaches of Southeastern China (page 78). However, no exact deposition of the type specimens was mentioned, although the authors listed three collections in the material and method. Based on Article 16.4.2 of the International Code of Zoological Nomenclature (ICZN 1999), the name *Rhabdoblatta carinata* is not available. Based on the material we examined, males of the species have intraspecific variation, with some individuals having dispersed large dark brown spots on tegmina, while others do not (Figure 7A–D).

Etymology. This species name is derived from the Latin word *ecarinatus*, referring to the outer-lateral margin of the sclerite L3 hook without carina.

Type material. *Holotype*: male, Hainan Prov., Yinggeling Nature Reserve, Nanfa Conservation Station, 650m, 21-IV-2015, Lu Qiu & Qi-kun Bai leg. *Paratype*: 8 males and 5 females, Hainan Prov., Yinggeling Nature Reserve, Nankai Conservation Station, 284–308m, 20-IV-2015, Xin-ran Li & Zhi-wei Qiu leg.; 2 females, Hainan Prov., Lingshui County, Diaoluoshan Mountain, 15-IV-2015, Lu Qiu & Qi-kun Bai leg.; 1 female, 1 male, 1 nymph, Hainan Prov., Lingshui County, Diaoluoshan Mountain, 24-V-2014, Shun-hua Gui & Xin-ran Li leg. (all in SWU).

Distribution. China (Hainan).

First descriptions of females including female genitalia of the 14 known *Rhabdoblatta* species

The DNA Barcode method allows us to successfully match *Rhabdoblatta* male and female samples, in spite of sexual dimorphism. Therefore, we take this opportunity to describe for the first time the female genitalia of 14 known *Rhabdoblatta* species.

Rhabdoblatta monticola (Kirby, 1903)

Figures 8A–D, 12E

Rhabdoblatta monticola, Princis, 1967: 664; Anisyutkin 2003: 542.

Measurements (mm). Female, overall length: 38.3–40.5.

Female. Female similar to male but slightly larger (Figure 8A–D).

Female genitalia. Weakly sclerotized. Ovipositor back to brood sac. Tergal process of the eighth abdominal tergite obviously vestigial, length ca. 1/2 of tergal process of the ninth abdominal tergite. Tergal process of the ninth abdominal tergite and the ninth tergum interlinked. First valves of ovipositor wide, apex membranous, inner margin with long bristles. Second valves of ovipositor fine, tube-shaped, completely covered by the first valves of ovipositor. Third valves of ovipositor slightly wider and flat, length shorter than the first valves of ovipositor. Gonangulum irregular. Sclerotized lobes of the second and third pairs of valves nearly triangular. Anterior arch of second valvifer slender. Basivalvula with semicircular arms, the mid sclerite incompletely separated, linked with membrane. Vestibular sclerite wide, wider than the basivalvula. Transverse sclerotized plate bowknot-shaped. Brood sac membranous and without sclerotized section (Figure 12E).

Material examined. 1 male and 7 females, Guangxi Prov., Shangsi County, Shiwandashan National Forest Park, 28-VI-2015, Lu Qiu & Qi-kun Bai leg.; 1 male and 1 female, Guangxi Prov., Jinxiu County, Dayaoshan Nature Reserve, Hekou Reserve Station, 4-VII-2015, Lu Qiu & Qi-kun Bai leg.; 1 female, Guangdong Prov., Zhaoqing City, Dinghushan Forest Park, 1–2-VII-2015, Zhi-wei Qiu & Yong-quan Zhao leg.; 1 male, Guangdong Prov., Zhaoqing City, Fenghuang Town, Jiulonghu Lake, 4-VII-2015, Zhi-wei Qiu & Yong-quan Zhao leg.

Distribution. China (Guangxi, Guangdong); Vietnam.

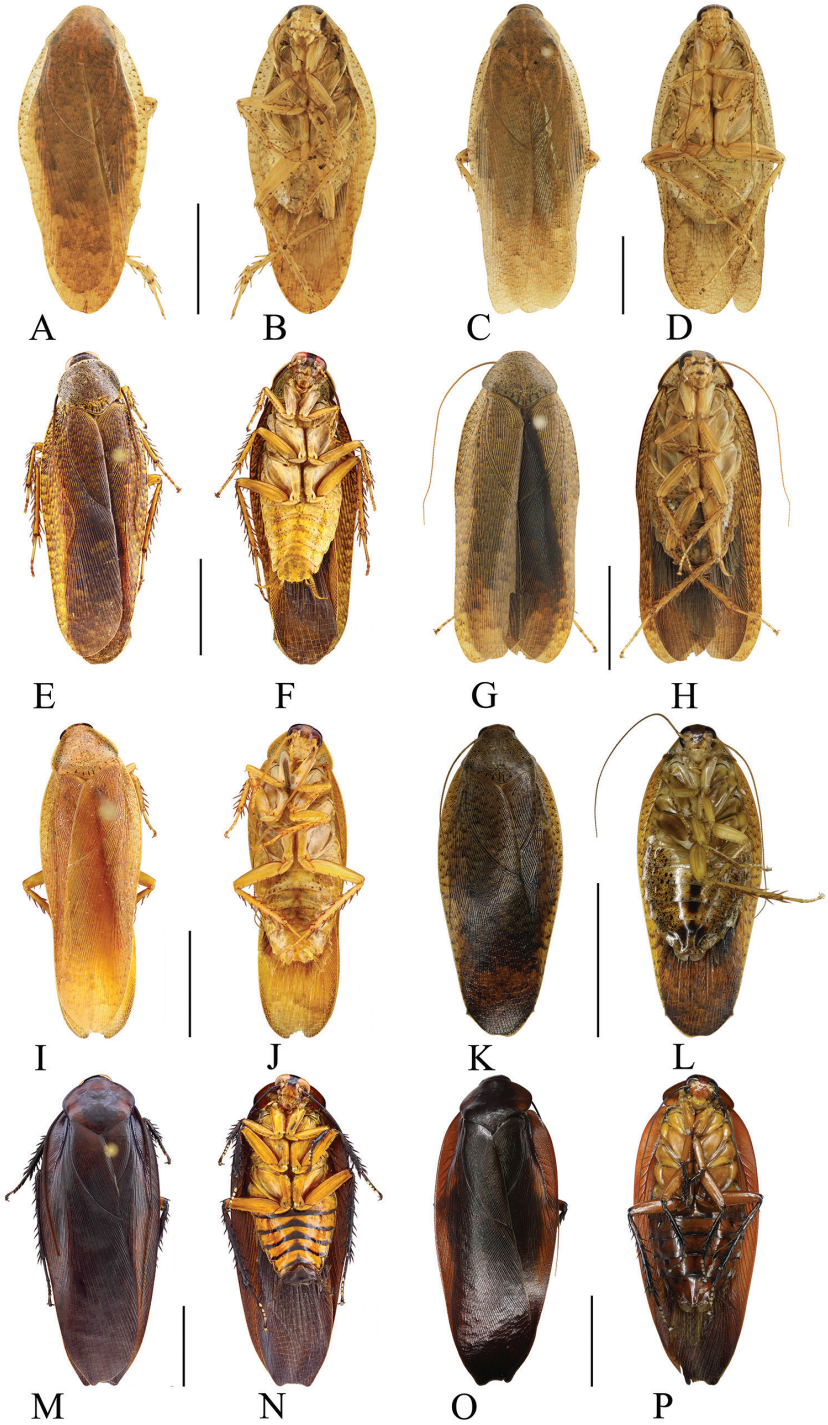

Figure 8. A–D *Rhabdoblatta monticola* (Kirby, 1903): **A, B** male **C, D** female **E–H** *Rhabdoblatta atra* Bey-Bienko, 1970: **E, F** male **G, H** female **I–L** *Rhabdoblatta rattanakiriensis* Anisyutkin, 1999: **I, J** male **K, L** female **M–P** *Rhabdoblatta elegans* Anisyutkin, 2000: **M, N** male **O, P** female. Scale bars: 1.0 cm.

***Rhabdoblatta atra* Bey-Bienko, 1970**
Figures 8E–H, 12F

Rhabdoblatta atra Bey-Bienko, 1970: 364; Anisyutkin 2003: 554.

Measurements (mm). Female, overall length: 29.0–33.0.

Female. Female similar to male but slightly larger. The hind margin of every abdominal sterna with scattered large brown spots (Figure 8E–H).

Female genitalia. Moderately sclerotized. Ovipositor back to brood sac. Tergal process of the eighth abdominal tergite slender, length ca. 1/2 of tergal process of the ninth abdominal tergite. Tergal process of the ninth abdominal tergite weakly sclerotized, linked with the ninth tergum. First valves of ovipositor with base wide, apex narrow, inner margin with obviously long bristles. Second valves of ovipositor tube-shaped, completely covered by the first valves of ovipositor. Third valves of ovipositor slightly wider, length shorter than the first valves of ovipositor. Gonangulum absent. Sclerotized lobes of the second and third pairs of valves not obvious. Anterior arch of second valvifer slender, middle narrow and both sides wide. Basivalvula with semicircular arms, the mid sclerite incompletely separated. Vestibular sclerite membranous, apical sclerite vestigial. Transverse sclerotized plate subelliptical. Brood sac membranous and without sclerotized section (Figure 12F).

Material examined. 40 males and 6 females, Guangxi Prov., Jinxiu County, Dayaoshan Nature Reserve, Hekou Reserve Station, 7–8-VII-2015, Qi-kun Bai & Lu Qiu leg.; 4 females, Guangxi Prov., Guiping City, Longtan Park, 31-V–2-VI-2014, Xin-ran Li & Shun-hua Gui leg.; 2 females, Guangxi Prov., Jinxiu County vicinity, Laoshan, 9-VII-2015, Lu Qiu & Qi-kun Bai leg.; 1 male, Yunnan Prov., Longchuan County, 7–8-VI-1981, Zhi-gang Zheng & Ying-shu Xie leg.

Distribution. China (Guangxi, Yunnan).

***Rhabdoblatta rattanakiriensis* Anisyutkin, 1999**
Figures 8I–L, 12G

Rhabdoblatta rattanakiriensis Anisyutkin, 1999: 253.

Measurements (mm). Female, overall length: 28.0–29.0.

Female. Female different from male. Body slightly larger. Color of female darker. Middle of every abdominal sterna with brown stripes (Figure 8I–L).

Female genitalia. Moderately sclerotized. Ovipositor back to brood sac. Tergal process of the eighth abdominal tergite slender, from the base to the end gradually narrowing, length ca. 1/2 of tergal process of the ninth abdominal tergite. Tergal process of the ninth abdominal tergite weakly sclerotized, linked with tergal process

of the eighth abdominal tergite. First valves of ovipositor slender, apex membranous, inner margin with fine bristles. Second valves of ovipositor tube-shaped, completely covered by the first valves of ovipositor. Third valves of ovipositor slightly wider, length shorter than the first valves of ovipositor. Gonangulum weakly sclerotized. Sclerotized lobes of the second and third pairs of valves nearly rectangular. Anterior arch of second valvifer slender. Basivalvula robust and with semicircular arms, the mid sclerite separate. Vestibular sclerite wide, apical sclerite vestigial. Transverse sclerotized plate absent. Brood sac membranous and without sclerotized section (Figure 12G).

Material examined. 26 males and 4 females, Hainan Prov., Wuzhishan Nature Reserve, 18–21-V-2014, Xin-ran Li, Shun-hua Gui & Jian-yue Qiu leg.; 1 male, Hainan Prov., Jianfengling, Mingfenggu, 26-IV-2015, Lu Qiu & Qi-kun Bai leg.; 4 males and 2 females, Hainan Prov., Diaoluoshan Mountain, 916 m, 18-IV-2015, Lu Qiu & Qi-kun Bai leg.

Distribution. China (Hainan).

***Rhabdoblatta elegans* Anisyutkin, 2000**

Figures 8M–P, 12H

Rhabdoblatta elegans Anisyutkin, 2000: 190.

Measurements (mm). Female, overall length: 38.3–42.7.

Female. Female similar to male but slightly larger (Figure 8M–P).

Female genitalia. Moderately sclerotized. Ovipositor back to brood sac. Tergal process of the eighth abdominal tergite slender, from the base to the end gradually narrowing, length ca. 1/2 of tergal process of the ninth abdominal tergite. Tergal process of the ninth abdominal tergite robust, linked with tergal process of the eighth abdominal tergite. First valves of ovipositor slender, apex membranous, inner margin with fine bristles. Second valves of ovipositor tube-shaped, completely covered by the first valves of ovipositor. Third valves of ovipositor slightly wider, length shorter than the first valves of ovipositor. Gonangulum boat-shaped. Sclerotized lobes of the second and third pairs of valves nearly rectangular. Anterior arch of second valvifer slender, middle narrow and both sides wide. Basivalvula robust and with semicircular arms, the mid sclerite incompletely separated. Vestibular sclerite wide, apical sclerite vestigial. Transverse sclerotized plate absent. Brood sac membranous and without sclerotized section (Figure 12H).

Material examined. 8 males and 10 females, Yunnan Prov., Jinping County, Maandi Township, Butterfly Valley, 14-V-2015, Jian-yue Qiu leg.; 1 female, Yunnan Prov., Baoshan City, Zaolong, 22-VIII-2015, Xin-ran Li & Zhi-wei Qiu leg.; 1 male, Yunnan Prov., Mengla County, 10-V-2015, Jian-yue Qiu leg.; 1 male, Jiangxi Prov., Fuzhou City, Gaoping Town, Qiayuan Village, 1298 m, 5-V-1980, Yan-bao Qiu leg.; 1 male,

Guangxi Prov., Jinzhongshan Mountain, 1-VIII-2014, Jian-hua Huang leg.; 1 male and 1 female, Guangdong Prov., Nanling Nature Reserve, 5–7-VI-2010, unknown.

Distribution. China (Yunnan, Guangxi, Guangdong, Jiangxi).

Rhabdoblatta nigrovittata Bey-Bienko, 1954

Figures 9A–D, 12I

Rhabdoblatta nigrovittata Bey-Bienko, 1954: 21; Princis 1967: 664; Feng, Guo et Wu 1997: 90; Anisyutkin 2003: 550.

Measurements (mm). Female, overall length: 43.0–45.0.

Female. Female slightly different from male and larger. Body pale yellow. Vertex and frons yellowish brown. Stripes on the sterna same as male (Figure 9A–D).

Female genitalia. Moderately sclerotized. Ovipositor back to brood sac. Tergal process of the eighth abdominal tergite obviously vestigial, sharp and slender, length ca. 1/3 of tergal process of the ninth abdominal tergite. Tergal process of the ninth abdominal tergite robust, linked with the ninth tergum. First valves of ovipositor with apex membranous, inner margin with fine bristles. Second valves of ovipositor tube-shaped, completely covered by the first valves of ovipositor. Third valves of ovipositor slightly wider, length slightly shorter than the first valves of ovipositor. Gonangulum and sclerotized lobes of the second and third pairs of valves nearly triangular. Anterior arch of second valvifer slender, middle narrow and both sides wide. Basivalvula robust and with semicircular arms, the mid sclerite incompletely separated. Vestibular sclerite wide and robust. Transverse sclerotized plate bowknot-shaped. Brood sac membranous and without sclerotized section (Figure 12I).

Material examined. 3 females, Hunan Prov., Mangshan Forest Park, 11–12-VII-2015, Zhi-wei Qiu & Yong-quan Zhao leg.; 3 females and 1 male, Guangxi Prov., Jinxiu County, Shengtangshan Mountain, 12-VII-2015, Lu Qiu & Qi-kun Bai leg.; 1 male, Guangdong Prov., Nanling Nature Reserve, 6–7-VI-2014, Cheng-hui Zhan leg.; 4 females, Chongqing City, Simianshan Mountain, Feilongmiao Temple, 5–6-VI-2015, Lu Qiu & Qi-kun Bai leg.; 10 males and 2 females, Guizhou Prov., Kuankuoshui Nature Reserve, Baishaogou, 4–5-VI-2010, Jia-jia Zhao leg.; 2 males, Zhejiang Prov., Tianmushan Mountain, 7–10-VI-2016, Lian Chen leg.; 1 male and 1 female, Sichuan Prov., Luzhou City, Gulin County, Guihua Township, Lou'e Village, 19-VII-2014, by light trap, Lu Qiu leg.; 1 female, Sichuan Prov., Leshan City, E'meishan Mountain, Sangenqiao, 1124 m, 22-VIII-2017, by light trap, Lu Qiu leg.; 1 female, Guangxi Prov., Jiuxiu City, Dayaoshan Nature Reserve, Hekou Reserve Station, 8-VII-2015, Lu Qiu & Qi-kun Bai leg.; 1 female, Guangxi Prov., Wuming County, Damingshan Mountain, 2-VII-2015, Qi-kun Bai & Lu Qiu leg.; 1 male and 1 female, Hubei Prov., Enshi City, Qizimeishan Mountain, 21-VI-2012, Mao Ye leg.

Distribution. China (Hunan, Hubei, Guangdong, Sichuan, Chongqing, Guizhou, Zhejiang, Guangxi, Yunnan, Fujian).

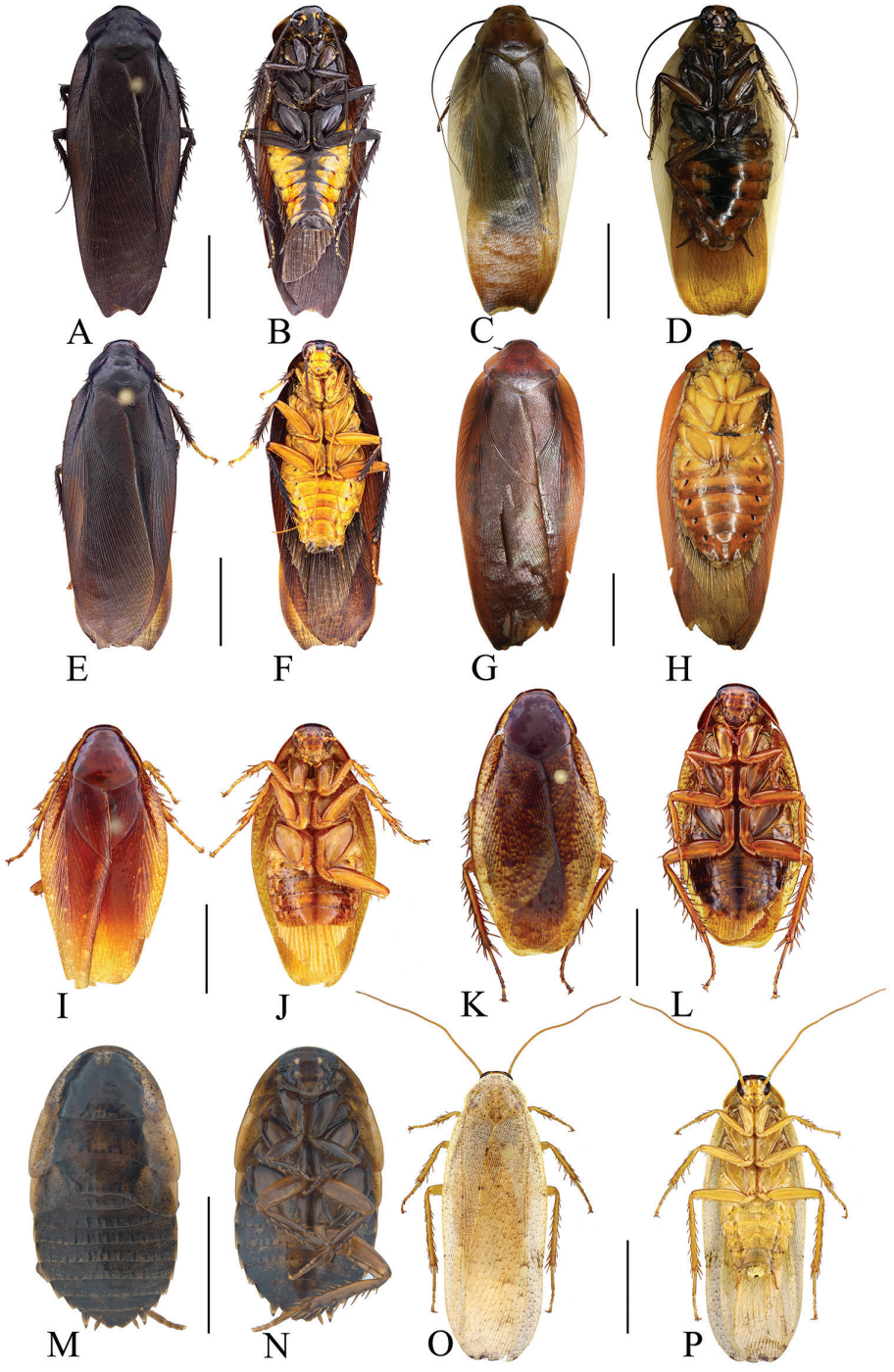

Figure 9. A–D *Rhabdoblatta nigrovittata* Bey-Bienko, 1954: **A, B** male **C, D** female **E–H** *Rhabdoblatta simulans* Anisyutkin, 2000: **E, F** male **G, H** female **I–N** *Rhabdoblatta marginata* Bey-Bienko, 1969: **I, J** male **K, L** female **M, N** nymph **O, P** *Rhabdoblatta sinuata* Bey-Bienko, 1958: **O, P** male. Scale bars: 1.0 cm.

***Rhabdoblatta simulans* Anisyutkin, 2000**
Figures 9E–H, 12J

Rhabdoblatta simulans Anisyutkin, 2000: 191.

Measurements (mm). Female, overall length: 42.7–43.1.

Female. Female slightly different from male and larger. Vertex and area of interocellus yellowish brown (Figure 9E–H).

Female genitalia. Moderately sclerotized. Ovipositor back to brood sac. Tergal process of the eighth abdominal tergite obvious and slender, length ca. 1/2 of tergal process of the ninth abdominal tergite. Tergal process of the ninth abdominal tergite robust, linked with the ninth tergum. First valves of ovipositor with apex wide and cambered, base thin. Second valves of ovipositor tube-shaped, completely covered by the first valves of ovipositor. Third valves of ovipositor slightly wider, length shorter than the first valves of ovipositor. Gonangulum boat-shaped. Sclerotized lobes of the second and third pairs of valves irregular. Anterior arch of second valvifer slender. Basivalvula with semicircular arms, mid sclerite incompletely separated. Vestibular sclerite membranous. Transverse sclerotized plate nearly circular. Brood sac membranous and without sclerotized section (Figure 12J).

Material examined. 1 male and 1 female, Yunnan Prov., Yingjiang County, Tongbiguan Township, 1345 m, 31-V-2018, Lu Qiu & Wen-bo Deng leg.; 1 female, Yunnan Prov., Yingjiang County, around Tongbiguan Township, 1345 m, 2-VI-2018, Lu Qiu & Wen-bo Deng leg.; 2 males and 1 female, Xizang Prov., Medog County, 3-VIII-2017, unknown.

Distribution. China (Yunnan, Xizang).

***Rhabdoblatta marginata* Bey-Bienko, 1969**
Figures 9I–N, 12K

Rhabdoblatta marginata Bey-Bienko, 1969: 843; Bey-Bienko 1970: 363; Princis 1971: 1158; Anisyutkin 2003: 547.

Measurements (mm). Female, overall length: 32.5–34.0.

Female. Female larger than male and color slightly darker (Figure 9I–L).

Female genitalia. Moderately sclerotized. Ovipositor back to brood sac. Tergal process of the eighth abdominal tergite obviously vestigial, length ca. 1/2 of tergal process of the ninth abdominal tergite. Tergal process of the ninth abdominal tergite robust, linked with the ninth tergum. First valves of ovipositor with apex membranous, inner margin with fine bristles. Second valves of ovipositor tube-shaped, completely covered by the first valves of ovipositor. Third valves of ovipositor slightly wider, length shorter than the first valves of ovipositor. Gonangulum boat-shaped. Sclerotized lobes of the second and third pairs of valves nearly triangle. Anterior arch of second valvifer

slender. Basivalvula with semicircular arms, the mid sclerite incompletely separated. Vestibular sclerite slender, the mid sclerite membranous. Transverse sclerotized plate nearly circular. Brood sac membranous and without sclerotized section (Figure 12K).

Nymph. Body dark brown. Pronotum black, lateral area with a yellow stripe and black spots on the surface. Abdominal terga dark brown, with short and bar-shaped convexity. Abdominal sterna dark brown and with scattered black spots on the surface (Figure 9M, N).

Material examined. 8 males and 8 females, Hainan Prov., Wuzhishan Nature Reserve, 18–21-V-2014, Shun-hua Gui, Xin-ran Li & Jian-yue Qiu leg.; 1 female and 1 nymph, Hainan Prov., Wuzhishan Mountain, 920 m, 21-XI-2013, Yan Shi leg.; 3 nymphs, Hainan Prov., Baoting County, Maogan Township, 549–776 m, 11–12-IV-2015, Lu Qiu & Qi-kun Bai leg.; 1 male and 1 female, Hainan Prov., Limushan Mountain, 15-IV-2015, Zhi-wei Qiu & Xin-ran Li leg.; 1 male, Hainan Prov., Changjiang County, Bawangling, Yajia, 29-VI-2015, Lu Qiu & Qi-kun Bai leg.; 10 males and 10 females, Guangdong Prov., Conghua District, Liuxihe National Forest Park, Wuzhishan Scenic, 7–8-VII-2015, Zhi-wei Qiu & Yong-quan Zhao leg.; 4 males and 5 females, Guangxi Prov., Shangsi County, Shiwandashan Forest Park, 28-VI-2015, Lu Qiu & Qi-kun Bai leg.; 1 male, Guangxi Prov., Jinxiu County, Shengtangshan Mountain, 4–5-VI-2014, Shun-hua Gui & Xin-ran Li leg.

Distribution. China (Hainan, Guangdong, Guangxi).

Rhabdoblatta sinuata Bey-Bienko, 1958

Figures 9O, P, 10A, B, 12L

Rhabdoblatta sinuata Bey-Bienko, 1958: 593; Bey-Bienko 1970: 368; Princis 1967: 675; Anisyutkin 2003: 552.

Measurements (mm). Female, overall length: 35.0–36.0.

Female. Female similar to male but slightly larger (Figure 9O, P, Figure 10A, B).

Female genitalia. Moderately sclerotized. Ovipositor extending toward brood sac. Tergal process of the eighth abdominal tergite obviously vestigial, from the base to the end gradually more narrow, length ca. 1/3 of tergal process of the ninth abdominal tergite. Tergal process of the ninth abdominal tergite wide, linked with the ninth tergum. First valves of ovipositor with apex membranous, inner margin with fine bristles. Second valves of ovipositor tube-shaped, completely covered by the first valves of ovipositor. Third valves of ovipositor slightly wider, length shorter than the first valves of ovipositor. Gonangulum boat-shaped. Sclerotized lobes of the second and third pairs of valves crescent-shaped. Anterior arch of second valvifer slender, middle narrow and both sides wide. Basivalvula with semicircular arms, the mid sclerite incompletely separated. Vestibular sclerite weakly scleritized, the mid sclerite nearly membranous. Transverse sclerotized plate nearly semicircle. Brood sac membranous and without sclerotized section (Figure 12L).

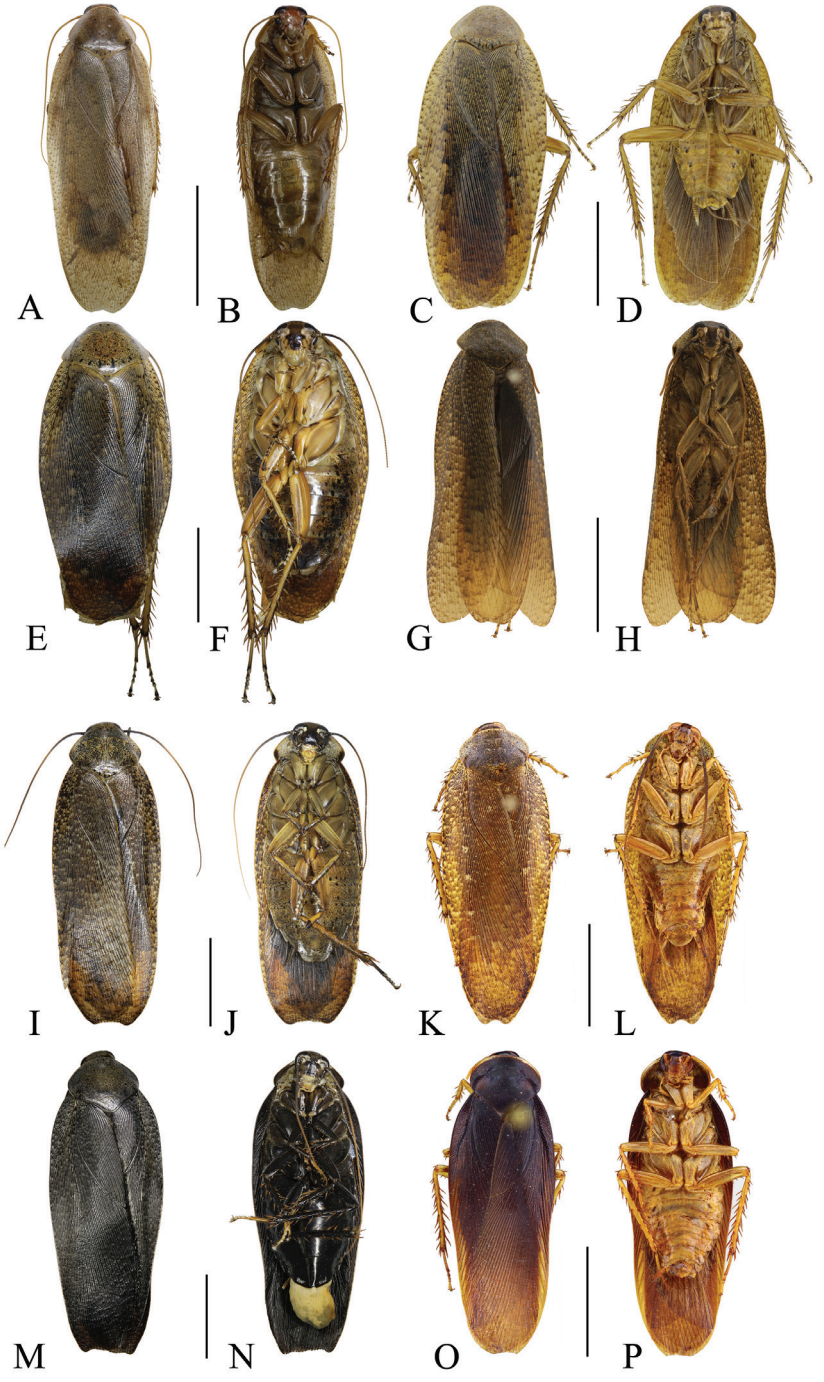

Figure 10. A, B *Rhabdoblatta sinuata* Bey-Bienko, 1958: **A, B** female **C–F** *Rhabdoblatta mascifera* Bey-Bienko, 1969: **C, D** male **E, F** female **G–J** *Rhabdoblatta incisa* Bey-Bienko, 1969: **G, H** male **I, J** female **K–N** *Rhabdoblatta krasnovi* (Bey-Bienko, 1969): **K, L** male **M, N** female **O, P** *Rhabdoblatta melancholica* (Bey-Bienko, 1954): **O, P** male. Scale bars: 1.0 cm.

Material examined. 12 males and 2 females, Yunnan Prov., Jinping County, Maandi Village, Butterfly Valley, 15-V-2015, Jian-yue Qiu leg.; 5 males and 1 female, Sichuan Prov., Panzhihua City, Daheishan Forest Park, 20–21-V-2011, unknown; 5 males, Guangdong Prov., Nanling Nature Reserve, 5–7-VI-2010, Ke-liang Wu & Jia-jia Wu leg.

Distribution. China (Yunnan, Sichuan, Guangdong).

Rhabdoblatta mascifera Bey-Bienko, 1969

Figures 10C–F, 12M

Rhabdoblatta mascifera Bey-Bienko, 1969: 844; Bey-Bienko 1970: 368; Princis 1971: 1158; Anisyutkin 2003: 547.

Measurements (mm). Female, overall length: 32.4.

Female. Female slightly bigger and frons dark brown (Figure 10C–F).

Female genitalia. Moderately sclerotized. Ovipositor back to brood sac. Tergal process of the eighth abdominal tergite from the base to the end gradually more narrow, length ca. 1/2 of tergal process of the ninth abdominal tergite. Tergal process of the ninth abdominal tergite linked to the ninth tergum. First valves of ovipositor with apex membranous, inner margin with fine bristles. Second valves of ovipositor tube-shaped, completely covered by the first valves of ovipositor. Third valves of ovipositor slightly wider, length shorter than the first valves of ovipositor. Gonangulum boat-shaped. Sclerotized lobes of the second and third pairs of valves irregular. Anterior arch of second valvifer slender. Basivalvula with semicircular arms, the mid-sclerite incompletely separated. Vestibular sclerite nearly membranous. Transverse sclerotized plate absent. Brood sac membranous and without sclerotized section (Figure 12M).

Material examined. 2 males, Yunnan Prov., Xishuangbanna, Mengla County, Shangyong Town, Longmen Village, 8–9-V-2015, Jian-yue Qiu leg.; 1 female, Yunnan Prov., Xishuangbanna, Menglun Town, Xishuangbanna Tropical Botanical Garden, Gouguyulin, 27-V-2016, Zhi-wei Qiu & Lu Qiu leg.

Distribution. China (Yunnan).

Rhabdoblatta incisa Bey-Bienko, 1969

Figures 10G–J, 12N

Rhabdoblatta incisa Bey-Bienko, 1969: 843; Princis 1971: 1158; Feng, Guo et Wu 1997: 95; Anisyutkin 2003: 547.

Measurements (mm). Female, overall length: 33.2.

Female. Female similar to male but slightly larger (Figure 10G–J).

Female genitalia. Moderately sclerotized. Ovipositor back to brood sac. Tergal process of the eighth abdominal tergite obvious, gradually narrowing from the base to the end, length ca. 1/2 of tergal process of the ninth abdominal tergite. Tergal process

of the ninth abdominal tergite robust, linked with the ninth tergum. First valves of ovipositor with apex membranous, inner margin with fine bristles. Second valves of ovipositor tube-shaped, completely covered by the first valves of ovipositor. Third valves of ovipositor slightly wider, whose length slightly shorter than the first valves of ovipositor. Gonangulum irregular. Sclerotized lobes of the second and third pairs of valves boat-shaped. Anterior arch of second valvifer slender, middle narrow and both sides wide. Basivalvula with semicircular arms, the mid sclerite incompletely separated. Vestibular sclerite weakly sclerotized, apical sclerite vestigial. Transverse sclerotized plate membranous. Brood sac membranous and without sclerotized section (Figure 12N).

Material examined. 20 males and 2 females, Yunnan Prov., Xinping County, Ailaoshan Mountain, Yaonan Village, 12-V-2016, Lu Qiu & Zhi-wei Qiu leg.; 1 female, Yunnan Prov., Pingbian County, Daweishan Mountain, Qianjin Village, 17-V-2016, Lu Qiu & Zhi-wei Qiu leg.

Distribution. China (Yunnan, Guizhou, Guangxi).

Rhabdoblatta krasnovi (Bey-Bienko, 1969)

Figures 10K–N, 12O

Stictolomapra krasnovi Bey-Bienko, 1969: 536; Princis 1971: 1159.
Rhabdoblatta krasnovi Anisyutkin, 2003: 552.

Measurements (mm). Female, overall length: 35.5.

Female. Female different from male and slightly larger. Body dark brown, darker than male. Frons dark brown. Tarsus and pretarsus yellowish, the remaining is dark brown (Figure 10K–N).

Female genitalia. Moderately sclerotized. Ovipositor back to brood sac. Tergal process of the eighth abdominal tergite slender, gradually narrowing from the base to the end, length ca. 1/2 of tergal process of the ninth abdominal tergite. Tergal process of the ninth abdominal tergite robust, linked with the ninth tergum. First valves of ovipositor with apex membranous, inner margin with fine bristles. Second valves of ovipositor tube-shaped, completely covered by the first valves of ovipositor. Third valves of ovipositor wider, length slightly shorter than the first valves of ovipositor. Gonangulum boat-shaped. Sclerotized lobes of the second and third pairs of valves flake-shaped. Anterior arch of second valvifer slender, with concavity in the middle. Basivalvula with semicircular arms, the mid sclerite incompletely separated. Vestibular sclerite membranous, apical sclerite vestigial. Transverse sclerotized plate absent. Brood sac membranous and without sclerotized section (Figure 12O).

Material examined. 7 males and 1 female, Yunnan Prov., Pingbian County, Daweishan Mountain, Hongqi Reservoir, 15-V-2016, Lu Qiu & Zhi-wei Qiu leg.; 10 males and 2 females, Yunnan Prov., Jinping County, Maandi Village, Butterfly Valley, 14-V-2015, Jian-yue Qiu leg.; 1 male, Guangxi Prov., Guilin City, Huaping Nature

Reserve, Hongtan, 11-VI-1963, Ji-kun Yang leg.; 1 male, Chongqing City, Jiangjing, Simianshan Mountain, 1000 m, 20-V-2007, Wei-wei Zhang leg.

Distribution. China (Yunnan, Guangxi, Chongqing).

Rhabdoblatta melancholica (Bey-Bienko, 1954)

Figures 10O, P, 11A–D, 12P

Stictolomapra melancholica Bey-Bienko, 1954: 21; Bey-Bienko 1957: 901; Princis 1967: 686.
Rhabdoblatta melancholica, Anisyutkin, 2003: 550.

Measurements (mm). Female, overall length: 20.3–22.0.

Female. Female similar to male. But individual color variable (Figures 10O, P, 11A–D).

Female genitalia. Moderately sclerotized. Ovipositor extending toward to brood sac. Tergal process of the eighth abdominal tergite slender, length ca. 1/2 of tergal process of the ninth abdominal tergite. Tergal process of the ninth abdominal tergite robust, linked with the ninth tergum. First valves of ovipositor with apex membranous, inner margin with fine bristles. Second valves of ovipositor tube-shaped, completely covered by the first valves of ovipositor. Third valves of ovipositor wider, length slightly shorter than the first valves of ovipositor. Gonangulum irregular. Sclerotized lobes of the second and third pairs of valves flake-shaped. Anterior arch of second valvifer narrow in middle and both sides wider. Basivalvula with semicircular arms, the mid-sclerite separate. Vestibular sclerite membranous, apical sclerite vestigial. Transverse sclerotized plate semicircular. Brood sac membranous and without sclerotized section (Figure 12P).

Material examined. 2 males, Guangxi Prov., Jinxiu County, Dayaoshan Nature Reserve, Hekou Reserve Station, 6–7-VII-2015, Lu Qiu & Qi-kun Bai leg.; 1 female, Guangxi Prov., Jinxiu County, Yinshan Park, 16–17-VII-2015, Lu Qiu & Qi-kun Bai leg.; 1 male, Guizhou Prov., Kuankuoshui Nature Reverse, Baishaogou, 5-VI-2010, Ke-liang Wu & Jia-jia Zhao leg.; 2 males and 1 female, Chongqing Prov., Simianshan Mountain, Ertai, 20-VI-2014, Hao Xu leg.; 10 males and 5 females, Sichuan Prov., Dujiangyan City, Qingchengshan Town, 19-V-2014, Lu Qiu; 50 males, Hubei Prov., Dabieshan Mountain, Taohuachong, 604 m, 27-VI-2014, Xin-ran Li & Yan Shi leg.; 10 females, Zhejiang Prov., Lin'an City, Tianmu Village, 23-VII-2016, Lu Qiu & Zhi-wei Qiu leg.; 2 females, Anhui Prov., Huangshan City, Tangkou Town, 10-VII-2014, Xin-ran Li & Jian-yue Qiu leg.; 8 males and 1 female, Hainan Prov., Diaoluoshan Mountain, 18-IV-2015, Lu Qiu & Qi-kun Bai leg.; 16 males and 2 females, Hainan Prov., Diaoluoshan Mountain, 916 m, 16-IV-2015, Lu Qiu & Qi-kun Bai leg.; 2 males, Fujian Prov., Wuyishan Mountain, 10-VI-1980, Shi-yang Xia leg.; 1 male, Guangdong Prov., Nankunshan Mountain, 15-VI-1981, Qin-jin Liu & Xue-feng Li leg.; 1 male, Jiangxi Prov., Jinggangshan Mountain, 23-V-1981, Jin Liu & Yao Liu leg.; 1 male, Shaanxi Prov., Foping County, 890 m, 26-VI-1999, You-wei Zhang leg.; 1 male, Gansu

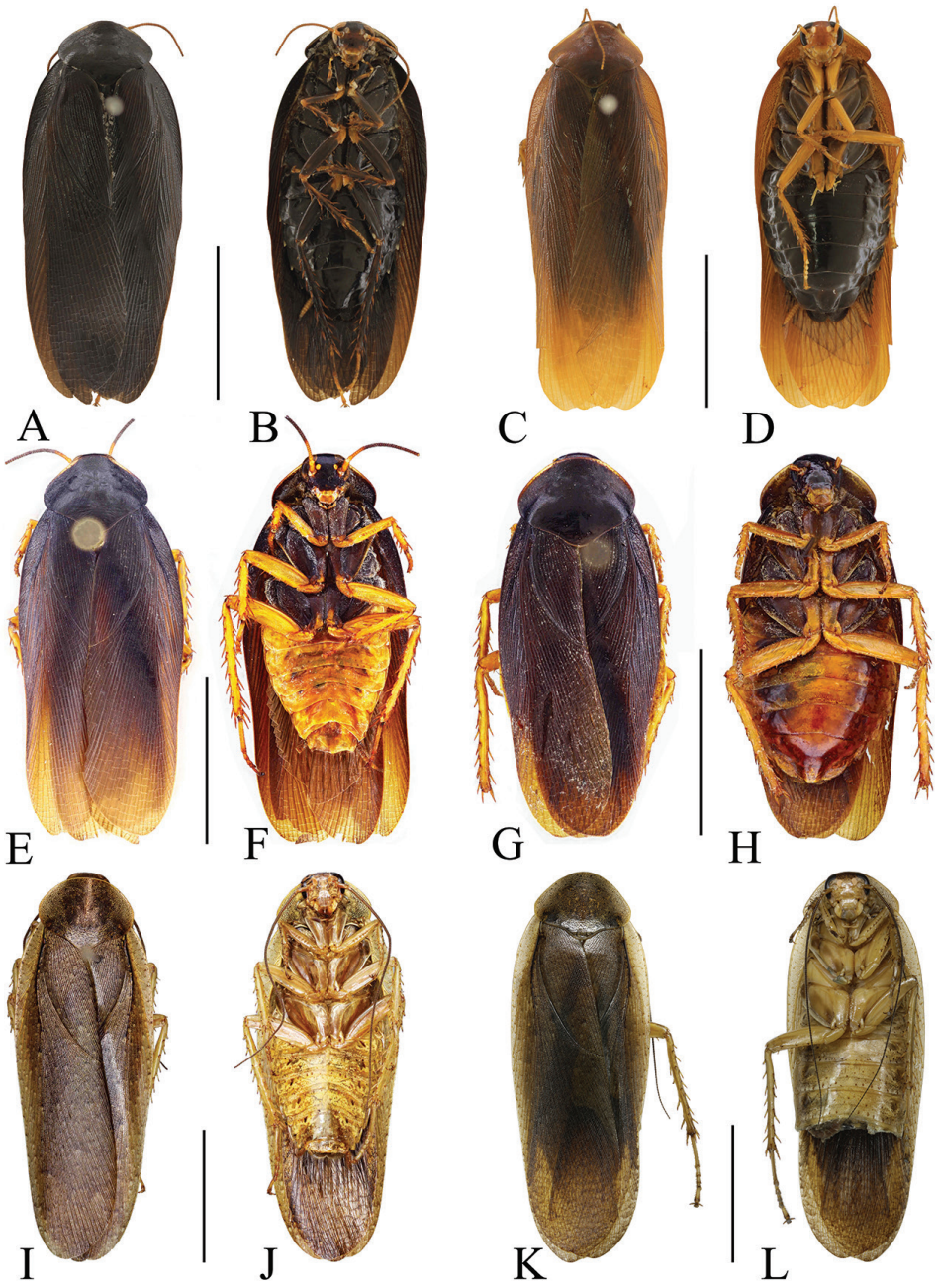

Figure 11. A–D *Rhabdoblatta melancholica* (Bey-Bienko, 1954): **A–D** female **E–H** *Rhabdoblatta bicolor* (Guo, Liu et Li, 2011): **E, F** male, **G, H** female **I–L** *Rhabdoblatta saussurei* (Kirby, 1903): **I, J** male **K, L** female. Scale bars: 1.0 cm.

Prov., Kangxian County, Yangba Town, 1020 m, 10-VII-1999, Hong-jian Wang leg.; l male, Huan Prov., Hengshan Mountain, Mojingtai, 21-VI-1963, Ji-kun Yang leg.; 1 male, Yunnan Prov., Cangyuan County, 750 m, 19-V-1980, Hong-xing Li leg.

Distribution. China (Fujian, Guangxi, Guangdong, Guizhou, Chongqing, Sichuan, Jiangxi, Shaanxi, Gansu, Hunan, Hubei, Zhejiang, Anhui, Yunnan, Hainan).

Rhabdoblatta bicolor (Guo, Liu & Li, 2011)

Figures 11E–H, 12Q

Rhabdoblatta bicolor Guo, Liu et Li, 2011: 723.

Measurements (mm). Female, overall length: 19.0–22.5.

Female. Female similar to male (Figure 11E–H).

Female genitalia. Moderately sclerotized. Ovipositor extends toward brood sac. Tergal process of the eighth abdominal tergite slender, length ca. 1/3 of tergal process of the ninth abdominal tergite. Tergal process of the ninth abdominal tergite robust, linked with the ninth tergum. First valves of ovipositor with apex membranous, inner margin with fine bristles. Second valves of ovipositor tube-shaped, completely covered by the first valves of ovipositor. Third valves of ovipositor wide and flat, length slightly shorter than the first valves of ovipositor. Gonangulum irregular. Sclerotized lobes of the second and third pairs of valves flake-shaped. Anterior arch of second valvifer narrow in middle and both sides wide. Basivalvula with semicircular arms, the mid-sclerite separate. Vestibular sclerite membranous, apical sclerite vestigial. Transverse sclerotized plate semicircle. Brood sac membranous and without sclerotized section (Figure 12Q).

Material examined. 3 males, Zhejiang Prov., Jiangshan City, Shuangxikou Village, 26–27-V-2017, Xin-ran Li, Li-li Wang & Meng Li leg.; 3 males and 1 female, Zhejiang Prov., Jiangshan City, Shuangxikou Village, 26–27-V-2017, Hua Zhang leg.; 1 female, Anhui Prov., Huangshan City, Tangkou Town, 10-VII-2014, Xin-ran Li & Jian-yue Qiu leg.; 1 female, Chongqing Ciry, Pengshui County, Taiyuan Village, 850 m, 10-VII-1989, Long-long Yang leg.; 1 female, Guizhou Prov., Qiandongnan Zhou, Shibing County, Shamuhe, 19-VI-1981, unknown; 1 female, Guangxi Prov., Jinxiu County, Wangshanzhuang, 20-V-1999, Fu-sheng Huang leg.

Distribution. China (Chongqing, Guizhou, Zhejiang, Anhui, Guangxi).

Rhabdoblatta saussurei (Kirby, 1903)

Figure 11I–L, 12R

Stictolomapra saussurei, Princis, 1952: 38; Bey-Bienko 1957: 901; Princis 1967: 683.
Rhabdoblatta saussurei, Anisyutkin, 2003: 555.

Measurements (mm). Female, overall length: 38.0–43.0.

Female. Female similar to male but slightly larger (Figure 11I–L).

Female genitalia. Moderately sclerotized. Ovipositor toward to brood sac. Tergal process of the eighth abdominal tergite vestigial, whose length ca. 1/2 of tergal process of the ninth abdominal tergite. Tergal process of the ninth abdominal tergite robust,

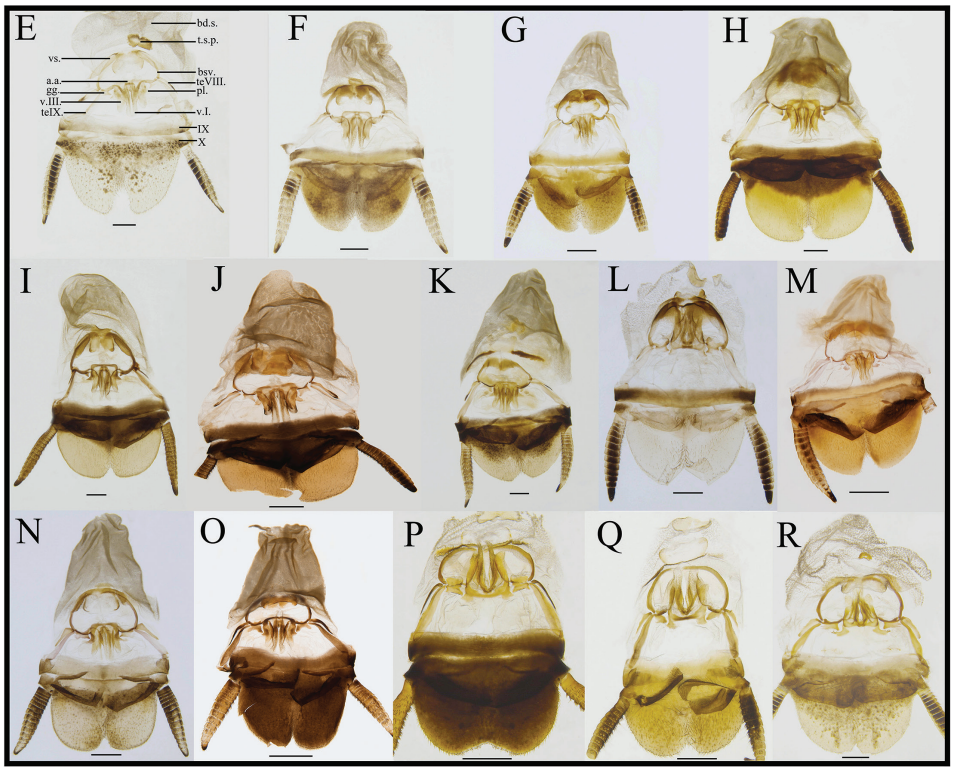

Figure 12. E–R Female genitalia. **E** *Rhabdoblatta monticola* (Kirby, 1903) **F** *Rhabdoblatta atra* Bey-Bienko, 1970 **G** *Rhabdoblatta rattanakiriensis* Anisyutkin, 1999 **H** *Rhabdoblatta* elegans Anisyutkin, 2000 **I** *Rhabdoblatta nigrovittata* Bey-Bienko, 1954 **J** *Rhabdoblatta simulans* Anisyutkin, 2000 **K** *Rhabdoblatta marginata* Bey-Bienko, 1969 **L** *Rhabdoblatta sinuata* Bey-Bienko, 1958 **M** *Rhabdoblatta mascifera* Bey-Bienko, 1969 **N** *Rhabdoblatta incisa* Bey-Bienko, 1969 **O** *Rhabdoblatta krasnovi* (Bey-Bienko, 1969) **P** *Rhabdoblatta melancholica* (Bey-Bienko, 1954) **Q** *Rhabdoblatta bicolor* (Guo, Liu et Li, 2011) **R** *Rhabdoblatta saussurei* (Kirby, 1903). Scale bars: 1.0 mm.

linked with the ninth tergum. First valves of ovipositor with apex membranous, inner margin with fine bristles. Second valves of ovipositor tube-shaped, completely covered by the first valves of ovipositor. Third valves of ovipositor wide and flat, length slightly shorter than the first valves of ovipositor. Gonangulum boat-shaped. Sclerotized lobes of the second and third pairs of valves nearly crescent-shaped, margin with scattered yellow spots. Anterior arch of second valvifer narrow in middle and both sides wider. Basivalvula with semicircular arms, the mid-sclerite weakly sclerotized and separated. Vestibular sclerite membranous, apical sclerite vestigial. Transverse sclerotized plate small, arc-shaped. Brood sac membranous and without sclerotized section (Figure 12R).

Material examined. 1 female, Guangxi Prov., Hechi City, Huanjiang County, Chuanshan Town, Shecun Village, 18–23-VII-2015, Jian-yue Qiu leg.; 1 male, Yunnan Prov., Mengla County, Shangyong Town, Longmen Village, 8–9-V-2015, Jian-yue Qiu leg.; 1 male, Guangdong Prov., Qingyuan City, Lianshan County, 1970, Ping Lin leg.

Distribution. China (Guangxi, Guangdong, Yunnan).

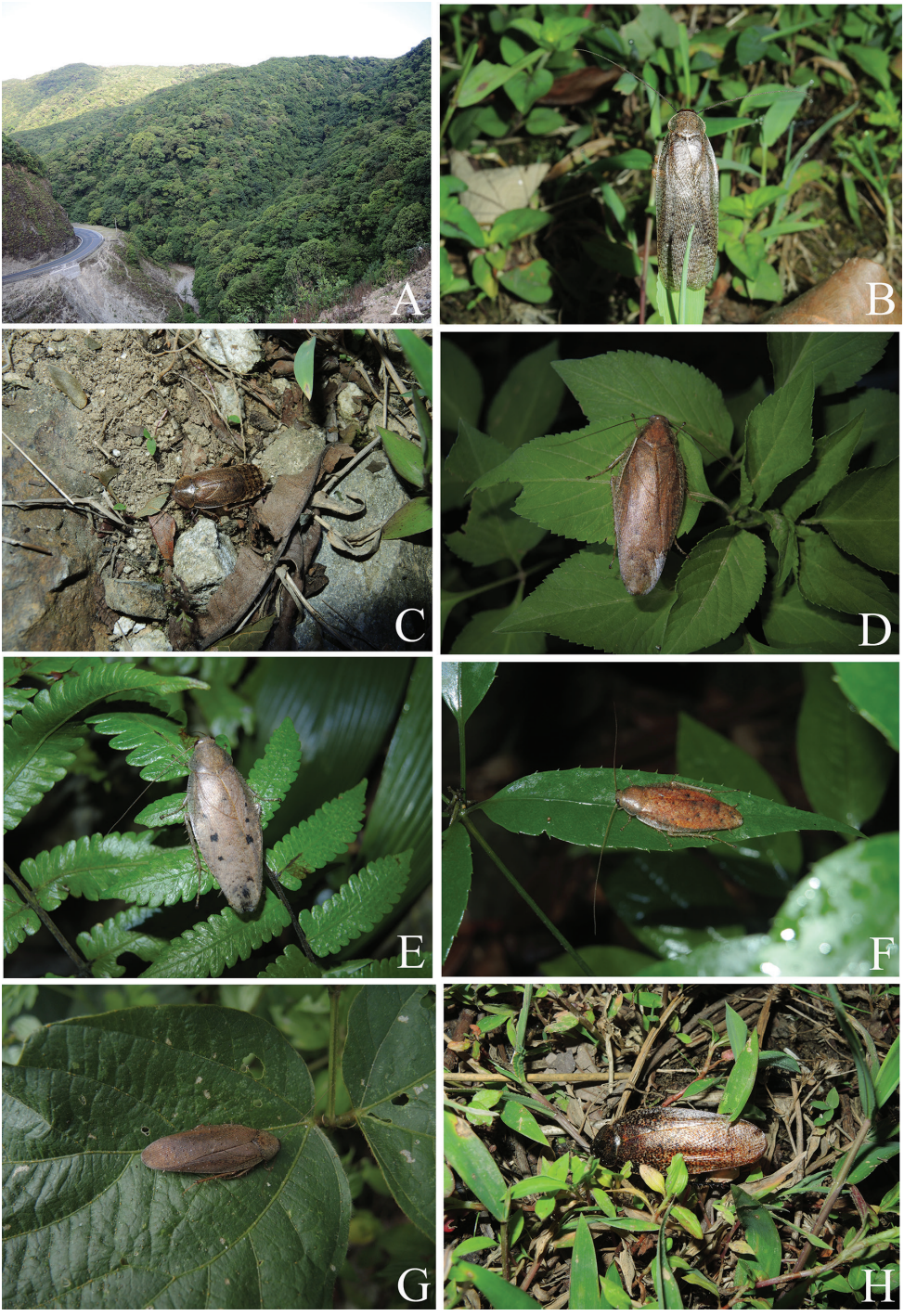

Figure 13. A Habitat of Ailao Mountain, Yunnan Prov. **B** male of *Rh. similsinuata* sp. n. from Ailao Mountain **C** female of *Rh. similsinuata* sp. n. from Ailao Mountain **D** *Rh. monticola* (Kirby, 1903) from Shiwandashan National Forest Park, Guangxi Prov. **E, F** male of *Rh. ecarinata* sp. n. from Yinggeling Nature Reserve, Hainan Prov. **G** *Rh. atra* Bey-Bienko, 1970 from Dayaoshan Nature Reserve, Guangxi Prov. **H** *Rh. densimaculata* sp. n. from Ailao Mountain, Yunnan Prov. All the photographs were taken by Lu Qiu.

Discussion

We examined the utility of DNA barcode data in *Rhabdoblatta* species identification. Some morphospecies have no morphological differences between different individuals, but their intraspecific genetic distance is much larger than that of other morphospecies. Some species (*Rh. marginata*, *Rh. melancholica*, *Rh. nigrovittata*, *Rh. sinuata*) confirm this issue. The maximum intraspecific genetic distance in *Rh. marginata* is 8.8%, while Hebert et al. (2003) indicated that divergence values between species are ordinarily greater than 3%. For example, the intraspecific and interspecific genetic distance of ectobiid cockroaches ranged from 0.0 to 7.0% and 4.6 to 30.8% (Che et al. 2017). The thrips is 0.0 to 7.91% and 8.65% to 31.15% (Rebijith et al. 2014) and the mosquitoes is 0 to 1.67% and 2.3 to 21.8% (Wang et al. 2012). And *Rh. marginata* was detected as having six MOTUs in ABGD and 7 MOTUs in GMYC. Morphologically, although expressing a larger genetic distance, all male samples of *Rh. marginata* showed no obvious variation in the shape of the male genitalia, only delicate differences in body color and size could be found. Hence we put forth the following view: there is a possibility of the existence of cryptic species for the following reasons: intraspecific genetic distances of same morphospecies of different regions reach to 8.8% in *Rh. marginata*, 7% in *Rh. nigrovittata*, 7.6% in *Rh. sinuata*, and 8.4% in *Rh. melancholica*; and the phenomenon of cryptic specie is not rare in cockroaches, such as the species of *Cryptocercus* are mainly delimitaed by molecular data and chromosome number (Burnside et al. 1999; Che et al. 2016; Bai et al. 2018). The view can be explored more by other methods, such as the numbers of chromosome, etc., in the future.

Our results show that DNA-based species delimitation methods perform well in detecting sexual dimorphism and in matching adults with nymphs. Five species have sexual dimorphism (differs of body color, size, spots, or other features): *Rh. rattanakiriensis*, *Rh. nigrovittata*, *Rh. simulans*, *Rh. krasnovi* and *Rh. similsinuata* sp. n. Their males and females were successfully matched using DNA barcoding, and also the nymph of *Rh. marginata* was successfully matched with the adult according to DNA data.

Acknowledgments

We are deeply grateful to the following collectors of specimens: Jianyue Qiu, Hao Xu, Guiqiang Huang (SWU), Zhiwei Dong (Kunming), Chao Wu (Beijing), Weiwei Zhang (Chongqing), and Chao Zhou (Chengdu). And we also thank Dr John Richard Schrock (Department of Biological Sciences, Emporia State University) for revising the English.

This study is supported by the National Natural Sciences Foundation of China (Nos. 31772506 & 31872271), the Program of the Ministry of Science and Technology of the People's Republic of China (2015FY210300) and the Fundamental Research Funds for the Central Universities (XDJK2017B032).

References

Anisyutkin LN (2000) New species of cockroaches of the genus *Rhabdoblatta* Kirby (Dictyoptera, Blaberidae) from southeast Asia. I. Entomological Review 79: 396–417.

Anisyutkin LN (2003) New and little known cockroaches of the genus *Rhabdoblatta* Kirby (Dictyoptera, Blaberidae) from Vietnam and Southern China. II. Entomological Review 82: 609–628.

Anisyutkin LN (2014) On cockroaches of the subfamily Epilamprinae (Dictyoptera: Blaberidae) from South India and Sri Lanka, with descriptions of new taxa. Zootaxa 3847: 301–332. https://doi.org/10.11646/zootaxa.3847.3.1

Bai QK, Wang LL, Wang ZQ, Lo N, Che YL (2018) Exploring the diversity of Asian *Cryptocercus* (Blattodea: Cryptocercidae): species delimitation based on chromosome numbers, morphology and molecular analysis. Invertebrate Systematics 32: 69–91. https://doi.org/10.1071/IS17003

Beccaloni GW (2014) Cockroach Species File Online. Version 5.0/5.0. http://Cockroach.SpeciesFile.org [accessed 5 July 2016]

Bey-Bienko GY (1950) Fauna of the USSR. Insects. Blattodea. Zoologicheskogo Instituta, Akademija Nauk SSSR, Moskva, n.s. 40, 342 pp.

Bey-Bienko GY (1954) Studies on the Blattoidea of Southeastern China. Trudy Zoologicheskogo Instituta, Rossijskaja Akademija Nauk SSSR 15: 5–26.

Bey-Bienko GY (1957) Blattoidea of Szechuan and Yunnan. Communication I. Entomologicheskoe Obozrenie 36: 895–915.

Bey-Bienko GY (1958) Blattoidea of Szechuan and Yunnan. Communication II. Entomologicheskoe Obozrenie 37: 670–690.

Bey-Bienko GY (1969) New genera and species of cockroaches (Blattoptera) from tropical and subtropical Asia. Entomological Review 199: 157–162.

Bey-Bienko GY (1970) Blattoptera of northern Viet-Nam in the collection of the Zoological Institute in Warsaw. Zoologicheskii Zhurnal 49: 362–375.

Burnside CA, Smith PT, Kambhampati S (1999) Three new species of the wood roach, *Cryptocercus* (Blattodea: Cryptocercidae), from the eastern United States. Journal of the Kansas Entomological Society 72: 361–378.

Che YL, Gui SH, Lo N, Ritchie A, Wang ZQ (2017) Species delimitation and phylogenetic relationships in ectobiid cockroaches (Dictyoptera, Blattodea) from China. PLoS ONE 12: 1–25. https://doi.org/10.1371/journal.pone.0169006

Che YL , Wang D, Shi Y, Du XH, Zhao YQ, Lo N, Wang ZQ (2016) A global molecular phylogeny and timescale of evolution for cryptocercus woodroaches. Molecular Phylogenetics and Evolution 98: 201–209. https://doi.org/10.1016/j.ympev.2016.02.005

Drummond AJ, Rambaut A (2007) BEAST: Bayesian evolutionary analysis by sampling trees. BMC Evolutionary Biology 7: 214. https://doi.org/10.1186/1471-2148-7-214

Evangelista D, Buss L, Ware JL (2013) Using DNA barcodes to confirm the presence of a new invasive cockroach pest in New York City. Journal of Economic Entomology 106: 2275–2279. https://doi.org/10.1603/EC13402

Ezard THG, Fujisawa T, Barraclough TG (2009) Splits: Species Limits by Threshold Statistics. http://R-Forge.R-project.org/projects/splits/ [accessed 5 July 2017]

Feng PZ, Shan YY, Wu FZ (1997) Species and control of cockroaches in China. Science and technology of China press, China, 206 pp.

Fujisawa T, Barraclough TG (2013) Delimiting species using single-locus data and the Generalized Mixed Yule Coalescent approach: a revised method and evaluation on simulated data sets. Systematic Biology 62: 707–724. https://doi.org/10.1093/sysbio/syt033

Guo JL, Liu XW, Fang Y, Li K (2011) Taxonomic study of Blattodea in Tianmu Mountain, Zhejiang Province. Zoological Systematics 36(3): 722–731.

Hanitsch R (1915) Malayan Blattidae. Part I. Journal Straits Branch Royal Asiatic Society, 69: 17–178.

Hebert PDN, Cywinska A, Ball SL, Dewaard JR (2003) Biological identifications through DNA barcodes. Proceedings of the Royal Society of London B: Biological Sciences 270: 313–321. https://doi.org/10.1098/rspb.2002.2218

Kimura M (1980) A simple method for estimating evolutionary rates of base substitutions through comparative studies of nucleotide sequences. Journal of Molecular Evolution 16: 111–120. https://doi.org/10.1007/BF01731581

Kirby WF (1903) Notes on Blattidae, with descriptions of new genera and species in the collection of the British Museum, South Kensington. No. II. Annals and Magazine of Natural History 12: 273–280. https://doi.org/10.1080/00222930308678853

Klass KD (1997) The external male genitalia and the phylogeny of Blattaria and Mantodea. Bonner Zoologische Monographien 42: 1–341.

Kumar S, Stecher G, Tamura K (2016) MEGA7: Molecular Evolutionary Genetics Analysis Version 7.0 for Bigger Datasets. Molecular Biology & Evolution 33: 1870–1874. https://doi.org/10.1093/molbev/msw054

Lanfear R, Calcott B, Ho SY, Guindon S (2012) Partitionfinder: combined selection of partitioning schemes and substitution models for phylogenetic analyses. Molecular Biology and Evolution 29: 1695–1701. https://doi.org/10.1093/molbev/mss020

Legendre F, Grandcolas P, Thouzé F (2017) Molecular phylogeny of Blaberidae (Dictyoptera, Blattodea) with implications for taxonomy and evolutionary studies. European Journal of Taxonomy 291: 1–13. https://doi.org/10.5852/ejt.2017.291

Liu XW, Zhu WB, Dai L, Wang HQ (2017) Cockroaches of Southeastern China. Henan Science and Technology Press, China, 228 pp.

Monaghan MT, Wild R, Elliot M, Fujisawa T, Balke M, Inward DJ, Lees DC, Ranaivosolo R, Eggleton P, Barraclough TG, Vogler AP (2009) Accelerated species inventory on Madagascar using coalescent-based models of species delineation. Systematic Biology 58: 298–311. https://doi.org/10.1093/sysbio/syp027

Pons J, Barraclough TG, Gomezzurita J, Cardoso A, Duran DP, Hazell S, Kamoun S, Sumlin WD, Vogler AP (2006) Sequence-based species delimitation for the DNA taxonomy of undescribed insects. Systematic Biology 55: 595–609. https://doi.org/10.1080/10635150600852011

Princis K (1952) Kritisches vergeichnis der Blattarien Chinas und Tibets. Opuscula Entomologica 17: 33–43.

Princis K (1958) Revision der Walkerschen und Kirbyschen Blattarientyen im British Museum of Natural History, London. II. Opuscula Entomologica 23: 59–75.

Princis K (1967) Blattariae: Suborbo [sic] Epilamproidea. Fam.: Nyctiboridae, Epilampridae. In: Beier M (Ed.) Orthopterorum Catalogus. Pars 11. W Junk's-Gravenhage, 617–710.

Princis K (1971) Blattariae: Subordo Epilamproidea; Fam. Ectobiidae (part fourteen). Orthopterorum Catalogus (Uitgeverijs'Gravenhage): 1039–1224.

Puillandre N, Lambert A, Brouillet S, Achaz G (2012) ABGD, Automatic Barcode Gap Discovery for primary species delimitation. Molecular Ecology 21: 1864–1877. hhttps://doi.org/10.1111/j.1365-294X.2011.05239.x

Rebijith KB, Asokan R, Krishna V, Ranjitha HH, Kumar NKK, Ramamurthy VV (2014) DNA Barcoding and Elucidation of Cryptic Diversity in Thrips (Thysanoptera). Florida Entomologist 97: 1328–1347. https://doi.org/10.1653/024.097.0407

Shelford R (1910) Orthoptera (Fam. Blattidae Subfam. Epilamprinae). In: Wytsman P (Ed.) Genera Insectorum 101: 1–21.

Stamatakis A, Hoover P, Rougemont J (2008) A rapid bootstrap algorithm for the RAxML web servers. Systematic Biology 57: 758–771. https://doi.org/10.1080/10635150802429642

Wang G, Li CX, Guo XX, Xing D, Dong YD, Wang ZM, Zhang YM, Liu MD, Zhong Z, Zhang HD, Zhu XJ, Wu ZM, Zhao TY (2012) Identifying the main mosquito species in China based on DNA barcoding. PLoS ONE 7: e47051. https://doi.org/10.1371/journal.pone.0047051

Wang ZZ (2018) The taxonomic and molecular phylogeny study of Epilamprinae from China. Masters thesis, Southwest University, China.

Yue QY, Wu KL, Qiu D, Hu J, Liu D, Wei XY, Chen J, Cook CE (2014) A formal re-description of the cockroach *Hebardina concinna* anchored on DNA barcodes confirms wing polymorphism and identifies morphological characters for field identification. PLoS ONE 9: e106789. https://doi.org/10.1371/journal.pone.0106789

ZooKeys 851: 71–89 (2019)
doi: 10.3897/zookeys.851.32956
http://zookeys.pensoft.net

RESEARCH ARTICLE

A peer-reviewed open-access journal
ZooKeys
Launched to accelerate biodiversity research

Species composition and elevational distribution of bumble bees (Hymenoptera, Apidae, *Bombus* Latreille) in the East Himalaya, Arunachal Pradesh, India

Martin Streinzer[1], Jharna Chakravorty[2], Johann Neumayer[3], Karsing Megu[2,4], Jaya Narah[2], Thomas Schmitt[5], Himender Bharti[6], Johannes Spaethe[7*], Axel Brockmann[4*]

1 *Department of Neurobiology, Faculty of Life Sciences, University of Vienna, Althanstraße 14, 1090 Vienna, Austria* **2** *Department of Zoology, Rajiv Gandhi University, Rono Hills, Doimukh, Papum Pare, Arunachal Pradesh 791112, India* **3** *Obergrubstraße 18, 5161 Elixhausen, Austria* **4** *National Centre for Biological Sciences, Tata Institute of Fundamental Research, Bellary Road, Bengaluru 560065, Karnataka, India* **5** *Department of Animal Ecology and Tropical Biology (Zoology III), Biocenter, University of Würzburg, Am Hubland, 97074 Würzburg, Germany* **6** *Department of Zoology and Environmental Sciences, Punjabi University, Patiala, Punjab 147002, India* **7** *Department of Behavioral Physiology and Sociobiology (Zoology II), Biocenter, University of Würzburg, Am Hubland, 97074 Würzburg, Germany*

Corresponding author: *Martin Streinzer* (martin.streinzer@univie.ac.at);
Johannes Spaethe (johannes.spaethe@uni-wuerzburg.de)

Academic editor: *Michael Ohl* | Received 15 January 2019 | Accepted 9 April 2019 | Published 3 June 2019

http://zoobank.org/4A2B5BAE-8D61-4B8F-AE62-6849D7EA18E8

Citation: Streinzer M, Chakravorty J, Neumayer J, Megu K, Narah J, Schmitt T, Bharti H, Spaethe J, Brockmann A (2019) Species composition and elevational distribution of bumble bees (Hymenoptera, Apidae, *Bombus* Latreille) in the East Himalaya, Arunachal Pradesh, India. ZooKeys 851: 71–89. https://doi.org/10.3897/zookeys.851.32956

Abstract

The East Himalaya is one of the world's most biodiverse ecosystems. However, very little is known about the abundance and distribution of many plant and animal taxa in this region. Bumble bees are a group of cold-adapted and high elevation insects that fulfil an important ecological and economical function as pollinators of wild and agricultural flowering plants and crops. The Himalayan mountain range provides ample suitable habitats for bumble bees. Systematic study of Himalayan bumble bees began a few decades ago and the main focus has centred on the western region, while the eastern part of the mountain range has received little attention and only a few species have been verified. During a three-year survey, more than 700 bumble bee specimens of 21 species were collected in Arunachal Pradesh, the largest of the north-eastern states of India. The material included a range of species that were previously known from a

* Co-senior authors

limited number of collected specimens, which highlights the unique character of the East Himalayan ecosystem. Our results are an important first step towards a future assessment of species distribution, threat, and conservation. Clear elevation patterns of species diversity were observed, which raise important questions about the functional adaptations that allow bumble bees to thrive in this particularly moist region in the East Himalaya.

Keywords
Alpine habitats, Apidae, conservation, global change, insect collection, pollination

Introduction

Bumble bees (Hymenoptera, Apidae, *Bombus* Latreille) are a group of conspicuous, large and colourful bees that mainly inhabit cold and temperate habitats at high latitudes and elevations. Their conspicuous appearance and abundance established them a prime object of study for numerous early naturalists and insect collectors. After extensive revision in the past decades, around 260 species are currently recognized (Williams 1998; updated online at http://www.nhm.ac.uk/research-curation/research/projects/bombus/index.html).

Current global sampling efforts focus on revising the bumble bee taxonomy at the subgeneric level and filling in blank spots in global distribution data for a worldwide IUCN red list assessment of all species (http://iucn.org/bumblebees). The latter is urgently needed, since a number of bumble bee species have recently shown dramatic declines in their abundance and range (Cameron et al. 2011). The reasons are only partially understood and most likely involve pathogen spill-over from commercial breeding and changes in agricultural practices and land use (Cameron et al. 2011, Jacobson et al. 2018). Moreover, climate change poses a threat to many bumble bee species worldwide, especially those adapted to high elevations, due to an ongoing decline of suitable habitats (Hoiss et al. 2012, Kerr et al. 2015, Rasmont et al. 2015).

Bumble bees are pollinators of many wild flowers. They are abundant throughout the season and, due to their thermoregulatory abilities, are able to be active at very low ambient temperatures (Corbet et al. 1993). Thus, they serve as important pollinators, especially in alpine environments and early in the flowering season (Kevan and Baker 1983, Yu et al. 2012). Besides their ecological importance, bumble bees serve as pollinators for many cultivated fruits, vegetables and spices, and thus become economically valuable, as well. In the industrialized western world, more than one million colonies per year are commercially reared and sold for pollination purposes (Velthuis and van Doorn 2006).

Bumble bees are cold adapted and therefore are most diverse and abundant in northern temperate habitats and in alpine environments. The Himalaya, the longest mountain range in the world, is home to a high bumble bee diversity due to its variety of suitable habitats. The mountain range spreads over 3,000 km between the Karakorum in the west and the Patkai and Hengduan mountain ranges in the east. As a major barrier for the south-eastern monsoon winds, it plays an important role in shaping the climate of entire South Asia (Zhisheng et al. 2001, Xu et al. 2009). The climate in the Himalaya is particularly diverse, e.g., the western end shows strong annual temperature

fluctuations and is relatively arid whereas the eastern end is rather stable in the annual temperatures and receives a high amount of annual rainfall. These climatic differences account for distinct differences in flora and fauna (Williams et al. 2010, Rawat 2017). The West Himalaya is characterized by temperate broad leaf forests and arid alpine meadows and pastures at high elevations with relatively low annual rainfall (Rawat 2017). At the eastern end, in contrast, annual precipitation can reach up to 5,000 mm (Dhar and Nandargi 2006) allowing for the formation of subtropical broadleaf forests and moist alpine meadows at higher elevations (Rawat 2017). Previous studies found that the biodiversity in the East Himalaya is particularly rich and the region is considered a global hotspot of biodiversity (Myers et al. 2000).

So far, bumble bee composition was intensively studied in the West (Williams 1991, Saini et al. 2015) and Central Himalaya (Williams et al. 2010). The highest diversity is reported for the Central Himalaya, i.e., from Nepal and the Indian state of Sikkim (Williams 2004, Williams et al. 2010, Saini et al. 2015). Many eastern and western species reach their respective distribution limit in Nepal and the overlap of both faunal regions may contribute to the high bumble bee diversity in this area (Williams et al. 2010). The eastern end of the Himalayan mountain range has received little attention so far and only few actually confirmed records are available (Williams 2004, Saini et al. 2015). The inaccessibility and the harsh climatic conditions cause field work in the East Himalaya to be extremely challenging (see comments in Saini et al. 2015, Rawat 2017) and has certainly contributed to the lack of bumble bee research. Arunachal Pradesh, the northernmost and largest of the Indian northeast region (NER) states, comprises the eastern end of the Himalayan range. Arunachal Pradesh is unique, in that it is densely forested, sparsely populated and agriculturally only extensively managed and thus barely fragmented in its landscape (Tripathi et al. 2016). Previous studies also showed an outstanding biodiversity and high endemism, e.g., in *Rhododendron* species, bamboos, orchids and many other plant taxa (Bhuyan et al. 2003, Mao 2010, Paul et al. 2010, Rawat 2017) as well as butterflies (Sondhi and Kunte 2016).

In this study, the results from the first systematic survey of bumble bees in Arunachal Pradesh are reported based on material collected during three major and a few minor field trips during the years 2015–2017. The survey represents the first phase of a project aiming to (1) document the bumble bee diversity in the East Himalaya to aid global distribution range assessments, (2) identify local pollinators of fruits, vegetables and other crops, and (3) describe functional adaptations that allow bumble bees to thrive in the particularly challenging climate of the East Himalaya.

Materials and methods

Study area and locations

Arunachal Pradesh is the largest of the North-East Indian states and is bordered by Bhutan in the west, the People's Republic of China (Autonomous region of Tibet) in the north, Myanmar in the east and the Indian states of Assam and Nagaland in the south (Fig. 1A).

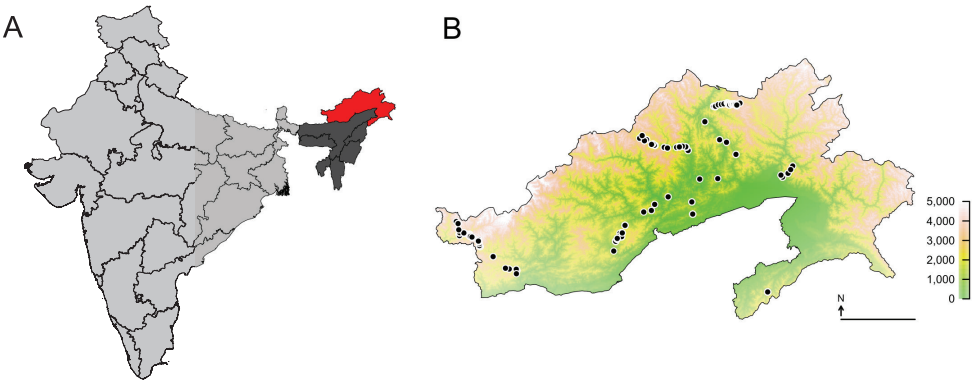

Figure 1. Sampling locations **A** Mainland India (light grey) showing the geographic location of Arunachal Pradesh (red) in the northeast region (NER, dark grey). Outlines denote Indian state borders. **B** Sampling locations within the state of Arunachal Pradesh for three major and a few minor field trips between 2015 and 2017. The locations are projected from GPS data to a SRTM elevation data set. The colour scale refers to elevation and does not reflect vegetation zone. Scale in B represents 100 km.

Bumble bee specimens were collected during three major field surveys in the years 2015–2017. The field trips covered the entire flowering season, pre-monsoon (May–Jun. 2016), during monsoon (Aug.–Sep. 2017), and post-monsoon (Sep.–Oct. 2015). Additional specimens were collected from the entire state during shorter field visits (post-monsoon) in the years 2016–2017 (Fig. 1B). We covered elevations between ca. 200 m and ca. 4,300 m above sea level and habitats ranging from foothill forests (tropical wet evergreen and semi-evergreen), temperate broadleaf forest, subalpine forest up to the alpine zone (Fig. 2; Rawat 2017). GPS locations and elevations were recorded using handheld GPS units or cell phones (Garmin Ltd., CH; Apple Inc., CA, USA) and later verified using Google Earth Pro (version 7.3.2, Google LLC, CA, USA). Elevation was read from the GPS unit and rounded to the closest 10 m for the analysis. Mapping of the occurrence data was performed using GPS coordinates and SRTM digital elevation data (Jarvis et al. 2008) using the "Raster" package (build 2.6-7; Hijmans 2017) in R (build 3.5.1; R Core Team 2018).

Sample collection

Bumble bees were collected by sweep netting and immediately killed with cyanide or ethyl acetate. The specimens were then stored in airtight containers with a few layers of tissue and the addition of a few drops of ethyl acetate to prevent the growth of mould during transport. After the field sampling, specimens were dry-mounted on standard insect pins for identification. The collected specimens were deposited in the NCBS Research Collection (National Centre for Biological Sciences, Tata Institute of Fundamental Research, Bangalore, India) for future reference. A full list of the col-

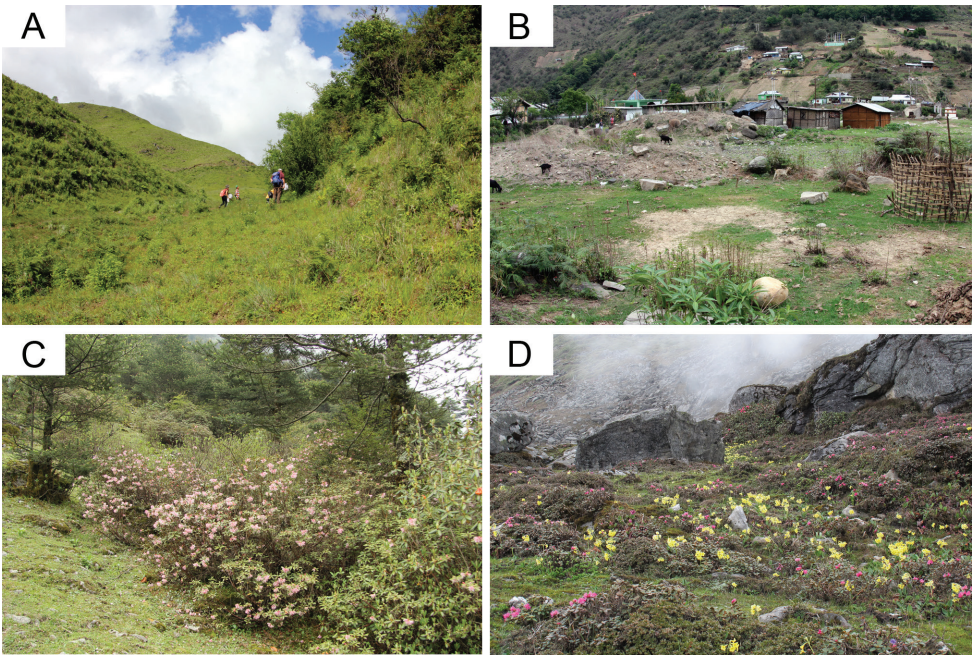

Figure 2. Bumble bee habitats in Arunachal Pradesh **A** Grass–/shrubland at 1,950–2,050 m elevation (Mechuka, West Siang district). Workers of *B. festivus* and *B. luteipes* and workers and males of *B. flavescens* were observed visiting *Cotoneaster* bushes **B** Agricultural crops located in a river valley at 1,500 m elevation (Old Dirang, West Kameng district). Workers of *B. flavescens* were collected from *Punica granatum* flowers **C** Ever-green deciduous *Rhododendron*– and *Pinus*-forests at 3,500 m (Karpo, Tawang district), where we collected queens of *B. festivus* and *B. pressus* **D** Alpine meadow with flowering *Primula* sp. and *Rhododendron* sp. (Se-La Pass, Tawang district) at 4,260 m, where we collected *B. mirus*, *B. lemniscatus*, *B. nobilis*, *B. festivus*, *B. rufofasciatus*, *B. miniatus*, and *B. novus*.

lecting information of the museum specimens is available upon request (curators: Dr Axel Brockmann and Dr Krushnamegh Kunte, NCBS Bangalore). In addition to the collected specimens, some field observations were conducted. Since the observed specimens are not available for later reference, only those are included that could be unambiguously identified and that were from locations where additional voucher specimens of the same species were collected. In addition to the specimens collected in this project, entomological collections were examined for bumble bees from Arunachal Pradesh.

Experimental ethics

Permits to sample bumble bees were issued by the Government of Arunachal Pradesh to Jharna Chakravorty (No. SFRI/APBB/9/2011-846, No. SFRI/APBB/09/2016/1168) and to Himender Bharti (No. CWL/G/13 (95)/2011-12/Pt./2471-75).

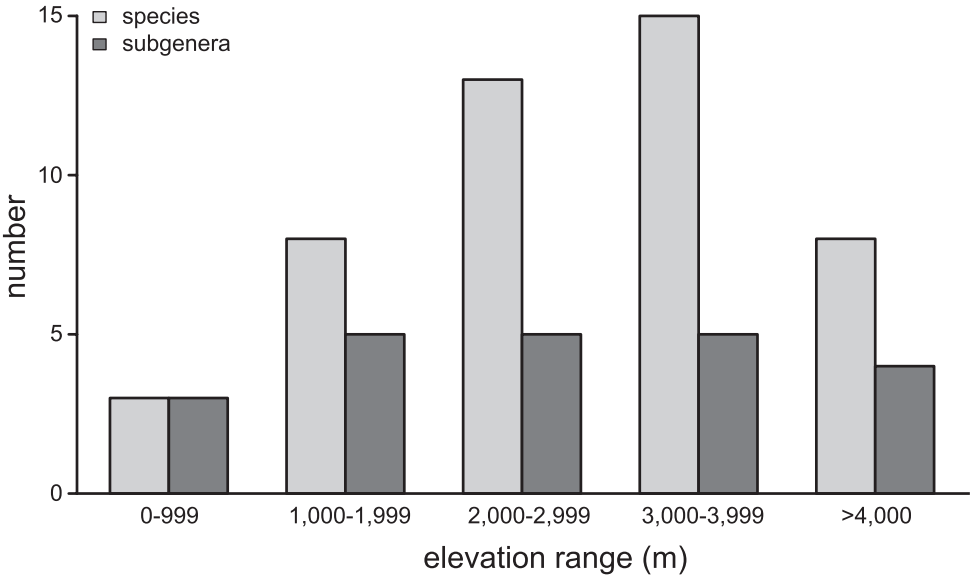

Figure 3. Species and subgeneric diversity along the elevational gradient. In the lowland tropical forest (< 1,000 m) only *B. haemorrhoidalis*, *B. albopleuralis*, and *B. breviceps* were observed. With increasing elevation, we found an increasing diversity of species. The relatively low diversity at > 4,000 m may represent a sampling bias, since only a few locations were accessible.

Species identification

Specimens were identified using published identification keys for adjacent regions, e.g., Kashmir (Williams 1991), Nepal (Williams et al. 2010), Sichuan (Williams et al. 2009), North China (An et al. 2014), and India (Saini et al. 2015). In addition, first descriptions and detailed species accounts were consulted (Linnaeus 1758, Smith 1852a, 1861, 1852b, Bingham 1897, Friese 1905, 1916, 1918, Skorikov 1912, Frison 1933, 1935, Richards 1934, Tkalcu 1968a, 1974).

Results

Between 2015 and 2017, 773 bumble bee specimens were either collected, identified in the field and from photographs or identified in entomological collections (Table 1). A total of 642 specimens were deposited in the NCBS Research Collection. The remaining voucher specimens are part of research project voucher collections (coll. Jaya Narah, Department of Zoology, Rajiv Gandhi University, Itanagar, Arunachal Pradesh – 15 specimens). An additional 16 specimens (collected 2014– 2017) were identified in entomological collections (Department of Entomology, University of Agricultural Sciences, GKVK, Bangalore – 15 specimens, India; NBCS Research Collection, Bangalore, India – 1 specimen).

The sampled region covers most of the state Arunachal Pradesh, and the least amount of sampling was carried out in the eastern-most region (Fig. 1B). Bumble bees were

Table 1. Summary of the collected bumble bee specimens. All specimens (N = 773) are listed that were examined and identified by the authors, including material collected during the field trips, specimens from research and museum collections, and specimens identified in the field. Subgenera are sorted according to their phylogenetic position (Williams et al. 2008). Within the subgenera, species are sorted alphabetically. Elevation has been rounded to the closest 10 m. Abbreviations: **Q** – number of queens, **W** –number of workers, **M** – number of males, † – includes one specimen of unspecified location or imprecise locality information.

Subgenus	Species	Σ	Q	W	M	Elevation	No. Localities
Orientalibombus	*B. funerarius* Smith,1852	3	0	2	1	2,400–3,230	2
	B. haemorrhoidalis Smith,1852	150	13	130	7	400–3,450	48†
Megabombus	*B. albopleuralis* Friese,1916	83	5	70	8	230–2,990	40†
Psithyrus	*B. cornutus* (Frison,1933)	1	0	NA	1	3,280	1
	B. novus (Frison,1933)	1	1	NA	0	4,200	1
Pyrobombus	*B. abnormis* (Tkalcu,1968)	4	4	0	0	3,680–3,940	2
	B. flavescens Smith,1852	31	2	22	7	1,510–3,130	8
	B. hypnorum s.l. (L.,1758)	9	0	4	5	2,850–3,980	5
	B. lemniscatus Skorikov,1912	10	6	1	3	3,500–4,260	5
	B. luteipes Richards,1934	76	0	70	6	1,150–3,500	21
	B. mirus (Tkalcu,1968)	98	17	51	30	2,850–4,260	24
	B. parthenius Richards,1934	20	0	16	4	2,950–3,680	8
	B. pressus (Frison,1935)	41	4	27	10	3,510–4,030	19
Alpigenobombus	*B. breviceps* Smith,1852	34	3	28	3	480–2,790	19
	B. genalis Friese,1918	6	0	6	0	1,560–1,850	3
	B. grahami (Frison,1933)	2	0	2	0	2,710	1
	B. nobilis Friese,1905	75	4	61	10	3,780–4,260	21
Melanobombus	*B. eximius* Smith,1852	9	1	8	0	1,090–1,720	6
	B. festivus Smith,1861	63	4	54	5	1,940–4,260	21
	B. miniatus Bingham,1897	31	1	17	13	2,400–4,240	11
	B. rufofasciatus Smith,1852	26	11	11	4	2,400–4,260	11

collected in a large elevation range from 230 m to 4,260 m above sea level, covering many different habitat types (Fig. 2). There was a clear elevational change in species composition (Fig. 3). In the moist evergreen forest at low elevations (230–1,090 m), only three species from three different subgenera were observed (*B.* (*Orientalibombus*) *haemorrhoidalis* Smith, *B.* (*Megabombus*) *albopleuralis* Friese, *B.* (*Alpigenobombus*) *breviceps* Smith; Table 1, Fig. 3, Suppl. material 1, Figs. S1B, 1C, 1N). Species diversity increased with elevation, climaxing in the region 3,000–4,000 m (mostly corresponding to the subalpine stage) with 15 species from five subgenera (Fig. 3). In total, the collected specimens belong to 21 currently recognized species from six subgenera (Table 1).

Discussion

Bumble bee diversity and species records in the East Himalaya

During several field trips in the Indian state of Arunachal Pradesh, over 700 bumble bee specimens were collected, belonging to 21 species. This survey represents the first systematic study of bumble bee diversity in the East Himalayan range, an area known as a biodiversity hotspot and an important region for conservation priority (Myers et al. 2000).

Previously, extremely few confirmed records for *Bombus* exist for Arunachal Pradesh. Williams (2004) listed eight species and predicted the occurrence of another 13 based on their known distribution. During a 12 year survey of India, and based on a total of almost 7,000 specimens, Saini et al. (2015) only recorded a single species, *B.* (*Melanobombus*) *eximius* Smith, from this state. In the present study, individuals of 21 currently recognized species were collected (Table 1), including almost all of the previously confirmed species (except for *B.* (*Psithyrus*) *turneri* (Richards)) and more than half of the predicted species (Williams 2004). Furthermore, a number of the species collected were previously assumed to either have a West Himalayan, e.g., *B.* (*Melanobombus*) *miniatus* Bingham, *B.* (*Psithyrus*) *novus* (Frison), *B.* (*Pyrobombus*) *parthenius* Richards, or Central Himalayan distribution, e.g., *B.* (*Pyrobombus*) *abnormis* (Tkalcu), *B.* (*Pyrobombus*) *mirus* (Tkalcu), *B.* (*Pyrobombus*) *pressus* (Frison), and were not expected to occur in Arunachal Pradesh (Williams 2004). Many of these species were previously classified as vulnerable, near threatened (Williams & Osborne, 2009) or extremely rare (Saini et al. 2015), are known from a limited number of specimens in entomological collections (PH Williams, personal communication, July 2018), and could not be found in recent field surveys across India (Saini et al. 2015). *Bombus mirus*, a species previously considered confined and rare (Tkalcu 1968a, Williams et al. 2010, Saini et al. 2015) represented ~13% of our entire collection (Table 1).

The present checklist for Arunachal Pradesh, comprising 22 species (including *B. turneri*, which was not found in our survey), places Arunachal Pradesh close to the species diversity found in the West Himalaya, e.g., Kashmir [29 species], Himachal Pradesh [25] and Uttarakhand [22] (Williams 2004, Williams et al. 2010). Contrary to the East Himalaya, these regions were intensively sampled in the last decades (Williams 1991, Saini et al. 2015). Based on the current sampling status and the predictions by Williams (2004), additional species are expected to be found in the future. Alpine regions above the tree line (> 4,000 m) are scarce and not easily accessible in Arunachal Pradesh (Mishra et al. 2006). A more intense survey of these areas will possibly confirm the presence of high elevation species (e.g., *B. waltoni* Cockerell, *B. kashmirensis* Friese, *B. ladakhensis* Richards, *B. keriensis* Morawitz), which are known to occur in south-east Tibet close to the Indian border (Williams 2004, Williams et al. 2015). The East Himalayan region is still vastly under-sampled and more thorough sampling is needed in the entire NER of India at the intersection between the Himalaya and the Patkai mountain range and in the mountain regions of Meghalaya, where the general occurrence of bumble bees is confirmed, but systematic surveys are lacking (Frison 1933, Tkalcu 1974, 1989, Williams 2004, Saini et al. 2015).

Future work in the region will also provide material for taxonomic revisions. Resulting from the large number of specific, subspecific, and infrasubspecific synonyms, a genus wide revision is still under progress (Williams 1998). The treatment by Saini et al. (2015) had not incorporated recent taxonomic changes from sub-generic revisions (e.g., Williams et al. 2011, 2012). While the identity of many species in our study is clear from the morphology, a few nominal taxa are currently treated as belonging to a species complex and future work will likely elucidate their taxonomic treatment (e.g., *B. hypnorum* s. l. (L.); see Tkalcu 1974, Williams et al. 2010).

Mimetic circles

Particularly high local convergence in colour pattern is often found within the genus *Bombus*. It is usually interpreted as Müllerian mimicry (Richards 1929, Williams 2007). One of the most remarkable mimetic circles is found in the Himalaya and South-East Asia, comprising *B.* (*Orientalibombus*) *haemorrhoidalis*, *B.* (*Alpigenobombus*) *breviceps*, *B.* (*Pyrobombus*) *rotundiceps* Friese and the closely related species of the *B.* (*Megabombus*) *trifasciatus*-group (Tkalcu 1968b, Williams 1991, Hines and Williams 2012). The species are members of four different subgenera, corroborating the interpretation that convergent evolution, rather than common ancestry, is responsible for the similarity of the colour pattern.

Three of these species were found in our study area and showed identical colour pattern across Arunachal Pradesh. Two other mimetic groups are present in the region, each comprising members of at least two different subgenera. First, *B.* (*Pyrobombus*) *abnormis*, *B.* (*Pyrobombus*) *hypnorum* s.l. and workers of *B.* (*Melanobombus*) *festivus* Smith all have a brown thorax and a white tail. The second group comprises *B.* (*Pyrobombus*) *flavescens* Smith, *B.* (*Melanobombus*) *eximius* and *B.* (*Alpigenobombus*) *genalis* Friese, which are characterized by black body pile, orange tinted wings and orange-brown cuticle and hairs on the legs (see examples in Fig. 4).

Colour pattern convergence within *Bombus* is also often observed between the parasitic species of the subgenus *Psithyrus* and their preferred host species (Reinig 1935, Williams 2008). The parasitic *B. novus*, recorded in our study, was previously assumed to develop in nests of *B.* (*Melanobombus*) *rufofasciatus* Smith (Tkalcu 1974). Although the female of *B. novus* shares with *B. rufofasciatus* a reddish band of pile just anterior to the white tail, it more closely resembles *B. miniatus* in the pale yellow (rather than white-grey) colouration of the anterior pale bands and the darker tint of the wings (Williams et al. 2010; Suppl. material 2, Fig. S2). Furthermore, the known distribution ranges of the latter match more closely, since both are (mostly) West Himalayan species that reach their eastern distribution limit in Arunachal Pradesh, whereas *B. rufofasciatus* is a widespread Himalayan and Tibetan species (Williams et al. 2015). However, most *Psithyrus* are to some extent flexible in their host choice and more observations, especially from breeding *Psithyrus* in their host nests, are necessary to confirm this suggested parasite-host association (Williams 2008).

Elevational distribution and adaptation

Covering a large range of elevations and habitat types, clear patterns of species-specific elevational ranges were recognised (Fig. 3). A number of species were only found in the subalpine and alpine region at the highest elevations, and they occupied similar elevational niches as in other regions of the world (e.g., *B. abnormis*, *B.* (*Pyrobombus*) *lemniscatus* Skorikov, *B. mirus*, *B.* (*Alpigenobombus*) *nobilis* Friese, *B. pressus*; Williams et al. 2009, 2010). The highest species diversity was observed at elevations between 3,000–4,000 m (Fig. 3), similar to observation in the Central

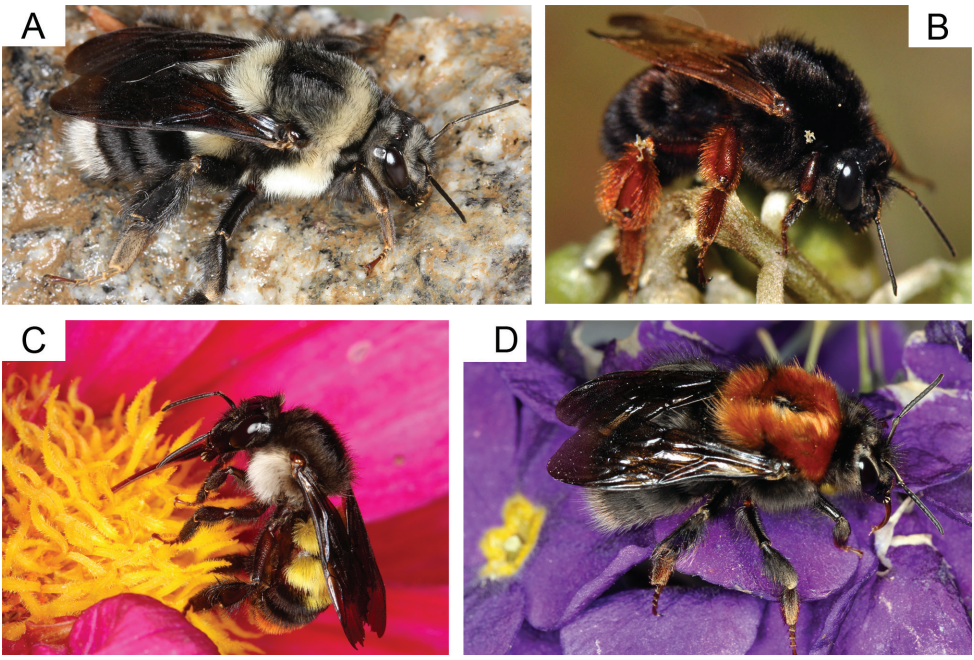

Figure 4. Examples of bumble bee species collected in Arunachal Pradesh **A** *Bombus miniatus* (queen) is a West Himalayan species of the subgenus *Melanobombus* reaching its eastern distribution limit in Arunachal Pradesh **B** *Bombus genalis* (worker), a rare species of the mid-elevation narrowly distributed in the East Himalaya **C** *Bombus albopleuralis* (worker), a widespread Himalayan species that occurs in a large elevational range from the tropical lowlands to the subalpine zone in Arunachal Pradesh **D** *Bombus abnormis* (queen), an elusive and very rare high elevation species of the subgenus *Pyrobombus* narrowly distributed in the East Himalaya.

Himalaya (Williams et al. 2010). However, at the current stage of study, this may also represent a sampling bias from the relatively lower number of sampling points at high elevations. In general, species diversity was found to decline towards lower elevations, and in the lowland (<1,000 m) only three species (*B. haemorrhoidalis*, *B. albopleuralis*, *B. breviceps*) were found. These species also occur at relatively low elevations throughout the Himalaya (lowest elevations: *B. haemorrhoidalis*: Kashmir—1,000 m, Nepal—850 m, *B. albopleuralis*: Kashmir—1,000 m, Nepal—950 m, *B. breviceps*: Nepal—980 m; Williams 1991, Williams et al. 2010). However, our records (*B. haemorrhoidalis*—400m, *B. albopleuralis*—230 m, *B. breviceps*—480 m; see Table 1), represent the lowest elevations at which these species, and bumble bees in general, have ever been recorded in the Himalayan range (Williams 1991, Williams et al. 2010). Bumble bees often occur in a wide elevational range, but only few species reach the tropical lowland, where conditions are usually unfavourable for these cold-adapted bees (Moure and Sakagami 1962, Williams 1991, Gonzalez et al. 2004, Williams et al. 2009).

Our observations may have multiple, not mutually exclusive, explanations. First, the specific climate of the East Himalaya probably allows certain bumble bee species

to thrive at relatively lower elevations (see below). Indeed, there seems to be a gradual decrease in the lower elevation limit from the west to the east that supports this interpretation (Williams 1991, Williams et al. 2010). Second, bumble bee workers can cover large horizontal and, particularly in steep terrain, vertical distances during their foraging trips (Osborne et al. 1999). In Arunachal Pradesh, most of the valleys are particularly steep and both lowland and higher elevations are within the foraging distance of a few kilometres. Therefore, the low records may represent foraging workers from a nest at higher elevation.

B. haemorrhoidalis, *B. albopleuralis*, and *B. breviceps* cover a wide range of elevations and usually were most abundant at medium elevations (Table 1, Suppl. material 1, Figs. S1B, S1C, S1N). Nevertheless, the wide range of foraging habitats, each posing their own challenges with respect to thermoregulation and energy expenditure, is remarkable. Future work is necessary to assess their specific individual and population-level adaptations that provide the plasticity to cover such a diversity in elevations and habitat types, while other species are restricted to narrow ranges and specific habitats (Williams et al. 2009, 2010, 2018). This plasticity (or absence of it) is of particular interest when we seek to understand potential threats due to climate change, making some species more vulnerable than others.

Several physiological and behavioural adaptations have been discussed in the context of elevational adaptation in bumble bees and previous work shows that behavioural plasticity enables quick adaptation to different elevations (Dillon et al. 2006, Dillon and Dudley 2014). At the morphological and physiological level, wing load and wing aspect ratio (Cartar 1992), variation of the cuticular hydrocarbon composition, which prevents bees from desiccation (Foley and Telonis-Scott 2010, Menzel et al. 2017), or changes in mitochondrial density and/or enzyme composition (Harrison et al. 2006, Zhang et al. 2013) may be important factors that vary among populations. However, the specific adaptations that allow these species to thrive in the particularly challenging habitats in the East Himalaya, where the peak of the monsoon season coincides with the peak of colony development in many species, is subject to future investigations. Our survey identified *B. haemorrhoidalis* and *B. albopleuralis* as suitable model taxa to investigate the potential adaptations to specific climatic conditions at the individual and population level. Both species cover a wide range of elevations and are widely distributed in Arunachal Pradesh (Table 1, Suppl. material 1, Figs. S1B, S1D).

Current and Future Threats and Conservation

The discovery of many rare and confined species of bumble bees in Arunachal Pradesh highlights the importance of extensive sampling in remote regions to better understand species distribution and ecological requirements (see also the discussion in Williams 2018). Although many species may be rare or confined to a particular region from a global perspective, they can be locally abundant and/or restricted to a very specific habitat. The specific climate of the East Himalaya, with the high amount of

precipitation, supports a high biodiversity including a large amount of endemism in the region (Myers et al. 2000, Mao 2010). Our observations suggest that some bumble bee species may be particularly adapted to these conditions since they are restricted to a limited region in the East Himalaya (e.g., *B. mirus*, *B. genalis*).

Arunachal Pradesh can currently be considered a remote region without serious recent land use changes, only small-scale agriculture and a low population density (Sikri 2006). However, locally distributed species and high elevation specialists may still be under future threat of extinction, due to changes in agricultural practices or climate change (Xu et al. 2009, Hoiss et al. 2012). Rising temperatures force bumble bee species to shift to higher elevations (Kerr et al. 2015), but high elevation refuges may be limited for species that are adapted to the East Himalayan climate. It is therefore crucial to better understand the adaptations of the local bumble bee fauna to assess their future threat status. Furthermore, it is urgent to develop general strategies for the future to preserve much of this remarkable region (Myers et al. 2000, Government of Arunachal Pradesh 2011).

In the Himalaya, bumble bees serve as important pollinators of many fruits, vegetables, e.g., cardamom (Deka et al. 2011), apple, and other crops (Raj et al. 2012, Raj and Mattu 2014, Tayeng and Gogoi 2018). Understanding their ecological requirements and preserving habitats that support pollinator diversity are crucial for a sufficient agricultural yield, especially in the extensively managed smallholder farming systems that are abundant in Arunachal Pradesh (Kala 2005). Bumble bees are used worldwide as pollinators for commercial fruit and vegetable production (Velthuis and van Doorn 2006). Initially, commercially reared species were used outside their native range, resulting both in the introduction of alien species (Morales et al. 2013) and spread of pathogens to native bumble bee populations (Arbetman et al. 2013). Nowadays, attempts are made to select suitable native species and develop methods for their commercial rearing in many world regions (Padilla et al. 2017). Laboratory rearing of *B. haemorrhoidalis* in India (Chauhan et al. 2014) and *B. breviceps* in Vietnam (Thai and Van Toan 2018) are first steps to produce native bumble bee colonies for commercial pollination. Both species are widespread in Arunachal Pradesh and would make excellent pollinators for many fruit and vegetables (Deka et al. 2011). Additional work is necessary to confirm their potential, or find other promising species for the future development of commercial fruit and crop pollination in Arunachal Pradesh.

Acknowledgements

We are particularly grateful to the students that assisted us during the field collections (Rajiv Gandhi University: Mosses Messar, Mohin Raza Naqvi, Nyaton Kitnya; Punjabi University: Joginder Singh, Sishal Sasi; University of Würzburg: Franziska Bandorf) as well as Tapir Darang, and the drivers and carriers who made the field trips possible.

We further thank the curators of the NCBS Research Collection (Dr K Kunte) and the Collection of the Entomology Department of the University of Agricultural Sciences, GKVK, Bangalore (Prof V Belavadi) for access and support during our

visits to the collections and the permit to use their data for our distribution records. PH Williams (National History Museum, London, UK) provided much valuable information and kindly identified some voucher specimens. We thank J Plant for linguistic support.

The bumble bee mapping project is part of the Chemical Ecology Network Programme funded by the Department of Biotechnology, Govt of India (Sanction number DBT-NER/Agri/24/2013). The field trips of researchers from RGU and NCBS were supported by funds from Chemical Ecology Project. Researchers from the University of Würzburg and Vienna were supported by institutional funds from the University of Würzburg to Thomas Schmitt and Johannes Spaethe. This publication was partially funded by the German Research Foundation (DFG) and the University of Wuerzburg in the funding programme Open Access Publishing.

References

An J, Huang J, Shao Y, Zhang S, Wang B, Liu X, Wu J, Williams PH (2014) The bumblebees of North China (Apidae, *Bombus* Latreille). Zootaxa 3830: 1–89. https://doi.org/10.11646/zootaxa.3830.1.1

Arbetman MP, Meeus I, Morales CL, Aizen MA, Smagghe G (2013) Alien parasite hitchhikes to Patagonia on invasive bumblebee. Biological Invasions 15: 489–494. https://doi.org/10.1007/s10530-012-0311-0

Bhuyan P, Khan ML, Tripathi RS (2003) Tree diversity and population structure in undisturbed and human-impacted stands of tropical wet evergreen forest in Arunachal Pradesh, Eastern Himalayas, India. Biodiversity & Conservation 12: 1753–1773. https://doi.org/10.1023/A:1023619017786

Bingham CT (1897) The Fauna of Bristish India including Ceylon and Burma. Hymenoptera (Vol. I.) – Wasps and Bees. Fauna of British India, including Ceylon and Burma. 539 pp. https://doi.org/10.5962/bhl.title.100738

Cameron SA, Lozier JD, Strange JP, Koch JB, Cordes N, Solter LF, Griswold TL (2011) Patterns of widespread decline in North American bumble bees. Proceedings of the National Academy of Sciences 108: 662–667. https://doi.org/10.1073/pnas.1014743108

Cartar RV (1992) Morphological senescence and longevity: An experiment relating wing wear and life span in foraging wild bumble bees. The Journal of Animal Ecology 61: 225. https://doi.org/10.2307/5525

Chauhan A, Rana BS, Katna S (2014) Successful rearing of bumble bee, *Bombus haemorrhoidalis* Smith year round in Himachal Pradesh in India. International Journal of Current Research 6: 10891–10896.

Corbet SA, Fussell M, Ake R, Fraser A, Gunson C, Savage A, Smith K (1993) Temperature and the pollinating activity of social bees. Ecological Entomology 18: 17–30. https://doi.org/10.1111/j.1365-2311.1993.tb01075.x

Deka TN, Sudharshan MR, Saju KA (2011) New record of bumble bee, *Bombus breviceps* Smith as a pollinator of large cardamom. Current Science 100: 926–928. https://www.jstor.org/stable/24076487

Dhar ON, Nandargi S (2006) Rainfall distribution over the Arunachal Pradesh Himalayas. Weather 59: 155–157. https://doi.org/10.1256/wea.87.03

Dillon ME, Dudley R (2014) Surpassing Mt. Everest: extreme flight performance of alpine bumble-bees. Biology Letters 10: 20130922. https://doi.org/10.1098/rsbl.2013.0922

Dillon ME, Frazier MR, Dudley R (2006) Into thin air: Physiology and evolution of alpine insects. Integrative and Comparative Biology 46: 49–61. https://doi.org/10.1093/icb/icj007

Foley B, Telonis-Scott M (2010) Quantitative genetic analysis suggests causal association between cuticular hydrocarbon composition and desiccation survival in *Drosophila melanogaster*. Heredity 106: 68–77. https://doi.org/10.1038/hdy.2010.40

Friese H (1905) Neue oder wenig bekannte Hummeln des Russischen Reiches (Hymenoptera). Ezhegodnik Zoologicheskago Muzeya 9: 507–523.

Friese H (1916) Über einige neue Hummelformen (*Bombus*), besonders aus Asien (Hym.). Deutsche entomologische Zeitschrift: 10–110. https://doi.org/10.1002/mmnd.48019160205

Friese H (1918) Über Hummelforumen aus dem Himalaja. Deutsche Entomologische Zeitschrift: 81–86.

Frison TH (1933) Records and descriptions of *Bremus* and *Psithyrus* from India (Bremidae: Hymenoptera). Record of the Indian Museum 35: 331–342.

Frison TH (1935) Records, notes and descriptions of *Bremus* from Asia (Bremidae: Hymenoptera). Record of the Indian Museum 37: 339–363.

Gonzalez VH, Mejia A, Rasmussen C (2004) Ecology and nesting behavior of *Bombus atratus* Franklin in Andean highlands (Hymenoptera: Apidae). Journal of Hymenoptera Research 13: 28–36.

Government of Arunachal Pradesh (2011) Arunachal Pradesh state action plan on climate change. Ministry of Environment, Forest and Climate Change, 128 pp. http://www.moef.nic.in/downloads/public-information/Arunachal-Pradesh-SAPCC.pdf.

Harrison J, Frazier MR, Henry JR, Kaiser A, Klok CJ, Rascón B (2006) Responses of terrestrial insects to hypoxia or hyperoxia. Respiratory Physiology and Neurobiology 154: 4–17. https://doi.org/10.1016/j.resp.2006.02.008

Hijmans RJ (2017) raster: Geographic Data Analysis and Modeling.https://rdrr.io/cran/raster/

Hines HM, Williams PH (2012) Mimetic colour pattern evolution in the highly polymorphic *Bombus trifasciatus* (Hymenoptera: Apidae) species complex and its comimics. Zoological Journal of the Linnean Society 166: 805–826. https://doi.org/10.1111/j.1096-3642.2012.00861.x

Hoiss B, Krauss J, Potts SG, Roberts S, Steffan-Dewenter I (2012) Altitude acts as an environmental filter on phylogenetic composition, traits and diversity in bee communities. Proceedings of the Royal Society B: Biological Sciences 279: 4447–4456. https://doi.org/10.1098/rspb.2012.1581

Jacobson MM, Tucker EM, Mathiasson ME, Rehan SM (2018) Decline of bumble bees in northeastern North America, with special focus on *Bombus terricola*. Biological Conservation 217: 437–445. https://doi.org/10.1016/j.biocon.2017.11.026

Jarvis A, Reuter HI, Nelson A, Guevara E (2008) Hole-filled seamless SRTM data V4, International Centre for Tropical Agriculture (CIAT). http://srtm.csi.cgiar.org

Kala CPP (2005) Ethnomedicinal botany of the Apatani in the Eastern Himalayan region of India. Journal of Ethnobiology and Ethnomedicine 1: 1–8. https://doi.org/10.1186/1746-4269-1-11

Kerr JT, Pindar A, Galpern P, Packer L, Potts SG, Roberts SM, Rasmont P, Schweiger O, Colla SR, Richardson LL, Wagner DL, Gall LF, Sikes DS, Pantotoja A (2015) Climate change impacts on bumblebees across continents. Science 349: 177–180. https://doi.org/10.1126/science.aaa7031

Kevan PG, Baker HG (1983) Insects as flower visitors and pollinators. Annual Review of Entomology 28: 407–453. https://doi.org/10.1146/annurev.en.28.010183.002203

Linnaeus C (1758) Systema naturæ per regna tria naturæ, secundum classes, ordines, genera, species, cum characteribus, differentiis, synonymis, locis. 1–824 pp. https://doi.org/10.5962/bhl.title.542

Mao AA (2010) The genus *Rhododendron* in north-east India. Plant Science 7: 26–34. https://doi.org/10.3126/botor.v7i0.4370

Menzel F, Blaimer BB, Schmitt T (2017) How do cuticular hydrocarbons evolve? Physiological constraints and climatic and biotic selection pressures act on a complex functional trait. Proceedings of the Royal Society B: Biological Sciences 284: 20161727. https://doi.org/10.1098/rspb.2016.1727

Mishra C, Madhusudan MD, Datta A (2006) Mammals of the high altitudes of western Arunachal Pradesh, eastern Himalaya: an assessment of threats and conservation needs. Oryx 40: 29–35. https://doi.org/10.1017/S0030605306000032

Morales CL, Arbetman MP, Cameron SA, Aizen MA (2013) Rapid ecological replacement of a native bumble bee by invasive species. Frontiers in Ecology and the Environment 11: 529–534. https://doi.org/10.1890/120321

Moure JS, Sakagami SF (1962) As mamangabas sociais do Brasil (*Bombus* Latr.)(Hym., Apoidea). Studia Entomologica 5: 65–194.

Myers N, Fonseca GAB, Mittermeier RA, Fonseca GAB, Kent J (2000) Biodiversity hotspots for conservation priorities. Nature 403: 853–858. https://doi.org/10.1038/35002501

Osborne JL, Clark SJ, Morris RJ, Williams IH, Riley JR, Smith AD, Reynolds DR, Edwards AS (1999) A landscape-scale of bumble bee foraging study range and constancy using harmonic radar. Journal of Applied Ecology 36: 519–533. https://doi.org/10.1046/j.1365-2664.1999.00428.x

Padilla SC, Cure JR, Riaño DA, Gutierrez AP, Rodriguez D, Romero E (2017) Gyne and drone production in *Bombus atratus* (Hymenoptera: Apidae). Journal of Apicultural Science 61. https://doi.org/10.1515/jas-2017-0005

Paul A, Khan ML, Das AK, Dutta PK (2010) Diversity and distribution of Rhododendrons in Arunachal Himalaya, India. Journal American Rhododendron Society 3: 200–205.

R Development Core Team (2018) R: A language and environment for statistical computing. R Foundation for Statistical Computing. https://www.r-project.org/

Raj H, Mattu VK (2014) Diversity and distribution of insect pollinators on various temperate fruit crops in Himachal Himalaya, India. International Journal of Science and Nature 5: 626–631.

Raj H, Mattu VK, Thakur ML (2012) Pollinator diversity and relative abundance of insect visitors on apple crop in Shimla Hills of Western Himalaya, India. International Journal of Science and Nature 3: 507–513.

Rasmont P, Franzén M, Lecocq T, Harpke A, Roberts Stuart PM, Biesmeijer J, Castro L, Cederberg B, Dvorák L, Fitzpatrick Ú, Gonseth Y, Haubruge E, Mahé G, Manino A, Michez D, Neumayer J, Ødegaard F, Paukkunen J, Pawlikowski T, Potts Simon G, Reemer M,

Settele J, Straka J, Schweiger O (2015) Climatic risk and distribution atlas of European bumblebees. BioRisk 10: 1–236. https://doi.org/10.3897/biorisk.10.4749

Rawat GS (2017) The Himalayan vegetation along horizontal and vertical gradients. In: Prins HT, Namgail T (Eds) Bird Migration in the Himalaya. Cambridge University Press, 189–204. https://doi.org/10.1017/9781316335420.015

Reinig WF (1935) On the variation of *Bombus lapidarius* L. and its cuckoo, *Psithyrus rupestris* Fabr., with notes on mimetic similarity. Journal of Genetics 30: 321–356. https://doi.org/10.1007/BF02982243

Richards OW (1929) Parallel colour variations in humble bees from the Himalayas. Proceedings of the Royal Entomological Society of London 3: 75–76.

Richards OW (1934) Some new species and varieties of oriental humble-bees (Hym. Bombidae). Stylops 3: 87–90. https://doi.org/10.1111/j.1365-3113.1934.tb01552.x

Saini MS, Raina RH, Ghator HS (2015) Indian Bumblebees. Bishen Singh Mahendra Pal Singh, Dehra Dun, 248 pp.

Sikri DK (2006) Census of India 2001 – Arunachal Pradesh Administrative Atlas. Government of India, Delhi.

Skorikov AC (1912) Neue Hummelformen (Hymenoptera, Bombidae) IV. Russkoe éntomologicheskoe Obozrênie 12: 606–610.

Smith F (1852a) Descriptions of some Hymenopterous Insects from Northern India. Transactions of The Royal Entomological Society of London 2: 45–48. https://doi.org/10.1111/j.1365-2311.1852.tb02209.x

Smith F (1852b) Descriptions of some new and apparently undescribed Hymenopterous Insects from North China, collected by R. Fortune, Esq. The Transactions of the Entomological Society of London 2: 33–44. https://doi.org/10.1111/j.1365-2311.1852.tb02208.x

Smith F (1861) Descriptions of new genera and species of exotic Hymenoptera. Journal of Entomology 1: 146–155.

Sondhi S, Kunte K (2016) Butterflies of the Kameng protected area complex, Western Arunachal Pradesh. Journal of Threatened Taxa 8: 9053–9124. https://doi.org/10.11609/jott.2984.8.8.9053-9124

Tayeng M, Gogoi H (2018) Insect pollinators of crops and fruits in Arunachal Pradesh, Eastern Himalaya: Rich diversity in flowers with yellow anther. Proceedings of the Zoological Society 71: 56–62. https://doi.org/10.1007/s12595-016-0185-8

Thai PH, Van Toan T (2018) Beekeeping in Vietnam. In: Chantawannakul P, Williams G, Neumann P (Eds), Asian Beekeeping in the 21st Century. Springer Singapore, Singapore, 247–267. https://doi.org/10.1007/978-981-10-8222-1_11

Tkalcu B (1968a) Neue Arten der Unterfamilie Bombinae der paläarktischen Region (Hymenoptera, Apoidea). Acta Entomologica Bohemoslovaca 65: 21–51.

Tkalcu B (1968b) Revision der vier sympatrischen, homochrome geographische Rassen bildenden Hummelarten SO-Asien (Hymenoptera, Apoidea, Bombinae). Annotationes Zoologicae at Botanicae 52: 1–31.

Tkalcu B (1974) Eine Hummel-Ausbeute aus dem Nepal-Himalaya (Insecta, Hymenoptera, Apoidea, Bombinae). Senckenbergiana Biologica 55: 311–349.

Tkalcu B (1989) Neue Taxa asiatischer Hummeln (Hymenoptera, Apoidea). Acta Entomologica Bohemoslovaca 86: 39–60.

Tripathi RS, Roy A, Kushwaha D, Lalnunmawia F, Lalnundanga, Lalraminghlova H, Lalnunzira C, Roy PS (2016) Perspectives of forest biodiversity conservation in Northeast India. Journal of Biodiversity, Bioprospecting and Development 3: 1–9. https://doi.org/10.4172/2376-0214.1000157

Velthuis HHWW, van Doorn A (2006) A century of advances in bumblebee domestication and the economic and environmental aspects of its commercialization for pollination. Apidologie 37: 421–451. https://doi.org/10.1051/apido:2006019

Williams PH (1991) The bumblebees of the Kashmir Himalaya (Hymenoptera: Apidae, Bombini). Bulletin of the British Museum 60: 1–204. https://biodiversitylibrary.org/page/41055963

Williams PH (1998) An annotated checklist of bumble bees with an analysis of patterns of description (Hymenoptera: Apidade, Bombini). Bulletin of The Natural History Museum (Entomology) 67: 79–152. https://biodiversitylibrary.org/page/40885412

Williams PH (2004) Genus Bombus Latreille. In: Gupta RK (Ed.) An annotated catalogue of the bee species of the Indian Region. Jai Narain Vyas University, Jodhpur. http://www.nhm.ac.uk/research-curation/research/projects/bombus/Williams04_India.pdf

Williams PH (2007) The distribution of bumblebee color patterns worldwide: possible significance for thermoregulation, crypsis, and warning mimicry. Biological Journal of the Linnean Society 92: 97–118. https://doi.org/10.1111/j.1095-8312.2007.00878.x

Williams PH (2008) Do the parasitic *Psithyrus* resemble their host bumblebees in colour pattern? Apidologie 39: 637–649. https://doi.org/10.1051/apido:2008048

Williams PH (2018) In a group of its own? Rediscovery of one of the world's rarest and highest mountain bumblebees, *Bombus tanguticus*. Journal of Natural History 52: 305–321. https://doi.org/10.1080/00222933.2018.1428377

Williams PH, An J, Huang J (2011) The bumblebees of the subgenus *Subterraneobombus*: Integrating evidence from morphology and DNA barcodes (Hymenoptera, Apidae, *Bombus*). Zoological Journal of the Linnean Society 163: 813–862. https://doi.org/10.1111/j.1096-3642.2011.00729.x

Williams PH, Brown MJF, Carolan JC, An J, Goulson D, Aytekin AM, Best LR, Byvaltsev AM, Cederberg B, Dawson R, Huang J, Ito M, Monfared A, Raina RH, Schmid-Hempel P, Sheffield CS, Šima P, Xie Z (2012) Unveiling cryptic species of the bumblebee subgenus *Bombus* s. str. worldwide with COI barcodes (Hymenoptera: Apidae). Systematics and Biodiversity 10: 21–56. https://doi.org/10.1080/14772000.2012.664574

Williams PH, Bystriakova N, Huang J, Miao Z, An J (2015) Bumblebees, climate and glaciers across the Tibetan plateau (Apidae: Bombus Latreille). Systematics and Biodiversity 13: 164–181. https://doi.org/10.1080/14772000.2014.982228

Williams PH, Cameron S, Hines HM, Cederberg B, Rasmont P (2008) A simplified subgeneric classification of the bumblebees (genus *Bombus*). Apidologie 39: 1–29. https://doi.org/10.1051/apido:2007052

Williams PH, Ito M, Matsumura T, Kudo I (2010) The Bumblebees of the Nepal Himalaya (Hymenoptera: Apidae). Insecta Matsumurana 66: 115–151. https://eprints.lib.hokudai.ac.jp/dspace/bitstream/2115/44628/1/05.pdf

Williams PH, Lobo JM, Meseguer AS (2018) Bumblebees take the high road: climatically integrative biogeography shows that escape from Tibet, not Tibetan uplift, is associated

with divergences of present-day *Mendacibombus*. Ecography 41: 461–477. https://doi.org/10.1111/ecog.03074

Williams PH, Osborne JL (2009) Bumblebee vulnerability and conservation world-wide. Apidologie 40: 367–387. https://doi.org/10.1051/apido/2009025

Williams PH, Tang Y, Yao J, Cameron S (2009) The bumblebees of Sichuan (Hymenoptera: Apidae, Bombini). Systematics and Biodiversity 7: 101–189. https://doi.org/10.1017/S1477200008002843

Xu J, Grumbine RE, Shresta A, Eriksson M, Yang X, Wang Y, Wilkes A (2009) The melting Himalayas - cascading effects of climate change on water, biodiversity, and livelihoods. Conservation Biology 23: 520–530. https://doi.org/10.1111/j.1523-1739.2009.01237.x

Yu W-B, Li D-Z, Wang H (2012) Highly efficient pollination by bumblebees ensures seed production in *Pedicularis lachnoglossa* (Orobanchaceae), an early-flowering Himalayan plant. Journal of Systematics and Evolution 50: 218–226. https://doi.org/10.1111/j.1759-6831.2012.00180.x

Zhang Z, Chen B, Zhao D, Kang L (2013) Functional modulation of mitochondrial cytochrome c oxidase underlies adaptation to high-altitude hypoxia in a Tibetan migratory locust. Proceedings of the Royal Society of London B: Biological Sciences 280: 20122758. https://doi.org/10.1098/rspb.2012.2758

Zhisheng A, Kutzbach JE, Prell WL, Porter SC (2001) Evolution of Asian monsoons and phased uplift of the Himalaya-Tibetan plateau since late miocene times. Nature 411: 62–66. https://doi.org/10.1038/35075035

Supplementary material 1

Distribution maps of all collected bumble bee species

Authors: Martin Streinzer, Jharna Chakravorty, Johann Neumayer, Karsing Megu, Jaya Narah, Thomas Schmitt, Himender Bharti, Johannes Spaethe, Axel Brockmann

Data type: occurrence

Explanation note: Distribution maps were created from projecting GPS collection data to an SRTM elevation dataset. The colour scale represents elevation and does not reflect vegetation zone. Each map is accompanied with a histogram of the elevations at which we collected the specimen. Species grouping follows Table 1 of the main text. Scale bar represents 100 km.

Link: https://doi.org/10.3897/zookeys.851.32956.suppl1

Supplementary material 2

Examples of bumble bee species collected in Arunachal Pradesh

Authors: Martin Streinzer, Jharna Chakravorty, Johann Neumayer, Karsing Megu, Jaya Narah, Thomas Schmitt, Himender Bharti, Johannes Spaethe, Axel Brockmann

Data type: species data

Explanation note: (A) Queens of the social parasite *Bombus* (*Psithyrus*) *novus* and two potential host species from the subgenus *Melanobombus*, (B) *B. miniatus* and (C) *B. rufofasciatus*. All species were found to co-occur in the west of Arunachal Pradesh (~ 4,200 m, Se-La Pass environment, Tawang Region).

Link: https://doi.org/10.3897/zookeys.851.32956.suppl2

ZooKeys 851: 91–111 (2019)
doi: 10.3897/zookeys.851.32157
http://zookeys.pensoft.net

RESEARCH ARTICLE

A peer-reviewed open-access journal
ZooKeys
Launched to accelerate biodiversity research

A new species of *Gracixalus* (Anura, Rhacophoridae) from Yunnan, China

Guohua Yu[1,2,*], Hong Hui[3,*], Jian Wang[4,*], Dingqi Rao[3], Zhengjun Wu[1,2], Junxing Yang[3]

1 *Key Laboratory of Ecology of Rare and Endangered Species and Environmental Protection (Guangxi Normal University), Ministry of Education, Guilin 541004, China* **2** *Guangxi Key Laboratory of Rare and Endangered Animal Ecology, College of Life Science, Guangxi Normal University, Guilin 541004, China* **3** *State Key Laboratory of Genetic Resources and Evolution, Kunming Institute of Zoology, Chinese Academy of Sciences, Kunming, Yunnan 650223, China* **4** *College of Life Science and technology, Honghe University, Mengzi, Yunnan 661199, China*

Corresponding author: *Dingqi Rao* (raodq@mail.kiz.ac.cn); *Zhengjun Wu* (wu_zhengjun@aliyun.com); *Junxing Yang* (yangjx@mail.kiz.ac.cn)

Academic editor: *A. Crottini* | Received 9 December 2018 | Accepted 24 March 2019 | Published 3 June 2019

http://zoobank.org/C026C8C4-E425-423D-8AED-FF96182B1975

Citation: Yu G, Hui H, Wang J, Rao D, Wu Z, Yang J (2019) A new species of *Gracixalus* (Anura, Rhacophoridae) from Yunnan, China. ZooKeys 851: 91–111. https://doi.org/10.3897/zookeys.851.32157

Abstract

A new species of the genus *Gracixalus*, *Gracixalus yunnanensis* **sp. n.**, is described based on a series of specimens collected from southwestern and southern Yunnan, China. This species is distinguished from all other known congeners by a combination of the following characters: relatively small body size in adult males (SVL 26.0–34.2 mm); dorsal surface yellow brown or red brown; distinctive conical asperities on dorsum; males with an external subgular vocal sac and linea masculina; throat, chest, and belly nearly immaculate; venter surface orangish with yellow spots, semi-transparent; snout rounded; supratympanic fold distinct; iris bronze; lack of white patch on temporal region; tibiotarsal projection absent; sides of body nearly smooth with no black blotch; finger webbing rudimentary; and toe webbing formula I1.5–2II1.5–2.7III.5–3IV2.5–1.5V. Genetically, the new species diverges from its congeners by 2.2%–14.1% (uncorrected p-distance) and is closest to *G. guangdongensis*. However, the new species can morphologically be separated from *G. guangdongensis* by distinctive conical tubercles on dorsum (versus absent), lateral surface nearly smooth with no black blotches on ventrolateral region (versus lateral surface rough, scattered with tubercles and black blotches on ventrolateral region), snout rounded (versus triangularly pointed), iris bronze (versus iris brown), and ventral surface orangish (versus throat and chest creamy white and belly light brown).

* These authors contributed equally to this work

Keywords
Gracixalus yunnanensis sp. n., taxonomy, Rhacophoridae, southwestern China

Introduction

The genus *Gracixalus* Delorme, Dubois, Grosjean & Ohler, 2005 is known from southern and southwestern China, Vietnam, Laos, Thailand, and Myanmar and contains 16 species including *G. ananjevae* (Matsui & Orlov, 2004), *G. carinensis* (Boulenger, 1893), *G. gracilipes* (Bourret, 1937), *G. guangdongensis* Wang, Zeng, Liu & Wang, 2018, *G. jinggangensis* Zeng, Zhao, Chen, Chen, Zhang & Wang, 2017, *G. jinxiuensis* (Hu, in Hu et al. 1978), *G. lumarius* Rowley, Le, Dau, Hoang & Cao, 2014, *G. medogensis* (Ye & Hu, 1984), *G. nonggangensis* Mo, Zhang, Luo, Zhou & Chen, 2013, *G. quangi*, Rowley, Dau, Nguyen, Cao & Nguyen, 2011, *G. quyeti* (Nguyen, Hendrix, Bohme, Vu & Ziegler, 2008), *G. sapaensis* Matsui, Ohler, Eto & Nguyen, 2017, *G. seesom* Matsui, Khonsue, Panha & Eto, 2015, *G. supercornutus* (Orlov, Ho & Nguyen, 2004), *G. tianlinensis* Chen, Bei, Liao, Zhou & Mo, 2018, and *G. waza* Nguyen, Le, Pham, Nguyen, Bonkowski & Ziegler, 2013 (Frost 2018). Of the 16 members of *Gracixalus*, ten were discovered in last decade (Nguyen et al. 2008, Rowley et al. 2011, Mo et al. 2013, Nguyen et al. 2013, Rowley et al. 2014, Matsui et al. 2015, Matsui et al. 2017, Zeng et al. 2017, Chen et al. 2018, Wang et al. 2018), indicating that species diversity of *Gracixalus* was very poorly understood in the past. Moreover, recent phylogenetic analyses (Matsui et al. 2017, Chen et al. 2018) showed that there are still several unnamed distinct lineages in the group of *G. jinxiuensis*, indicating that species richness of *Gracixalus* remains underestimated.

During recent fieldworks in Yunnan, China, we collected some specimens of a small-sized tree frog, which morphologically can be assigned to the genus *Gracixalus* by the presence of intercalary cartilage between terminal and penultimate phalanges of digits, tips of digits enlarged to discs bearing circummarginal grooves, vomerine teeth absent, inner (first and second) and outer (third and fourth) fingers non-opposable, and an inversed Y-shaped dark brown marking on dorsum (Fei 1999, Rowley et al. 2011, Chen et al. 2018), but morphologically and genetically can be distinguished from all recognized species of genus *Gracixalus*. Thus, we describe these specimens as a new species of *Gracixalus*.

Materials and methods

Sampling

Specimens were collected during fieldworks in Menghai County, Lancang County, and Lvchun County of Yunnan, China in 2014 to 2018 (Fig. 1). They were fixed and then

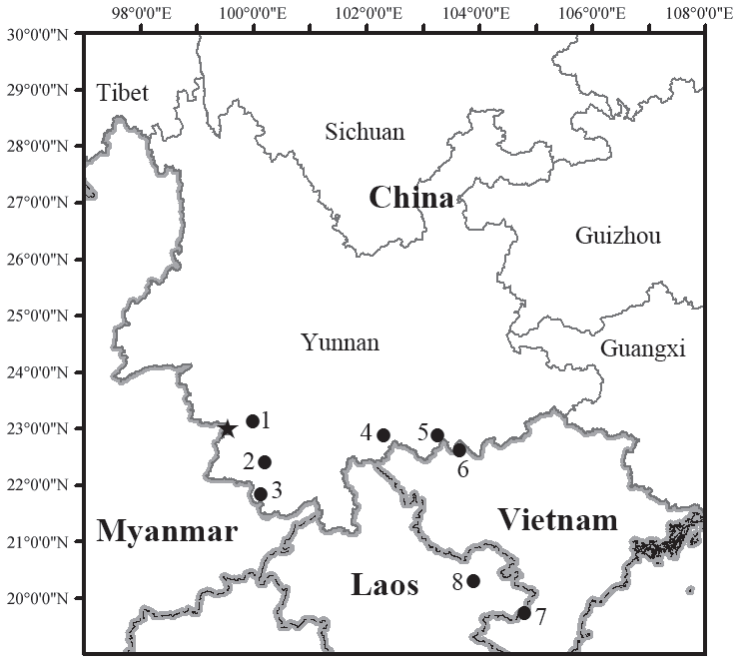

Figure 1. Map showing collection sites of *Gracixalus yunnanensis* sp. n. Star indicates the type locality (Xuelin) and circles indicate Fudong Township (**1**), Fazhanhe Township (**2**), Bada Township (**3**), Mt. Huanglian (**4**), Jinping (**5**), Lao Cai (**6**), Nghe An (**7**), and Houapan (**8**), respectively. Sequences of samples from sites 5–8 came from previous studies.

stored in 80% ethanol after taking photos. Liver tissues were preserved in 99% ethanol. Specimens were deposited at the Kunming Institute of Zoology (KIZ), Chinese Academy of Sciences and Guangxi Normal University (GXNU).

Morphology

Morphometric data were taken using digital calipers to the nearest 0.1 mm. Morphological terminologies follow Matsui et al. (2017) and Wang et al. (2018). Measurements include:

SVL snout-vent length (from tip of snout to vent);
HL head length (from tip of snout to rear of jaws);
HW head width (width of head at its widest point);
SL snout length (from tip of snout to anterior border of eye);
IND internarial distance (distance between nares);
IOD interorbital distance (minimum distance between upper eyelids);

UEW upper eyelid width (maximum width of upper eyelid);
ED eye diameter (diameter of exposed portion of eyeball);
TD tympanum diameter;
FHL forearm and hand length (from elbow to tip of third finger);
THL thigh length (from vent to knee);
TL tibia length (distance from knee to heel);
FL foot length (from proximal end of inner metatarsal tubercle to tip of fourth toe);
TFL length of foot and tarsus (from tibiotarsal joint to tip of fourth toe).

Comparative morphological data of other *Gracixalus* species were taken from their original descriptions or re-descriptions (Boulenger 1893, Hu et al. 1981, Ye and Hu 1984, Matsui and Orlov 2004, Orlov et al. 2004, Nguyen et al. 2008, Rowley et al. 2011, Mo et al. 2013, Nguyen et al. 2013, Rowley et al. 2014, Matsui et al. 2015, Matsui et al. 2017, Zeng et al. 2017, Chen et al. 2018, Wang et al. 2018).

Molecular analyses

Total genomic DNA was extracted from liver tissues. Tissue samples were digested using proteinase K, and subsequently purified following a standard phenol/chloroform isolation and ethanol precipitation. A fragment encoding partial 16S rRNA gene was amplified and sequenced following Yu et al. (2010). All new sequences have been deposited in GenBank under Accession Nos. MK234876–MK234883 (Table 1). Available homologous sequences of *Gracixalus* were obtained from GenBank. *Rhacophorus borneensis* Matsui, Shimada & Sudin, 2013 and *Kurixalus idiootocus* (Kuramoto & Wang, 1987) were selected as outgroups according to Matsui et al. (2017) and sequences of them were also downloaded from GenBank.

Sequences were aligned using MUSCLE with the default parameters in MEGA version 7 (Kumar et al. 2016). Uncorrected pairwise distances between species were calculated in MEGA version 7. The best substitution model was selected using the corrected Akaike Information Criterion (AICc) in jMODELTEST version 2.1.10 (Darriba et al. 2012). Three methods were used to construct phylogeny of the genus *Gracixalus*. Firstly, Bayesian inference (BI) was performed in MRBAYES version 3.2.6 (Ronquist et al. 2012) based on the selected substitution model (TIM2 + I + G). Two runs were performed simultaneously with four Markov chains starting from random tree. The chains were run for 5,000,000 generations and sampled every 100 generations. Convergence and burn-in were checked using the program Tracer version 1.6. (Rambaut et al. 2014) and plot of the generation versus the log likelihood values. The first 25% of the sampled trees were discarded as burn-in and the remaining trees were used to create a consensus tree and to estimate Bayesian posterior probabilities (BPPs). Secondly, maximum likelihood (ML) analysis was conducted in RAXML-HPC version 8.2.10 (Stamatakis 2014) with 1000 rapid bootstrap replicates. Finally, a neighbor-joining (NJ) tree was constructed using PAUP* version 4.0b10 (Swofford 2002) and nodal supports were assessed by 1000 bootstrap replicates.

Table 1. Species used in phylogenetic analysis of this study.

Species	Locality	Voucher no.	GenBank no.
Rhacophorus borneensis	Sabah, Malaysia	BORN 22410	AB781693
Kurixalus idiootocus	Taiwan, China	KUHE 12979	AB933306
Gracixalus ananjevae	Nghe An, Vietnam	VNMN 03012	JN862546
Gracixalus gracilipes	Ha Giang, Vietnam	AMNH A163897	DQ283051
	Pingbian, Yunnan, China	060821196Rao	GQ285668
	Lao Cai, Vietnam	AMS R 177672	KT374014
Gracixalus guangdongensis	Hunan, China	CIB HN201108200	LC011936
	Guangdong, China	SYS a004902	MG520193
	Guangdong, China	SYS a005750	MG520197
Gracixalus jinggangensis	Mt. Jinggang, Jiangxi	SYS a003186	KY624587
Gracixalus jinxiuensis	Jinxiu, Guangxi, China	SYS a002182	KY624584
	Jinxiu, Guangxi, China	SYS a002183	KY624585
	Jinxiu, Guangxi, China	KIZ 060821013	EF564524
	Jinxiu, Guangxi, China	KIZ 061210YP	EU215525
Gracixalus lumarius	Kon Tum, Vietnam	AMS R 176202	KF918412
Gracixalus nonggangensis	Guangxi, China	NHMG 200910010	JX841318
Gracixalus quyeti	Cha Noi, Vietnam	VNUH 160706	EU871428
Gracixalus quangi	Nghe An, Vietnam	AMS R173417	JN862539
Gracixalus sapaensis	Lao Cai, Vietnam	MNHN 1999.5961	AY880503
	Lai Chau, Vietnam	IEBR 2351	EU871425
	Lao Cai, Vietnam	CIB XM-439	GQ285670
	Lao Cai, Vietnam	KUHE 46401	LC011938
	Lao Cai, Vietnam	KUHE 46402	LC011939
	Lao Cai, Vietnam	MNHN 1999.5966	LC140970
	Lao Cai, Vietnam	VNMN 4211	LC140971
	Lao Cai, Vietnam	VNMN 4212	LC140972
	Lao Cai, Vietnam	VNMN 4358	LC140973
Gracixalus seesom	Kanchanaburi, Thailand	KUHE 35084	LC011932
Gracixalus supercornutus	Kon Tum, Vietnam	AMS R173887	JN862545
	Gia Lai, Vietnam	AMS R176287	KT374016
Gracixalus tianlinensis	Guangxi, China	NHMG 1705015	MH117960
	Guangxi, China	NHMG 1705016	MH117961
Gracixalus waza	Cao Bang, Vietnam	IEBR A.2012.2	JX896681
	Cao Bang, Vietnam	VNMN A.2012.2	JX896684
Gracixalus sp.	Wenshan, Yunnan, China	03320Rao	GQ285669
Gracixalus yunnanensis sp. n.	Houapan, Laos	KUHE 32453	LC011937
	Lao Cai, Vietnam	VNMN 4355	LC140985
	Lao Cai, Vietnam	VNMN 4357	LC140986
	Lao Cai, Vietnam	VNMN 4371	LC140987
	Nghe An, Vietnam	AMS R173454	JN862547
	Jinping, Yunnan, China	KIZ 060821126	EF564525
	Lvchuan, Yunnan, China	GXNU YU000060	MK234876
	Bada, Menghai, Yunnan, China	KIZ 20160216	MK234877
	Xuelin, Lancang, Yunnan, China	KIZ 20160222	MK234878
	Xuelin, Lancang, Yunnan, China	KIZ 20160223	MK234879
	Fudong, Lancang, Yunnan, China	KIZ 20160226	MK234880
	Fazhanhe, Lancang, Yunnan, China	KIZ 20160228	MK234881
	Fazhanhe, Lancang, Yunnan, China	KIZ 20160229	MK234882
	Fazhanhe, Lancang, Yunnan, China	KIZ 20160230	MK234883

Results

The obtained alignment of 16S rRNA sequences is 543 bp in length after cutting off both ragged sides. The newly collected samples from Bada, Xuelin, Fudong, Fazhanhe, and Lvchun of Yunnan, China form a distinct lineage together with samples from Houapan of Laos (KUHE 32453), Nghe An (AMS R173454) and Lao Cai (VNMN 4355, 4357, 4371) of Vietnam, and Jinping of Yunnan (KIZ 060821126) that were sequenced by previous studies (Yu et al. 2008, Rowley et al. 2011, Matsui et al 2015, Matsui et al. 2017) (Figs 2, 3). Both Bayesian inference and Maximum likelihood analyses recovered this lineage as the sister to the clade consisting of *G. ananjevae* and *Gracixalus* sp. (GQ285669) with weak support (Fig. 2), whereas the NJ analysis revealed that it is closest to *G. guangdongensis* with weak support (Fig. 3). Average uncorrected pairwise distances (p-distance) between the new species and other species ranged from 2.2% (*G. guangdongensis*) to 14.1% (*G. lumarius*) (Table 2).

Morphologically, these newly collected specimens can be distinguished from *G. guangdongensis* by a series of characters, including distinctive conical tubercles on dorsum (versus absent), lateral surfaces nearly smooth with no black blotches on ventrolateral region (versus lateral surfaces rough, scattered with tubercles and black blotches on ventrolateral region), snout rounded (versus triangularly pointed), iris bronze (versus iris brown), and ventral surface orangish (versus throat and chest creamy white and belly light brown). These specimens also differ from other members of *Gracixalus* in a series of characters. Herein we describe these specimens as a new species.

Table 2. Uncorrected p-distances (%) between *Gracixalus* species estimated from 16S rRNA sequences.

	Species	1	2	3	4	5	6	7	8	9	10	11	12	13	14	15	16
1	*Gracixalus yunnanensis* sp. n.	–															
2	*G. ananjevae*	3.9	–														
3	*Gracixalus* sp. (GQ285669)	5.1	2.3	–													
4	*G. sapaensis*	4.7	6.0	6.6	–												
5	*G. quangi*	8.0	9.6	9.5	9.1	–											
6	*G. supercornutus*	9.2	10.9	10.7	10.5	3.0	–										
7	*G. nonggangensis*	7.1	8.8	8.9	7.9	10.5	11.5	–									
8	*G. waza*	6.3	8.7	9.3	7.3	11.6	12.8	2.5	–								
9	*G. lumarius*	14.1	14.5	14.6	15.9	14.3	15.3	16.0	16.0	–							
10	*G. gracilipes*	10.3	11.0	11.3	10.4	5.2	6.2	12.4	13.3	15.0	–						
11	*G. jinxiuensis*	6.0	7.3	7.5	7.2	9.6	10.9	7.7	7.9	16.1	11.4	–					
12	*G. jinggangensis*	5.0	7.3	7.7	6.3	8.0	9.5	7.5	7.5	14.5	11.3	7.0	–				
13	*G. seesom*	8.6	10.4	9.7	8.8	6.0	6.7	10.2	10.1	16.0	6.1	9.6	9.9	–			
14	*G. quyeti*	10.5	11.4	11.0	10.9	6.5	6.1	11.2	12.2	14.0	7.3	10.2	11.1	8.1	–		
15	*G. tianlinensis*	4.3	6.3	6.5	3.0	9.4	10.5	7.2	6.4	14.8	10.3	5.9	6.5	7.8	10.0	–	
16	*G. guangdongensis*	2.2	4.6	5.4	5.0	7.8	9.5	7.2	6.7	14.2	10.1	5.6	5.3	8.3	10.6	4.4	–

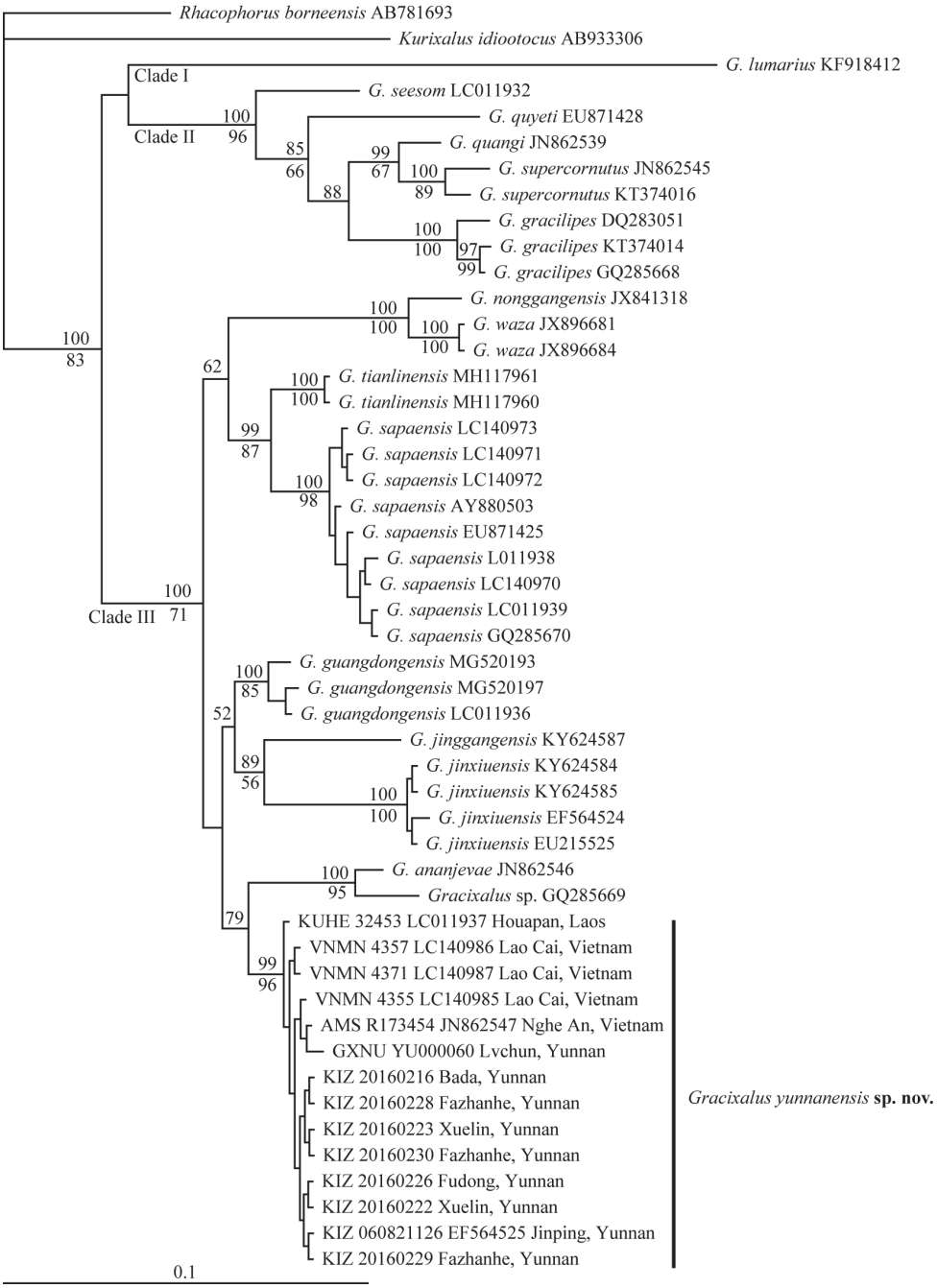

Figure 2. Bayesian phylogram of *Gracixalus* inferred from 543 bp of 16S rRNA gene. Numbers above and below branches are Bayesian posterior probabilities and ML bootstrap values (only values above 50% are shown), respectively.

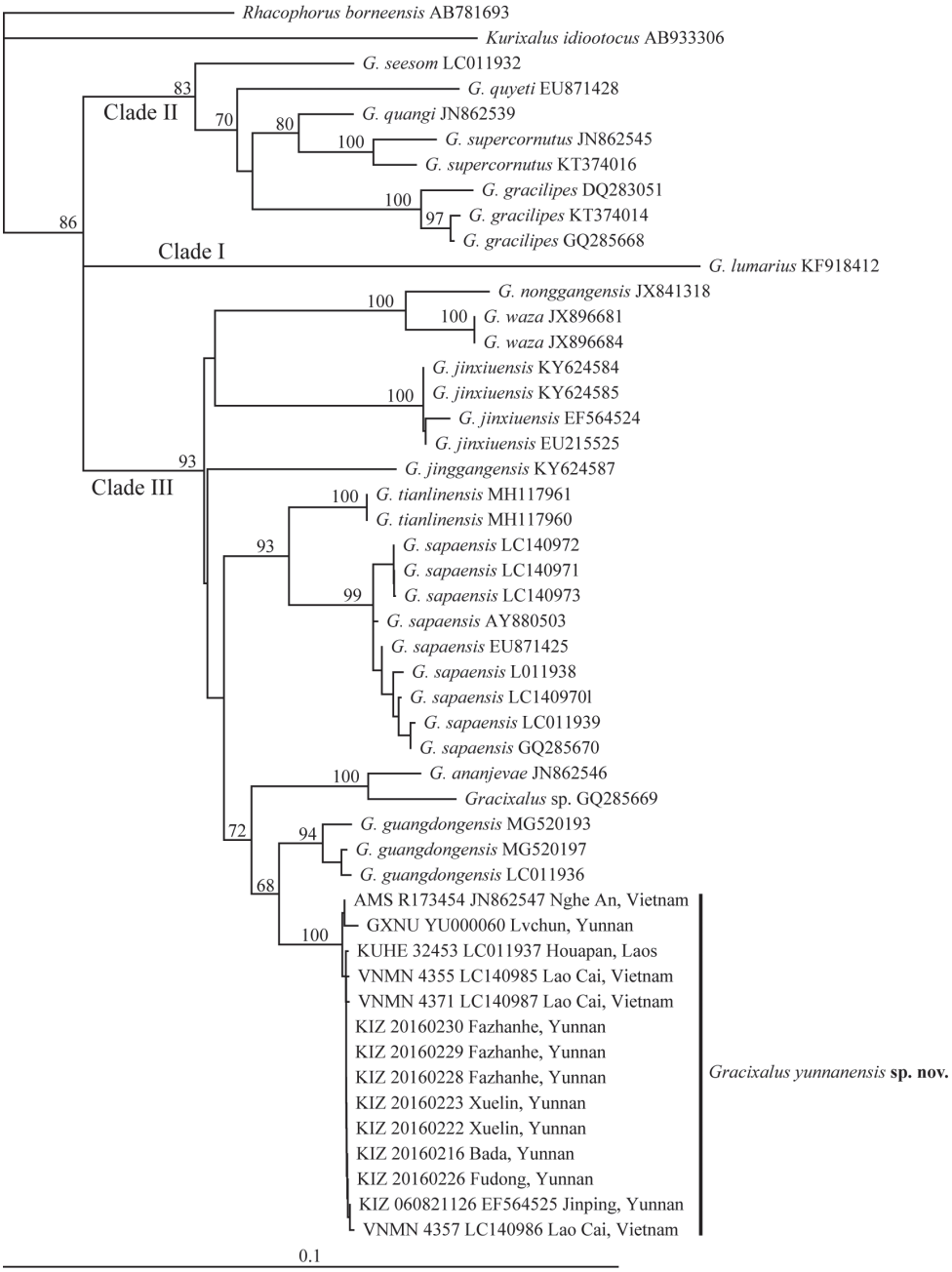

Figure 3. Neighbor-joining (NJ) tree of *Gracixalus* inferred from 543 bp of 16S rRNA gene. Numbers above branches are bootstrap values (only values above 50% are shown).

***Gracixalus yunnanensis* sp. n.**
http://zoobank.org/1D19A62E-B4B2-4EDA-975D-4DCFD58DEDAD
Figs 4–6

Type material. ***Holotype.*** KIZ 20160222, an adult male, collected at 21:05 on 1 June 2017 by Hong Hui from Xuelin Township, Lancang County, Yunnan Province, China (23°0'39.4"N, 99°31'54"E, 1864 m elevation).

Paratypes. Seven adult males: KIZ 20160223 collected at 21:05 on 1 June 2017 by Hong Hui from the type locality; KIZ 20160216 collected at 21:00 on 7 June 2014 by Hong Hui from Bada Township, Menghai County, Yunnan Province, China (21°50'8.9"N, 100°6'57.8"E, 1870 m elevation); KIZ 20160226 collected at 21:50 on 27 May 2017 by Hong Hui from Fudong Township, Lancang County, Yunnan Province, China (23°7'13.6"N, 99°58'33.9"E, 2166 m elevation); KIZ 20160228–20160230 collected at 21:40–22:15 on 10 June 2017 by Hong Hui from Fazhanhe Township, Lancang County, Yunnan Province, China (22°24'3.4"N, 100°12'4.2"E, 1822 m elevation); and GXNU YU000060 collected at 21:00 on 7 June 2018 by Jian Wang from Mt. Huanglian, Lvchun County, Yunnan Province, China (22°53'N, 102°18'E, 1918 m elevation).

Etymology. The specific epithet *yunnanensis* refers to the distribution of this species in China, Yunnan Province.

Diagnosis. The new species is assigned to genus *Gracixalus* based upon molecular data and the following morphological characters: the presence of intercalary cartilage between terminal and penultimate phalanges of digits, tips of digits enlarged to discs bearing circummarginal grooves, vomerine teeth absent, inner (first and second) and outer (third and fourth) fingers non-opposable, and an inversed Y-shaped dark brown marking on dorsum (Fei 1999, Rowley et al. 2011, Chen et al. 2018). The new species is distinguished from its congeners by a combination of 1) SVL 26.0–34.2 mm in males; 2) dorsal surface yellow brown or red brown; 3) distinctive conical tubercles on dorsum; 4) males with an external subgular vocal sac; 5) throat granular; 6) finger webbing rudimentary; 7) linea masculina, a band of connective tissue between the rectus abdominus muscle and oblique abdominus muscle, present in males; 8) tibiotarsal articulation reaching eye; 9) snout rounded; 10) white patch absent on temporal region; 11) tibiotarsal projection absent; 12) supratympanic fold distinct; 13) ventral surface orangish, nearly immaculate, and semi-transparent; 14) nuptial pads present on finger I; 15) heels overlapping when legs at right angle to body; 16) iris bronze; and 17) body sides nearly smooth with no black blotch.

Description of holotype. Adult male (SVL 29.7 mm); head wider (HW 10.9 mm) than long (HL 9.5 mm); snout rounded, slightly projecting beyond margin of lower jaw in ventral view, rounded in profile; canthus rostralis rounded; loreal region oblique, slightly concave; nostril oval, protuberant, closer to tip of snout than eye; IND (2.9 mm) slightly narrower than IOD (3.0 mm) and wider than UEW (2.5 mm); eye large, horizontal diameter (ED 4.2 mm) equal to snout length (SL 4.2 mm); pupil oval, horizontal; pineal ocellus absent; tympanum distinct, diameter (TD 1.5 mm)

smaller than half of ED; supratympanic fold distinct, extending from posterior corner of eye to above insertion of arm; vomerine teeth absent; tongue notched posteriorly; a pair of vocal sac slits on floor of mouth at both corners; an external subgular vocal sac.

Forelimb relatively robust; length of forearm and hand (FHL 14.1 mm) 47% of SVL; relative length of fingers I < II < IV < III; tips of all fingers expanded into discs with circummarginal grooves; disc of third finger large, slightly wider than tympanum; nuptial pads present on base of finger I; webbing between fingers rudimentary; subarticular tubercles prominent, rounded, single, formula 1, 1, 2, 2; supernumerary tubercles present; an inner metacarpal tubercle, oval; one outer metacarpal tubercle, rounded.

Heels overlapping when legs at right angle to body; tibiotarsal articulation reaching to middle of eye when hindlimb adpressed to body; relative length of toes I < II < III < V < IV; tips of toes expanded into discs with circummarginal grooves; discs of toes smaller than those of fingers; toes webbed, webbing formula I1.5–2II1.5–2.7III.5–3IV2.5–1.5V following Savage (1975); subarticular tubercles distinct and rounded, formula 1, 1, 2, 3, 2; supernumerary tubercles present; inner metatarsal tubercle oval; outer metatarsal tubercle absent.

Dorsal surface scattered with many small conical tubercles on head, upper eyelids, and dorsum; flanks of body and dorsal surface of limbs smooth, few small conical tubercles on hindlimbs and forearms; throat, chest, belly, and venter of thigh granulated; few small conical tubercles scattered on venter of thigh, tibia, and forearm.

Coloration of holotype. In life, iris bronze; dorsal surface yellow brown with a dark brownish Y-shaped marking across back, covering interorbital region and posterior eyelids, bifurcating into two branches on the shoulder, and reaching the posterior of the back; limbs dorsally brown with dark brown bars; sides of head faint brown; flanks yellow brown, mottled with faint pink on lower part; minute dark spots densely scattered on lower part of flanks, temporal region, and upper jaw; skin of ventral surface semi-transparent, orangish with yellow spots; nuptial pads and discs faint yellow; linea masculina visible, white (Fig. 4b).

In preservative, color faded, pattern same as in life. Dorsal surface grayish brown, with a darker brown Y-shaped marking; dorsal side of limbs barred with dark brown; ventral surface of throat, chest, belly, forelimbs, and hindlimbs faded to whitish.

Morphological variation. Measurements are shown in Table 3. Because the holotype and paratypes of the new species are all male, sexual dimorphism could not be determined. IOD is slightly wider than IND in holotype and most paratypes with the exception of KIZ 20160228, and TL is longer than FL in holotype and most paratypes with exceptions of KIZ 20160226 and KIZ 20160229.

Color of dorsal and ventral surfaces varied among individuals. Dorsal ground color of the holotype and four paratypes (KIZ 20160216, KIZ 20160223, KIZ 20160228, and KIZ 20160230) is yellow brown, and dorsal ground color of remaining paratypes (KIZ 20160226, KIZ 20160229, and GXNU YU000060) is red brown. Ventral surface of all specimens is nearly immaculate with the exception of paratype GXNU YU000060, which has dark marbling on throat, chest, and belly (Fig. 6). Conical tubercles on dorsum of specimens with red brown ground color are more distinct visually (Fig. 6).

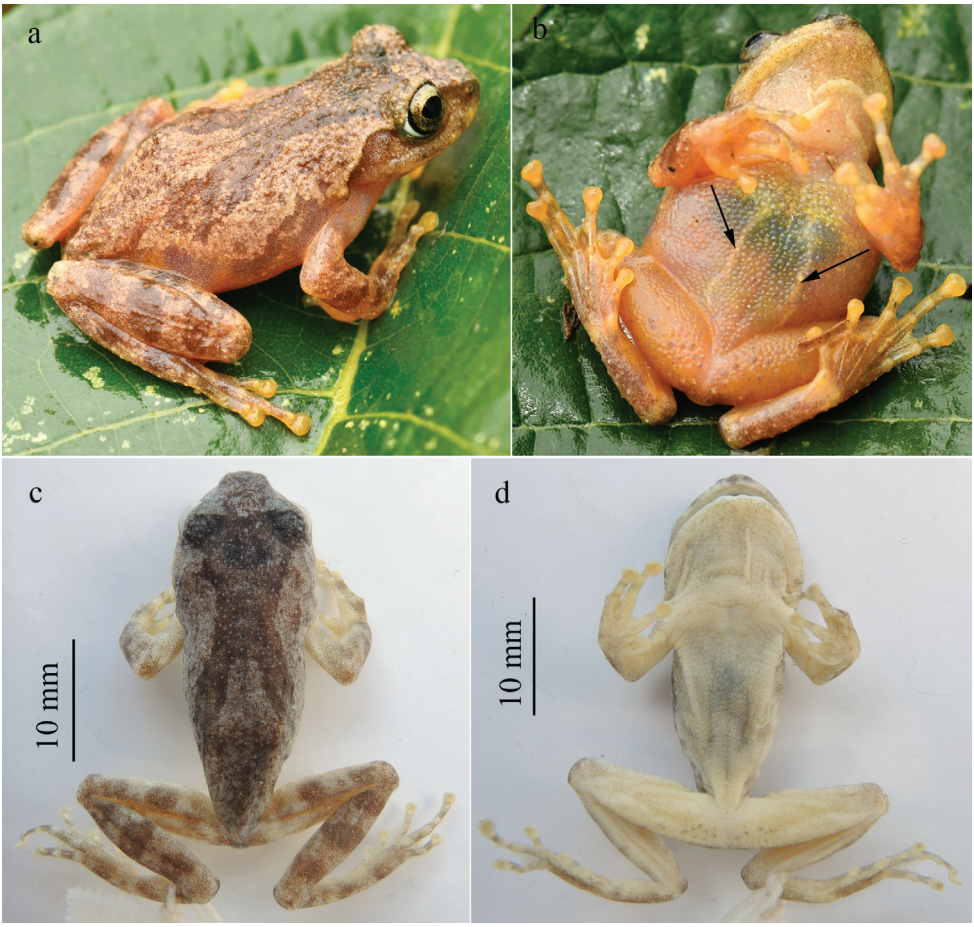

Figure 4. Dorsolateral (**a**) and ventral (**b**) views of the holotype of *Gracixalus yunnanensis* sp. n. in life and dorsal (**c**) and ventral (**d**) views of the holotype of *Gracixalus yunnanensis* sp. n. in preservative. Linea masculina is pointed by arrow.

Distribution. In China, the new species is known from Yunnan (Lancang County, Menghai County, Lvchun County, and Jinping County). In addition, the new species also occurs in Laos (Houapan) and Vietnam (Lao Cai and Nghe An) because our molecular analyses revealed that samples from Houapan (KUHE 32453), Lao Cai (VNMN 4355, 4357, 4371), and Nghe An (AMS R173454) that were sequenced by previous studies also belong to the new species (Figs 2, 3). In Yunnan, specimens were found sitting on leaves of herbaceous plants (e.g., *Amomum tsaoko* and *Eupatorium adenophorum*). No eggs and tadpoles were found.

Comparisons. A summary of morphological comparisons presents in Table 4. The new species can be distinguished from *G. ananjevae* by having distinctive conical tubercles on dorsum (versus absent), sides of body smooth (versus coarsely granular), skin of throat granular (versus plain), and snout rounded (versus slightly pointed);

Table 3. Measurements (mm) of *Gracixalus yunnanensis* sp. n. Abbreviations defined in text.

Voucher no.	Sex	SVL	HL	HW	SL	IND	IOD	UEW	ED	TD	DNE	DNS	FHL	THL	TL	TFL	FL
KIZ 20160216	m	30.0	9.5	11.4	4.0	3.4	3.5	2.5	4.4	1.9	2.4	1.8	15.4	13.1	13.8	20.2	13.3
KIZ 20160222	m	29.7	9.5	10.9	4.2	2.9	3.0	2.5	4.2	1.5	2.4	1.7	14.1	12.3	13.2	18.8	12.9
KIZ 20160223	m	28.5	9.4	10.5	4.0	2.9	3.0	2.5	4.0	1.8	2.2	1.6	13.9	12.6	13.0	18.7	12.5
KIZ 20160226	m	34.2	10.1	12.1	4.7	3.3	3.8	2.8	4.4	1.9	2.5	2.1	15.6	13.3	14.1	21.1	14.2
KIZ 20160228	m	28.7	9.4	11.0	4.2	3.0	3.0	2.5	4.1	1.6	2.4	1.7	14.6	12.6	13.3	19.2	12.8
KIZ 20160229	m	26.0	9.0	9.4	3.5	2.6	2.8	2.3	3.5	1.3	2.0	1.3	12.8	11.0	11.6	17.0	11.6
KIZ 20160230	m	26.4	8.3	10.0	3.8	2.9	3.3	2.5	3.8	1.6	2.2	1.7	13.4	12.0	12.7	18.3	11.8
GXNU YU000060	m	27.3	8.7	9.5	4.1	2.7	2.8	2.5	3.7	1.7	2.3	1.7	13.4	11.9	12.7	18.8	12.3

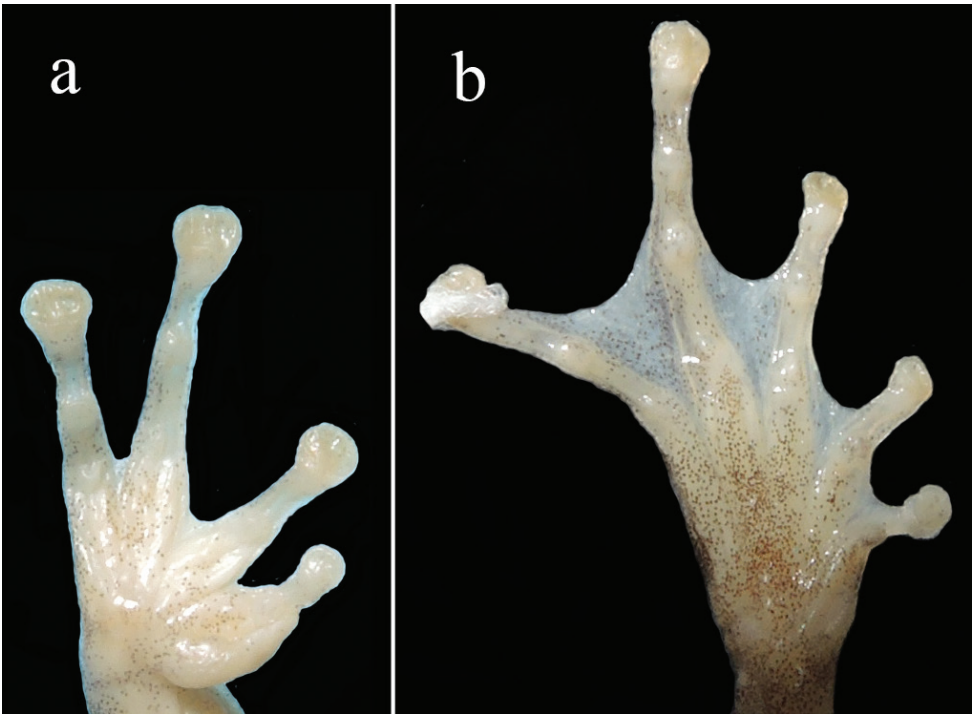

Figure 5. Ventral views of hand (**a**) and foot (**b**) of the holotype of *Gracixalus yunnanensis* sp. n. in preservative.

from *G. carinensis* by having smaller body size in males (SVL 26.0–34.2 mm versus 30.2–38.1 mm), having distinctive conical tubercles on dorsum (versus absent), having an external vocal sac in males (versus an internal vocal sac), ventral surface orangish (versus white), and less developed toe webbing (Fig. 7); from *G. gracilipes* by having bigger body size in males (SVL 26.0–34.2 mm versus 20–24 mm), distinctive conical tubercles present on dorsum (versus absent), dorsal surface yellow brown or red brown (versus greenish), males with an external vocal sac (versus internal), throat granular (versus smooth), finger webbing rudimentary (versus absent), tibiotarsal articulation reaching to eye (versus reaching to between eye and nostril), snout rounded (versus triangular pointed), white patch absent on temporal region (versus present),

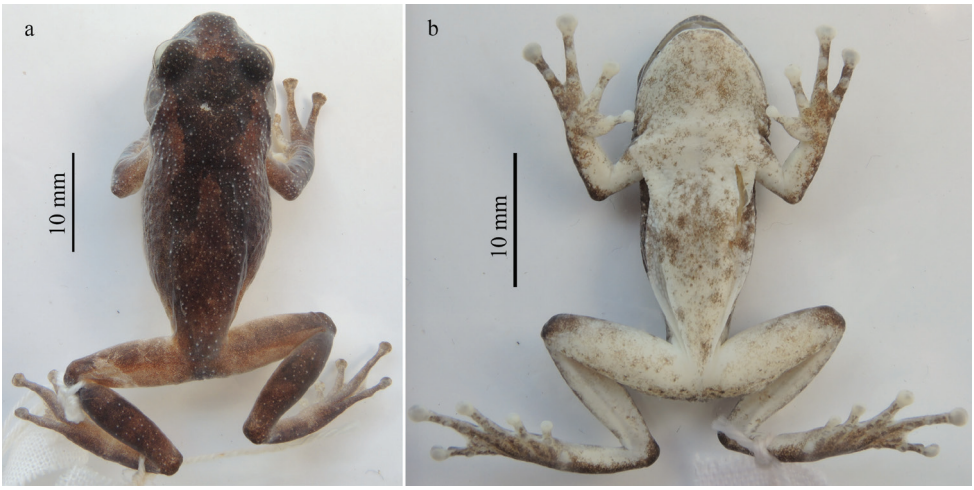

Figure 6. Dorsal view of paratype KIZ 20160226 (**a**) and ventral view of paratype GXNU YU000060 (**b**).

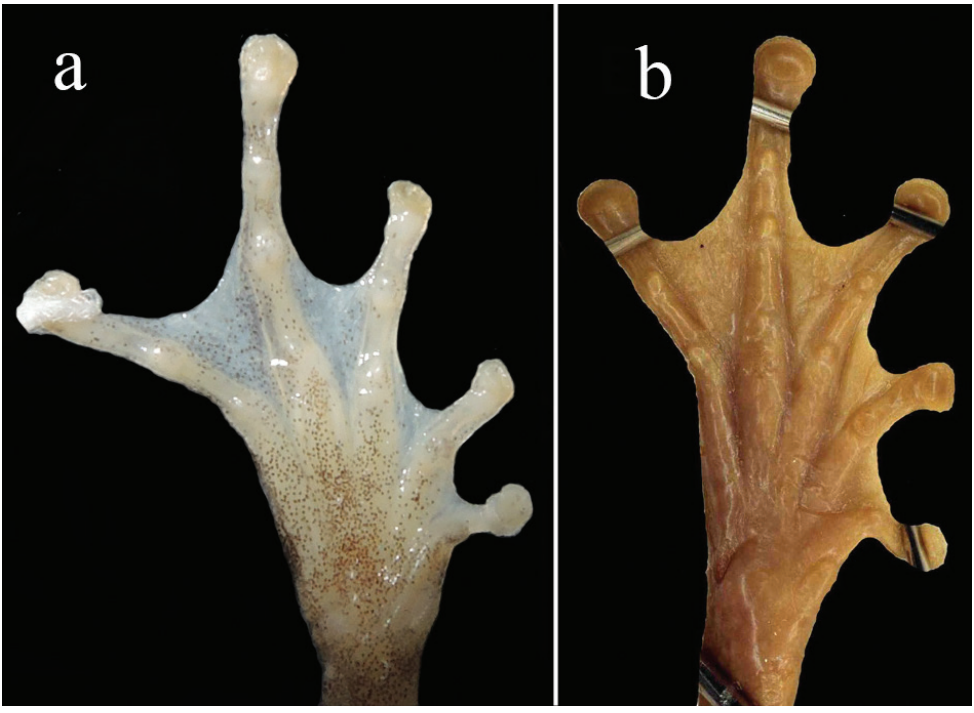

Figure 7. Ventral views of foot of the holotype of *Gracixalus yunnanensis* sp. n. (**a**) and lectotype of *Gracixalus carinensis* (**b**; reproduced from Matsui et al. 2017).

tibiotarsal projection absent (versus present), and iris bronze (versus brown); and from *G. guangdongensis* by having distinctive conical tubercles on dorsum (versus absent), dorsal surface yellow brown or red brown (versus brown), flanks nearly smooth with

Table 4. Morphological characters for comparisons among *Gracixalus* species. "?" = not known or not clearly defined in the literature.

Species	Adult male SVL (mm)	Conical tubercles on dorsum	Dorsal color in life	Vocal sac	Skin of body sides	Skin of throat
G. yunnanensis sp. n.	26.0–34.2	present, small	yellow brown or red brown	external	smooth, no black blotches	granular
G. ananjevae	32	absent	?	?	coarsely granular	plain
G. carinensis	30.2–38.1	absent	purplish, reddish, or greyish brown	internal	?	granular
G. gracilipes	20–24	absent	greenish	internal	smooth with white stripe	smooth
G. guangdongensis	26.1–34.7	absent	brown	?	rough, black blotches	granular
G. jinggangensis	27.9–33.8	absent	brown to beige	?	rough with tubercles	granular
G. jinxiuensis	23.5–26.3	?	brown	internal	rough with tubercles	granular
G. lumarius	38.9–41.6	present	yellow	external	?	granular
G. medogensis	26.5	absent	grass green	internal	?	granular
G. nonggangensis	29.9–35.3	absent	yellowish-olive with dark-green mark	internal	rough with tubercles	granular
G. quangi	< 25	present, small	olive-green	external	with black blotches	smooth
G. quyeti	?	present	brownish to moss-green	?	rough with sharp tubercles	smooth
G. sapaensis	21–37	absent	Golden ochre	?	coarsely scattered with large tubercles	?
G. seesom	21.6–23.0	absent	tan	?	with large tubercles and white blotches	smooth
G. supercornutus	22.0–24.1	present, bigger horn-like	green with brown spots	?	?	granular
G. tianlinensis	30.3–35.9	absent	brown to beige	external	?	granular
G. waza	27.1–32.9	absent	greyish-green to moss-green	?	with small granulars	smooth

Table 4. (Continued).

Species	Finger webbing	Linea masculina	Tibiotarsal articulation	Snout	White patch on temporal region	Tibiotarsal projection	Supratympanic fold
G. yunnanensis sp. n.	rudimentary	present,	reaching eye	rounded	absent	absent	distinct
G. ananjevae	rudimentary	?	reaching eye	slightly pointed	absent	absent	distinct
G. carinensis	rudimentary	?	reaching eye	rounded	absent	absent	distinct
G. guangdongensis	rudimentary	?	reaching eye	triangularly pointed	absent	absent	distinct
G. gracilipes	absent	present	reaching between eye and nostril	triangularly pointed	present	present	distinct
G. jinggangensis	rudimentary	?	reaching eye	triangularly pointed	absent	absent	distinct

Species	Finger webbing	Linea masculina	Tibiotarsal articulation	Snout	White patch on temporal region	Tibiotarsal projection	Supratympanic fold
G. jinxiuensis	rudimentary	absent	reaching eye	rounded	absent	absent	distinct
G. lumarius	rudimentary	?	?	rounded	absent	absent	indistinct
G. medogensis	absent	present	reaching eye	rounded	absent	absent	distinct
G. nonggangensis	absent	absent	reaching tip of snout	rounded	absent	absent	distinct
G. quangi	absent	?	?	triangularly pointed	present	present	distinct
G. quyeti	rudimentary	?	reaching to snout	rounded	absent	absent	indistinct
G. sapaensis	rudimentary	?	reaching eye	rounded	absent	absent	distinct
G. seesom	rudimentary	?	reaching between eye and nostril	triangularly pointed	absent	absent	distinct
G. supercornutus	?	?	?	pointed	present	present	distinct
G. tianlinensis	absent	?	?	rounded	absent	absent	distinct
G. waza	absent	?	?	rounded	absent	absent	distinct

Table 4. (Continued).

Species	venter	Nuptial pads	heels	iris
G. yunnanensis sp. n.	orangish with yellow spots, immaculate, semi-transparent	on finger I	overlapping	bronze
G. ananjevae	immaculate	on finger I	overlapping	?
G. carinensis	immaculate white	?	?	?
G. gracilips	yellowish white	on fingers I and II	overlapping	brown
G. guangdongensis	throat and chest creamy white, belly light brown , semi-transparent	on finger I	overlapping	brown
G. jinggangensis	Throat and chest dirty white with dark specks, belly white anteriorly with dark marking and posteriorly yellowish, semi-transparent	on fingers I and II	just meeting	golden
G. jinxiuensis	gray-brown with dark marbling	on finger I	just meeting	?
G. lumarius	opaque pink	on finger I	?	dark gold
G. medogensis	pale green	on finger I	overlapping	?
G. nonggangensis	white with dark marbling, semi-transparent	absent	overlapping	olive
G. quangi	opaque white with translucent pale green margins	on finger I	?	bronze
G. quyeti	belly immaculate white	?	overlapping	?
G. sapaensis	throat, chest, and belly light yellow, with dark marking	on finger I	overlapping	golden
G. seesom	anterior belly opaque white and posterior belly translucent	absent	overlapping	golden
G. supercornutus	light with white spots	?	?	?
G. tianlinensis	throat and chest gray with dark specks, belly creamy white, opaque	on fingers I and II	?	bronze
G. waza	Throat and chest white with dark marbling, belly immaculate white, semi-transparent	on finger I	overlapping	?

no black blotches on ventrolateral region (versus flanks rough, scattered with tubercles and black blotches on ventrolateral region), snout rounded (versus triangularly pointed), ventral surface orangish (versus throat and chest creamy white and belly light brown), and iris bronze (versus iris brown).

Gracixalus yunnanensis sp. n. differs from *G. jinggangensis* by having distinctive conical tubercles on dorsum (versus absent), flanks nearly smooth (versus rough with tubercles), snout rounded (versus triangularly pointed), ventral surface orangish and immaculate (versus throat and chest dirty white with dark specks, belly white anteriorly with dark marking and posteriorly yellowish), nuptial pads present only on finger I (versus nuptial pads present on fingers I and II), heels overlapping when hindlimbs held at right angles to the body (versus just meeting), and iris bronze (versus iris golden); from *G. jinxiuensis* by larger body size in males (SVL 26.0–34.2 mm versus 23.5–26.3 mm), males with an external vocal sac (versus vocal sac internal), flanks nearly smooth (versus rough with tubercles), linea masculina present (versus absent), ventral surface orangish and immaculate (versus ventral surface gray-brown with dark marbling), and sole of feet and palms smooth (versus rough with dense large tubercles); and from *G. lumarius* by smaller body size in males (SVL 26.0–34.2 mm versus 38.9–41.6 mm), dorsal surface yellow brown or red brown (versus yellow), and venter orangish and semi-transparent (versus venter opaque pink), supratympanic fold distinct (versus indistinct), and iris bronze (versus dark gold).

Gracixalus yunnanensis sp. n. can be distinguished from *G. medogensis* by having distinctive conical tubercles on dorsum (versus absent), dorsal surface yellow brown or red brown (versus grass green), males with an external vocal sac (versus an internal vocal sac), finger webbing rudimentary (versus absent), and venter orangish (versus pale green); from *G. nonggangensis* by having conical tubercles on dorsum (versus absent), dorsum yellow brown or red brown with a dark brown marking (versus yellowish-olive with a dark-green marking), males with an external vocal sac (versus internal), flanks smooth (versus rough with tubercles), finger webbing rudimentary (versus absent), linea masculina present in males (versus absent), tibiotarsal articulation reaching to eye (versus reaching to tip of snout), ventral surface immaculate (versus throat, chest, and belly white with dark marbling), nuptial pads present on finger I (versus absent), and iris bronze (versus olive); from *G. quangi* by having bigger body size in males (SVL 26.0–34.2 mm versus < 25 mm), dorsal surface yellow brown or red brown (versus olive-green), black spots absent on flanks and ventral surface of thighs (versus present), throat granular (versus smooth), finger webbing rudimentary (versus absent), snout rounded (versus triangular pointed), white patch absent on temporal region (versus present), tibiotarsal projection absent (versus present), and ventral surface orangish (versus opaque white with translucent pale green margins); and from *G. quyeti* by dorsal surface yellow brown or red brown (versus brownish to moss-green), flanks nearly smooth (versus rough with sharp tubercles), throat granular (versus smooth), tibiotarsal articulation reaching to eye (versus reaching to snout), supratympanic fold distinct (versus indistinct), and throat and chest immaculate (versus throat, margin of throat, and chest yellow-white with brown marbling).

Gracixalus yunnanensis sp. n. differs from *G. sapaensis* by having distinctive conical tubercles on dorsum (versus absent) and sides of body nearly smooth (versus coarsely scattered with large round tubercles); from *G. seesom* by bigger body size in males (SVL 26.0–34.2 mm versus 21.6–23.0 mm), conical tubercles present on dorsum (versus absent), dorsal surface yellow brown or red brown (versus tan), flanks nearly smooth with no white blotches (versus flanks with large tubercles and white blotches), throat granular (versus smooth), snout rounded (versus triangular pointed), nuptial pads present on finger I (versus absent), and iris bronze (versus golden); and from *G. supercornutus* by bigger body size in males (SVL 26.0–34.2 mm versus 22.0–24.1 mm), conical tubercles on dorsum small (versus considerable bigger horn-like projections in supraorbital area, around cloaca, and on dorsal surface, forelimbs and hindlimbs), dorsal surface yellow brown or red brown (versus greenish), snout rounded (versus triangular pointed), white patch absent on temporal region (versus present), and tibiotarsal projection absent (versus present).

The new species can be distinguished from *G. tianlinensis* by smaller body size in males (SVL 26.0–34.2 mm versus 30.3–35.9 mm), distinctive conical tubercles present on dorsum (versus absent), dorsal surface yellow brown or red brown (versus brown to beige), finger webbing rudimentary (versus absent), ventral surface orangish, immaculate, and semi-transparent (versus throat and chest gray with dark specks and belly creamy white, opaque), and nuptial pads present on finger I (versus on fingers I and II); and from *G. waza* by having distinctive conical tubercles on dorsum (versus absent), dorsal surface yellow brown or red brown (versus greyish-green to moss-green), throat granular (versus smooth), finger webbing rudimentary (versus absent), and ventral surface immaculate (versus throat and chest with dark marbling).

Discussion

Although *G. yunnanensis* sp. n. only diverges from *G. guangdongensis* by a distance of 2.2%, it can be morphologically separated from *G. guangdongensis* by a series of characters including distinctive conical tubercles on dorsum (versus absent), dorsal surface yellow brown or red brown (versus brown), flanks nearly smooth with no black blotches on ventrolateral region (versus flanks rough, scattered with tubercles and black blotches on ventrolateral region), snout rounded (versus triangularly pointed), ventral surface orangish (versus throat and chest creamy white and belly light brown), and iris bronze (versus iris brown) (Table 4). In addition, the new species has linea masculina (Fig. 4b), whereas *G. guangdongensis* likely lacks linea masculina (Fig. 8), although it was not described in Wang et al. (2018). Moreover, the new species and *G. guangdongensis* were recovered as reciprocally monophyletic and the new species is not directly related to *G. guangdongensis* or other known congeners with strong support (Figs 2, 3). Therefore, we think that *G. yunnanensis* sp. n. should be diagnosed as an independent species. It has been revealed that low interspecific genetic distance seems to be very common in frogs from Southeast Asia (e.g., 2.2%–21.2% in Megophryidae, 1.8%–16.0% in Ranidae, and 1.5%–19.8% in Rhacophoridae; Grosjean et al. 2015).

Figure 8. Ventral view of male holotype of *G. guangdongensis* (SYS a005724) in life (reproduced from Wang et al. 2018).

Historically, *G. yunnanensis* sp. n. was once confused with *G. jinxiuensis* in that the Jinping specimen (KIZ 060821126), Houapan specimen (KUHE 32453), Nghe An specimen (AMS R173454), and Lao Cai specimens (VNMN 4355, 4357, 4371) were originally identified as *G. jinxiuensis* by Yu et al. (2008), Matsui et al. (2015), Rowley et al. (2011), and Matsui et al. (2017), respectively. However, the new species can easily be distinguished from *G. jinxiuensis* by having bigger body size, an external vocal sac, and linea masculina in males (Table 4).

Gracixalus now contains a total of 17 species and our phylogenetic analyses revealed that this genus consists of three major clades, one consisting of *G. lumarius* (Clade I), one consisting of *G. seesom*, *G. quyeti*, *G. quangi*, *G. supercornutus*, and *G. gracilipes* (Clade II), and one consisting of all other species (Clade III) (Figs 2, 3). This result is consistent with Zeng et al. (2017), Chen et al. (2018), and Wang et al. (2018). However, like these previous studies, the present study did not achieve a complete resolution of phylogenetic relationships among these three clades and phylogenetic relationships within clades II and III. Thus, more studies will be needed to resolve the phylogenetic relationships among this genus. Additionally, taxonomic confusions still exist in *Gracixalus*: Matsui et al. (2015) and Wang et al. (2018) considered that *G. nonggangensis* should be synonymized with *G. waza* because of low genetic distance between them. However, morphologically, males of *G. waza* have developed nuptial pads on finger I according to Nguyen et al. (2013), whereas males of *G. nonggongensis* lack nuptial pad according to Mo et al. (2013). If indeed this is the case, we would

prefer that *G. nonggangensis* and *G. waza* represent two different species. Furthermore, cryptic species might exist in *G. nonggangensis* because its monophyly was not supported in Matsui et al. (2015) and Wang et al. (2018). In addition, studies will be necessary to confirm whether the specimen from Wenshan, Yunnan, China (voucher number: 03320Rao; GenBank accession no.: GQ285669) belongs to *G. ananjevae* or not. We found that they are sister to each other with strong support values (Figs 2, 3), which is consistent with Mo et al. (2013); the genetic distance between them is moderate (2.3%; Table 2).

Acknowledgements

We thank Tan He and Wenjing Jiang for their assistances with fieldworks. Thanks also to the three reviewers for their helpful comments on the manuscript. This work was supported by the National Natural Science Foundation of China (Nos. 31872212 and 31301870) and CAS "Light of West China" Program to Guohua Yu.

References

Boulenger GA (1893) Concluding report on the reptiles and batrachians obtained in Burma by Signor L. Fea dealing with the collection made in Pegu and the Karin Hills in 1887–88. Annali del Museo Civico di Storia Naturale di Genov 13: 304–347. https://doi.org/10.5962/bhl.part.9543

Bourret R (1937) Notes herpétologiques sur l'Indochine française. XIV. Les batraciens de la collection du Laboratoire des Sciences Naturelles de l'Université. Descriptions de quinze espèces ou variétés nouvelles. Annexe au Bulletin Général de l'Instruction Publique 1937: 5–56. https://doi.org/10.5962/bhl.part.22065

Chen W, Bei Y, Liao X, Zhou S, Mo Y (2018) A new species of *Gracixalus* (Anura: Rhacophoridae) from West Guangxi, China. Asian Herpetological Research 9: 74–84. https://doi.org/10.11646/zootaxa.3616.1.5

Darriba D, Taboada GL, Doallo R, Posada D (2012) jModelTest 2: more models, new heuristics and parallel computing. Nature Methods 9: 772–772. https://doi.org/10.1038/nmeth.2109

Delorme M, Dubois A, Grosjean S, Ohler A (2005) Une nouvelle classification générique et subgénérique de la tribu des Philautini (Amphibia, Anura, Rhacophorinae). Bulletin Mensuel de la Société Linnéenne de Lyon 74: 165–171. https://doi.org/10.3406/linly.2005.13595

Fei L (1999) Atlas of Amphibians of China. Henan Publishing House of Science and Technology, Zhengzhou, China, 432 pp.

Frost DR (2018) Amphibian Species of the World: and Online Reference. Version 6.0. American Museum of Natural History, New York, USA. http://research.amnh.org/herpetology/amphibia/index.html/ [Accessed 27 November 2018]

Grosjean S, Ohler A, Chuaynkern Y, Cruaud C, Hassanin A (2015) Improving biodiversity assessment of anuran amphibians using DNA barcoding of tadpoles. Case studies from Southeast Asia. Comptes Rendus Biologies 338: 351–361. https://doi.org/10.1016/j.crvi.2015.03.015

Hu S, Fei L, Ye C (1978) Three new amphibian species in China. Materials for Herpetological Research 4: 20.

Hu S, Tian W, Wu G (1981) Three new species of Amphibians from Guangxi. Acta Herpetological Sinica 17: 111–120.

Kumar S, Stecher G, Tamura K (2016) MEGA7: Molecular Evolutionary Genetics Analysis version 7.0 for bigger datasets. Molecular Biology and Evolution 33: 1870–1874. https://doi.org/10.1093/molbev/msw054

Kuramoto M, Wang C (1987) A new rhacophorid treefrog from Taiwan, with comparisons to *Chirixalus eiffingeri* (Anura, Rhacophoridae). Copeia 1987: 931–942. https://doi.org/10.2307/1445556

Matsui M, Khonosue W, Panha S, Eto K (2015) A new tree frog of the genus *Gracixalus* from Thailand (Amphibia: Rhacophoridae). Zoological Science 32: 204–210. https://doi.org/10.2108/zs140238

Matsui M, Ohler A, Eto K, Nguyen TT (2017) Distinction of *Gracixalus carinensis* from Vietnam and Myanmar, with description of a new species. Alytes 33: 25–37.

Matsui M, Orlov N (2004) A new species of *Chirixalus* from Vietnam (Anura: Rhacophoridae). Zoological Science 21: 671–676. https://doi.org/10.2108/zsj.21.671

Matsui M, Shimada T, Sudin A (2013) A new gliding frog of the genus *Rhacophorus* from Borneo. Current Herpetology 32: 112–124. https://doi.org/10.5358/hsj.32.112

Mo Y, Zhang W, Luo Y, Zhou S, Chen W (2013) A new species of the genus *Gracixalus* (Amphibia: Anura: Rhacophoridae) from Southern Guangxi, China. Zootaxa 3616: 61–72. https://doi.org/10.11646/zootaxa.3616.1.5

Nguyen TQ, Hendrix R, Böhme W, Vu TN, Ziegler T (2008) A new species of the genus *Philautus* (Amphibia: Anura: Rhacophoridae) from the Truong Son Range, Quang Binh Province, central Vietnam. Zootaxa 1925: 1–13.

Nguyen TQ, Le MD, Pham CT, Nguyen TT, Bonkowski M, Ziegler T (2013) A new species of *Gracixalus* (Amphibia: Anura: Rhacophoridae) from northern Vietnam. Organisms Diversity & Evolution 13: 203–214. https://doi.org/10.1007/s13127-012-0116-0

Orlov NL, Ho TC, Nguyen QT (2004) A new species of the genus *Philautus* from central Vietnam (Anura: Rhacophoridae). Russian Journal of Herpetology 11: 51–64.

Rambaut A, Suchard MA, Xie D, Drummond AJ (2014) Tracer v1.6. http://tree.bio.ed.ac.uk/softeare/tracer

Ronquist F, Teslenko M, van der Mark P, Ayres DL, Darling A, Höhna S, Larget B, Liu L, Suchard MA, Huelsenbeck JP (2012) MrBayes 3.2: efficient Bayesian phylogenetic inference and model choice across a large model space. Systematic Biology 61: 539–542. https://doi.org/10.1093/sysbio/sys029

Rowley JJL, Dau QV, Nguyen TT, Cao TT, Nguyen SN (2011) A new species of *Gracixalus* (Anura: Rhacophoridae) with a hyperextended vocal repertoire from Vietnam. Zootaxa 3125: 22–38. https://doi.org/10.1163/15685381-00003007

Rowley JJL, Le DTT, Dau VQ, Hoang HD, Cao TT (2014) A striking new species of phytotelm-breeding tree frog (Anura: Rhacophoridae) from central Vietnam. Zootaxa 3785: 25–37. https://doi.org/10.11646/zootaxa.3785.1.2

Savage JM (1975) Systematics and distribution of the Mexican and Central American stream frogs related to Eleutherodactylus rugulosus. Copeia 1975: 254–306. https://doi.org/10.2307/1442883

Stamatakis A (2014) RAxML Version 8: A tool for phylogenetic analysis and post-analysis of large phylogenies. Bioinformatics 30: 1312–1313. https://doi.org/10.1093/bioinformatics/btu033

Swofford DL (2002) PAUP: Phylogenetic Analysis Using Parsimony (*and other Methods), Version 4.0. Sinauer Associates, Sunderland, MA.

Wang J, Zeng Z, Lyu Z, Liu Z, Wang Y (2018) Description of a new species of *Gracixalus* (Amphibia: Anura: Rhacophoridae) from Guangdong Province, southeastern China. Zootxa 4420: 251–269. https://doi.org/10.11646/zootaxa.4420.2.7

Ye C, Hu S (1984) A new species of *Philautus* (Anura: Rhacophoridae) from Xizang Autonomous Region. Acta Herpetologica Sinica 3: 67–69.

Yu G, Zhang M, Yang J (2010) A species boundary within the Chinese *Kurixalus odontotarsus* species group (Anura: Rhacophoridae): New insights from molecular evidence. Molecular Phylogenetics and Evolution 56: 942–950. https://doi.org/10.1016/j.ympev.2010.05.008

Zeng Z, Zhao J, Chen C, Chen G, Zhang Z, Wang Y (2017) A new species of the genus *Gracixalus* (Amphibia: Anura: Rhacophoridae) from Mount Jinggang, southeastern China. Zootaxa 4250: 171–185. https://doi.org/10.11646/zootaxa.4250.2.3

ZooKeys 851: 113–164 (2019)
doi: 10.3897/zookeys.851.29107
http://zookeys.pensoft.net

RESEARCH ARTICLE

A peer-reviewed open-access journal
ZooKeys
Launched to accelerate biodiversity research

Description of six new species of the subgenus *Panophrys* within the genus *Megophrys* (Anura, Megophryidae) from southeastern China based on molecular and morphological data

Jian Wang[1], Zhi-Tong Lyu[1], Zu-Yao Liu[1], Cheng-Kai Liao[2], Zhao-Chi Zeng[1], Jian Zhao[1], Yu-Long Li[1], Ying-Yong Wang[1]

1 *State Key Laboratory of Biocontrol / The Museum of Biology, School of Life Sciences, Sun Yat-sen University, Guangzhou 510275, China* **2** *Jiulianshan National Nature Reserve, Longnan County, Jiangxi 341700, China*

Corresponding author: *Yingyong Wang* (wangyy@mail.sysu.edu.cn)

Academic editor: *J. Penner* | Received 15 August 2018 | Accepted 11 April 2019 | Published 3 June 2019

http://zoobank.org/F0AB358B-811E-42EE-B25A-5CF24658E6CA

Citation: Wang J, Lyu Z-T, Liu Z-Y, Liao C-K, Zeng Z-C, Zhao J, Li Y-L, Wang Y-Y (2019) Description of six new species of the subgenus *Panophrys* within the genus *Megophrys* (Anura, Megophryidae) from southeastern China based on molecular and morphological data. ZooKeys 851: 113–164. https://doi.org/10.3897/zookeys.851.29107

Abstract

The diversity of the subgenus *Panophrys* within the genus *Megophrys* has been revealed to be extremely underestimated from southeastern China. Herpetological surveys coupled with extensive sampling in a longitudinal mountain belt located in southeastern China resulted in the discoveries of six new species of the subgenus *Panophrys*. Furthermore, the new discoveries support the findings of "micro-endemism", "sympatric phenomenon" and "sympatric but distant phylogenetically" which appear to be common among *Panophrys* species, and also indicates that the Asian horned toads would be good candidates for studies on speciation and biogeography, and additionally emphasizes the conservation difficulties of these toads.

Keywords

Conservation, *Megophrys*, southeastern China, species diversity, subgenus *Panophrys*, speciation, biogeography

Introduction

The Asian horned toads (*Megophrys*) comprise 85 recognized species which were previously classified in the subfamily Megophryinae (Frost 2019). They are widespread in montane forest area in tropical and subtropical Asia, including southern mainland

China, southern and eastern Himalayas, across Indochina to Malay, to the islands of the Sunda Shelf and the Philippines (Chen et al. 2017; Deuti et al. 2017; Mahony et al. 2017; Mahony et al. 2018; Li et al. 2018; Liu et al. 2018; Munir et al. 2018; Messenger et al. 2019; Tapley et al. 2018; Frost 2019). As a consequence of both morphological similarity among species and the complex patterns of genetic divergence, the taxonomy of these toads always has been controversial. Although several researchers have proposed different taxonomic schemes in recent decades (Dubois 1987; Rao and Yang 1997; Dubois and Ohler 1998; Jiang et al. 2003; Zheng et al. 2004; Frost et al. 2006; Li and Wang 2008; Fei et al. 2009; Fei and Ye 2016; Chen et al. 2017; Mahony et al. 2017), the debate remains. Based on a large-scale molecular analysis, Chen et al. (2017) considered that subfamily Megophryinae is composed of five genera, namely *Atympanophrys* Tian & Hu, 1983, *Brachytarsophrys* Tian & Hu, 1983, *Megophrys* Kuhl & Van Hasselt, 1822, *Ophryophryne* Boulenger, 1903 and *Xenophrys* Günther, 1864. Almost at the same time, based on the integrative analysis with phylogeny and morphological examination, Mahony et al. (2017) treated the entire subfamily Megophryinae as a single genus *Megophrys* and divided it into seven subgenera, i.e. *Atympanophrys*, *Brachytarsophrys*, *Megophrys*, *Ophryophryne*, *Panophrys* Rao & Yang, 1997, *Pelobatrachus* Beddard, 1908 and *Xenophrys*, and 25 known species were placed in the subgenus *Panophrys*. Subsequently, Liu et al. (2018) partially agreed with this taxonomic system based on a substantial study on phylogenetic similarity, and revealed unusually high levels of species diversity in the subgenus *Panophrys* with a total number of 60 species, 2.4 times of previously known, including 41 unnamed cryptic species and 39 of which were from southeastern China. Therefore, *Panophrys* species diversity from southeastern China is extremely underestimated.

In the past years, we have carried out continual herpetological surveys coupled with extensive sampling in a longitudinal mountain belt with a west-east width of 100 km, north-south length of 800 km in the middle of southeastern China, from Hong Kong and Shenzhen in the Pearl River Delta, across the Jiulian Mountains and Luoxiao Mountains, north to the Yangtze River (Fig. 1). The surveys resulted in the discovery of 15 unnamed *Panophrys* species (Liu et al. 2018) and descriptions of 14 new species of amphibians and reptiles, namely *Leptobrachella laui* (Sung, Yang & Wang, 2014), *Megophrys* (*Brachytarsophrys*) *popei* (Zhao, Yang, Chen, Chen & Wang, 2014), *M.* (*Panophrys*) *cheni* (Wang & Liu, 2014), *M.* (*Pa.*) *lini* (Wang & Yang, 2014), *Megophrys* (*Pa.*) *jinggangensis* (Wang, 2012), *Nidirana nankunensis* Lyu, Zeng, Wang, Lin, Liu & Wang, 2017, *Amolops albispinus* Sung, Hu, Wang, Liu & Wang, 2016, *Gracixalus jinggangensis* Zeng, Zhao, Chen, Chen, Zhang & Wang, 2017 and *Gr. guangdongensis* Wang, Zeng, Lyu, Liu & Wang, 2018; *Goniurosaurus yingdeensis* Wang, Yang & Cui, 2010, *Go. zhelongi* Wang, Jin, Li & Grismer, 2014, *Takydromus albomaculosus* Wang, Gong, Liu & Wang, 2017, *Rhabdophis guangdongensis* Zhu, Wang, Takeuchi & Zhao, 2014 and *Opisthotropis shenzhenensis* Wang, Guo, Liu, Lyu, Wang, Luo, Sun & Zhang, 2017.

In the present study, we re-reviewed several species defined by Liu et al. (2018) from this mountain belt based on molecular and morphological data and formally described six new species of *Megophrys*.

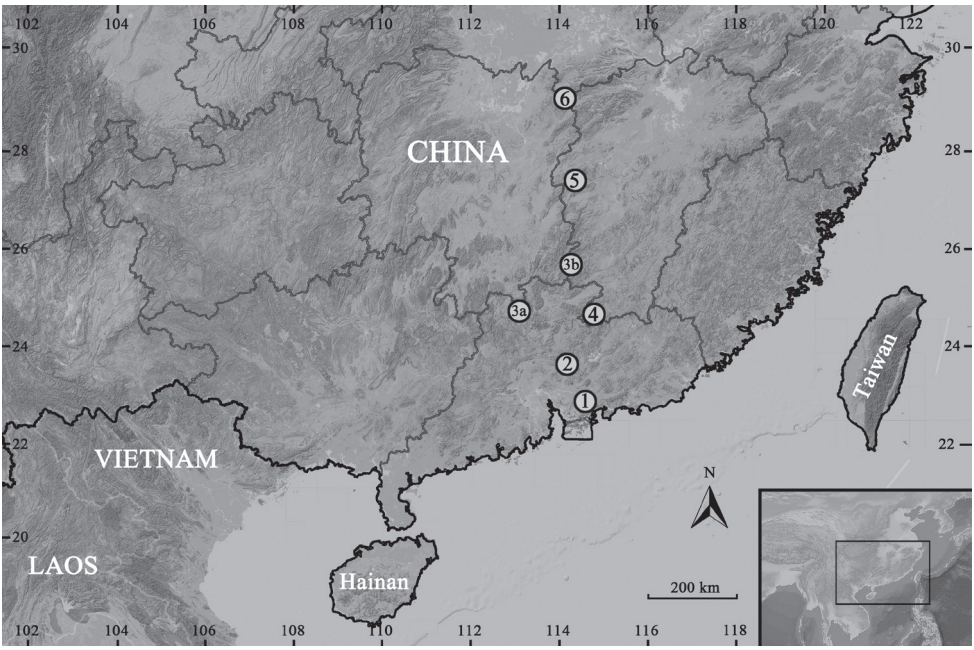

Figure 1. Collection localities of the six new *Megophrys* species in this study: **1** Mt. Yinping in Dongguan City of Guangdong Province, the type locality of *M. dongguanensis* sp. nov. **2** Mt. Nankun in Huizhou City of Guangdong Province, the type locality of *M. nankunensis* sp. nov., and one of the localities of its sympatric species, *M. jiulianensis* sp. nov. **3a** Nanling Nature Reserve in Shaoguan City of Guangdong Province, the type locality of *M. nanlingensis* sp. nov. **3b** Mt. Qiyun in Ganzhou City of Jiangxi Province, the other collection locality of *M. nanlingensis* sp. nov. **4** Mt. Jiulian in Ganzhou City of Jiangxi Province, the type locality of *M. jiulianensis* sp. nov. **5** Yangshimu Scenic Area in Pingxiang City and adjacent Wugongshan Scenic Area in Ji'an City of Jiangxi Province, the type locality of *M. wugongensis* sp. nov. **6** Mt. Mufu in Yueyang City of Hunan Province, the type locality of *M. mufumontana* sp.nov.

Material and methods

Sampling

For molecular analysis, a total of 42 samples (17 were attained from GenBank and 25 were new materials in this study) from the collection of unnamed specimens of the subgenus *Panophrys*, together with 39 samples (37 from GenBank and two new materials) from 21 recognized species of *Panophrys* were used as in-groups in this study. In addition, four samples (all from GenBank) from two recognized species of the subgenus *Atympanophrys*, four samples (three from GenBank and one new materials) from two recognized species of the subgenus *Brachytarsophrys*, three samples (one from GenBank and two new materials) from two recognized species of the subgenus *Ophryophryne*, two samples (all from GenBank) from two recognized species of the subgenus *Pelobatrachus*, and six samples (five from GenBank and one new materials) of three recognized species of the subgenus *Xenophrys* were incorporated into our dataset and used as out-groups. Details see Table 1. All muscle samples were preserved in 95% ethanol and stored at -40 °C.

Table 1. Localities, voucher information, and GenBank accession numbers for all specimens used in this study.

Subgenus of *Megophrys* s. l.	ID	Species name	Locality	Specimen voucher no.	Genbank Accession No.	
					16S	CO1
Panophrys	1	*M. dongguanensis* sp. nov.	China: Mt. Yinping, Dongguan City, Guangdong	SYS a001971/ CIB110006	MK524097	MK524128
	2	*M. dongguanensis* sp. nov.	China: Mt. Yinping, Dongguan City, Guangdong	SYS a001972	MK524098	MK524129
	3	*M. dongguanensis* sp. nov.	China: Mt. Yinping, Dongguan City, Guangdong	SYS a001973	MH406647	MH406083
	4	*M. dongguanensis* sp. nov.	China: Mt. Yinping, Dongguan City, Guangdong	SYS a001974	MH406648	MH406084
	5	*M. dongguanensis* sp. nov.	China: Mt. Yinping, Dongguan City, Guangdong	SYS a001975	MH406649	MH406085
	6	*M. dongguanensis* sp. nov.	China: Mt. Yinping, Dongguan City, Guangdong	SYS a002007	MH406654	MH406090
	7	*M. jiulianensis* sp. nov.	China: Mt. Jiulian, Ganzhou City, Jiangxi	SYS a002107	MK524099	MK524130
	8	*M. jiulianensis* sp. nov.	China: Mt. Jiulian, Ganzhou City, Jiangxi	SYS a002108	MK524100	MK524131
	9	*M. jiulianensis* sp. nov.	China: Mt. Jiulian, Ganzhou City, Jiangxi	SYS a002109	MK524101	MK524132
	10	*M. jiulianensis* sp. nov.	China: Mt. Jiulian, Ganzhou City, Jiangxi	SYS a004219	MH406791	MH406253
	11	*M. jiulianensis* sp. nov.	China: Mt. Nankun, Huizhou City, Guangdong	SYS a003622	MK524102	MK524133
	12	*M. jiulianensis* sp. nov.	China: Mt. Nankun, Huizhou City, Guangdong	SYS a003623	MK524103	MK524134
	13	*M. mufumontana* sp. nov.	China: Mt. Mufu, Pingjiang County, Hunan	SYS a006390/ CIB110012	MK524104	MK524135
	14	*M. mufumontana* sp. nov.	China: Mt. Mufu, Pingjiang County, Hunan	SYS a006391	MK524105	MK524136
	15	*M. mufumontana* sp. nov.	China: Mt. Mufu, Pingjiang County, Hunan	SYS a006392	MK524106	MK524137
	16	*M. mufumontana* sp. nov.	China: Mt. Mufu, Pingjiang County, Hunan	SYS a006419	MK524107	MK524138
	17	*M.nankunensis* sp. nov.	China: Mt. Nankun, Huizhou City, Guangdong	SYS a004498	MK524108	MK524139
	18	*M.nankunensis* sp. nov.	China: Mt. Nankun, Huizhou City, Guangdong	SYS a004499	MK524109	MK524140
	19	*M.nankunensis* sp. nov.	China: Mt. Nankun, Huizhou City, Guangdong	SYS a004500	MK524110	MK524141
	20	*M.nankunensis* sp. nov.	China: Mt. Nankun, Huizhou City, Guangdong	SYS a004501	MH406822	MH406284
	21	*M.nankunensis* sp. nov.	China: Mt. Nankun, Huizhou City, Guangdong	SYS a004502	MH406823	MH406285
	22	*M.nankunensis* sp. nov.	China: Mt. Nankun, Huizhou City, Guangdong	SYS a004503	MH406824	MH406286

Subgenus of *Megophrys* s. l.	ID	Species name	Locality	Specimen voucher no.	Genbank Accession No.	
					16S	CO1
Panophrys	23	*M.nanlingensis* sp. nov.	China: Nanling Nature Reserve, Shaoguan City, Guangdong	SYS a001959	MK524111	MK524142
	24	*M.nanlingensis* sp. nov.	China: Nanling Nature Reserve, Shaoguan City, Guangdong	SYS a001960	MK524112	MK524143
	25	*M.nanlingensis* sp. nov.	China: Nanling Nature Reserve, Shaoguan City, Guangdong	SYS a001964	MH406646	MH406082
	26	*M.nanlingensis* sp. nov.	China: Mt. Qiyun, Chongyi County, Jiangxi	SYS a002334	MH406686	MH406132
	27	*M.nanlingensis* sp. nov.	China: Mt. Qiyun, Chongyi County, Jiangxi	SYS a002356	MK524113	MK524144
	28	*M.nanlingensis* sp. nov.	China: Mt. Qiyun, Chongyi County, Jiangxi	SYS a002357	MH406687	MH406133
	29	*M.nanlingensis* sp. nov.	China: Mt. Qiyun, Chongyi County, Jiangxi	SYS a002358	MH406688	MH406134
	30	*M. wugongensis* sp. nov.	China: Wugongshan Scenic Area, Anfu County, Jiangxi	SYS a002610	MK524114	MK524145
	31	*M. wugongensis* sp. nov.	China: Wugongshan Scenic Area, Anfu County, Jiangxi	SYS a002611	MK524115	MK524146
	32	*M. wugongensis* sp. nov.	China: Yangshimu Scenic Area, Pingxiang City, Jiangxi	SYS a002625	MK524116	MK524147
	33	*M. wugongensis* sp. nov.	China: Wugongshan Scenic Area, Anfu County, Jiangxi	SYS a004777/ CIB110011	MK524117	MK524148
	34	*M. wugongensis* sp. nov.	China: Wugongshan Scenic Area, Anfu County, Jiangxi	SYS a004796	MK524118	MK524149
	35	*M. wugongensis* sp. nov.	China: Wugongshan Scenic Area, Anfu County, Jiangxi	SYS a004797	MK524119	MK524150
	36	*M. wugongensis* sp. nov.	China: Wugongshan Scenic Area, Anfu County, Jiangxi	SYS a004798	MK524120	MK524151
	37	*M. wugongensis* sp. nov.	China: Wugongshan Scenic Area, Anfu County, Jiangxi	SYS a004799	MH406852	MH406314
	38	*M. wugongensis* sp. nov.	China: Wugongshan Scenic Area, Anfu County, Jiangxi	SYS a004800	MH406853	MH406315
	39	*M. wugongensis* sp. nov.	China: Wugongshan Scenic Area, Anfu County, Jiangxi	SYS a004801	MH406854	MH406316
	40	*M. wugongensis* sp. nov.	China: Wugongshan Scenic Area, Anfu County, Jiangxi	SYS a004802	MH406855	MH406317
	41	*M. wugongensis* sp. nov.	China: Wugongshan Scenic Area, Anfu County, Jiangxi	SYS a004803	MH406856	MH406318
	42	*M. wugongensis* sp. nov.	China: Wugongshan Scenic Area, Anfu County, Jiangxi	SYS a004804	MK524121	MK524152
	43	*M. acuta*	China: Heishiding Nature Reserve, Zhaoqing City, Guangdong	SYS a001957	KJ579118	MF667898
	44	*M. acuta*	China: Heishiding Nature Reserve, Zhaoqing City, Guangdong	SYS a002159	MF667869	MF667899

Subgenus of *Megophrys* s. l.	ID	Species name	Locality	Specimen voucher no.	Genbank Accession No.	
					16S	CO1
Panophrys	45	*M. binlingensis*	China: Mt. Wawu, Meishan City, Sichuan	SYS a005313	MH406892	MH406354
	46	*M. binlingensis*	China: Mt. Wawu, Meishan City, Sichuan	SYS a005314	MH406893	MH406355
	47	*M. boettgeri*	China: Longhu Forest Station, Shaowu City, Fujian	SYS a004126	MH406785	MH406245
	48	*M. boettgeri*	China: Mt. Wuyi, Fujian	SYS a004150	MF667879	MF667914
	49	*M. brachykolos*	China: Hongkong	SYS a005563	MK524122	MK524153
	50	*M. brachykolos*	China: Hongkong	SYS a005564	MK524123	MK524154
	51	*M. caudoprocta*	China: Mt. Badagongshan, Zhangjiajie City, Hunan	SYS a004281	MH406795	MH406257
	52	*M. caudoprocta*	China: Mt. Badagongshan, Zhangjiajie City, Hunan	SYS a004293	MH406796	MH406258
	53	*M. cheni*	China: Taoyuandong Nature Reserve, Zhuzhou City, Hunan	SYS a002123	KJ560396	MF667904
	54	*M. cheni*	China: Taoyuandong Nature Reserve, Zhuzhou City, Hunan	SYS a002140	MF667872	MF667905
	55	*M. huangshanensis*	China: Mt. Huangshan, Anhui	SYS a002702	MF667882	MF667919
	56	*M. huangshanensis*	China: Mt. Huangshan, Anhui	SYS a002703	MF667883	MF667920
	57	*M. insularis*	China: Nan'ao Island, Guangdong	SYS a002169 (Holotype)	MF667887	MF667924
	58	*M. insularis*	China: Nan'ao Island, Guangdong	SYS a002170	MF667888	MF667925
	59	*M. jingdongensis*	China: Mt. Wuliang, Yunnan	SYS a003928	MH406773	MH406232
	60	*M. jingdongensis*	China: Mt. Wuliang, Yunnan	SYS a003929	MH406774	MH406233
	61	*M. jinggangensis*	China: Mt. Jinggang, Jiangxi	SYS a004028	MH406780	MH406239
	62	*M. jinggangensis*	China: Mt. Sifang, Hengdong County, Hunan	SYS a004825	MH406858	MH406320
	63	*M. kuatunensis*	China: Mt. Wuyi, Jiangxi	SYS a003449	MF667881	MF667916
	64	*M. lini*	China: Nanfengmian Nature Reserve, Jiangxi	SYS a002128	KJ560416	MF667907
	65	*M. lini*	China: Nanfengmian Nature Reserve, Jiangxi	SYS a002381	MF667874	MF667908
	66	*M. minor*	China: Dujiangyan City, Sichuan	SYS a003209	MF667862	MF667891
	67	*M. minor*	China: Dujiangyan City, Sichuan	SYS a003210	MF667863	MF667892
	68	*M. obesa*	China: Heishiding Nature Reserve, Guangdong	SYS a002271	KJ579121	MH406123
	69	*M. obesa*	China: Heishiding Nature Reserve, Guangdong	SYS a005025	MH406868	MH406330
	70	*M. ombrophila*	China: Mt. Wuyi, Fujian	WUYI2015101	KX856397	/
	71	*M. omeimontis*	China: Mt. Laojunshan, Yibin City, Sichuan	SYS a002741	MH406710	MH406162

Subgenus of *Megophrys* s. l.	ID	Species name	Locality	Specimen voucher no.	Genbank Accession No.	
					16S	CO1
Panophrys	72	*M. omeimontis*	China: Hejiang County, Sichuan	SYS a004916	MH406864	MH406326
	73	*M. sangzhiensis*	China: Mt. Badagongshan, Hunan	SYS a004307	MH406798	MH406260
	74	*M. sangzhiensis*	China: Mt. Badagongshan, Hunan	SYS a004313	MH406802	MH406264
	75	*M. spinata*	China: Mt. Leigong, Guizhou	SYS a002226	MH406675	MH406115
	76	*M. spinata*	China: Mt. Leigong, Guizhou	SYS a002227	MH406676	MH406116
	77	*M. tuberogranulatus*	China: Mt. Badagongshan, Hunan	SYS a004310	MH406801	MH406263
	78	*M. wushanensis*	China: Shennongjia Forestry District, Hubei	SYS a003008	MH406732	MH406184
	79	*M. wushanensis*	China: Shennongjia Forestry District, Hubei	SYS a003009	MH406733	MH406185
	80	*M. wuliangshanensis*	China: Mt. Wuliang, Yunnan	SYS a003924	MH406771	MH406230
	81	*M. wuliangshanensis*	China: Mt. Wuliang, Yunnan	SYS a003925	MH406772	MH406231
Atympanophrys	82	*M. gigantica*	China: Mt. Ailao, Yunnan	SYS a003883	MH406766	MH406225
	83	*M. gigantica*	China: Mt. Wuliang, Yunnan	SYS a003933	MH406775	MH406234
	84	*M. shapingensis*	China: Mt. Wawu, Sichuan	SYS a005310	MH406890	MH406352
	85	*M. shapingensis*	China: Zhaojue County, Sichuan	SYS a005339	MH406897	MH406359
Brachytarsophrys	86	*M. chuannanensis*	China: Hejiang County, Sichuan	SYS a004926	MH406901	MH406364
	87	*M. chuannanensis*	China: Hejiang County, Sichuan	SYS a004927	MH406902	MH406365
	88	*M. popei*	China: Taoyuandong Nature Reserve, Hunan	SYS a001864	MH406361	KM504256
	89	*M. popei*	China: Mt. Jinggang, Jiangxi	SYS a004209	MK524124	MK524155
Ophryophryne	90	*M. hansi*	Vietnam: Quang Nam, Tra My District	AMNH 163680	KY022203	/
	91	*M. microstoma*	China: Mt. Wuhuang, Pubei County, Guangxi	SYS a003492	MK524125	MK524156
	92	*M. microstoma*	China: Mt. Wuhuang, Pubei County, Guangxi	SYS a003493	MK524126	MK524157
Pelobatrachus	93	*M. nasuta*	Malaysia: Sabah, Lahad Datu District	FMNH 231281	KY022186	/
	94	*M. stejnegeri*	Philippines: Mindanao, Bukidnon Province	FMNH 250842	KY022190	/
Xenophrys	95	*M. glandulosa*	China: Mt. Gaoligong, Yunnan	SYS a003758	MH406755	MH406214
	96	*M. glandulosa*	China: Mt. Gaoligong, Yunnan	SYS a003794	MH406759	MH406218
	97	*M. mangshanensis*	China: Mt. Longtou, Guangdong	SYS a002750	MF667866	MF667895
	98	*M. mangshanensis*	China: Mt. Dayao, Guangxi	SYS a004870	MH406861	MH406323
	99	*M. medogensis*	China: Medog County, Tibet	SYS a002932	MH406725	MH406177
	100	*M. medogensis*	China: Medog County, Tibet	SYS a002933	MK524127	MK524158

DNA Extraction, PCR and sequencing

Genomic DNA was extracted from muscular tissue using a DNA extraction kit from Tiangen Biotech (Beijing) Co., Ltd. All samples were sequenced for two mitochondrial genes, i.e., partial 16S ribosomal RNA gene (16S) and complete cytochrome C oxidase 1 gene (CO1). Primers used for 16S were L3975 (5'-CGCCTGTTTACCAAAAACAT-3') and H4551 (5'-CCGGTCTGAACTCAGATCACGT-3') following Simon et al. (1994), and for CO1 were Chmf4 (5'-TYTCWACWAAYCAYAAAGAYATCGG-3') and Chmr4 (5'-ACYTCRGGRTGRCCRAARAATCA-3') following Meyer et al. (2005). PCR amplifications were processed in a 20-reaction volume with the cycling conditions that initial denaturing step at 95 °C for 4 min, 35 cycles of denaturing at 94 °C for 40 s, annealing at 53 °C for 40 s and extending at 72 °C for 1 min, and final extending step of 72 °C for 10 min. PCR products were purified with spin columns. The purified products were sequenced with both forward and reverse primers using BigDye Terminator Cycle Sequencing Kit per the guidelines, on an ABI Prism 3730 automated DNA sequencer by Shanghai Majorbio Bio-pharm Technology Co., Ltd and Beijing Genomics Institute. All sequences have been deposited in GenBank (Table 1).

Phylogenetic analyses

DNA sequences were aligned in MEGA 6 (Tamura et al. 2013) by the Clustal W algorithm with default parameters (Thompson et al. 1997). Two gene segments, 535 base pairs (bp) of 16S and 645 bp of CO1, were concatenated seriatim into a 1180-bp single sequence. The dataset was partitioned according to the genes and codon positions, and then tested respectively in jmodeltest v2.1.2 with Akaike and Bayesian information criteria, all resulting in the best-fitting nucleotide substitution models of GTR + I + G. Sequenced data was analyzed using Bayesian inference (BI) in MrBayes 3.2.4 (Ronquist et al. 2012). Three independent runs were conducted in BI analysis, each of which was performed for 2,000,000 generations and sampled every 1000 generations with the first 25% samples were discarded as burn-in, resulting a potential scale reduction factor (PSRF) of < 0.01. Pairwise distances (p-distance) were calculated in MEGA 6 using the uncorrected p-distance model.

Morphometrics

All specimens were fixed in 10 % buffered formalin and later transferred to 70% ethanol for preservation, and deposited at the Museum of Biology, Sun Yat-sen University (**SYS**) and Chengdu Institute of Biology, the Chinese Academy of Sciences (**CIB**), China.

Measurements follow Fei et al. (2009), and were taken with digital calipers to the nearest 0.1 mm. These measurements were as follows:

SVL snout−vent length (from tip of snout to vent);
HDL head length (from tip of snout to rear of jaws);
HDW head width (head width at commissure of jaws);
SNT snout length (from tip of snout to anterior corner of eye);
ED eye diameter (diameter of exposed portion of eyeball);
IOD interorbital distance (minimum distance between upper eyelids);
IND internasal distance (distance between nares);
TD tympanum diameter (horizontal diameter of tympanum);
TED tympanum–eye distance (distance from anterior edge of tympanum to posterior corner of eye);
HND hand length (distance from distal end of radioulna to tip of phalanx of finger III);
RAD radioulna length;
TIB tibia length (distance from knee to heel);
FTL foot length (distance from distal end of tibia to tip of distal phalanx of toe IV).

Sex was determined by direct observation of calls, the presence of internal vocal sac openings and the presence of testicles observed through dissection for males, as well as the presence of eggs and ovaries on the abdomen through anatomise for females. Presence or absence of nuptial pads/spines was examined with a microscope.

Comparative morphological data of *Megophrys* species allocated to the subgenus *Panophrys* (currently contains 32 species) (Mahony et al. 2017; Tapley et al. 2017; Wang et al. 2017a; Wang et al. 2017b; Zhang et al. 2017; Li et al. 2018; Tapley et al. 2018), and a small-sized species *M. feii* (incertae sedis), were obtained from examination of museum specimens (see Appendix 1) and from the literature (Table 2). The order of the new species accounts follows the distributions of the new species that located in the longitudinal mountain belt from the south to the north.

Results

Phylogenetics

The Bayesian inference (BI) phylogenetic tree was integrated in Figure 2; the *p*-distances at the mitochondrial 16S rRNA gene fragment among all samples of the subgenus *Panophrys* were given in Table 3.

In our phylogenic tree, all sequences of the genus *Megophrys* grouped into six clades with strong node support values, which were consistent with the results from Mahony et al. (2017) and Liu et al. (2018), and corresponded to the six subgenera: *Panophrys*, *Ophryophryne*, *Xenophrys*, *Atympanophrys*, *Brachytarsophrys* and *Pelobatrachus*. The subgenus *Panophrys* is further divided into three subclades, named western subclade A, western subclade B and eastern subclade.

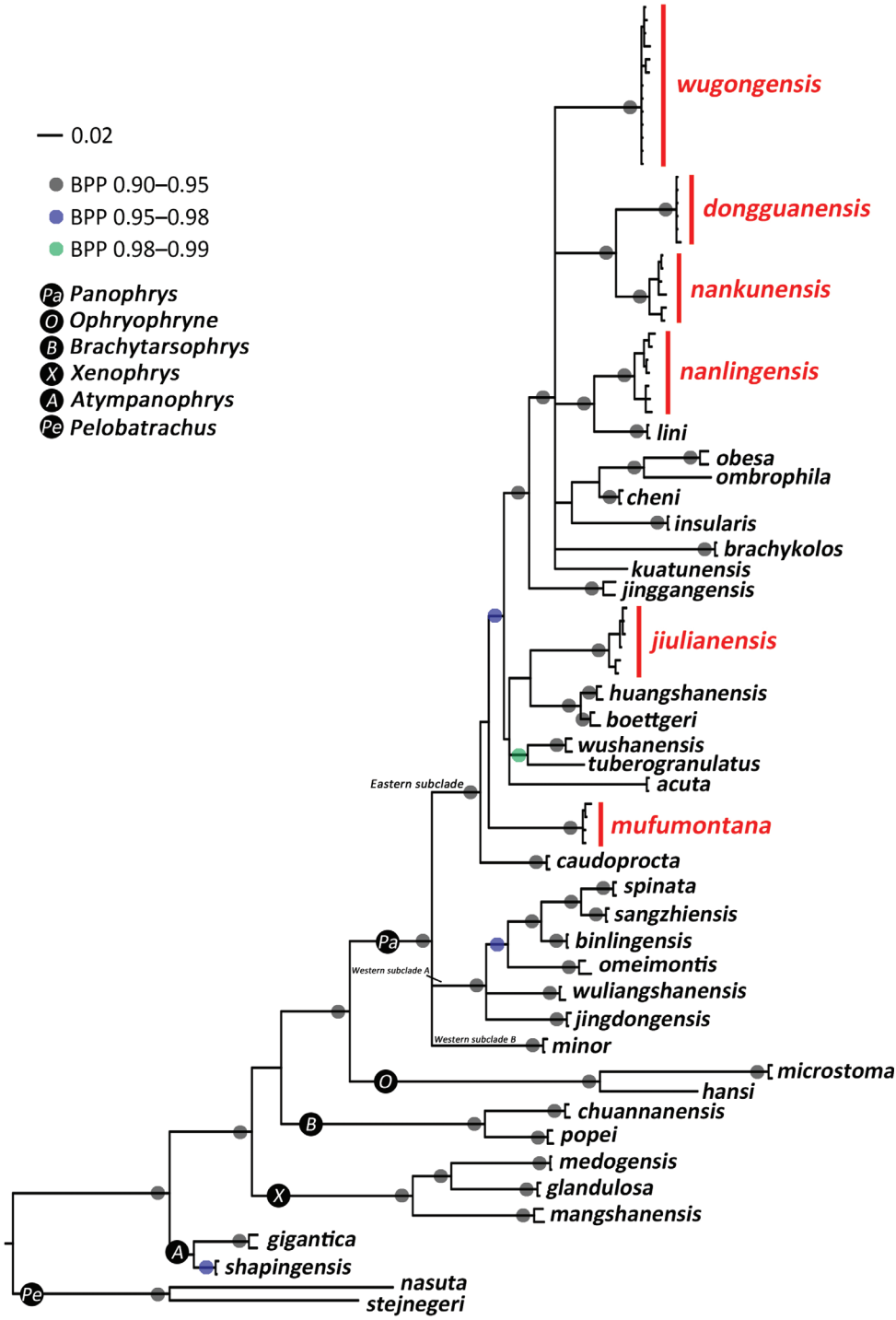

Figure 2. Bayesian inference tree derived from partial DNA sequences of the mitochondrial 16S rRNA + CO1 genes.

Table 2. References for morphological characters for congeners of the subgenus *Panophrys* and *Megophrys feii* (incertae sedis).

ID	Subgenus *Panophrys*	Literature obtained
1	*M. acuta* Wang, Li & Jin, 2014	Li et al. 2014
2	*M. baolongensis* Ye, Fei & Xie, 2007	Ye et al. 2007
3	*M. binchuanensis* Ye & Fei, 1995	Ye and Fei 1995
4	*M. binlingensis* Jiang, Fei & Ye, 2009	Fei et al. 2009
5	*M. boettgeri* (Boulenger, 1899)	Fei et al. 2012
6	*M. brachykolos* Inger & Romer, 1961	Inger and Romer 1961
7	*M. caudoprocta* Shen, 1994	Fei et al. 2012
8	*M. cheni* (Wang & Liu, 2014)	Wang et al. 2014
9	*M. daweimontis* Rao & Yang, 1997	Fei et al. 2012
10	*M. fansipanensis* Tapley, Cutajar, Mahony, Nguyen, Dau, Luong, Le, Nguyen, Nguyen, Portway, Luong & Rowley, 2018	Tapley et al. 2018
11	*M. huangshanensis* Fei & Ye, 2005	Fei et al. 2012
12	*M. hoanglienensis* Tapley, Cutajar, Mahony, Nguyen, Dau, Luong, Le, Nguyen, Nguyen, Portway, Luong &, 2018	Tapley et al. 2018
13	*M. insularis* (Wang, Liu, Lyu, Zeng & Wang, 2017)	Wang et al. 2017b
14	*M. jingdongensis* Fei & Ye, 1983	Fei et al. 2012
15	*M. jinggangensis* (Wang, 2012)	Wang et al. 2012
16	*M. kuatunensis* Pope, 1929	Fei et al. 2012
17	*M. latidactyla* Orlov, Poyarkov & Nguyen, 2015	Orlov et al. 2015
18	*M. leishanensis* Li, Xu, Liu, Jiang, Wei & Wang, 2018	Li et al. 2018
19	*M. liboensis* (Zhang, Li, Xiao, Li, Pan, Wang, Zhang & Zhou, 2017)	Zhang et al. 2017
20	*M. lini* (Wang &Yang, 2014)	Wang et al. 2014
21	*M. lishuiensis* (Wang, Liu & Jiang, 2017)	Wang et al. 2017a
22	*M. minor* Stejneger, 1926	Wang et al. 2017b
23	*M. obesa* Wang, Li & Zhao, 2014	Li et al. 2014
24	*M. ombrophila* Messenger & Dahn, 2019	Messenger et al. 2019
25	*M. omeimontis* Liu, 1950	Fei et al. 2009
26	*M. palpebralespinosa* Bourret, 1937	Fei et al. 2012
27	*M. rubrimera* Tapley, Cutajar, Mahony, Chung, Dau, Nguyen, Luong & Rowley, 2017	Tapley et al. 2017
28	*M. sangzhiensis* Jiang, Ye & Fei, 2008	Jiang et al. 2008
29	*M. shuichengensis* Tian & Sun, 1995	Tian et al. 2000
30	*M. spinata* Liu & Hu, 1973	Fei et al. 2012
31	*M. tuberogranulatus* Shen, Mo & Li, 2010	Mo et al. 2010
32	*M. wuliangshanensis* Ye & Fei, 1995	Ye and Fei 1995
33	*M. wushanensis* Ye & Fei, 1995	Ye and Fei 1995
Incertae sedis		
1	*M. feii* Yang, Wang & Wang, 2018	Yang et al. 2018

The western subclade A is composed of *Megophrys omeimontis*, *M. binglingensis*, *M. sangzhiensis*, *M. spinata*, *M. wuliangshanensis* and *M. jingdongensis*, and the western subclade B is composed of *M. minor*, all of which are distributed in southwestern China.

The eastern subclade contains 14 known species from southeastern China, i.e. *M. boettgeri*, *M. huangshanensis*, *M. kuatunensis*, *M. brachykolos*, *M. insularis*, *M. cheni*, *M. lini*, *M. jinggangensis*, *M. obesa*, *M. ombrophila*, *M. acuta*, *M. sangzhiensis*, *M. caudoprocta*, *M. tuberogranulatus* and *wushanensis*, and other six lineages made up of samples from the aforementioned longitudinal mountain belt in the middle of southeastern China with significant genetic differences (Table 3).

Table 3. Uncorrected *p*-distances among *Megophrys* species of the subgenus *Panophrys* in this study, based on mitochondrial 16S r RNA genes.

Species & ID No.	(1)–(6)	(7)–(12)	(13)–(16)	(17)–(22)	(23)–(29)	(30)–(42)	(43)–(44)	(45)–(46)	(47)–(48)	(49)–(50)	(51)–(52)	(53)–(54)	(55)–(56)	(57)–(58)
M. dongguanensis sp. nov. (1)–(6)	0–0.2													
M. jiulianensis sp. nov. (7)–(12)	5.3–5.8	0–0.7												
M. mufumontana sp. nov. (13)–(16)	6.3	3.7–4	0											
M. nankunensis sp. nov. (17)–(22)	2.6–2.8	4.7–4.9	4.9–5.1	0–0.7										
M. nanlingensis sp. nov. (23)–(29)	5.3–6.1	5.3–6.3	5.8–6.5	4.9–5.8	0–0.7									
M. wugongensis sp. nov. (30)–(42)	5.3–5.4	4–4.2	6–6.1	4.7–4.9	4.9–5.4	0								
M. acuta (43)–(44)	7.4–7.5	7–7.4	7.9	7.9–8.1	6.7–7.2	8.1–8.2	0							
M. binlingensis (45)–(46)	6.3	4.9–5.4	5.1	5.8–6.1	5.6–6.1	5.4	8.2	0						
M. boettgeri (47)–(48)	5.1–5.4	2.3–2.8	2.8–3	4–4.4	4.4–5.4	4.2–4.4	6.5–6.8	4.2–4.4	0–0.2					
M. brachykolos (49)–(50)	6.8	5.8–6.3	6.8	5.8–6.1	6.1–7.5	7.7	7.2	7.7	6.1	0–0.1				
M. caudoprocta (51)–(52)	6.3	3.5–3.7	4	4.9–5.1	6.8–7.5	5.8	6.8	4.4	3.3	6.5	0			
M. cheni (53)–(54)	3–3.3	3.5–4	4.2–4.4	5.8–6	3.5–4.4	5.7–6.6	7–7.2	4.7–4.9	2.6	5.1–5.4	4.4–4.7	0–0.2		
M. huangshanensis (55)–(56)	5.6	3–3.3	3.7	4.7–4.9	5.1–5.8	4.7	6.5	4.9	0.9–1.2	6.5	3.5	3.3–3.5	0	
M. insularis (57)–(58)	4.4–4.9	5.1–5.8	5.1–6.5	3.5–4.2	4.4–5.8	4.9–5.1	7.7–8.4	5.8	4.4–5.1	6.3–6.5	6.1–6.5	3.3–3.5	4.7–5.4	0
M. jingdongensis (59)–(60)	7.4	6–6.3	5.8	5.8–6	6.7–7.5	5.3–5.4	7.9	6.2–6.7	4.9–5.1	7.9	4.7	4.7–4.9	5.6	6.7
M. jinggangensis (61)–(62)	5.8–6.3	4.4–4.9	4.2–4.4	4.7–5.1	4.9–5.8	4.4	6.7	4.9	3.7–4	6.1	5.4	3–3.3	4.4	4.7
M. kuatunensis (63)	3.3	4–4.2	4.2	2.8–3	4.7–5.4	5.1	7.4	5.4	3.3–3.5	4.7	4.4	2.6–2.8	3.7	3.5
M. lini (64)–(65)	5.1	5.1–5.6	6–6.1	4.7–4.9	3.7–4.4	5.6	6.5	6.3	4.2–4.4	4.9	5.8	3.3–3.5	4.7	4.9
M. minor (66)–(67)	7.9–8.2	7–7.7	6.8–7	7.7–8.2	7–7.2	6.5–6.8	8.9–9.1	6.3–6.5	5.6–5.8	8.7–8.9	7–7.2	6.5–6.8	6.3–6.5	8.4–8.6
M. obesa (68)–(69)	4.7–5.8	5.6–6	6.3	4.2	4.4–4.9	5.1	7.4	7.2	4.2–4.4	6.3	6.8	2.8–3	4.9–5.1	4.9
M. ombrophila (70)	5.1	5.6–5.8	6–6.1	4.4–4.7	6–6.8	5.3–5.4	8.8	6.8	4.7–4.9	7	6.8	3–3.3	5.1–5.4	4.7
M. omeimontis (71)–(72)	5.8	4.2–4.4	4.9	4.7–4.9	5.1–5.8	4.3–4.4	7.9	5.5	4–4.2	7	4.2	3.7–4	4.7	5.4
M. sangzhiensis (73)–(74)	6.3	5.3–5.8	5.8	6.3	5.6–6	5.1	8.6	6.9	4.7–4.9	8.2	4.9	4.7–4.9	5.4	5.6
M. spinata (75)–(76)	6.5	5.1–5.6	5.8	6.3–6.5	5.3–6.1	4.9	8.4	4.5	4.4–4.7	8.4	5.1	4.7–4.9	4.7	6.3
M. tuberogranulatus (77)	4.7	2.6–2.8	3	3.3–3.5	4.7–5.1	4	6.5	7.5	3.4	5.4	3	2.1–2.3	2.3	4.2
M. wushanensis (78)–(79)	4.9–5.4	3.5–4	5.8	4.2–4.7	5.6–6.3	4.9–5.1	7.2–7.5	7.5–7.6	3–3.5	5.8	4.2–4.4	3.3–3.7	3.7–4	3.7–4
M. wuliangshanensis (80)–(81)	7.2	5.3–5.8	4	5.8–6	7–7.2	6–6.1	8.4	6.5–6.7	4.9–5.1	7.5	5.6	5.1–5.4	5.4–5.6	6.7

Table 3. (Continued) Uncorrected *p*-distances among *Megophrys* species of the subgenus *Panophrys* in this study, based on mitochondrial 16S r RNA genes.

Species & ID No.	(59)–(60)	(61)–(62)	(63)	(64)–(65)	(66)–(67)	(68)–(69)	(70)	(71)–(72)	(73)–(74)	(75)–(76)	(77)	(78)–(79)	(80)–(81)
M. jingdongensis (59)–(60)	0												
M. jinggangensis (61)–(62)	5.3	0–0.5											
M. kuatunensis (63)	5.8	4.4	0										
M. lini (64)–(65)	6.3	4.4	3.7	0									
M. minor (66)–(67)	7.2–7.5	6.8–7	6.5–6.8	7.7–7.9	0–0.2								
M. obesa (68)–(69)	6.3	4.9–5.3	4.2	4.2	7.2–7.5	0							
M. ombrophila (70)	6.7	5.3–5.8	4.9	5.8	8.2–8.4	3	0						
M. omeimontis (71)–(72)	3	4.4–4.9	4.7	5.1	5.8–6.1	5.6	5.6	0					
M. sangzhiensis (73)–(74)	3.9	5.6	5.8	6.3	7.2–7.5	7.2	6.5	4	0				
M. spinata (75)–(76)	3.9	5.8	6	5.6	6.5–6.8	7	6.7	3	2	0			
M. tuberogranulatus (77)	4	3	3	4.7	5.8–6.1	4.7–5.8	4.4	3.7	3.7	3.7	0		
M. wushanensis (78)–(79)	5.4–5.6	3.7–4	3.7–4	5.6–5.8	7.2–7.5	5.4–5.8	4.7–4.9	3.7–4	5.1–5.4	5.1–5.4	2.1	0	
M. wuliangshanensis (80)–(81)	3.7	5.8	5.1	6.7	6.5–6.8	5.8	6.5	3.5	4.9	4.4	4.2	4.7–5.1	0–0.5

Among them, all samples from Mt. Mufu, Hunan (samples 13–16 in Table 1) clustered into a basal lineage of an eastern subclade with strong node supports and almost have no molecular differences; further, this population can be distinguished from all known species and other undescribed lineages by distinctive morphological characters and significant molecular differences with a lowest *p*-distance of 2.8%. Therefore, the population from Mt. Mufu represented a separately evolving lineage, and is described as a new species, *Megophrys* (*Panophrys*) *mufumontana* sp. nov., below.

All samples from Mt. Wugong, Jiangxi (samples 30–42 from Yangshimu Scenic Area and Wugongshan Scenic Area) clustered into a lineage with strong node supporting values and almost no genetic differences, which was defined as a species and recognized as *M.* sp12 by Liu et al. (2018); further, the population from Mt. Wugong can be distinguished from all known species and other undescribed lineages by distinctive morphological differences and significant molecular differences with a lowest *p*-distance of 4%. Therefore, the population from Mt. Wugong represented a separately evolving lineage and is described as a new species, *Megophrys* (*Panophrys*) *wugongensis* sp. nov., below.

All samples from Mt. Yinping, Guangdong (samples 1–6) clustered into a lineage with strong node supportg values and small genetic differences (highest *p*-distance 0.2%), which was defined as a species and recognized as *M.* sp11 by Liu et al. (2018); samples 17–22 from Mt. Nankun, Guangdong clustered into a lineage with strong node support values and small genetic differences (highest *p*-distance 0.7%), which was defined as a species and recognized as *M.* sp10 by Liu et al. (2018); these two populations are sister taxa to each other with significant genetic differences (*p*-distances 2.6–2.8%), and can be further distinguished from all known species and other undescribed lineages by distinctive morphological differences and significant molecular differences. Therefore, the populations from Mt. Yinping and Mt. Nankun represented two separately evolving lineages, and are described as new species, *Megophrys* (*Panophrys*) *dongguanensis* sp. nov. and *Megophrys* (*Panophrys*) *nankunensis* sp. nov., below.

Samples 7–10 from Mt. Jiulian, Jiangxi and samples 11–12 from Mt. Nankun, Guangdong clustered into a lineage with small genetic differences (highest *p*-distance 0.7%), which is a sister subclade to *M. boettgeri* and *M. huangshanensis* with large genetic differences (lowest p-distance 2.3%); therefore, these samples represented a separately evolving lineage, which was defined as a species and recognized as *M.* sp30 by Liu et al. (2018), and is described as a new species, *Megophrys* (*Panophrys*) *jiulianensis* sp. nov., below.

Samples 26–29 from Mt. Qiyun, Jiangxi were defined as a species and recognized as *M.* sp6 by Liu et al. (2018) and the samples 23–25 from Nanling Nature Reserve, Guangdong were defined as a species and recognized as *M.* sp7 by Liu et al. (2018). Although the populations from two locations are divided into two branches, the highest *p*-distance is only 0.7%. Moreover, there are no distinct morphological characters that can distinguish them from each other. Herein, we considered these two populations as one taxon, which is the sister taxon to *M. lini* with large genetic differences (*p*-distances 3.7–4.4%), representing a new species and described as, *Megophrys* (*Panophrys*) *nanlingensis* sp. nov., below.

Taxonomic accounts

***Megophrys* (*Panophrys*) *dongguanensis* J. Wang & Y.Y. Wang, sp. nov.**
http://zoobank.org/94DBE153-5A7C-4820-8E27-E9BE41C3A764
Fig. 3, Table 4

Holotype. SYS a001973, adult male, collected by Run-Lin Li on 13 December 2012 from Mt. Yinping, Xiegang County (22°54'17.20"N, 114°13'23.88"E; 132 m a.s.l.), Dongguan City, Guangdong Province, China.

Paratypes (10 males). SYS a002007, adult male, collected on 17 March 2013 by Run-Lin Li from Mt. Yinping, Qingxi County (22°53'26.21"N, 114°10'14.82"E; 277 m a.s.l.), Dongguan City, China; adult males, SYS a001971/CIB110006, SYS a001972, 1974–1975, collected on 12–13 December 2012, SYS a001492–1495, collected on 23 December 2012 by Run-Lin Li from the same locality as the holotype (100–300 m a.s.l.).

Diagnosis. (1) Body size small to moderate, SVL 30.2–39.3 mm in 11 adult male specimens; (2) head width slightly larger than head length, HDW/HDL ratio 1.04–1.09; (3) snout pointed in dorsal view; (4) tympanum distinct, moderate-sized, TD/ED ratio 0.42–0.60; (5) strong vomerine ridge bearing vomerine teeth; (6) margin of tongue not notched behind; (7) hindlimbs short, heels not meeting, tibio-tarsal articulation reaching the region between tympanum and eye; (8) presence of subarticular tubercles and absence of lateral fringes on fingers, relative finger lengths II < I ≤ IV < III; (9) toes with rudiment of webbing at their bases and without lateral fringes, subarticular tubercles only present at the base of each toe; (10) numerous granules present on dorsal surface of body, several large tubercles present on surface of flanks; (11) presence of a barely visible reddish horn-like tubercle at the edge of the upper eyelid; (12) supratympanic fold distinct, whitish; (13) yellowish brown dorsally, with an incomplete dark triangular marking between eyes and usually an X-shaped marking on back of trunk; (14) ventral surface black brown, with white spots on posterior surface of abandon; (15) males with a single subgular vocal sac; (16) presence of nuptial pads with darker nuptial spines on dorsal surface of the first and second fingers in adult males during breeding season, respectively.

Comparisons. Comparative data of *Megophrys dongguanensis* sp. nov. with *M. feii* and the 33 recognized members of *Megophrys* s.l. allocated to the subgenus *Panophrys* are listed in Table 5.

With significantly smaller body size, SVL 30.2–39.3 mm in males, *Megophrys dongguanensis* sp. nov. differs from the eight members with larger SVL values: *M. baolongensis* (42.0–45.0 mm in males), *M. binlingensis* (45.1–51.0 mm in males), *M. caudoprocta* (81.3 mm in male), *M. jingdongensis* (53.0–56.5 mm in males), *M. omeimontis* (56.0–59.5 mm in males), *M. sangzhiensis* (54.7 mm in single male), *M. spinata* (47.2–54.4 mm in males) and *M. shuichengensis* (102.0–118.3 mm in males).

Megophrys dongguanensis sp. nov. differs from 12 species occurring in eastern and southern China (*M. acuta*, *M. brachykolos*, *M. boettgeri*, *M. cheni*, *M. huangshanensis*,

Table 4. Measurements (in mm; minimum-maximum, mean ± SD) of the type series of *Megophrys dongguanensis* sp. nov. and *M. nankunensis*. sp. nov., respectively.

Species	*Megophrys dongguanensis* sp. nov.	*Megophrys nankunensis* sp. nov.	
	Males (n = 9)	Males (n = 11)	Females (n = 2)
SVL	30.2–39.3 (36.3 ± 3.3)	29.9–34.9 (32.7 ± 1.5)	39.4–41.9
HDL	11.1–12.6 (12.0 ± 0.5)	9.0–11.3 (10.0 ± 0.7)	11.9–12.5
HDW	11.5–13.2 (12.8 ± 0.6)	10.1–12.6 (10.9 ± 0.7)	13.0–13.7
SNT	3.7–4.6 (4.2 ± 0.3)	2.8–3.7 (3.3 ± 0.3)	4.1–4.4
IND	3.7–3.9 (3.6 ± 0.2)	2.2–3.8 (3.1 ± 0.5)	3.1–3.9
IOD	3.2–3.6 (3.5 ± 0.2)	2.4–3.4 (2.8 ± 0.3)	3.1–3.2
ED	4.6–5.2 (4.9 ± 0.2)	3.1–4.4 (3.8 ± 0.4)	4.7–5.2
TD	2.1–2.8 (2.5 ± 0.3)	1.4–2.4 (1.9 ± 0.3)	2.6–2.7
TED	1.9–2.4 (2.1 ± 0.1)	0.8–1.7 (1.2 ± 0.2)	2.2–2.3
HND	8.3–9.8 (9.2 ± 0.5)	6.7–8.6 (7.5 ± 0.5)	9.7–10.2
RAD	8.2–9.7 (9.2 ± 0.5)	5.5–8.4 (6.6 ± 0.7)	8.0–8.4
FTL	13.4–16.5 (15.5 ± 1.08)	10.9–14.1 (12.2 ± 0.7)	14.6–15.3
TIB	19.9–23.4 (22.2 ± 1.11)	16.3–21.6 (18.2 ± 1.4)	22.6–25.5
HDL/SVL	0.32–0.37 (0.33 ± 0.02)	0.27–0.33 (0.31 ± 0.02)	0.30
HDW/SVL	0.33–0.40 (0.35 ± 0.02)	0.30–0.37 (0.33 ± 0.02)	0.33
HDW/HDL	1.04–1.09 (1.06 ± 0.02)	1.00–1.20 (1.10 ± 0.06)	1.09–1.10
SNT/HDL	0.33–0.37 (0.35 ± 0.01)	0.28–0.40 (0.33 ± 0.03)	0.35
SNT/SVL	0.11–0.12 (0.12 ± 0.01)	0.08–0.11 (0.10 ± 0.01)	0.10–0.11
IND/HDW	0.26–0.30 (0.28 ± 0.01)	0.21–0.34 (0.28 ± 0.04)	0.24–0.28
IOD/HDW	0.27–0.28 (0.27 ± 0.01)	0.23–0.30 (0.26 ± 0.02)	0.23–0.24
ED/HDL	0.37–0.44 (0.40 ± 0.02)	0.34–0.41 (0.38 ± 0.02)	0.39–0.42
ED/SVL	0.12–0.16 (0.14 ± 0.02)	0.09–0.13 (0.11 ± 0.01)	0.12
TD/ED	0.42–0.60 (0.51 ± 0.06)	0.43–0.61 (0.50 ± 0.06)	0.49–0.57
TED/TD	0.73–1.09 (0.88 ± 0.14)	0.58–0.74 (0.66 ± 0.05)	0.85
HND/SVL	0.24–0.28 (0.25 ± 0.01)	0.21–0.25 (0.23 ± 0.01)	0.24–0.25
RAD/SVL	0.24–0.28 (0.25 ± 0.01)	0.16–0.25 (0.20 ± 0.02)	0.20
TIB/SVL	0.41–0.46 (0.43 ± 0.02)	0.35–0.42 (0.37 ± 0.01)	0.37
FTL/SVL	0.58–0.70 (0.61 ± 0.04)	0.53–0.62 (0.56 ± 0.03)	0.57–0.61

M. insularis, *M. jinggangensis*, *M. kuatunensis*, *M. lini*, *M. lishuiensis*, *M. obesa* and *M.ombrophila*) by the following combination of characters: presence of vomerine teeth (vs. absent in *M. acuta*, *M. boettgeri*, *M. brachykolos*, *M. cheni*, *M. huangshanensis*, *M. kuatunensis*, *M. lini*, *M. lishuiensis*, *M. obesa* and *M.ombrophila*), margin of tongue not notched posteriorly (vs. notched in *M. boettgeri*, *M. cheni*, *M. huangshanensis*, *M. insularis* and *M. kuatunensis*), absence of lateral fringes on toes (vs. presence of narrow lateral fringes on toes in *M. acuta*, *M. jinggangensis* and *M. kuatunensis*; presence of wide lateral fringes on toes in *M. boettgeri*, *M. cheni* and *M. lini*), toes with rudimentary webbing (vs. toes without webbing in *M. lishuiensis*, *M. kuatunensis* and *M.ombrophila*), hindlimbs short, with heels not meeting when the flexed hindlimbs are held at right angles to the body axis (vs. hindlimbs comparatively longer, with heels meeting or overlapping in *M. cheni*, *M. boettgeri*, *M. kuatunensis*, *M. jinggangensis* and *M. lini*), tibio-tarsal articulation reaching the region between tympanum and eye when hindlimb is stretched along the side of the body (vs. reaching forward to the shoulder in *M. brachykolos* and to the posterior edge of tympanum in *M. insularis*).

Table 5. Diagnostic characters separating the seven new species described in this study from *Megophrys feii* (incertae sedis) and 33 recognizing species of the *Megophrys* s.l. allocated to the subgenus *Panophrys*.

Species	SVL		Horn-like tubercle at edge of upper eyelid[1]	Vomerine teeth[2]	Tongue[3]	Lateral fringes on toes[4]	Toes[5]	TD/ED	TIB/SVL
	males (N)	females (N)							
M. dongguanensis	30.2–39.3 (9)	/	+	+	−	−	+	0.42–0.60	0.41–0.46
M. nankunensis	29.9–34.9 (11)	39.4–41.9 (2)	+	+	−	−	+	0.43–0.61	0.35–0.42
M. jiulianensis	30.4–33.9 (9)	34.1–37.5 (2)	+	+	+	−	+	0.50–0.59	0.44–0.48
M. nanlingensis	30.5–37.3 (10)	/	+	+	+	+	+	0.43–0.57	0.45–0.51
M. wugongensis	31.0–34.1 (4)	38.5–42.8 (9)	+	−	−	−	+	0.45–0.53	0.37–0.44
M. mufumontana	30.1–30.8 (2)	36.3 (2)	+	−	−	+	+	0.51–0.58	0.47–0.53
M. acuta	27.1–33.0 (10)	28.1–33.6 (4)	++	−	−	+	+	0.57–0.71	0.38–0.45
M. baolongensis	42.0–45.0 (5)	/	+	−	+	−	−	0.41	0.46
M. binchuanensis	32.0–36.0 (4)	40.2–42.5 (2)	−	−	+ or −	++	+	0.33–0.50	0.46–0.48
M. binlingensis	45.1–51.0 (3)	/	−	−	+	/	+	0.47–0.52	0.52–0.53
M. boettgeri	34.5–37.8 (20)	39.7–46.8 (10)	+	−	+	++	+	0.40–0.67	0.45–0.49
M. brachykolos	33.7–39.3 (5)	33.9–45.9 (2)	+	−	−	−	+	> 0.50	0.37–0.42
M. caudoprocta	81.3 (1)	/	++	+	−	/	+	0.50	0.51
M. cheni	26.2–29.5 (15)	31.8–34.1 (3)	+	−	++	++	+	0.41–0.54	0.50–0.54
M. daweimontis	34.0–37.0 (18)	40.0–46.0 (3)	+	+	/	−	−	/	0.54
M. fansipanensis	30.9–44.3 (13)	41.7–42.5 (2)	+	+	+	−	−	0.53–0.80	0.49–0.59
M. feii	24.3–25.1 (4)	28.2–28.9 (2)	+	−	+	++	+	0.51–0.58	0.48–0.55
M. hoanglienensis	37.4–47.6 (11)	59.6 (1)	+	+	+	−	−	0.54–0.75	0.44–0.63
M. huangshanensis	36.0–41.6 (4)	44.2 (1)	+	−	+	−	−	<0.50	0.42–0.45
M. insularis	36.8–41.2 (5)	47.1 (1)	+	+	+	−	+	0.46–0.57	0.40–0.43
M. jingdongensis	53.0–56.5 (3)	63.5 (1)	+	+	+	++	+++	/	0.58–0.59
M. jinggangensis	35.1–36.7 (2)	38.4–41.6 (3)	++	+	−	+	+	0.73–0.88	0.47–0.50
M. kuatunensis	26.2–29.6 (13)	37.4 (1)	+	−	+	+	−	0.44	0.38–0.48
M. latidactyla	38.9 (1)	/	++	+	−	++	+	0.85	0.52
M. leishanensis	30.4–38.7 (10)	42.3 (2)	+	−	−	−	+	/	/
M. liboensis	34.7–67.7 (5)	60.8–70.6 (8)	+++	+	+	++	+	0.48–0.78	0.44–0.61
M. lini	34.1–39.7 (20)	37.0–39.9 (4)	+	−	−	++	+	0.40–0.60	0.46–0.53
M. lishuiensis	30.7–34.7 (13)	36.9–40.4 (3)	+	−	−	−	−	/	/
M. minor	34.5–41.2 (4)	/	−	−	+	−	+	0.8–0.83	0.46–0.48
M. obesa	35.6 (1)	37.5–41.2 (6)	+	−	−	−	+	0.51–0.66	0.41–0.47
M. ombrophila	27.4–34.5 (5)	32.8–35.0 (4)	+	−	−	−	−	0.52–0.69	0.32–0.41
M. omeimontis	56.0–59.5 (10)	68.0–72.5 (3)	+	+	+	+	+	/	0.52–0.56
M. palpebralespinosa	36.2–38.0 (2)	/	++	+	−	++	+++	/	0.55
M. rubrimera	26.7–30.5 (8)	/	+	+	+	+	−	0.58–0.76	0.48–0.56
M. sangzhiensis	54.7 (1)	/	+	+	+	+	+	0.62	0.59
M. shuichengensis	102.0–118.3 (7)	99.8–115.6 (6)	++	−	+	++	+++	0.67	0.43–0.47
M. spinata	47.2–54.4 (18)	54.0–55.0 (2)	−	−	+	++	+++	0.43	0.56–0.58
M. tuberogranulatus	33.2–39.6 (9)	50.5 (1)	+ or −	−	−	−	+	0.50	0.45–0.51
M. wuliangshanensis	27.3–31.6 (10)	41.0–41.5 (2)	−	−	+ or −	−	−	0.50	0.50–0.51
M. wushanensis	30.4–35.5 (10)	38.4 (1)	−	−	−	− (in female), ++ (in male)	+	0.50	0.47–0.48

[1] long point (+++); slightly large (++), small (+), absent or indistinct (−); [2] present (+), or absent (−); [3] notched (++), feebly notched (+), or not notched (−); [4] wide (++), narrow (+), lacking (−); [5] at least one-fourth webbed (+++), at most one-fourth webbed (++), with rudimentary webbing (+), or without webbing (−).

From the remaining 10 species occurring in China, *Megophrys dongguanensis* sp. nov. can be distinguished by the presence of vomerine teeth (vs. absent in *M. binchuanensis*, *M. leishanensis*, *M. minor*, *M. tuberogranulatus*, *M. wuliangshanensis* and *M. wushanensis*), by the unnotched tongue (vs. tongue notched in *M. daweimontis*, *M. liboensis*, *M. minor* and *M. rubrimera*), by the absence of lateral fringes on toes (vs. wide in *M. binchuanensis*, *M. liboensis*, *M. palpebralespinosa* and *M. wushanensis* (in males); narrow in *M. rubrimera*), by the rudimentary webbing on toes (vs. toes without webbing in *M. rubrimera* and *M. wuliangshanensis*; at least one-fourth webbed in *M. palpebralespinosa*), by the heels not meeting when the flexed hindlimbs are held at right angles to the body axis (vs. heels meeting in *M. binchuanensis* and *M. tuberogranulatus*; heels meeting or overlapping in *M. minor* and *M. wushanensis*; heels overlapping in *M. leishanensis*, *M. liboensis*, *M. palpebralespinosa* and *M. wuliangshanensis*).

Megophrys dongguanensis sp. nov. differs from the remaining species, *M. fansipanensis*, *M. hoanglienensis* and *M. latidactyla*, by the small horn-like tubercle at edge of upper eyelid (vs. slightly large in *M. latidactyla*), by the unnotched tongue (vs. tongue notched in *M. fansipanensis*, *M. hoanglienensis* and *M. latidactyla*), by the absence of lateral fringes on toes (vs. wide in *M. latidactyla*), by the presence of rudimentary webbing on toes (vs. webbing indistinct or absent in *M. fansipanensis* and *M. hoanglienensis*).

Megophrys dongguanensis sp. nov. further differs from *M. feii*, for which molecular data are lacking and cannot be allocated to any subgenus base on morphology only (Yang et al. 2018) by the larger body size, SVL 30.2–39.3 mm in males (VS. 24.3–25.1 mm in males), presence of nuptial pad with nuptial spines in males during breeding season (vs. absent), presence of vomerine teeth (vs. absent), unnotched tongue (vs. slightly notched), absence of lateral fringes on toes (vs. moderate or wide), heels not meeting when the flexed hindlimbs are held at right angles to the body axis (vs. heels overlapping).

Description of holotype. Adult male. Body moderate-sized, SVL 38.0 mm; head width slightly larger than head length, HWD/HDL 1.09; snout pointed in dorsal view, projecting, sloping backward to mouth in profile, protruding well beyond margin of lower jaw; top of head flat; eye large, ED/HDL 0.40, pupil vertical; nostril oblique ovoid; canthus rostralis well developed, forming the beginning of a fleshy, protruding ridge, that continues over the upper eyelid, and transitions into a supratympanic fold that terminates in the scapular region; loreal region slightly oblique; internasal distance slightly larger than interorbital distance; tympanum distinct, moderate-sized, TD/ED 0.54; large ovoid choanae at the base of the maxilla; presence of vomerine ridge bearing vomerine teeth; margin of tongue not notched posteriorly; internal vocal slits present near the rear of the lower mandible.

Radioulna length and hand length 0.24 of SVL; fingers without webbing and lateral fringes, relative finger length II < I < IV < III; tips of fingers slightly dilated, round; presence of subarticular tubercles on finger III, and one subarticular tubercle at the bases of each finger; outer metacarpal tubercles indistinct, inner metacarpal tubercles distinct and observably enlarged. Hindlimbs short, tibio-tarsal articulation reaching the region between tympanum and eye when hindlimb is stretched along the side of the body; heels not meeting when the flexed hindlimbs are held at right angles to the

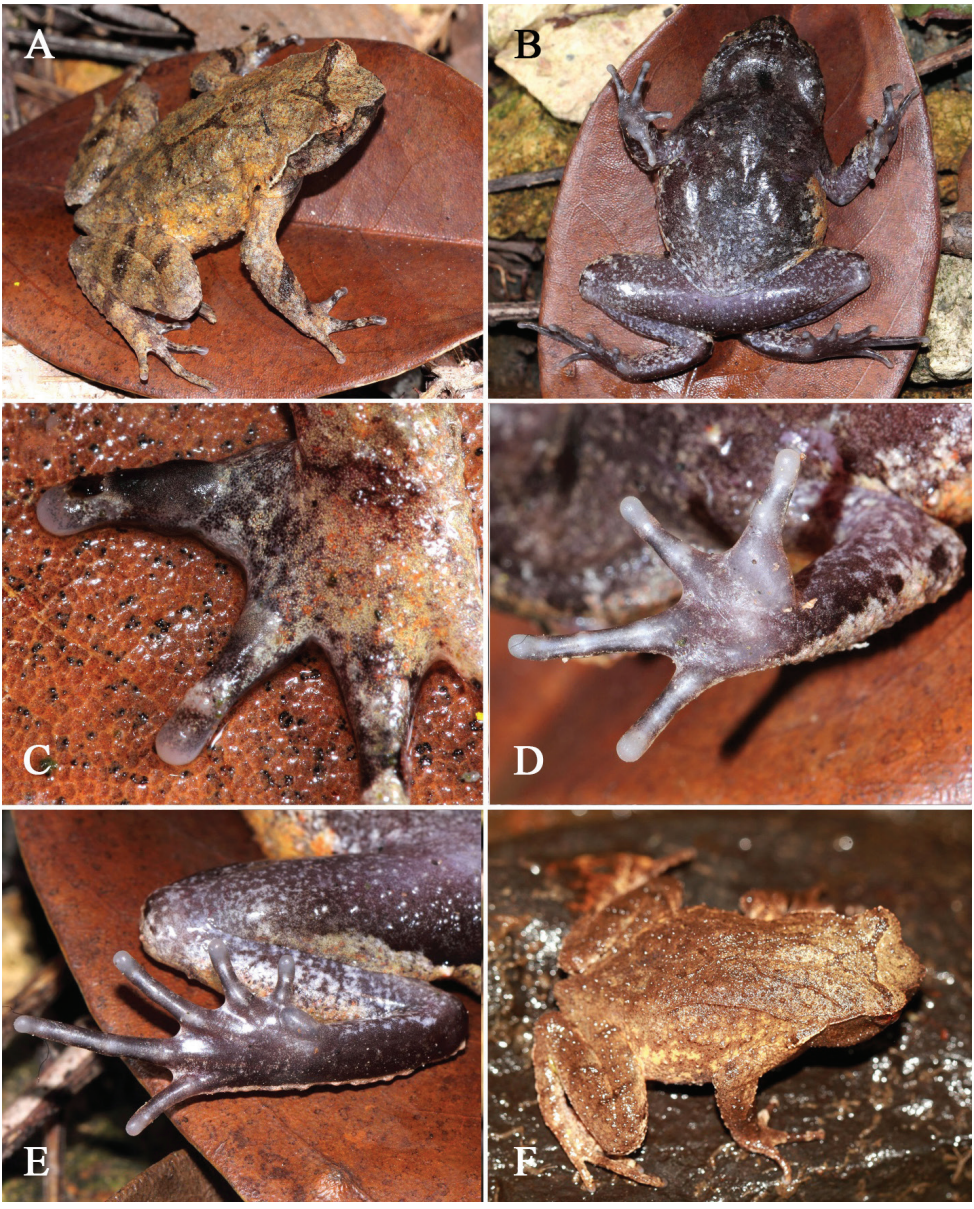

Figure 3. *Megophrys dongguanensis* sp. nov. in life: **A–E** SYS a001973, the male holotype **F** SYS a001492, a male paratype with more distinct skin ridges, granules and tubercles on dorsal surface of body.

body axis; tibia length 0.41 of SVL and foot length 0.61 of SVL; relative toe length I < II < V < III < IV; tips of toes round and slightly dilated; presence of rudimentary webbing on toes but absence of lateral fringes and tarsal folds; one subarticular tubercle at the bases of each toe; presence of a long ovoid inner metatarsal tubercle and absence of outer metatarsal tubercle.

Dorsal skin texture rough with dense granules; granules forming discontinuous X-shaped ridge with two discontinuous dorsolateral ridges on both sides at the central trunk; several large tubercles present on dorsal surface of flanks, thighs, shanks and forearms; four small tubercles present on the edge of upper eyelid, one of which is more prominent; distinct narrow supratympanic fold curving posteroventrally from posterior corner of eye to a level above insertion of arm; ventral skin texture smooth, several granules present on surface of abandon, ventral and posterior surface of thighs; pectoral gland small, closer to axilla; single femoral gland on rear of thigh.

Measurements of holotype (in mm). SVL 38.0, HDL 12.0, HDW 13.1, SNT 4.5, IND 3.9, IOD 3.6, ED 4.8, TD 2.6, TED 2.1, HND 9.1, RAD 9.2, FTL 23.2, TIB 15.6.

Coloration of holotype in life. (Fig. 3A–E) Yellowish brown dorsally, with a dark triangular marking between eyes. A wide oblique black band present on forearm. Dorsal surface of fingers and hindlimbs with dark grey transverse bands. Point of snout dark brown, presence of a vertical dark brown band below the eye. Tubercles on the edge of upper eyelid reddish. Supratympanic fold whitish tan. Ventral surface dark brown, with a black longitudinal band on surface of throat, several white spots present on ventral surface of limbs. Digits, inner and outer metacarpal tubercles greyish white, inner metatarsal tubercle greyish brown. Pectoral glands and femoral glands white. Iris yellowish brown.

Coloration of holotype in preservative. Yellowish brown fades to greyish brown dorsally. Triangular marking between eyes, oblique bands on dorsal forearms, transverse bands on dorsal fingers and hindlimbs become indistinct. Color of ventral surface fades, all bands and spots become indistinct.

Variation. Measurements of type series are listed in Table 4. All paratypes are very similar to holotype in morphology and color pattern. However, one male (SYS a001492) has more distinct skin ridges, granules and tubercles on dorsal surface of body (Fig. 3, F).

Etymology. The specific epithet "dongguanensis" is in reference to the type locality, Dongguan City of the new species. We propose the common English name "Dongguan Horned Toad" and Chinese name "Dong Guan Jiao Chan (东莞角蟾)".

Distribution and natural history. Currently, *Megophrys dongguanensis* sp. nov. is only known from Mt. Yinping, Guangdong Province, China. It inhabits flowing montane streams and the nearby forest floor and leaf litter at elevations between 100–300 m. Advertisement calls of males were noticed from mid-December until April of the next year just before the rainy season. Males were found calling on rocks in the flowing streams. Tadpoles could be found in this period.

***Megophrys* (*Panophrys*) *nankunensis* J. Wang, Zeng & Y.Y. Wang, sp. nov.**
http://zoobank.org/1F85DDB8-298D-47BB-B5BD-CA6D5A3E66A8
Fig. 4, Table 4

Holotype. SYS a004498, adult male, collected by Jian Wang and Hai-Long He on 20 October 2015 from Mt. Nankun (23°38'19"N, 113°53'24"E; 400 m a.s.l.), Longmen County, Huizhou City, Guangdong Province, China.

Figure 4. *Megophrys nankunensis* sp. nov. in life: **A–D** SYS a004498, the male holotype **E–F** SYS a004507, the female paratype.

Paratypes (10 males & two females). Adult females, SYS a004506–4507, collected by Jian Wang and Hai-Long He on 20 October 2015; adult males, SYS a002023, 2032–2033, collected by Run-Lin Li on 20 March 2013, SYS a004499–4504, SYS a004505/CIB110007, collected by Jian Wang and Hai-Long He on 20 October 2015, all from Mt. Nankun at elevations between 300–650 m.

Diagnosis. (1) Body size small, SVL 29.9–34.9 mm in 11 adult males, 39.4–41.9 mm in two adult females; (2) head width slightly larger than head length, HDW/HDL ratio 1.00–1.20; (3) snout rounded in dorsal view, tip of snout slightly sharpened; (4) tympanum distinct, moderate-sized, TD/ED ratio 0.43–0.61; (5) strong vomerine ridge bearing vomerine teeth; (6) margin of tongue not notched behind; (7) shanks short, heels not meeting when the flexed hindlimbs are held at right angles

to the body axis; tibia-tarsal articulation reaching forward to the region between tympanum and eye when hindlimb is stretched along the side of the body; (8) TIB/SVL ratio 0.35–0.42, FTL/SVL ratio 0.53–0.62; (9) absence of lateral fringes on fingers, presence of an indistinct subarticular tubercle on the bases of each finger, relative finger lengths II < I < IV < III; (10) toes with rudimentary webbing at their bases and without lateral fringes, subarticular tubercles only present on the bases of each toes; (11) dorsal surface with dense granules, surface of flanks and dorsal surface of limbs with large tubercles; (12) edge of eye lid with a small reddish horn-like tubercle; (13) supratympanic fold distinct, forming a depressed supraaxillary gland above insertion of arm; (14) dorsum beige to dark brown, with indistinct light brown patches, with an incomplete dark triangular marking between eyes; (15) males with a single subgular vocal sac, and dense dark villiform nuptial spines present on dorsal surface of first and second fingers during breeding season, respectively; (16) gravid females bear creamy yellow oocytes.

Comparisons. Comparative data of *Megophrys nankunensis* sp. nov. with *M. dongduanensis* sp. nov., *M. feii* and the 33 recognized members of *Megophrys* s.l. allocated to the subgenus *Panophrys* are listed in Table 5.

In the ML and BI phylogenetic trees (Fig. 2), *Megophrys nankunensis* sp. nov. is a sister taxon to *M. dongguanensis* sp. nov. (p=4.6–5.0%) with high node-supporting value (0.1 in BI, 100% in ML%), and differs from the later by the snout rounded in dorsal view, tip of snout slightly sharpened (vs. snout pointed in dorsal view, tip of snout not sharpened), supratympanic fold forming a depressed supraaxillary gland above insertion of arm (vs. supraaxillary gland absent).

With significantly smaller body size, SVL 29.9–34.9 mm in males and 39.4–41.9 mm in females, *Megophrys nankunensis* sp. nov. differs from the 12 members with larger SVL values: *M. baolongensis* (42.0–45.0 mm in males), *M. binlingensis* (45.1–51.0 mm in males), *M. caudoprocta* (81.3 mm in single male), *M. hoanglienensis* (37.4–47.6 mm in males), *M. jingdongensis* (53.0–56.5 mm in males, 63.5 mm in single female), *M. latidactyla* (38.9 mm in single male), *M. omeimontis* (56.0–59.5 mm in males, 68.0–72.5 mm in females), *M. palpebralespinosa* (36.2–38.0 mm in males), *M. sangzhiensis* (54.7 mm in single male), *M. shuichengensis* (102.0–118.3 mm in males, 99.8–115.6 mm in females), *M. spinata* (47.2–54.4 mm in males, 54.0–55.0 mm in females) and *M. tuberogranulatus* (50.5 in single female).

Megophrys nankunensis sp. nov. differs from 12 species occurring in eastern and southern China (*M. acuta*, *M. brachykolos*, *M. boettgeri*, *M. cheni*, *M. huangshanensis*, *M. insularis, M. jinggangensis*, *M. kuatunensis*, *M. lini*, *M. lishuiensis*, *M. obesa* and *M. ombrophila*) by the following combination of characters: presence of vomerine teeth (vs. absent in *M. acuta*, *M. boettgeri*, *M. brachykolos*, *M. cheni*, *M. huangshanensis*, *M. kuatunensis*, *M. lini*, *M. lishuiensis*, *M. obesa* and *M. ombrophila*), absence of lateral fringes on toes (vs. presence of narrow lateral fringes on toes in *M. acuta*, *M. jinggangensis* and *M. kuatunensis*; presence of wide lateral fringes on toes in *M. boettgeri*, *M. cheni* and *M. lini*), toes with rudimentary webbing (vs. toes without webbing in *M. lishuiensis*, *M. kuatunensis* and *M. ombrophila*), hindlimbs short, with heels not meeting when the flexed hindlimbs are held at right angles to the body axis (vs. hindlimbs

comparatively longer, with heels meeting or overlapping in *M. cheni*, *M. boettgeri*, *M. kuatunensis*, *M. jinggangensis* and *M. lini*), tibio-tarsal articulation reaching forward to the region between tympanum and eye when hindlimb is stretched along the side of the body (vs. reaching forward to the shoulder in *M. brachykolos* and to the posterior edge of tympanum in *M. insularis*), relative finger lengths II < I < IV < III (vs. IV < I < II < III in *M. brachykolos* and I < II < IV < III in *M. obesa* and *M. ombrophila*); supratympanic fold forming a depressed supraaxillary gland above insertion of arm (vs. supraaxillary gland swollen in *M. insularis*; absent in other 11 species).

Megophrys nankunensis sp. nov. differs from the remaining nine members of the *Megophrys s.l.* allocated to the subgenus *Panophrys* which share a moderate or small body size, by the by the small horn-like tubercle at edge of upper eyelid (vs. horn-like tubercle indistinct or absent in *M. binchuanensis*, *M. minor*, *M. wuliangshanensis* and *M. wushanensis*; long point in *M. liboensis*), presence of vomerine teeth (vs. absent in *M. binchuanensis*, *M. leishanensis*, *M. minor*, *M. wuliangshanensis* and *M. wushanensis*), absence of lateral fringes on toes (vs. wide in *M. binchuanensis*, *M. liboensis*, *M. wushanensis* (wide in males); narrow in *M. rubrimera*), toes with rudimentary webbing (vs. toes without webbing in *M. daweimontis*, *M. rubrimera*, *M. wuliangshanensis* and *M. wushanensis* (in females); webbing indistinct or absent in *M. fansipanensis*), tibio-tarsal articulation reaching forward to the region between tympanum and eye when hindlimb is stretched along the side of the body (vs. reaching forward to the tip of snout in *M. daweimontis*), finger II shortest (vs. finger I shortest in *M. liboensis*), presence of an indistinct subarticular tubercle on the bases of each finger (vs. subarticular tubercle absent in *M. fansipanensis*), heels not meeting when the flexed hindlimbs are held at right angles to the body axis (heels meeting in *M. binchuanensis*; heels meeting or overlapping in *M. minor* and *M. wushanensis*; heels overlapping in *M. leishanensis*, *M. liboensis* and *M. wuliangshanensis*).

Megophrys nankunensis sp. nov. further differs from *M. feii*, for which molecular data are lacking and cannot be allocated to any subgenus base on morphology only (Yang et al. 2018) by the larger body size, SVL 29.9–34.9 mm in males and 39.4–41.9 mm in females (VS. 24.3–25.1 mm in males, 28.2–28.9 mm in females), presence of nuptial pad with nuptial spines in males during breeding season (vs. absent), presence of vomerine teeth (vs. absent), absence of lateral fringes on toes (vs. moderate or wide), heels not meeting when the flexed hindlimbs are held at right angles to the body axis (vs. heels overlapping).

Description of holotype. Adult male. Habitus small, SVL 31.3 mm; head width slightly larger than head length, HDW/HDL 1.12; snout rounded in dorsal view, tip of snout slightly sharpened, sloping backward to mouth in profile, protruding well beyond margin of lower jaw; top of head flat; eye large, ED/HDL 0.38; nostril oblique ovoid; pupil vertical; canthus rostralis well developed, forming the beginning of a fleshy, protruding ridge, that continues over the upper eyelid, and transitions into a supratympanic fold that terminates in the scapular region; loreal region vertical; internasal distance slightly larger than interorbital distance; tympanum distinct, moderate-sized, TD/ED 0.44; large ovoid choanae at the base of the maxilla; strong vomerine

ridge bearing vomerine teeth; margin of tongue weakly notched posteriorly; internal vocal slits present near the rear of the lower mandible.

RAD/SVL 0.22, HND/SVL 0.22; absence of lateral fringes and webbing on fingers, relative finger lengths II < I < IV < III; tip of finger rounded, slightly swollen; presence of a distinct subarticular tubercle on the base of each finger; outer metacarpal tubercles indistinct, inner metacarpal tubercles distinct and observably enlarged. Hindlimbs short, tibio-tarsal articulation reaching forward the anterior margin of tympanum when hindlimb is stretched along the side of the body; heels not meeting when the flexed hindlimbs are held at right angles to the body axis; TIB/SVL 0.37 and FTL/SVL 0.55; relative toe lengths I < II < V < III < IV; tips of toes round and slightly dilated; presence of rudimentary webbing on toes but absence of lateral fringes and tarsal folds; presence of a subarticular tubercle only at the bases of each toes; presence of a long ovoid inner metatarsal tubercle and absence of outer metatarsal tubercle.

Dorsal skin texture smooth with dense granules, some of which forming a weak X-shaped skin ridge on center of trunk; surface of flanks with large tubercles; presence of a small horn-like tubercle at the edge of eyelid; distinct supratympanic fold curving posteroventrally from posterior corner of eye to a level above insertion of arm, forming a swollen supraaxillary gland above insertion of arm; ventral skin texture smooth with granules on the surface of abdomen; pectoral gland large, equal size to tip of fingers, closer to axilla; single large femoral gland on rear of thigh.

Measurements of holotype (in mm). SVL 31.3, HDL 9.6, HDW 10.8, SNT 3.4, IND 3.4, IOD 2.4, ED 3.7, TD 1.6, TED 1.0, HND 6.9, RAD 7.0, FTL 17.3, TIB 11.6.

Coloration of holotype in life. (Fig. 4A–D) Dorsal surface beige with obscure darker patches, with a distinct and incomplete dark triangular marking between eyes, unconnected with an incomplete X-shaped marking on center of trunk. Forearm with dark bands dorsally; hindlimb with broad black transverse bands. Tip of snout dark brown. A dark brown vertical band below the eye. Supratympanic fold white. Horn-like tubercle at the edge of the upper eyelid orange. Surface of throat and chest dark brown, with scarlet spots. Posterior region of abdomen white, with dark brown and scarlet spots. Ventral surface of limbs white with brown patches. Ventral surface of hand and foot light brown, subarticular tubercle at the base of each fingers and toes, outer metacarpal tubercle, inner metatarsal tubercle and inner metacarpal tubercle pink. Pectoral and femoral glands white. Iris white.

Coloration of holotype in preservative. On dorsal surface the beige fades to dark grey. Dark interorbital triangular marking becomes more indistinct. Ventral surface pale in color, grey-brownish grounding, markings and mottling more distinct, all scarlet spots absent.

Variation. Measurements and body proportions of type series are given in Table 4.

All paratype specimens were very similar in morphology and color pattern. However, the holotype has the dorsal surface beige (vs. reddish brown in paratypes SYS a002033, 4501, and dark brown in paratypes SYS a004502–4506, 4507 (Fig. 4E–F)), dorsal skin texture smooth, granules and tubercles weak (vs. dorsal skin texture relatively rough with more distinct granules and tubercles in paratypes SYS a004502,

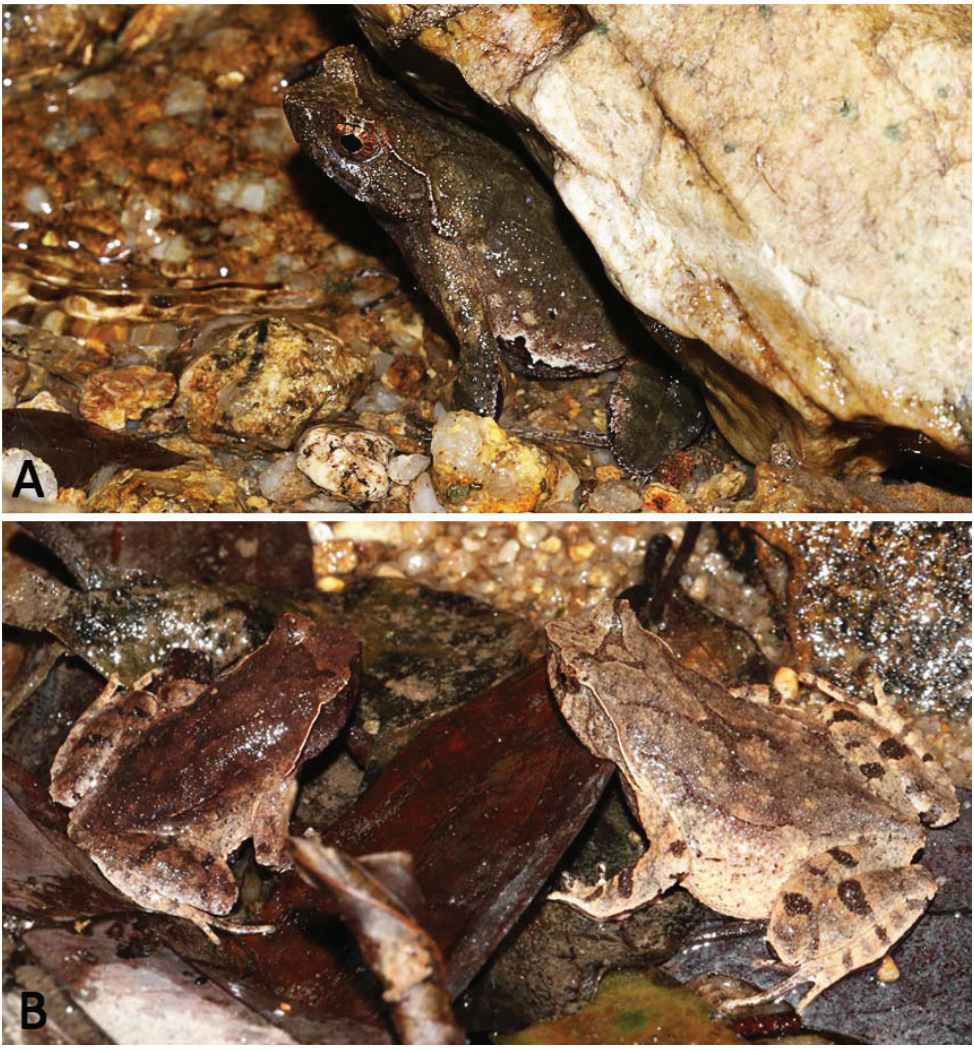

Figure 5. Ecology and behavior of *Megophrys nankunensis* sp. nov. **A** an adult male observed under the rock in the flowing stream **B** pair of *M. nankunensis* sp. nov. observed exposed on leave litters in a flowing stream, about 2.5 m wide, prior to amplexus.

4504–4507), and ventral surface of hand and foot light brown (vs. ventral surface of hand and foot grey white in paratypes SYS a004502–4504).

Etymology. The specific epithet "nankunensis" is in reference to the type locality of the new species: Mt. Nankun. We propose the common English name "Nankunshan Horned Toad" and Chinese name "Nan Kun Shan Jiao Chan (南昆山角蟾)".

Distribution and habits. Currently, *Megophrys nankunensis* sp. nov. is known only from the type locality, Mt. Nankun in Longmen County, Guangdong Province, China. It inhabits forest floor, leaf litter and the nearby undergrowth rocky mountainous streams (2–3 m wide) surrounded by moist subtropical evergreen broadleaved forests

at elevations between 300–600 m. Breeding season of *M. nankunensis* sp. nov. is from October to the following March, males were found calling under the leaf litter or rocks (Fig. 5A) on the ground in the flowing streams, besides, a pair were observed exposed on the floor in a flowing stream, about 2.5 m wide, prior to amplexus (Fig. 5B) at 20:09 P.M. on 20 October 2015. Tadpoles were not observed in this period.

***Megophrys* (*Panophrys*) *jiulianensis* J. Wang, Zeng, Lyu & Y.Y. Wang, sp. nov.**
http://zoobank.org/2B18FD8D-520D-4531-AA9B-852E0E2AC92A
Fig. 6, Table 6

Holotype. SYS a002112, adult male, collected by Yu-Long Li on 2 May 2013 from Daqiutian Protection Station (24°34'34.99"N, 114°26'28.53"E; 560 m a.s.l.) of Mt. Jiulian, Longnan County, Ganzhou City, Jiangxi Province, China.

Paratypes (nine males & two females). SYS a002110, 2111, adult females, collected by Yu-Long Li on 3 May 2013 from Xiagongtang Protection Station (24°32'16.74"N, 114°27'56.82"E; 770 m a.s.l.) of Mt. Jiulian; SYS a001007, 1009, adult males, collected by Run-Lin Li on 23 July 2010 from Daqiutian Protection Station of Mt. Jiulian; SYS a002107–2109, 2113–2114, SYS a002115/CIB110008, adult males, collected by Yu-Long Li on 1–4 May 2013 from Xiagongtang Protection Station and Daqiutian Protection Station of Mt. Jiulian at elevations between 400–800 m a.s.l.; SYS a002031, adult male, collected by Run-Lin Li on 20 Marth 2013 from Mt. Nankun (23°38'21.94"N, 113°50'39.49"E; 610 m a.s.l.), Longmen County, Huizhou City, Guangdong Province, China.

Diagnosis. (1) Body slender and small-sized, SVL 30.4–33.9 mm in nine adult males, 34.1–37.5 mm in two adult females; (2) head width slightly larger than head length, HDW/HDL ratio 1.04–1.06; (3) snout rounded in dorsal view; (4) eye large, tympanum distinct, moderate-sized, TD/ED ratio 0.50–0.59; (5) weak vomerine ridge bearing vomerine teeth; (6) tongue weakly notched posteriorly; (7) hindlimbs slender, heels overlapping when the flexed hindlimbs are held at right angles to the body axis, tibia-tarsal articulation reaching forward to the middle of eye when hindlimb is stretched along the side of the body; (8) absence of lateral fringes on fingers, presence of an indistinct subarticular tubercle on the bases of each finger, relative finger lengths II < I < IV < III; (9) toes with rudimentary webbing at their bases and without lateral fringes, subarticular tubercles only present at the base of toe I and II; (10) dorsal skin rough, presence of black spines on granules of dorsal skin, and occasionally present on canthus rostralis and margin of tympanum, presence of large tubercles on flanks, dorsal body and limbs; (11) four prominent parallel dorsolateral ridges with granules bearing black spines on back of trunk, the middle two ridges forming a X-shaped ridge occasionally; (12) a reddish horn-like tubercle bearing a black spine at its tip at the edge of eye lid; (13) distinct supratympanic fold bearing black spines; (14) beige to brownish red above, with an hollow dark triangle between eyes and a rectangular dark marking on the center of the back of trunk; (15) males with a single subgular vocal sac, and presence of nuptial pads bear-

ing darker nuptial spines on dorsal surface of the first and second fingers in adult males during breeding season, respectively; (16) gravid females bear creamy yellow oocytes.

Comparisons. Comparative data of *Megophrys jiulianensis* sp. nov. with *M. dongduanensis* sp. nov., *M. nankunensis* sp. nov., *M. feii* and the 33 recognized members of the *Megophrys* s.l. allocated to the subgenus *Panophrys* are listed in Table 5.

Megophrys jiulianensis sp. nov. is sympatric with *M. nankunensis* sp. nov. in Mt. Nankun, but it can be easily distinguished from the later by heels overlapping when the flexed hindlimbs are held at right angles to the body axis (vs. heels not meeting), TIB/SVL ratio 0.61–0.68 (vs. TIB/SVL ratio 0.35–0.42), supratympanic fold not forming a supraaxillary gland above insertion of arm (vs. supratympanic fold forming a depressed supraaxillary gland), presence of black spines on dorsal skin (vs. absent); besides, *M. jiulianensis* sp. nov. differs from *M. dongguanensis* sp. nov. by the notched tongue vs. (not notched), heels overlapping when the flexed hindlimbs are held at right angles to the body axis (vs. heels not meeting), TIB/SVL ratio 0.61–0.68 (vs. TIB/SVL ratio 0.41–0.46).

With significantly smaller body size, SVL 30.4–33.9 mm in males and 34.1–37.5 mm in females, *M. jiulianensis* sp. nov. differs from the 17 members with larger SVL values: *M. baolongensis* (42.0–45.0 mm in males), *M. binchuanensis* (40.2–42.5 mm in females), *M. binlingensis* (45.1–51.0 mm in males), *M. caudoprocta* (81.3 mm in single male), *M. daweimontis* (40.0–46.0 mm in females), *M. fansipanensis* (41.7–42.5 mm in females), *M. hoanglienensis* (37.4–47.6 mm in males, 59.6 mm in single female), *M. jingdongensis* (53.0–56.5 mm in males, 63.5 mm in single female), *M. liboensis* (34.7–67.7 mm in males, 60.8–70.6 mm in females), *M. minor* (34.5–41.2 mm in males), *M. omeimontis* (56.0–59.5 mm in males, 68.0–72.5 mm in females), *M. palpebralespinosa* (36.2–38.0 mm in males), *M. sangzhiensis* (54.7 mm in single male), *M. shuichengensis* (102.0–118.3 mm in males, 99.8–115.6 mm in females), *M. spinata* (47.2–54.4 mm in males, 54.0–55.0 mm in females), *M. tuberogranulatus* (50.5 mm in single female) and *M. wuliangshanensis* (41.3 mm in single female).

Megophrys jiulianensis sp. nov. differs from 12 species occurring in eastern and southern China (*M. acuta*, *M. brachykolos*, *M. boettgeri*, *M. cheni*, *M. huangshanensis*, *M. insularis*, *M. jinggangensis*, *M. kuatunensis*, *M. lini*, *M. lishuiensis*, *M. obesa* and *M.ombrophila*) by the following combination of characters: presence of vomerine teeth (vs. absent in *M. acuta*, *M. boettgeri*, *M. brachykolos*, *M. cheni*, *M. huangshanensis*, *M. jinggangensis*, *M. kuatunensis*, *M. lini*, *M. lishuiensis*, *M. obesa* and *M.ombrophila*), tongue notched posteriorly (vs. not notched in *M. acuta*, *M. brachykolos*, *M. jinggangensis*, *M. lini*, *M. lishuiensis*, *M. obesa* and *M.ombrophila*), absence of lateral fringes on toes (vs. narrow in *M. acuta*, *M. jinggangensis* and *M. kuatunensis*; wide in *M. boettgeri*, *M. cheni* and *M. lini*), heels overlapping when the flexed hindlimbs are held at right angles to the body axis (vs. heels not meeting in *M. acuta*, *M. brachykolos*, *M. insularis, M. obesa* and *M.ombrophila*).

Megophrys jiulianensis sp. nov. differs from the remaining four members of the *Megophrys* s.l. allocated to the subgenus *Panophrys* which share a moderate or small body size, by the presence of vomerine teeth (vs. absent in *M. leishanensis* and *M. wushanensis*), tongue notched posteriorly (vs. not notched in *M. leishanensis*, *M. wushanen-*

sis and *M. latidactyla*), absence of lateral fringes on toes (vs. narrow in *M. rubrimera*; wide in *M. latidactyla* and *M. wushanensis* (wide in females)), toe webbing rudimentary (vs. absence of webbing on toes in *M. rubrimera*).

Megophrys jiulianensis sp. nov. further differs from *M. feii*, for which molecular data are lacking and cannot be allocated to any subgenus base on morphology only (Yang et al. 2018) by the larger body size, SVL 30.4–33.9 mm in males and 34.1–37.5 mm in females (VS. 24.3–25.1 mm in males, 28.2–28.9 mm in females), presence of nuptial pad with nuptial spines in males during breeding season (vs. absent), presence of vomerine teeth (vs. absent), absence of lateral fringes on toes (vs. moderate or wide).

Description of holotype. Adult male. Habitus slender and small, SVL 32.0 mm; head width slightly larger than head length, HDW/HWL 1.04; snout rounded in dorsal view, projecting, sloping backward to mouth in profile, protruding well beyond margin of lower jaw; top of head flat; eye large, ED/HDL 0.39; nostril oblique ovoid; pupil vertical; canthus rostralis well developed, forming the beginning of a fleshy, protruding ridge, that continues over the upper eyelid, and transitions into a supratympanic fold that terminates in the scapular region; loreal region vertical; internasal distance slightly larger than interorbital distance; tympanum distinct, moderate-sized, TD/ED 0.52; large ovoid choanae at the base of the maxilla; weak vomerine ridge bearing vomerine teeth; margin of tongue weakly notched posteriorly; internal vocal slits present near the rear of the lower mandible..

RAD/SVL 0.25; absence of lateral fringes and webbing on fingers, relative finger lengths II < I < IV < III; tip of finger rounded, slightly swollen; presence of an indistinct subarticular tubercle on the base of each finger; outer metacarpal tubercles indistinct, inner metacarpal tubercles distinct and observably enlarged. Hindlimbs long, tibio-tarsal articulation reaching forward to the middle of eye when hindlimb is stretched along the side of the body; heels overlapping when the flexed hindlimbs are held at right angles to the body axis; TIB/SVL 0.46 and FTL/SVL 0.62; relative toe lengths I < II < V < III < IV; tips of toes round and slightly dilated; presence of rudimentary webbing on toes but absence of lateral fringes and tarsal folds; presence of a subarticular tubercle only at the bases of the first and second toes; presence of a long ovoid inner metatarsal tubercle and absence of outer metatarsal tubercle.

Dorsum rough with dense granules bearing spines; canthus rostralis, margin of tympanum, supratympanic fold and upper lip with dense spines; presence of large tubercles bearing spines on dorsal surface of body, surface of flanks and dorsal and posterolateral surface of limbs; prominent parallel dorsolateral ridges with granules bearing spines on back of trunk; presence of a horn-like tubercle bearing a spine at its tip at the edge of eye lid; distinct supratympanic fold curving posteroventrally from posterior corner of eye to a level above insertion of arm; ventral skin texture smooth, the lower lip bears spines; sides of belly with large tubercles; ventral skin texture of thighs smooth with a few small tubercles, posterior surface and surface around anus with large tubercles bearing spines; surface of tibia-tarsal with a few tubercles bearing spines; presence of spines on lateral sides of fingers and toes; pectoral

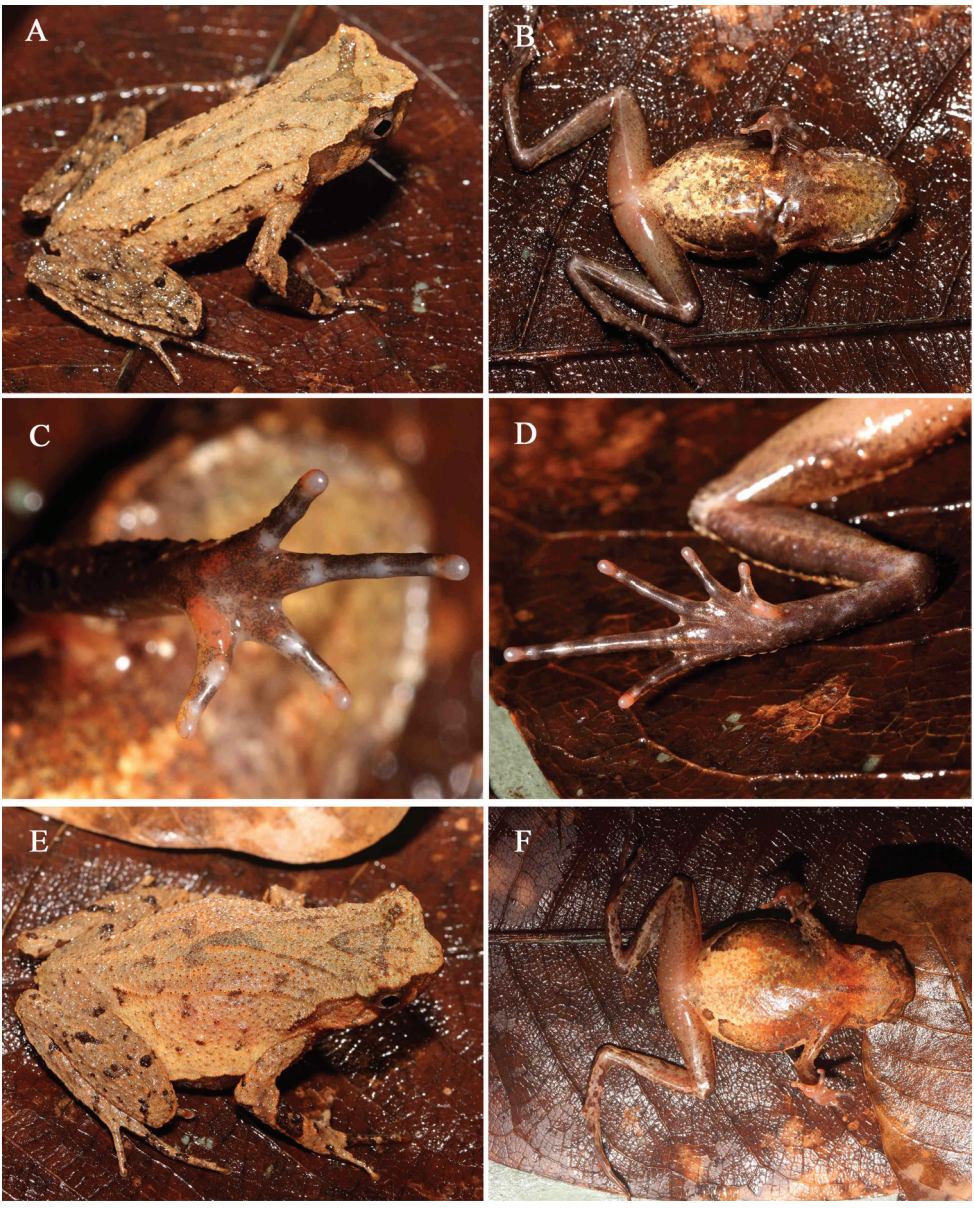

Figure 6. General life aspect in life of *Megophrys jiulianensis* sp. nov.: **A–D** SYS a002112, the male holotype **E–F** SYS a002111, the female paratype.

gland moderate-sized, closer to axilla; single femoral gland on rear of thigh, distinctly smaller than pectoral gland.

Measurements of holotype (in mm). SVL 32.2, HDL 11.5, HDW 11.4, SNT 3.6, IND 3.5, IOD 3.3, ED 4.2, TD 2.3, TED 1.7, HND 8.0, RAD 8.1, FTL 20.5, TIB 14.7.

Table 6. Measurements (in mm; minimum-maximum, mean ± SD) of the type series of *Megophrys jiulianensis* sp. nov.

Species	*Megophrys jiulianensis* sp. nov.	
	Males (n = 9)	Females (n = 2)
SVL	30.4–33.9 (32.2 ± 1.2)	34.1–37.5
HDL	10.7–11.6 (11.2 ± 0.4)	12.0–12.4
HDW	10.9–11.8 (11.4 ± 0.4)	12.5–13.2
SNT	3.4–3.8 (3.6 ± 0.2)	3.9–4.1
IND	3.2–3.6 (3.5 ± 0.1)	3.5–3.8
IOD	3.2–3.5 (3.3 ± 0.1)	3.6
ED	3.9–4.4 (4.2 ± 0.2)	4.3–4.4
TD	2.1–2.5 (2.3 ± 0.1)	2.2–2.4
TED	1.6–2.0 (1.7 ± 0.1)	2.1–2.5
HND	7.4–10.6 (8.0 ± 0.4)	8.3–9.5
RAD	7.7–8.5 (8.1 ± 0.3)	8.3–9.8
FTL	14.1–15.2 (14.7 ± 0.4)	16.0–17.8
TIB	19.8–21.1 (20.5 ± 0.5)	21.6–25.5
HDL/SVL	0.34–0.37 (0.35 ± 0.01)	0.33–0.35
HDW/SVL	0.34–0.37 (0.35 ± 0.01)	0.35–0.37
HDW/HDL	1.00–1.04 (1.02 ± 0.02)	1.04–1.06
SNT/HDL	0.32–0.34 (0.32 ± 0.01)	0.33
SNT/SVL	0.11–0.12 (0.11 ± 0.00)	0.11
IND/HDW	0.29–0.33 (0.30 ± 0.01)	0.28–0.29
IOD/HDW	0.28–0.30 (0.29 ± 0.01)	0.27–0.29
ED/HDL	0.36–0.39 (0.38 ± 0.01)	0.35–0.36
ED/SVL	0.12–0.14 (0.13 ± 0.01)	0.12–0.13
TD/ED	0.50–0.59 (0.55 ± 0.03)	0.51–0.55
TED/TD	0.68–0.87 (0.75 ± 0.07)	0.95–1.04
HND/SVL	0.24–0.26 (0.25 ± 0.01)	0.24–0.25
RAD/SVL	0.24–0.27 (0.25 ± 0.01)	0.24–0.26
TIB/SVL	0.44–0.48 (0.46 ± 0.01)	0.47
FTL/SVL	0.61–0.67 (0.64 ± 0.02)	0.63–0.68

Coloration of holotype in life. (Fig. 6A–D) Dorsal surface yellowish brown, with an incomplete dark triangular marking between eyes. Spines on dorsal surface, granules and tubercles black. Forearm with a distinct, black oblique band. Transverse bands on hindlimb indistinct. Tip of snout grayish brown. A grayish-brown vertical band below the eye. Tubercle at the edge of the upper eyelid red. Ventral surface yellow, scattered with dense dark gray spots and black scarlet blotches; ventral surface of limbs flesh colored with pink and black spots. Palms and soles dark brown, inner metatarsal tubercle, outer metacarpal tubercle and inner metacarpal tubercle orange red, tip of digits orange-red. Pectoral glands and femoral glands white. Iris white.

Coloration of holotype in preservative. Dorsum yellowish brown fades to greyish brown, scattered with black spots. Greyish black triangular marking between the eyes become more distinct. Ventral surface paled in color, brown grounding, markings and mottling become more distinct.

Variation. Measurements and body proportions of type series are given in Table 6.

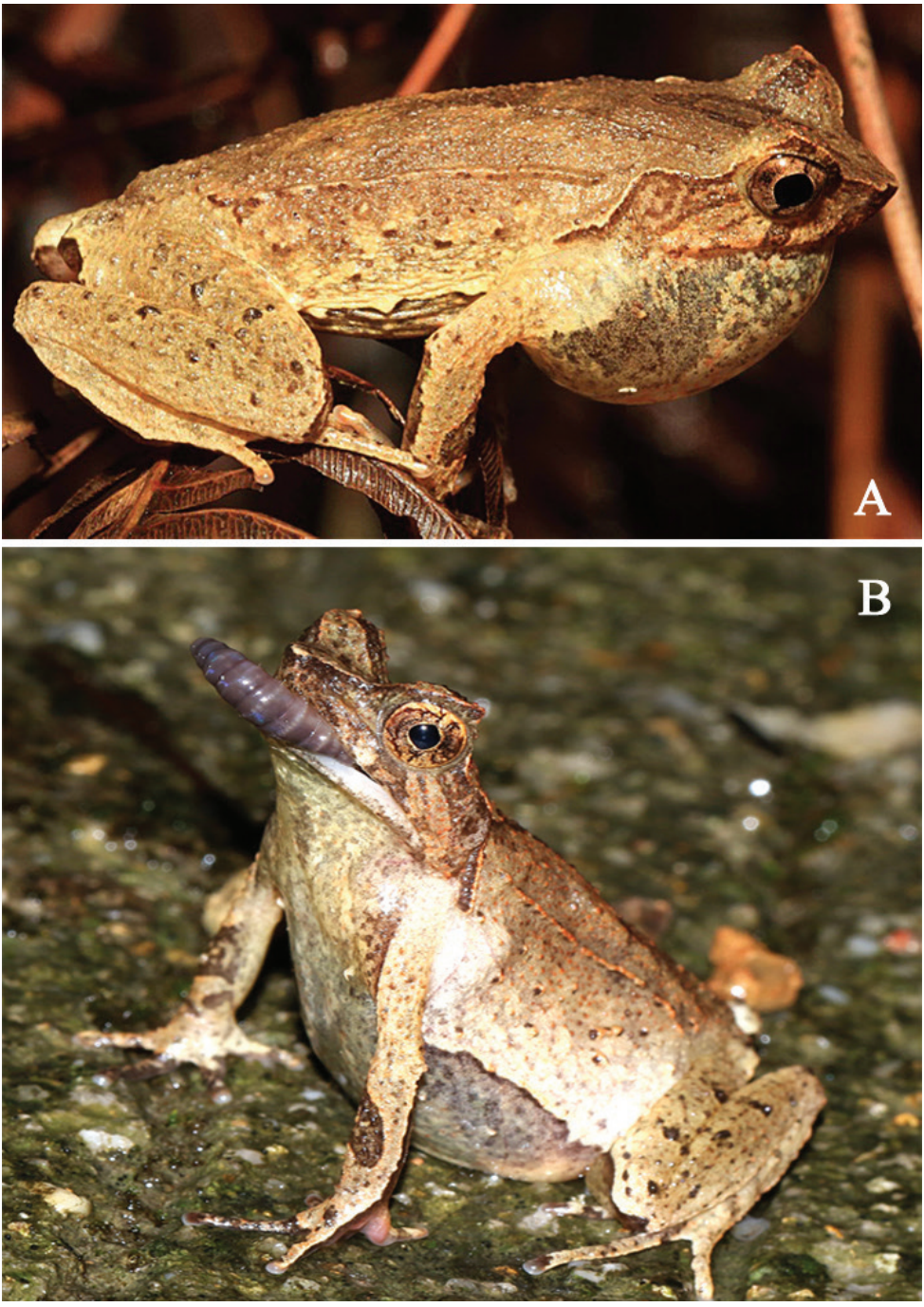

Figure 7. Ecology and behavior of *Megophrys jiulianensis* sp. nov.: **A** The male paratype SYS a002031 observed calling on a leaf (showing subgular vocal sac) **B** a female individual observed feeding on an earthworm after rain, both from Mt. Nankun in Guangdong Province.

All paratype specimens were very similar in morphology and color pattern. However, dorsal skin texture is more rough with well-developed spines in the female specimen SYS a002111 (Fig. 6E–F), dorsal surface yellowish brown in the other female specimen SYS a002110, and the middle two ridges on dorsum forming an X-shape skin ridge in the male specimen SYS a002108.

Etymology. The specific epithet "jiulianensis" is in reference to the known localities of the new species: Mt. Jiulian and Nankunshan Natuire Reserve located in the Jiulian Mountains range. We propose the common English name "Jiulianshan Horned Toad" and Chinese name "Jiu Lian Shan Jiao Chan (九连山角蟾)".

Distribution and natural history. Currently, *Megophrys jiulianensis* sp. nov. is known from Mt. Nankun in Guangdong Province and the type locality, Jiulian Nature Reserve in Jiangxi Province, China. It inhabits forest floor, leaf litter and the nearby undergrowth mountainous streams surrounded by moist subtropical evergreen broadleaved forests at elevations between 500–800 m. Breeding season of *M. jiulianensis* sp. nov. is from March to July, males were usually found staying while calling on leaves (Fig. 7A), about 0.1–0.3 m above the ground. After the rain, numerous individuals can be easily found on the road, and a female individual from Mt. Nankun was observed feeding on an earthworm (Fig. 7B) on 20:45 p.m., 21 March 2016. Tadpoles could be found all year round.

Megophrys jiulianensis sp. nov. is sympatric with *M. nankunensis* sp. nov. and *M. mangshanensis* at Mt. Nankun.

Megophrys (*Panophrys*) *nanlingensis* Lyu, J. Wang, Liu & Y.Y. Wang, sp. nov.

http://zoobank.org/F9567F3F-D374-4CE8-A3A6-01C5F6A17A2D
Fig. 8, Table 7

Holotype. SYS a001964, adult male, collected by Run-Lin Li on 21 December 2012 from Nanling Nature Reserve (24°54'48.80"N, 113°01'12.34"E; 1008m a.s.l.), Ruyuan County, Shaoguan City, Guangdong Province, China.

Paratypes (nine males). SYS a001959–1962, SYS a001963/CIB110010, adult males, collected on 21 December 2012 by Run-Lin Li from the same stream as the holotype (1000–1300 m a.s.l.); SYS a002334, 2356–2358, collected on 1–3 October 2013 by Ying-Yong Wang and Zu-Yao Liu from Mt. Qiyun (25°52'22.84"N, 114°01'52.09"E; 691–1355m a.s.l.), Chongyi County, Ganzhou City, Jiangxi Province, China.

Diagnosis. (1) Body small-sized, SVL 30.5–37.3 mm in 10 adult males; (2) snout rounded in dorsal view; (3) tympanum distinct, moderate-sized, TD/ED ratio 0.43–0.57; (4) vomerine ridge and vomerine teeth present; (5) tongue notched posteriorly; (6) absence of lateral fringes and webbing on fingers, presence of narrow lateral fringes and rudimentary webbing on toes; (7) presence of a subarticular tubercle at the base of each finger and toe; (8) hindlimbs slender, heels overlapping, tibio-tarsal articulation reaching between the posterior corner to the center of eye; (9) TIB/SVL ratio 0.45–0.51 and FTL/SVL ratio 0.61–0.73; (10) dense conical granules present on surface of temporal region, upper lip, and from loreal region to the tip of snout; (11) granules

and tubercles on dorsal surface forming a discontinuous X-shaped ridge and a pair of discontinuous dorsolateral ridges on back of trunk; (12) supratympanic fold distinct, whitish tan; (13) brown dorsally, with a dark triangular marking with light yellow edge between eyes, and an X-shaped or V-shaped marking with light yellow edge on the center of the back of trunk; (14) presence of a single subgular vocal sac in males; (15) nuptial pads and nuptial spines invisible in males during breeding season.

Comparisons. Comparative data of *Megophrys nanlingensis* sp. nov. with *M. dongduanensis* sp. nov., *M. nankunensis* sp. nov., *M. jiulianensis* sp. nov., *M. feii* and the 33 recognized members of *Megophrys* s.l. allocated to the subgenus *Panophrys* are listed in Table 5.

Megophrys nanlingensis sp. nov. differs from *M. dongguanensis* sp. nov., *M. nankunensis* sp. nov. and *M. jiulianensis* sp. nov. by the heels overlapping when hindlimb is stretched along the side of the body (vs. heels not meeting in *M. dongguanensis* sp. nov. and *M. nankunensis* sp. nov.), presence of lateral fringes on toes (vs. absent in *M. dongguanensis* sp. nov., *M. nankunensis* sp. nov. and *M. jiulianensis* sp. nov.), tongue notched posteriorly (vs. not notched in *M. dongguanensis* sp. nov. and *M. nankunensis* sp. nov.), skin relatively smooth and lacking black horny spines (vs. skin rough with black horny spines in *M . jiulianensis* sp. nov.).

With the smaller body size, SVL 30.5–37.3 mm in males, *Megophrys nanlingensis* sp. nov. differs from the nine members with larger SVL values: *M. baolongensis* (42.0–45.0 mm in males), *M. binlingensis* (45.1–51.0 mm in males), *M. caudoprocta* (81.3 mm in single male), *M. jingdongensis* (53.0–56.5 mm in males), *M. latidactyla* (38.9 mm in single male), *M. omeimontis* (56.0–59.5 mm in males), *M. sangzhiensis* (54.7 mm in single male), *M. shuichengensis* (102.0–118.3 mm in males) and *M. spinata* (47.2–54.4 mm in males).

Megophrys nanlingensis sp. nov. differs from 12 species occurring in eastern and southern China (*M. acuta*, *M. brachykolos*, *M. boettgeri*, *M. cheni*, *M. huangshanensis*, *M. insularis*, *M. jinggangensis*, *M. kuatunensis*, *M. lini*, *M. lishuiensis*, *M. obesa* and *M.ombrophila*) by the following combination of characters: presence of vomerine teeth (vs. absent in *M. acuta*, *M. boettgeri*, *M. brachykolos*, *M. cheni*, *M. huangshanensis*, *M. kuatunensis*, *M. lini*, *M. lishuiensis*, *M. obesa* and *M.ombrophila*), margin of tongue notched posteriorly (vs. not notched in *M. acuta*, *M. brachykolos*, *M. jinggangensis*, *M. lini*, *M. lishuiensis*, *M. obesa* and *M.ombrophila*), toes with narrow lateral fringes (vs. wide in *M. boettgeri*, *M. cheni* and *M. lini*; absent in *M. brachykolos*, *M. huangshanensis*, *M. insularis*, *M. lishuiensis*, *M. obesa* and *M.ombrophila*), toes with rudimentary webbing (vs. toes without webbing in *M. lishuiensis*, *M. kuatunensis* and *M.ombrophila*), hindlimbs comparatively longer, with heels overlapping when the flexed hindlimbs are held at right angles to the body axis (vs. hindlimbs short, with heels not meeting in *M. acuta*, *M. brachykolos*, *M. huangshanensis*, *M. insularis*, *M. obesa* and *M.ombrophila*).

Megophrys nanlingensis sp. nov. differs from the remaining 12 members of the *Megophrys s.l.* allocated to the subgenus *Panophrys* which share a moderate or small body size, by the small horn-like tubercle at edge of the upper eyelid (vs. horn-like tubercle indistinct or absent in *M. binchuanensis*, *M. minor*, *M. wuliangshanensis* and *M. wushanensis*; slightly large in *M. palpebralespinosa*; long point in *M. liboensis*), presence of vomerine teeth (vs. absent in *M. binchuanensis*, *M. leishanensis*, *M. minor*,

M. wuliangshanensis and *M. wushanensis*), tongue notched posteriorly (vs. tongue not notched in *M. palpebralespinosa*, *M. tuberogranulatus* and *M. wushanensis*), toes with narrow lateral fringes (vs. wide in *M. binchuanensis*, *M. liboensis*, *M. palpebralespinosa* and *M. wushanensis* (in males)); absent in *M. daweimontis*, *M. leishanensis*, *M. minor*, *M. tuberogranulatus*, *M. wuliangshanensis*, *M. wushanensis* (in females); indistinct or absent in *M. hoanglienensis*), toes webbing rudimentary (vs. toes without webbing in *M. daweimontis*, *M. fansipanensis*, *M. rubrimera* and *M. wuliangshanensis*; indistinct or absent in *M. fansipanensis* and *M. hoanglienensis*; at least one-fourth webbed in *M. palpebralespinosa*), subarticular tubercles present (vs. absent in *M. palpebralespinosa* and *M. rubrimera*).

Megophrys nanlingensis sp. nov. further differs from *M. feii*, for which molecular data are lacking and cannot be allocated to any subgenus based on morphology only (Yang et al. 2018) by the larger body size, SVL 30.5–37.3 mm in males (VS. 24.3–25.1 mm in males), presence of nuptial pad with nuptial spines in males during breeding season (vs. absent), presence of vomerine teeth (vs. absent), presence of narrow lateral fringes on toes (vs. moderate or wide).

Description of holotype. Adult male. Body size small, SVL 32.5 mm; head length and head width almost isometric, HDW/HDL 0.99; snout rounded in dorsal view, projecting, sloping backward to mouth in profile, protruding well beyond margin of lower jaw; top of head flat; eye large, ED/HDL 0.37, pupil vertical; nostril oblique ovoid; canthus rostralis well developed; loreal region slightly oblique; internasal distance slightly larger than interorbital distance; tympanum distinct, moderate-sized, TD/ED 0.48; large ovoid choanae at the base of the maxilla; presence of vomerine ridge bearing vomerine teeth; margin of tongue notched posteriorly; internal vocal slits present near the rear of the lower mandible.

RAD/SVL 0.25, HND/SVL 0.24; fingers without webbing and lateral fringes, relative finger length II < I < IV < III; tips of fingers slightly dilated, round; one subarticular tubercle at the bases of each finger; outer and inner metacarpal tubercles distinct, and the inner one observably enlarged. Hindlimbs slender, tibio-tarsal articulation reaching forward to the center of the eye when hindlimb is stretched along the side of the body; heels overlapping when the flexed hindlimbs are held at right angles to the body axis; TIB/SVL 0.49 and FTL/SVL 0.69; relative toe length I < II < V < III < IV; tips of toes round and slightly dilated; toes with narrow lateral fringes, rudimentary webbing; one subarticular tubercle at the bases of each toes; presence of a long ovoid inner metatarsal tubercle and absence of outer metatarsal tubercle.

Dorsal skin texture rough; head surface rough, with small tapered granules densely covering from temporal region, upper lip, loreal region to tip of snout; granules forming discontinuous X-shaped ridge with two discontinuous dorsolateral ridges on both sides at the central trunk; large tubercles on flanks; a horn-like prominent tubercle on the edge of the upper eyelid; distinct supratympanic fold curving posteroventrally from posterior corner of eye to a level above insertion of arm; ventral skin texture smooth, with several large granules and tubercles on two sides; ventral skin texture of thighs

Figure 8. *Megophrys nanlingensis* sp. nov. in life: **A–D** SYS a001964, male holotype **E, F** SYS a001963, female paratype.

smooth, with a few small tubercles; pectoral gland larger, closer to axilla; single femoral gland on rear of thigh.

Measurements of holotype (in mm). SVL 32.5, HDL 11.5, HDW 11.4, SNT 3.7, IND 3.5, IOD 3.3, ED 4.2, TD 2.0, TED 1.7, HND 8.0, RAD 7.8, FTL 22.3, TIB 15.9.

Coloration of holotype in life. (Fig. 8A–D) Brown dorsally, with a dark triangular marking with light yellow edge between eyes, and an X-shaped marking with light yellow edge on the center of the back of trunk. Dark brown transverse bands dorsally on lower arms and hindlimbs. Surface of snout brown. Black brown vertical band below the eye on each side. Temporal region brown, supratympanic fold white. Ventral surface pale grey, an indistinct longitudinal stripe on surface of throat. Scarlet spots on surface of chest. Belly whitish grey with dark brown marbling. A pair of black longitudinal stripes scattered with several white tubercles on surface of lateroventral flanks. Ventral surface of limbs light red and scattered with white spots. Ventral surface of hands and feet dark brown, tips of digits pale-grey. Metacarpal tubercle and metatarsal tubercle light red. Pectoral glands and femoral glands white. Iris reddish brown.

Coloration of holotype in preservative. Coloration of dorsal and ventral surface turned pale; transverse bands on limbs, dark longitudinal stripe on surface of throat and black patches on surface of lateroventral flanks became more distinct; scarlet spots on surface of chest faded.

Variation. Measurement data of type series are listed in Table 7.

All paratypes are very similar to holotype in morphology and color pattern. However, the male specimen SYS a001963 (Fig. 8E, F) is obviously large in snout-vent

Table 7. Measurements (in mm; minimum-maximum, mean ± SD) of the type series of *Megophrys nanlingensis* sp. nov.

Species	*Megopgrys nanlingensis* sp. nov. Males (n = 10)
SVL	30.5–37.3 (33.2 ± 1.9)
HDL	10.9–12.7 (11.6 ± 0.5)
HDW	10.7–13.8 (11.8 ± 0.9)
SNT	3.4–3.8 (3.6 ± 0.1)
IND	3.5–4.0 (3.7 ± 0.2)
IOD	3.2–4.0 (3.4 ± 0.3)
ED	4.1–4.9 (4.5 ± 0.3)
TD	1.9–2.5 (2.2 ± 0.2)
TED	1.6–2.2 (1.8 ± 0.2)
HND	7.1–9.6 (8.0 ± 0.6)
RAD	7.1–9.0 (8.1 ± 0.5)
FTL	18.6–27.1 (22.4 ± 2.3)
TIB	13.9–18.8 (16.0 ± 1.3)
HDL/SVL	0.33–0.36 (0.35 ± 0.01)
HDW/SVL	0.33–0.37 (0.35 ± 0.01)
HDW/HDL	0.97–1.09 (1.02 ± 0.04)
SNT/HDL	0.30–0.33 (0.31 ± 0.01)
SNT/SVL	0.10–0.12 (0.11 ± 0.01)
IND/HDW	0.29–0.35 (0.31 ± 0.02)
IOD/HDW	0.28–0.32 (0.29 ± 0.01)
ED/HDL	0.37–0.41 (0.39 ± 0.01)
ED/SVL	0.13–0.14 (0.14 ± 0.01)
TD/ED	0.43–0.57 (0.48 ± 0.04)
TED/TD	0.67–0.95 (0.83 ± 0.10)
HND/SVL	0.23–0.26 (0.24 ± 0.01)
RAD/SVL	0.23–0.26 (0.24 ± 0.01)
TIB/SVL	0.45–0.51 (0.48 ± 0.02)
FTL/SVL	0.61–0.73 (0.68 ± 0.04)

length than other specimens, with lighter reddish-brown iris, yellowish brown background coloration and comparatively smooth skin. The heels are significantly overlapping in all specimens from Nanling Nature Reserve but slightly overlapping in specimens from Mt. Qiyun.

Etymology. The specific epithet "nanglingensis" is in reference to the type locality of the new species, Nanling Nature Reserve of the Nanling Mountains. We propose the common English name "Nanling Horned Toad" and Chinese name "Nan Ling Jiao Chan (南岭角蟾)".

Distribution and natural history. Currently, *Megophrys nanglingensis* sp. nov. is known from Nanling Nature Reserve and the neighboring Mangshan Nature Reserve (between elevations of 1000–1300 m), together with Mt. Qiyun (between elevations of 690–1400 m). It inhabits streams in bamboo forests. Males are frequently heard calling during August and December. Tadpoles could be found in this period.

Megophrys nanlingensis sp. nov. is sympatric with *M. mangshanensis* and *M. popei* in Nanling Nature Reserve and the neighboring Mangshan Nature Reserve.

***Megophrys* (*Panophrys*) *wugongensis* J. Wang, Lyu & Y.Y. Wang, sp. nov.**
http://zoobank.org/51EED805-C594-4FA0-A03E-9BE8C11EAA40
Fig. 9, Table 8

Holotype. SYS a002625, adult male, collected by Guo-Ling Chen and Jian Zhao on 9 May 2014 from Yangshimu Scenic Area (27°34'47.93"N, 114°15'7.34"E; 550 m a.s.l.), Pingxiang City, Jiangxi Province, China.

Paratypes (three males & nine females). Adult males, SYS a004777/CIB110011, SYS a004796, 4800, collected by Zhi-Tong Lyu and Ying-Yong Wang on 23 May 2016, and adult females, SYS a002610–2611, collected by Guo-Ling Chen and Jian Zhao on 8 May 2014, SYS a004797–4799, 4801–4804, collected by Zhi-Tong Lyu and Ying-Yong Wang on 23 May 2016, from Wugongshan Scenic Area (27°34'3.94"N, 114°10'28.38"E; 1050–1080 m a.s.l.), Anfu County, Ji'an City, Jiangxi Province, China.

Diagnosis. (1) Body size small, SVL 31.0–34.1 mm in four adult males and body size moderate, SVL 38.5–42.8 mm in nine adult females; (2) tympanum distinct, slightly convex, moderate-sized, TD/ED ratio 0.47–0.52; (3) vomerine teeth absent; (4) margin of tongue not notched posteriorly; (5) hindlimbs short, heels not meeting, tibia-tarsal articulation reaching forward to the region between posterior corner of eye and posterior margin of tympanum; (6) TIB/SVL ratio 0.39–0.44, FTL/SVL ratio 0.56–0.64; (7) fingers without lateral fringes, presence of a subarticular tubercle at the bases of each finger, relative finger lengths II < I = IV < III; (8) toes with rudimentary webbing at their bases and without lateral fringes, subarticular tubercles only present at the base of each toe; (9) numerous granules present on dorsal surface of body, several large tubercles present on surface of flanks and dorsal surface of limbs; (10) presence of a small horn-like tubercle at the edge of the upper eyelid; (11) supratympanic fold distinct, whitish; (12) yellowish brown or reddish brown dorsally, with an incomplete dark triangular marking between eyes and an X-shaped marking on back of trunk; (13) ventral surface greyish brown, ventral surface of abdomen with creamy white nebulous patches and black spots; (14) males with a single subgular vocal sac; (15) gravid females bear creamy yellow oocytes.

Comparisons. Comparative data of *Megophrys wugongensis* sp. nov. with *M. dongduanensis* sp. nov., *M. nankunensis* sp. nov., *M. jiulianensis* sp. nov., *Megophrys nanlingensis* sp. nov., *M. feii* and the 33 recognized members of *Megophrys* s.l. allocated to the subgenus *Panophrys* are listed in Table 5.

Megophrys wugongensis sp. nov. differs from *M. dongguanensis* sp. nov., *M. nankunensis* sp. nov., *M. jiulianensis* sp. nov. and *M. nanlingensis* sp. nov. by a combination of following characters: vomerine teeth absent (vs. vomerine teeth present), tongue not notched posteriorly (vs. tongue notched in *M. jiulianensis* sp. nov. and *M. nanlingensis* sp. nov.), absence of lateral fringes on toes (vs. presence of narrow lateral fringes on toes in *M. nanlingensis* sp. nov.), heels not meeting when the flexed hindlimbs are held at right angles to the body axis (vs. heels overlapping in *M. jiulianensis* sp. nov. and *M. nanlingensis* sp. nov.), absence of black spines on dorsal skin (vs. present in *M. jiulianensis* sp. nov.), relative finger lengths II < I = IV < III (vs. II < I < IV < III in *M. nan-*

kunensis sp. nov., *M. jiulianensis* sp. nov. and *M. nanlingensis* sp. nov.), ventral surface with creamy white nebulous patches (vs. absence of such patched on ventral surface in *M. dongguanensis* sp. nov. and *M. nankunensis* sp. nov.).

With the smaller body size, SVL 31.0–34.1 mm in males and 38.5–42.8 mm in females, *Megophrys wugongensis* sp. nov. differs from the 13 members with larger SVL values: *M. baolongensis* (42.0–45.0 mm in males), *M. binlingensis* (45.1–51.0 mm in males), *M. caudoprocta* (81.3 mm in single male), *M. hoanglienensis* (37.4–47.6 mm in males, 59.6 mm in single female), *M. jingdongensis* (53.0–56.5 mm in males 63.5 in single female), *M. latidactyla* (38.9 mm in single male), *M. liboensis* (34.7–67.7 mm in males, 60.8–70.6 mm in females), *M. omeimontis* (56.0–59.5 mm in males, 68.0–72.5 mm in females), *M. palpebralespinosa* (36.2–38.0 mm in males), *M. sangzhiensis* (54.7 mm in single male), *M. shuichengensis* (102.0–118.3 mm in males, 99.8–115.6 mm in females), *M. spinata* (47.2–54.4 mm in males, 54.0–55.0 mm in females), and *M. tuberogranulatus* (33.2–39.6 mm in males, 50.5 mm in single female).

Megophrys wugongensis sp. nov. differs from 12 species occurring in eastern and southern China (*M. acuta*, *M. brachykolos*, *M. boettgeri*, *M. cheni*, *M. huangshanensis*, *M. insularis*, *M. jinggangensis*, *M. kuatunensis*, *M. lini*, *M. lishuiensis*, *M. obesa* and *M.ombrophila*) by the following combination of characters: vomerine teeth absent (vs. present in *M. insularis* and *M. jinggangensis*), tongue not notched posteriorly (vs. tongue notched in *M. boettgeri*, *M. huangshanensis*, *M. kuatunensis* and *M. insularis*), toes without lateral fringes (vs. laterals fringes on toes narrow in *M. acuta*, *M. kuatunensis* and *M. jinggangensis*; wide in *M. boettgeri*, *M. cheni* and *M. lini*), toes with rudimentary webbing (vs. toes without webbing in *M. huangshanensis*, *M. lishuiensis* and *M.ombrophila*), hindlimbs short, with heels not meeting when the flexed hindlimbs are held at right angles to the body axis (vs. hindlimbs comparatively longer, with heels overlapping in *M. boettgeri*, *M. cheni*, *M. kuatunensis*, *M. jinggangensis* and *M .lini*), relative finger lengths II < I = IV < III (vs. I < II ≤ IV < III in *M. acuta* and *M.ombrophila*; IV < II < I < III in *M. brachykolos*; I < II = IV < III in *M. lishuiensis*; I < II ≤ IV < III in *M. obesa*), males bearing nuptial pads with nuptial spines during breeding season (vs. nuptials absence in adult males of *M. acuta*), ventral surface with creamy white nebulous patches (vs. absence of such patched in *M. brachykolos* and *M. obesa*).

Megophrys nanlingensis sp. nov. differs from the remaining eight members of the *Megophrys* s.l. allocated to the subgenus *Panophrys* which share a moderate or small body size, by a combination of following characters: horn-like tubercle small at edge of the upper eyelid (vs. horn-like tubercle indistinct or absent in *M. binchuanensis*, *M. minor*, *M. wuliangshanensis* and *M. wushanensis*), absence of vomerine teeth (vs. present in *M. daweimontis*, *M. fansipanensis* and *M. rubrimera*), tongue not notched posteriorly (vs. tongue notched in *M. minor*, *M. fansipanensis* and *M. rubrimera*), toes without lateral fringes (vs. lateral fringes wide in *M. binchuanensis*, *M. wushanensis* (in males); narrow in *M. rubrimera*), toes with rudimentary webbing (vs. toes without webbing in *M. daweimontis*, *M. fansipanensis*, *M. rubrimera* and *M. wuliangshanensis*), heels not meeting when the flexed hindlimbs are held at right angles to the body axis (vs. heels overlapping in *M. minor* and *M. wuliangshanensis*), heels not meeting when the flexed hindlimbs are held at right angles

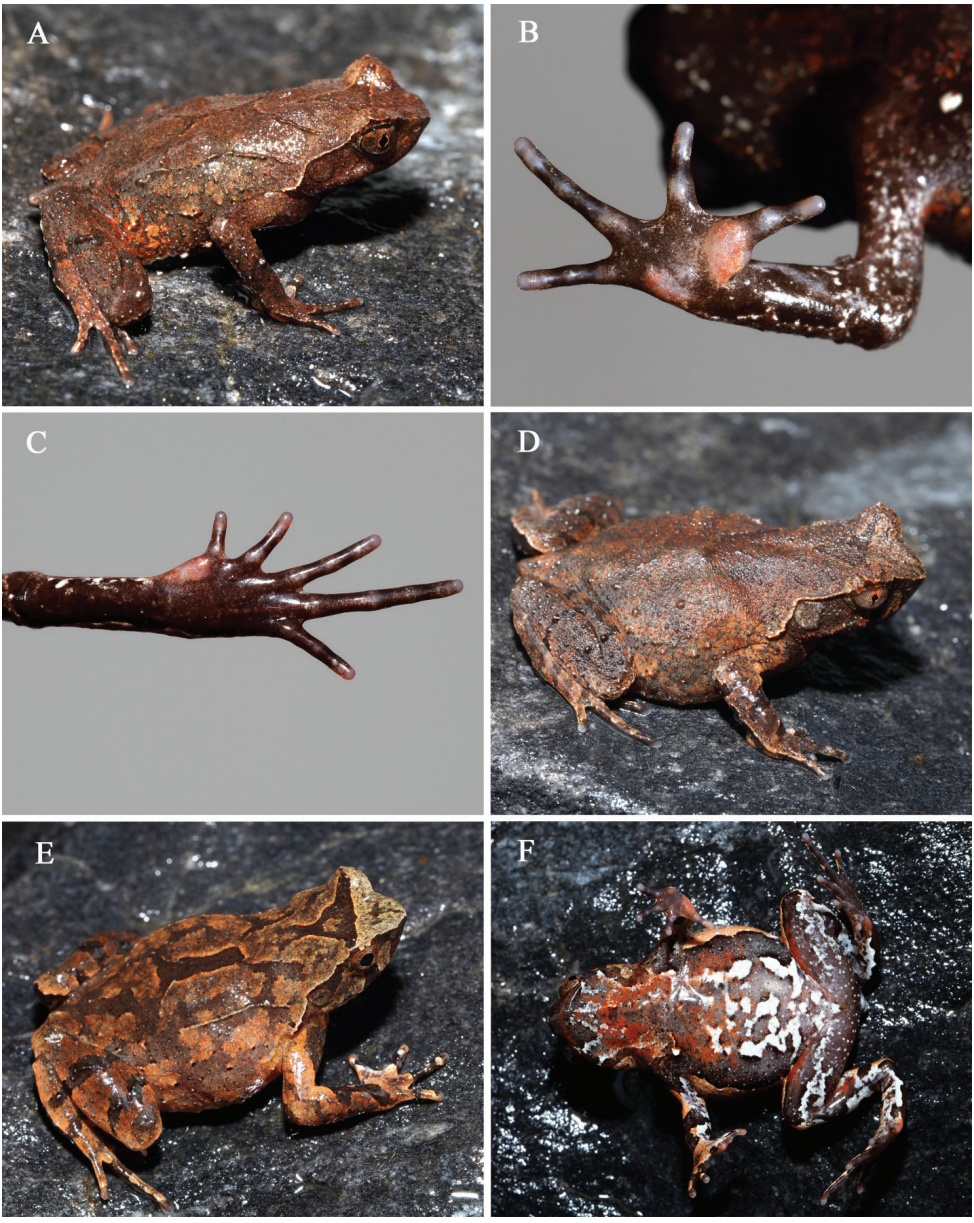

Figure 9. *Megophrys wugongensis* sp. nov. in life: **A–C** SYS a002625, male holotype **D** SYS a002610, female paratype **E, F** SYS a002611, female paratype.

to the body axis (heels meeting in *M. binchuanensis*; heels meeting or overlapping in *M. minor* and *M. wushanensis*; heels overlapping in *M. leishanensis*, and *M. wuliangshanensis*).

Megophrys wugongensis sp. nov. further differs from *M. feii*, for which molecular data are lacking and cannot be allocated to any subgenus base on morphology only

(Yang et al. 2018) by the larger body size, SVL 31.0–34.1 mm in males and 38.5–42.8 mm in females (VS. 24.3–25.1 mm in males, 28.2–28.9 mm in females), presence of nuptial pad with nuptial spines in males during breeding season (vs. absent), absence of lateral fringes on toes (vs. moderate or wide).

Description of holotype. Adult male. Habitus small, SVL 31.0 mm; head width slightly larger than head length, HDW/HWL 1.03; snout rounded in dorsal view, tip of snout slightly sharpened, sloping backward to mouth in profile, protruding well beyond margin of lower jaw; top of head flat; eye large, ED/HDL 0.41; nostril oblique ovoid; pupil vertical; canthus rostralis well developed; loreal region vertical; internasal distance slightly larger than interorbital distance; tympanum distinct, moderate-sized, TD/ED 0.47; large ovoid choanae at the base of the maxilla; weak vomerine ridge present, vomerine teeth absent; margin of tongue not notched posteriorly; internal vocal slits present near the rear of the lower mandible.

RAD/SVL 0.24, HND/SVL 0.22; absence of lateral fringes and webbing on fingers, relative finger lengths II < I = IV < III; tip of finger rounded, slightly swollen; presence of a distinct subarticular tubercle on the base of each finger; outer metacarpal tubercles indistinct, inner metacarpal tubercles distinct and observably enlarged. Hindlimbs short, tibio-tarsal articulation reaching forward the posterior corner of eye when hindlimb is stretched along the side of the body; heels not meeting when the flexed hindlimbs are held at right angles to the body axis; TIB/SVL 0.43 and FTL/SVL 0.61; relative toe lengths I < II < V < III < IV; tips of toes round and slightly dilated; presence of rudimentary webbing on toes but absence of lateral fringes and tarsal folds; presence of a subarticular tubercle only at the bases of each toes; presence of a long ovoid inner metatarsal tubercle and absence of outer metatarsal tubercle.

Dorsal skin texture rough with dense granules, some of which forming an X-shaped skin ridge on center of trunk; surface of flanks with large tubercles; presence of a small horn-like tubercle at the edge of eye lid; distinct supratympanic fold curving posteroventrally from posterior corner of eye to a level above insertion of arm; superior margin of tympanum in connect with supratympanic fold; ventral skin texture smooth with granules on the surface of abdomen; pectoral gland large, closer to axilla; single large femoral gland on rear of thigh.

Measurements of holotype (in mm). SVL 30.8, HDL 11.9, HDW 11.7, SNT 3.5, IND 3.0, IOD 2.8, ED 3.5, TD 1.8, TED 1.7, HND 8.5, RAD 7.2, FTL 21.8, TIB 15.1

Coloration of holotype in life. (Fig. 9A–C) Dorsal surface reddish brown, with a distinct and dark triangular marking with yellow edges between eyes. Hindlimb with broad black transverse bands. A dark brown vertical band below the eye. Canthus rostralis and supratympanic fold white. Horn-like tubercle at the edge of the upper eyelid yellow. Surface of throat and chest dark brown, with scarlet marbling, posterior region of abdomen white. Ventral surface of limbs brown with white spots and patches. Ventral surface of hand and foot brown, inner and outer metatarsal tubercles and inner metacarpal tubercle pink. Pectoral and femoral glands white. Iris reddish brown.

Coloration of holotype in preservative. Dorsum dark brown, markings on dorsal surface became indistinct, transverse bands on limbs became dark grey and became more

Table 8. Measurements (in mm; minimum-maximum, mean ± SD) of the type series of *Megophrys wugongensis* sp. nov.

Species	*Megophrys wugongensis* sp. nov.	
	Males (n = 4)	Females (n = 9)
SVL	31.0–34.1 (32.4 ± 1.3)	38.5–42.8 (40.8 ± 1.3)
HDL	10.2–11.2 (10.7 ± 0.4)	11.8–13.2 (12.6 ± 0.4)
HDW	10.4–11.9 (11.0 ± 0.6)	12.6–13.9 (13.4 ± 0.4)
SNT	3.4–3.9 (3.8 ± 0.2)	4.2–4.8 (4.6 ± 0.2)
IND	3.6–3.7 (3.7 ± 0.1)	3.6–4.2 (4.0 ± 0.2)
IOD	3.1–3.4 (3.2 ± 0.1)	3.6–3.8 (3.7 ± 0.1)
ED	4.1–4.4 (4.3 ± 0.1)	4.1–5.1 (4.4 ± 0.3)
TD	2.0–2.2 (2.1 ± 0.1)	2.1–2.3 (2.2 ± 0.1)
TED	1.7–2.2 (1.9 ± 0.2)	2.1–2.6 (2.4 ± 0.2)
HND	6.5–7.3 (7.0 ± 0.3)	8.2–9.7 (8.7 ± 0.5)
RAD	6.7–7.8 (7.4 ± 0.5)	8.1–9.8 (8.9 ± 0.6)
FTL	17.8–20.9 (19.2 ± 1.3)	21.8–25.0 (23.3 ± 1.1)
TIB	12.4–14.3 (13.3 ± 0.8)	15.0–17.9 (16.0 ± 0.9)
HDL/SVL	0.31–0.34 (0.33 ± 0.01)	0.30–0.33 (0.31 ± 0.01)
HDW/SVL	0.32–0.36 (0.34 ± 0.02)	0.32–0.35 (0.33 ± 0.01)
HDW/HDL	1.01–1.06 (1.03 ± 0.02)	1.03–1.08 (1.06 ± 0.02)
SNT/HDL	0.32–0.37 (0.35 ± 0.02)	0.33–0.40 (0.36 ± 0.02)
SNT/SVL	0.11–0.12 (0.12)	0.11–0.12 (0.11 ± 0.01)
IND/HDW	0.31–0.35 (0.33 ± 0.02)	0.27–0.32 (0.30 ± 0.02)
IOD/HDW	0.27–0.31 (0.29 ± 0.02)	0.27–0.30 (0.28 ± 0.01)
ED/HDL	0.37–0.41 (0.40 ± 0.02)	0.31–0.40 (0.35 ± 0.03)
ED/SVL	0.13–0.14 (0.13 ± 0.01)	0.10–0.13 (0.11 ± 0.01)
TD/ED	0.47–0.52 (0.49 ± 0.02)	0.45–0.53 (0.51 ± 0.03)
TED/TD	0.85–1.10 (0.92 ± 0.12)	0.91–1.14 (1.09 ± 0.07)
HND/SVL	0.20–0.22 (0.21 ± 0.01)	0.20–0.23 (0.21 ± 0.01)
RAD/SVL	0.21–0.24 (0.23 ± 0.02)	0.20–0.25 (0.22 ± 0.02)
TIB/SVL	0.39–0.44 (0.41 ± 0.02)	0.37–0.44 (0.39 ± 0.02)
FTL/SVL	0.56–0.64 (0.59 ± 0.04)	0.54–0.60 (0.57 ± 0.02)

distinct. Surface of throat and chest light brown, posterior region of abdomen light yellow, ventral surface of limbs light brown, inner and outer metatarsal tubercles and inner metacarpal tubercle light yellow, all marbling, colored spots and patches absent.

Variation. Measurement data of type series are listed in Table 8.

All paratypes are very similar to holotype in morphology and color pattern. However, dorsal surface yellowish brown in female paratypes SYS a004798, 4801, 4804, markings on dorsal skin indistinct in male paratypes SYS a004777/CIB110011 and SYS a004796, and female paratypes SYS a002610 (Fig. 9D), 4797, 4799, presence of a rectangle marking on central back of trunk in the female paratype SYS a002611 (Fig. 9E–F).

Etymology. The specific epithet "wugongensis" is in reference to the type locality of the new species in the Wugong Mountains. We propose the common English name "Wugongshan Horned Toad" and Chinese name "Wu Gong Shan Jiao Chan (武功山角蟾)".

Distribution and habits. Currently, *Megophrys wugongensis* sp. nov. is known from the type locality, Yangshimu Scenic Area, Pingxiang City, Jiangxi Province at approximate 550 m a.s.l., Wugongshan Scenic Area, Ji'an City, Jiangxi Province at approximate

1050–1080 m a.s.l., all located in the Luoxiao Mountains in eastern China. All specimens were collected on leaf litter near a stream in the bamboo forest, males were not heard calling. In consideration of the invisible nuptial pad and nuptial spines in all male specimens and the undeveloped fallopian tubes in all female specimens, the breeding season of *M. wugongensis* sp. nov. still remains unknown. Tadpoles were not observed. *Megophrys wugongensis* sp. nov. is sympatric with *M. jinggangensis* in all localities.

Megophrys (*Panophrys*) *mufumontana* J. Wang, Lyu & Y.Y. Wang, sp. nov.

http://zoobank.org/4FD2EE4D-A6D7-4F72-896C-A3866D74DFB7
Fig. 10, Table 9

Holotype. SYS a006391, adult male, collected by Zhi-Tong Lyu on 3 August 2017 from Mt. Mufu (28°58'18.45"N, 113°48'58.53"E; 1300 m a.s.l.), Pingjiang County, Yueyang City, Hunan Province, China.

Paratypes (one male & two females). Adult females, SYS a006390/CIB110012, SYS a006419, and the other adult male, SYS a006392, all collected by Zhi-Ting Lyu on 3 August 2017 from the same locality as the holotype.

Diagnosis. (1) Body size small, SVL 30.1–30.8 mm in two adult males and SVL 36.3 mm in two adult females; (2) head length slightly larger than head width, HDW/HDL ratio 0.98–0.99; (3) tympanum distinct, moderate-sized, TD/ED ratio 0.51–0.58, upper 1/4 part of the tympanum concealed by supratympanic fold; (4) vomerine teeth absent; (5) margin of tongue not notched posteriorly; (6) heels overlapping, tibia-tarsal articulation reach forward to the tympanum in males and to the eye in females; (7) TIB/SVL ratio 0.47–0.53, FTL/SVL ratio 0.68–0.74; (8) fingers without lateral fringes, presence of a subarticular tubercle at the bases of each finger, relative finger lengths II = IV < I < III; (9) toes with rudimentary webbing at their bases and narrow lateral fringes, subarticular tubercles only present at the base of each toe; (10) numerous granules scattered with tubercles present on dorsal surface of body, limbs and surface of flanks, some of which forming a V-shaped, \ /-shaped or X-shaped skin ridge on central back of trunk; (11) presence of a small horn-like tubercle at the edge of the upper eyelid; (12) supratympanic fold distinct; (13) light brown to dark brown dorsally, with a dark triangular marking between eyes; (14) a pair of dark longitudinal and irregular marking with white edges on its upper side on ventrolateral surface of flanks; (15) surface of throat and chest greyish brown with dark brown patches and creamy white spots, surface of abdomen greyish white with creamy white and orange spots; (16) ventral surface of thighs with dense small whitish tubercles.

Comparisons. Comparative data of *Megophrys mufumontana* sp. nov. with *M. dongduanensis* sp. nov., *M. nankunensis* sp. nov., *M. jiulianensis* sp. nov., *Megophrys nanlingensis* sp. nov., *Megophrys wugongensis* sp. nov., *M. feii* and the 33 recognized members of *Megophrys* s.l. allocated to the subgenus *Panophrys* are listed in Table 5.

Megophrys mufumontana sp. nov. differs from *M. dongguanensis* sp. nov., *M. nankunensis* sp. nov., *M. jiulianensis* sp. nov. and *M. wugongensis* sp. nov. by upper 1/4 part

of the tympanum concealed by supratympanic fold (vs. tympanum entirely visible), the heels overlapping when hindlimb is stretched along the side of the body (vs. heels not meeting in *M. dongguanensis* sp. nov., *M. nankunensis* sp. nov., *M. jiulianensis* sp. nov. and *M. wugongensis* sp. nov.), presence of narrow lateral fringes on toes (vs. absent in *M. dongguanensis* sp. nov., *M. nankunensis* sp. nov. and *M. jiulianensis* sp. nov.), absence of vomerine teeth (vs. present in *M. dongguanensis* sp. nov., *M. nankunensis* sp. nov., *M. jiulianensis* sp. nov. and *M. nanlingensis* sp. nov.), tongue not notched posteriorly (vs. tongue notched in *M. jiulianensis* sp. nov. and *M. nanlingensis* sp. nov.), skin relatively smooth and lacking black horny spines (vs. skin rough with black horny spines in *M . jiulianensis* sp. nov.).

With the smaller body size, SVL 30.1–30.8 mm in males and 36.3 mm in females, *Megophrys mufumontana* sp. nov. differs from the 19 members with larger SVL values: *M. baolongensis* (42.0–45.0 mm in males), *M. binchuanensis* (32.0–36.0 mm in males, 40.2–42.5 mm in females), *M. binlingensis* (45.1–51.0 mm in males), *M. caudoprocta* (81.3 mm in single male), *M. daweimontis* (34.0–37.0 mm in males, 40.0–46.0 mm in females), *M. fansipanensis* (41.7–42.5 mm in females), M. hoanglienensis (37.4–47.6 mm in males, 59.6 mm in single female), *M. jingdongensis* (53.0–56.5 mm in males 63.5 in single female), *M. latidactyla* (38.9 mm in single male), *M. liboensis* (34.7–67.7 mm in males, 60.8–70.6 mm in females), *M. minor* (34.5–41.2 mm in males), *M. omeimontis* (56.0–59.5 mm in males, 68.0–72.5 mm in females), *M. palpebralespinosa* (36.2–38.0 mm in males), *M. sangzhiensis* (54.7 mm in single male), *M. shuichengensis* (102.0–118.3 mm in males, 99.8–115.6 mm in females), *M. spinata* (47.2–54.4 mm in males, 54.0–55.0 mm in females), *M. tuberogranulatus* (33.2–39.6 mm in males, 50.5 mm in single female), *M. wushanensis* (38.4 mm in single female) and *M. wuliangshanensis* (41.3 mm in single female).

Megophrys mufumontana sp. nov. differs from 12 species occurring in eastern and southern China (*M. acuta*, *M. brachykolos*, *M. boettgeri*, *M. cheni*, *M. huangshanensis*, *M. insularis*, *M. jinggangensis*, *M. kuatunensis*, *M. lini*, *M. lishuiensis*, *M. obesa* and *M.ombrophila*) by the following combination of characters: upper 1/4 part of the tympanum concealed by supratympanic fold (vs. tympanum entirely visible in the 12 species above), absence of vomerine teeth (vs. present in *M. insularis* and *M. jinggangensis*), tongue not notched posteriorly (vs. tongue notched in *M. boettgeri*, *M. cheni*, *M. huangshanensis*, *M. insularis* and *M. kuatunensis*), presence of narrow lateral fringes on toes (vs. absent in *M. brachykolos*, *M. huangshanensis*, *M. insularis*, *M. lishuiensis*, *M. obesa* and *M.ombrophila*; wide in *M. boettgeri* and *M. cheni*), toes with rudimentary webbing (vs. toes without webbing in *M. huangshanensis*, *M. kuatunensis, M. lishuiensis* and *M.ombrophila*), the heels overlapping when hindlimb is stretched along the side of the body (vs. heels not meeting in *M. acuta*, *M. brachykolos*, *M. insularis, M. obesa* and *M.ombrophila*).

Megophrys mufumontana sp. nov. differs from the remaining *M. leishanensis* and *M. rubrimera* allocated to the subgenus *Panophrys* by the absence of vomerine teeth (vs. present in *M. rubrimera*), tongue not notched posteriorly (vs. tongue notched in *M. rubrimera*), upper 1/4 part of the tympanum concealed by supratympanic fold (vs.

Figure 10. *Megophrys mufumontana* sp. nov. in life: **A–D** SYS a006391, male paratype **E–F** SYS a006392, female paratype.

tympanum entirely visible in *M. leishanensis* and *M. rubrimera*), toes with narrow lateral fringes (vs. absent in *M. leishanensis*; indistinct or absent in *M. rubrimera*).

Megophrys mufumontana sp. nov. further differs from *M. feii*, for which molecular data are lacking and cannot be allocated to any subgenus base on morphology only (Yang et al. 2018) by the larger body size, SVL 30.1–30.8 mm in males and 36.3 mm in females (VS. 24.3–25.1 mm in males, 28.2–28.9 mm in females), tongue not notched posteriorly (vs. tongue notched), toes with narrow lateral fringes (vs. moderate or wide).

Description of holotype. Adult male. Habitus small, SVL 30.8 mm; head length slightly larger than head width, HDW/HWL 0.98; snout rounded in dorsal view, sloping backward to mouth in profile, protruding well beyond margin of lower jaw; top of head flat; eye large, ED/HDL 0.30; nostril oblique ovoid; pupil vertical; canthus

Table 9. Measurements (in mm; minimum-maximum, mean ± SD) of the type series of *Megophrys mufumontana* sp. nov.

Species	*Megophrys mufumontana* sp. nov.	
	Males (n = 2)	Females (n = 2)
SVL	30.1–30.8	36.3
HDL	11.6–11.9	11.8–12.4
HDW	11.4–11.7	11.7–12.3
SNT	3.5–3.7	3.7–4.2
IND	3.0–3.1	3.5–3.6
IOD	2.8–2.9	3.2–3.3
ED	3.5–3.6	3.7–3.8
TD	1.7–1.8	2.1–2.2
TED	1.7–1.8	1.8–1.9
HND	8.5–9.2	9.4–9.9
RAD	7.2–7.7	8.0–8.2
FTL	21.8–22.9	24.8–25.1
TIB	15.1–16.3	16.9–17.5
HDL/SVL	0.39	0.33–0.34
HDW/SVL	0.38	0.32–0.34
HDW/HDL	0.98	0.99
SNT/HDL	0.30–0.31	0.31–0.34
SNT/SVL	0.12	0.10–0.12
IND/HDW	0.26	0.29–0.30
IOD/HDW	0.25	0.27
ED/HDL	0.30	0.31
ED/SVL	0.12	0.10
TD/ED	0.51–0.56	0.57–0.58
TED/TD	0.90–0.94	0.86
HND/SVL	0.28–0.30	0.26–0.27
RAD/SVL	0.24–0.25	0.22–0.23
TIB/SVL	0.50–0.53	0.47–0.48
FTL/SVL	0.72–0.74	0.68–0.69

rostralis well developed; loreal region vertical; internasal distance slightly larger than interorbital distance; tympanum distinct, moderate-sized, TD/ED 0.56; large ovoid choanae at the base of the maxilla; weak vomerine ridge present, vomerine teeth absent; margin of tongue not notched posteriorly.

RAD/SVL 0.25, HND/SVL 0.30; absence of lateral fringes and webbing on fingers, relative finger lengths II = IV < I < III; tip of finger rounded, slightly swollen; presence of a distinct subarticular tubercle on the base of each finger; outer metacarpal tubercles indistinct, inner metacarpal tubercles distinct and observably enlarged. Hindlimbs long, tibio-tarsal articulation reaching forward to the tympanum when hindlimb is stretched along the side of the body; heels overlapping when the flexed hindlimbs are held at right angles to the body axis; TIB/SVL 0.53 and FTL/SVL 0.74; relative toe lengths I < II < V < III < IV; tips of toes round and slightly dilated; presence of rudimentary webbing and narrow lateral fringes on toes but absence of tarsal folds; presence of a subarticular tubercle only at the bases of each toes; presence of a long ovoid inner metatarsal tubercle and absence of outer metatarsal tubercle.

Dorsal skin texture rough with dense granules and scattered with small tubercles, some of which forming a \ /-shaped skin ridge on central back of trunk; presence of a small horn-like tubercle at the edge of upper eye lid; distinct supratympanic fold curving posteroventrally from posterior corner of eye to a level above insertion of arm; upper 1/4 part of the tympanum covered by supratympanic fold; ventral skin texture smooth with granules; pectoral gland large, closer to axilla; single large femoral gland on rear of thigh.

Measurements of holotype (in mm). SVL 30.1, HDL 11.6, HDW 11.4, SNT 3.5, IND 3.0, IOD 2.8, ED 3.5, TD 18, TED 1.7, HND 8.5, RAD 7.2, FTL 21.8, TIB 15.1.

Coloration of holotype in life. (Fig. 10A–D) Dorsal surface brown, with a distinct and incomplete dark triangular marking between eyes. Hindlimb with black transverse bands. A dark brown vertical band below the eye. Horn-like tubercle at the edge of the upper eyelid red. Surface of throat and chest greyish brown with dark brown patches. Surface of abdomen greyish white with creamy white and orange spots. Ventral surface of limbs pink with white spots and light-yellow patches. Ventral surface of hand and foot brown, inner and outer metatarsal tubercles and inner metacarpal tubercle pink. Pectoral and femoral glands white. Iris white.

Coloration of holotype in preservative. Coloration of dorsum dark brown, markings on dorsal surface and transverse bands on limbs became indistinct. Ventral surface of throat, chest and abdomen dark grey. All patches on ventral surface indistinct, all colored spots absent. Ventral surface of limbs light yellow.

Variation. Measurement data of type series are listed in Table 9.

All paratypes are very similar to holotype SYS a006391 in morphology and color pattern. However, tibia-tarsal articulation reaching forward to the eye when hindlimb is stretched along the side of the body in all females, and granules and tubercles forming a \ /-shaped skin ridge on central back of trunk in the holotype (vs. X-shaped in SYS a006390, 6419; V-shaped in SYS a006392 (Fig. 10E–F)).

Etymology. The specific epithet "mufumontana" is in reference to the type locality of the new species, Mt. Mufu. We propose the common English name "Mufushan Horned Toad" and Chinese name "Mu Fu Shan Jiao Chan (幕阜山角蟾)".

Distribution and habits. Currently, *Megophrys mufumontana* sp. nov. is known only from Mt. Mufu, Pingjiang County, Yueyang City, Hunan Province, China at approximate 1300 m a.s.l.. All specimens were collected on leaf litter near a stream (about 5 m wide) surrounded by moist subtropical evergreen broadleaved forests, males were not heard calling. Tadpoles were not observed. Because none of the males have nuptial pads developed and none of the females have fallopian tubes and eggs developed, the breeding season of *M. mufumontana* sp. nov. remains unknown.

Discussion

Megophrys dongguanensis sp. nov. is easily confused with *M. brachykolos* because of the relatively short shanks. In addition, the type locality of the new species is at a straight-line distance of approximately 72 km from the type locality (Hongkong Island), and at

a straight-line distance of approximately 32 km from the closest locality (Sanzhoutian of Shenzhen City) of *M. brachykolos*. Currently, eight *Megophrys* species in the subgenus *Panophrys* were found to have comparatively short shanks with heels not meeting when thighs are adpressed at right angles with respect to the body axis: *M. dongguanensis* sp. nov., *M. nankunensis* sp. nov., *M. wugongensis* sp. nov., *M. acuta*, *M. brachykolos*, *M. insularis*, *M. megacephala* and *M. obesa*.

In our previous study (Liu et al. 2018), 41 cryptic species within the subgenus *Panophrys* were revealed, and one of them was recently described as *Megophrys leishanensis* by Li et al. (2018). Moreover, except for *M. mufumontana* sp. nov. (not mentioned in Liu et al. (2018)), five of them are described in this study. Currently, the total number of recognized species of the subgenus *Panophrys* rises to 39, which makes it the most species-rich subgenus of *Megophrys* (≈46.4%). It's worth noting that there remain still 33 undescribed species according to Liu et al. (2018), and 27 of them are found in southeastern China, which further reveals the unusually high level of species diversity in this region.

As the diversity of the subgenus *Panophrys* was confirmed to be extremely underestimated (Chen et al. 2017; Mahony et al. 2017; Liu et al. 2018), a number of new *Panophrys* species have been described since 2017 (i.e. *Megophrys lishuiensis*, *M. insularis*, *M. rubrimera*, *M. liboensis*, and six new species in this study). However, all of these species have narrow distributions. For example, *M. insularis* is currently known only from an offshore island in Guangdong (Wang et al. 2017b), and *M. liboensis* is currently known only from a cave in Libo, Guizhou (Zhang et al. 2017). For the six new species in this study, *M. dongguanensis* sp. nov., *M. nankunensis* sp. nov., *M. wugongensis* sp. nov. and *M. mufumontana* sp. nov. are currently only found in their type localities. This situation of "micro-endemism" (Liu et al. 2018) has brought great challenges for the protection of these unique toads.

Among the six new species described in this paper, *M. jiulianensis* sp. nov. is sympatric with *M. nankunensis* sp. nov. in Mt. Nankun while also being sympatric with *M. hongshanensis* sp. nov. in Mt. Jiulian. Further, *M. mufumontana* sp. nov. is sympatric with a known congener *M. jinggangensis* in Mt. Mufu and *M. wugongensis* sp. nov. is sympatric with *M. jinggangensis* in Mt. Wugong. By combining the localities of these species in our phylogenetic trees (Fig. 2), our results also support the conclusion of "sympatric but distant phylogenetically" (Liu et al. 2018), that is, sympatric distribution is very common in horned toads within the subgenus *Panophrys* while they are distantly related in the phylogeny (Fei et al. 2012; Li et al. 2014; Wang et al. 2014; Liu et al. 2018). These geographical patterns of "sympatric but distant phylogenetically" and "micro-endemism" indicate that the Asian horned toads would be good candidates for studies on speciation and biogeography.

Acknowledgments

We thank Yao Li from the Biology Museum of Sun Yet-sen University, for her help in the lab work, and thank Runlin Li, Hailong He, Chaoyu Lin, Siyu Zhang and Guoling Chen from the Biology Museum of Sun Yet-sen University, for their help in the field work.

The work was supported by Project of Comprehensive Scientific Survey of Luoxiao Mountains Range (No. 2013FY111500) of Ministry of Science and Technology of China to Ying-Yong Wang.

References

Boulenger GA (1899) Descriptions of three new reptiles and a new batrachian from Mount Kina Balu, North Borneo. Annals and Magazine of Natural History Series 7(4): 453. https://doi.org/10.1080/00222939908678228

Chen JM, Zhou WW, Poyarkov NA, Stuart BL, Brown RM, Lathrop A, Wang YY, Yuan ZY, Jiang K, Hou M, Chen HM, Suwannapoom C, Nguyen SN, Duong TV, Papenfuss TJ, Murphy RW, Zhang YP, Che J (2017) A novel multilocus phylogenetic estimation reveals unrecognized diversity in Asian horned toads, genus *Megophrys* sensu lato (Anura: Megophryidae). Molecular Phylogenetics and Evolution 106: 28–43. https://doi.org/10.1016/j.ympev.2016.09.004

Deuti K, Grosjean S, Nicolas V, Vasudevan K, Ohler A (2017) Nomenclatural puzzle in early *Xenophrys* nomina (Anura, Megophryidae) solved with description of two new species from India (Darjeeling hills and Sikkim). Alytes (34): 20–48.

Dubois A (1987) Miscellanea taxinomica batrachologica (I). Alytes 1987[1986]: 7–95.

Dubois A, Ohler A (1998) A new species of *Leptobrachium* (*Vibrissaphora*) from northern Vietnam, with a review of the taxonomy of the genus *Leptobrachium* (Pelobatidae, Megophyinae). Dumerilia 4(14): 1–32.

Fei L, Hu SQ, Ye CY, Huang YZ (2009) Fauna Sinica. Amphibia Vol. 2 Anura. Science Press, Beijing, 957 pp. [In Chinese]

Fei L, Ye CY (2016) Amphibians of China. Vol. 1. Science Press, Beijing, 1040 pp.

Fei L, Ye CY, Jiang JP (2012) Colored atlas of Chinese amphibians and their distributions. Sichuan Publishing House of Science & Technology, Chengdu, 619 pp. [In Chinese]

Frost DR (2019) Amphibian Species of the World: an Online Reference. Version 6.0. Electronic Database. American Museum of Natural History, New York, USA. http://research.amnh.org/herpetology/amphibia/index.html [accessed 17 Jan 2019]

Frost DR, Grant T, Faivovich J, Bain RH, Haas A, Haddad CFB, De Sa, Rafael O, Channing A, Wilkinson M, Donnellan SC, Raxworthy CJ, Campbell JA, Blotto BL, Moler P, Drewes RC, Nussbaum RA, Lynch JD, Green DM, Wheeler WC (2006) The amphibian tree of life. Bulletin of the American Museum of natural History 297: 1–370. https://doi.org/10.1206/0003-0090(2006)297[0001:TATOL]2.0.CO;2

Huang YZ, Fei L (1981) Two new species of amphibians from Xizang. Acta Zootaxonomica Sinica/Dong Wu Fen Lei Xue Bao 6: 211–215.

Inger RF (1989) Four new species of frogs from Borneo. Malayan Nature Journal, Kuala Lumpur 42: 229–243.

Inger RF, Romer JD (1961) A new pelobatid frog of the genus *Megophrys* from Hong Kong. Fieldiana: Zoology 39 (46): 533–538. https://doi.org/10.5962/bhl.title.3373

Jiang JP, Ye CY, Fei L (2008) A new horn toad *Megophrys sangzhiensis* from Hunan, China (Amphibia, Anura). Zoological Research 29(2): 219–222. [in Chinese with English abstract] https://doi.org/10.3724/SP.J.1141.2008.00219

Jiang JP, Yuan FR, Xie F, Zheng ZH (2003) Phylogenetic relationships of some species and genera in megophryids inferred from partial sequences of mitochondrial 12S and 16S rRNA genes. Zoological Research 24: 241–248.

Li C, Wang YZ (2008) Taxonomic review of *Megophrys* and *Xenophrys*, and a proposal for Chinese species (Megophryidae, Anura). Acta Zootaxonomica Sinica 33(1): 104–106.

Li YL, Jin MJ, Zhao J, Liu ZY, Wang YY, Pang H (2014) Description of two new species of the genus *Xenophrys* (Amphibia: Anura: Megophryidae) from Heishiding Natural Resreve, Fengkai, Guangdong, China, based on molecular and morphological data. Zootaxa 3795: 449–471. https://doi.org/10.11646/zootaxa.3795.4.5

Li SZ, Xu N, Liu J, Jiang JP, Wei G, Wang B (2018) A new species of the asian toad genus *Megophrys* sensu lato (Amphibia: Anura: Megophryidae) from Guizhou Province, China. Asian Herpetological Research 9(4): 224–239.

Liu ZY, Chen GL, Zhu TQ, Zeng ZC, Lyu ZT, Wang J, Messenger K, Greenberg AJ, Guo ZX, Yang ZH, Shi SH, Wang YY (2018) Prevalence of cryptic species in morphologically uniform taxa – fast speciation and evolutionary radiation in Asian toads. Molecular Phylogenetics and Evolution. https://doi.org/10.1016/j.ympev.2018.06.020

Mahony S, Foley NM, Biju SD, Teeling EC (2017) Evolutionary history of the Asian Horned Frogs (Megophryinae): integrative approaches to timetree dating in the absence of a fossil record. Molecular Biology and Evolution 34(3): 744–771. https://doi.org/10.1093/molbev/msw267

Mahony S, Kamei RG, Teelin EC, Biju SD (2018) Cryptic diversity within the *Megophrys major* species group (Amphibia: Megophryidae) of the Asian Horned Frogs: Phylogenetic perspectives and a taxonomic revision of South Asian taxa, with descriptions of four new species. Zootaxa 4523: 1–96. https://doi.org/10.11646/zootaxa.4523.1.1

Messenger KR, Dahn HA, Liang Y, Xie P, Wang Y, Lu C (2019) A new species of the genus *Megophrys* Gunther, 1864 (Amphibia: Anura: Megophryidae) from Mount Wuyi, China. Zootaxa 4554: 561–583. https://doi.org/10.11646/zootaxa.4554.2.9

Malkmus R, Manthey U, Vogel G, Hoffmann P, Kosuch J (2002) Amphibians & Reptiles of Mount Kinabalu (North Borneo). Ruggell: A.R.G. Gantner Verlag, 424pp.

Meyer CP, Geller JB, Paulay G (2005) Fine scale endemism on coral reefs: archipelagic differentiation in turbinid gastropods. Evolution 59(1): 113–125. https://doi.org/10.1111/j.0014-3820.2005.tb00899.x

Mo XY, Shen YH, Li HH, Wu XS (2010) A new species of *Megophrys* (Amphibia: Anura: Megophryidae) from the northwestern Hunan Province, China. Current Zoology 56(4): 432–436.

Orlov NL, Poyarkov NA, Nguyen TT (2015) Taxonomic notes on *Xenophrys* frogs (Megophryidae: Anura) of Vietnam, with description of a new species. Russian Journal of Herpetology 22: 206–218.

Rao DQ, Yang DT (1997) The karyotypes of Megophryinae (Pelobatinae) with a discussion on their classification and phylogenetic relationships. Asiatic Herpetological Research 7: 93–102. https://doi.org/10.5962/bhl.part.18858

Ronquist F, Teslenko M, Van Der Mark P, Ayres DL, Darling A, Höhna S, Larget B, Liu L, Suchard MA, Huelsenbeck JP (2012) MrBayes 3.2: efficient Bayesian phylogenetic inference and model choice across a large model space. Systematic Biology 61: 539–542. https://doi.org/10.1093/sysbio/sys029

Stuart BL, Sok K, Neang T (2006) A collection of amphibians and reptiles from hilly eastern Cambodia. Raffles Bulletin of Zoology, Singapore 54: 129–155.

Simon C, Frati F, Beckenbach A, Crespi B, Liu H, Flook P (1994) Evolution, weighting, and phylogenetic utility of mitochondrial gene sequences and a compilation of conserved polymerasechain reaction primers. Annals of the Entomological Society of America 87: 651–701. https://doi.org/10.1093/aesa/87.6.651

Taylor EH (1920) Philippine Amphibia. Philippine Journal of Science 16: 213–359. https://doi.org/10.5962/bhl.part.4751

Tapley B, Cutajar TP, Mahony S, Chung NT, Dau VQ, Nguyen TT, Luong HV, Rowley JJL (2017) The Vietnamese population of *Megophrys kuatunensis* (Amphibia: Megophryidae) represents a new species of Asian horned frog from Vietnam and southern China. Zootaxa 4344: 465–492. https://doi.org/10.11646/zootaxa.4344.3.3

Tapley B, Cutajar TP, Mahony S, Nguyen CT, Dau VQ, Luong AM, Le DT, Nguyen TT, Nguyen TQ, Portway C, Luong HV, Rowley JJL (2018) Two new and potentially highly threatened *Megophrys* Horned frogs (Amphibia: Megophryidae) from Indochina's highest mountains. Zootaxa 4508: 301–333. https://doi.org/10.11646/zootaxa.4508.3.1

Tamura K, Stecher G, Peterson D, Filipski A, Kumar S (2013) MEGA6: molecular evolutionary genetics analysis, version 6.0. Molecular Biology and Evolution 30: 2725–2729. https://doi.org/10.1093/molbev/mst197

Thompson JD, Gibson TJ, Plewniak F, Jeanmougin F, Higgins DG (1997) The CLUSTAL_X windows interface: flexible strategies for multiple sequence alignment aided by quality analysis tools. Nucleic Acids Research 25: 4876–4882. https://doi.org/10.1093/nar/25.24.4876

Tian YZ, Gu XM, Sun AQ (2000) A new species of *Xenophrys* in China (Amphibia: Pelobatidae). Acta Zootaxonomica Sinica 25: 462–466.

Wang YF, Liu BQ, Jiang K, Jin W, Xu JN, Wu CH (2017a) A new species of the horn toad of the genus *Xenophrys* from Zhejiang, China (Amphibia: Megophryidae). Chinese Journal of Zoology 52(1): 19–29. [in Chinese with English abstract]

Wang J, Liu ZY, Lyu ZT, Zeng ZC, Wang YY (2017b) A new species of the genus *Xenophrys* (Amphibia: Anura: Megophryidae) from an offshore island in Guangdong Province, southeastern China. Zootaza 4324: 541–556. https://doi.org/10.11646/zootaxa.4324.3.8

Wang YY, Zhao J, Yang JH, Zhou ZX, Chen GL, Liu Y (2014) Morphology, molecular genetics, and bioacoustics support two new sympatric *Xenophrys* (Amphibia: Anura: Megophryidae) species in Southeast China. PLoS ONE 9: e93075. https://doi.org/10.1371/journal.pone.0093075

Wang YY, Zhang TD, Zhao J, Sung YH, Yang JH, Pang H, Zhang Z (2012) Description of a new species of the genus *Xenophrys* Günther, 1864 (Amphibia: Anura: Megophryidae) from Mount Jinggang, China, based on molecular and morphological data. Zootaxa 3546: 53–67. https://doi.org/10.11646/zootaxa.3546.1.4

Yang JH, Wang J, Wang YY (2018) A new species of the genus *Megophrys* (Anura: Megophryidae) from Yunnan Province, China. Zootaxa 4413(2): 325–338. https://doi.org/10.11646/zootaxa.4413.2.5

Ye CY, Fei L (1995) Taxonomic studies on the small type *Megophrys* in China including descriptions of the new species (subspecies) (Pelobatidae: genus *Megophrys*). Acta Herpetologica Sinica/Liangqi Paxing Dongwu Yanjiu 4–5: 72–81.

Ye CY, Fei L, Xie F (2007). A new species of Megophryidae – *Megophrys baolongensis* from China (Amphibia, Anura). Herpetologica Sinica 11: 38–41.

Zhang YG, Li N, Xiao JL, Pan T, Wang H, Zhang B, Zhou J (2017) A new species of the genus *Xenophrys* (Amphibia: Anura: Megophryidae) from Libo County, Guizhou, China. Asian Herpetological Research 8: 75–85.

Zheng YC, Zeng XM, Yuan YZ, Liu ZJ (2004) Phylogenetic positions of *Ophryophryne* and four *Leptobrachium* group genera in Megophryidae (Anura). Sichuan Journal of Zoology 23: 290–295.

Appendix 1

Specimens of comparative species examined

Megophrys boettgeri (n = 13): China: Jiangxi Provence: Guixi City: Yangjifeng Nature Reserve (the middle area of Wuyi Mountains, 600–883 m a.s.l.): SYS a000312, 000315, 000328–000330, 000376, 000378; Guangfeng County: Tongboshan Nature Reserve (the eastern area of Wuyi Mountains, 450–821 m a.s.l.): SYS a001671–001673, 001683, 001700.

Megophrys brachykolos (n = 21): China: Hong Kong: SYS a001502–001503; Guangdong Province: Shenzhen City: Yangtaishan Forest Park (60–150 m a.s.l.): SYS a2051–002056, 002069–002074, 002413; Qiniangshan Geological Park (30–50 m a.s.l.): SYS a002405–002410.

Megophrys caudoprocta (n = 3): China: Hunan Province: Zhangjiajie City: Sangzhi County: Mt. Badagong (1100–1200 m a.s.l.): SYS a004281, 004308–4309.

Megophrys cheni (n = 19): China: Jiangxi Province: Jinggangshan City: Mt. Jinggang (1200–1260 m a.s.l.): SYS a001427–001429, SYS a001871–001873; Hunan Province: Yanling County: Taoyuandong Nature Reserve: Lishuzhou Village (1480–1530 m a.s.l.): SYS a002123–002127, Dayuan Farm (1480 m a.s.l.): SYS a002140–002145.

Megophrys huangshanensis (n = 10): China: Jiangxi Province: Wuyuan County: Mount Dazhang (600–900 m a.s.l.): SYS a001314–001323.

Megophrys insularis (n = 6): China: Guangdong Province: Shantou City: Nan'ao Island (50–500 m a.s.l.): SYS a002167–002171, SYS a003666/CIB 106881.

Megophrys jingdongensis (n = 2): Yunnan Province: Jingdong County: Mt. Wuliang (1800 m a.s.l.): SYS a003928–3929.

Megophrys jinggangensis (n = 10): China: Jiangxi Province: Jinggangshan City: Mt. Jinggang (700–900m a.s.l.): SYS a001413–001416, 001430; Hunan Province: Yanling County: Taoyuandong Nature Reserve (800–1000 m a.s.l.): SYS a001859–001863.

Megophrys kuatunensis (n = 3): China: Fujian Province: Wuyishan City (=Ch'ungan Hsien): Guadun Village (= Kuatun Village, 1060–1220 m a.s.l.): SYS a001579 and 001590; Jiangxi Province: Guixi City: Yangjifeng Nature Reserve (the middle area of Wuyi Mountains, 950 m a.s.l.): SYS a000241.

Megophrys lini (n = 27): China: Jiangxi Province: Jinggangshan City: Mt. Jinggang (1100–1610 m a.s.l.): SYS a001417–001424, SYS a002375–002386; Suichuan County: Nanfengmian Nature Reserve (1150–1250 m a.s.l.): SYS a002369–002374; Hunan Province: Yanling County: Taoyuandong Nature Reserve: Niushiping Village (1360 m a.s.l.): SYS a002128.

Megophrys minor (n = 4): China: Sichuan Province: Dujiangyan City: Mt. Qingcheng: SYS a003209, 003211–3213.

Megophrys omeimontis (n = 6): China: Sichuan Province: Mt. Emei: SYS a001798–001801, 001940–001941.

Megophrys sangzhiensis (n = 6): China: Hunan Province: Zhangjiajie City: Sangzhi County: Mt. Badagong (1100–1200 m a.s.l.): SYS a004306–004307, 004313–004316.

Megophrys spinata (n = 2): China: Guizhou Province: Leishan County: Mt. Leigong: SYS a002226–002227.

Megophrys tuberogranulatus (n = 1): China: Hunan Province: Zhangjiajie City: Sangzhi County: Mt. Badagong (1100–1200 m a.s.l.): SYS a004310.*Megophrys wuliangshanensis* (n = 2): Yunnan Province: Jingdong County: Mt. Wuliang (1800 m a.s.l.): SYS a003924–3925.